



TECHNISCHE UNIVERSITÄT MÜNCHEN

Lehrstuhl für Entwicklungsgenetik

**The long-term effects of low dose ionizing radiation
on the adult mouse brain and consequences for behavior**

Marie-Claire Ung

Vollständiger Abdruck der von der TUM School of Life Sciences der Technischen Universität München zur Erlangung des akademischen Grades eines Doktors der Naturwissenschaften genehmigten Dissertation.

Vorsitzende:

Prof. Angelika Schnieke, Ph.D.

Prüfer der Dissertation:

1. Prof. Dr. Wolfgang Wurst
2. Prof. Dr. Michael J. Atkinson

Die Dissertation wurde am 21.10.2020 bei der Technischen Universität München eingereicht und durch die TUM School of Life Sciences am 30.06.2021 angenommen.

CONTENTS

List of figures.....	10
List of tables	14
Abbreviations.....	15
Abstract.....	17
Zusammenfassung.....	19
I. Introduction	21
1. Exposure to ionizing radiation	21
1.1. What is ionizing radiation?.....	21
1.2. Where is ionizing radiation present?	21
1.3. How is ionizing radiation measured?	21
1.4. What is a low dose radiation?	22
2. Damages caused by ionizing radiation	23
2.1.Direct damages.....	23
2.1.a. Double strands breaks (DSBs)	23
2.1.b. Reactive oxygen species	25
2.2.Indirect damages	26
3. Effects of unrepaired damages consecutive to exposure to ionizing radiation	26
3.1.Stochastic effects.....	26
3.2.Non-stochastic/deterministic effects/tissues reaction.....	27
4. Threshold for biological effects	29
5. Adaptive responses	29
6. Effects of unrepaired damages caused by ionizing radiation on the brain	30
6.1.Brain development and neurogenesis	30
6.2.Brain regions	30
6.3.Behavior	31
6.3.a. Acoustic Startle Response (ASR)	31
6.3.b. Open Field test (OF)	32
6.3.c. Social Discrimination test (SD)	32
6.4. Effects of high-dose radiation exposure on the brain	33
6.5. Effects of low-dose radiation exposure on the brain	33
7. Ercc2 ^{S737P} biology.....	34
8. Importance of the research	35

9. Unresolved questions	36
II. Aims of the study	37
1. Research questions	37
2. Objectives	37
3. Hypotheses	37
III. Materials and methods.....	38
1. Animals.....	38
1.1. F1 hybrid C57/C3H animals	38
1.2. Ercc2 ^{S737P} heterozygous mice.....	38
2. Irradiation	39
3. Behavioral tests	39
3.1. Open Field test (OF)	40
3.2. Acoustic Startle Response/Prepulse inhibition test (ASR/PPI)	41
3.3. Social discrimination (SD).....	41
4. Tissue sampling procedure	41
5. Immunohistochemistry	42
5.1. Reagents and solutions	42
5.2. Consumables.....	43
5.3. Technical equipment.....	44
5.4. Nissl, Iba1 and GFAP staining.....	45
5.6. Cell quantification (stereology)	47
5.7. Golgi staining	49
5.8. Analysis of microglial and astrocytic morphology	49
6. Statistical analyses.....	50
IV. Results.....	52
A. Wildtype animals.....	52
1. Open field (OF)	52

1.1. OF - 4 months after exposure	52
1.1.a. OF - 4 months after exposure to 0.063 Gy	52
1.1.b. OF - 4 months after exposure to 0.125 Gy	53
1.1.c. OF - 4 months after exposure to 0.5 Gy	54
1.2. OF - 12 months after exposure	55
1.2.a. OF - 12 months after exposure to 0.063 Gy	55
1.2.b. OF - 12 months after exposure to 0.125 Gy	56
1.2.c. OF - 12 months after exposure to 0.5 Gy	57
1.3. OF - 18 months after exposure	58
1.3.a. OF - 18 months after exposure to 0.063 Gy	58
1.3.b. OF - 18 months after exposure to 0.125 Gy	59
1.3.c. OF - 18 months after exposure to 0.5 Gy	60
2. Acoustic Startle Response (ASR)	62
2.1. ASR - 4 months after exposure	62
2.1.a. ASR - 4 months after exposure to 0.063 Gy	62
2.1.b. ASR - 4 months after exposure to 0.125 Gy	64
2.1.c. ASR - 4 months after exposure to 0.5 Gy	65
2.2. ASR - 12 months after exposure	65
2.2.a. ASR - 12 months after exposure to 0.063 Gy	65
2.2.b. ASR - 12 months after exposure to 0.125 Gy	66
2.2.c. ASR - 12 months after exposure to 0.5 Gy	67
2.3. ASR - 18 months after exposure	67
2.3.a. ASR - 18 months after exposure to 0.063 Gy	68
2.3.b. ASR - 18 months after exposure to 0.125 Gy	68
2.3.c. ASR - 18 months after exposure to 0.5 Gy	70
3. Social discrimination (SD)	72
3.1. SD - 4 months after exposure	72
3.1.a. SD - 4 months after exposure to 0.063 Gy	73
3.1.b. SD - 4 months after exposure to 0.125 Gy	74
3.1.c. SD - 4 months after exposure to 0.5 Gy	75
3.2. SD - 12 months after exposure	76
3.2.a. SD - 12 months after exposure to 0.063 Gy	76
3.2.b. SD - 12 months after exposure to 0.125 Gy	77
3.2.c. SD - 12 months after exposure to 0.5 Gy	78
3.3. SD - 18 months after exposure	79
3.3.a. SD - 18 months after exposure to 0.063 Gy	79
3.3.b. SD - 18 months after exposure to 0.125 Gy	80
3.3.c. SD - 18 months after exposure to 0.5 Gy	81

B. Heterozygous Ercc2 ^{S737P} mice.....	82
1. Open field (OF)	82
1.1. OF - 4 months after exposure	82
1.1.a. OF - 4 months after exposure to 0.063 Gy	82
1.1.b. OF – 4 months after exposure to 0.125 Gy	83
1.1.c. OF – 4 months after exposure to 0.5 Gy	84
1.2. OF – 12 months after exposure	85
1.2.a. OF – 12 months after exposure to 0.063 Gy	85
1.2.b. OF – 12 months after exposure to 0.125 Gy.....	86
1.2.c. OF – 12 months after exposure to 0.5 Gy	87
1.3. OF - 18 months after exposure	88
1.3.a. OF – 18 months after exposure to 0.063 Gy	88
1.3.b. OF – 18 months after exposure to 0.125 Gy.....	89
1.3.c. OF – 18 months after exposure to 0.5 Gy	90
2. Acoustic Startle Response (ASR).....	91
2.1. ASR - 4 months after exposure	91
2.1.a. ASR – 4 months after exposure to 0.063 Gy	91
2.1.b. ASR – 4 months after exposure to 0.125 Gy	92
2.1.c. ASR – 4 months after exposure to 0.5 Gy	93
2.2. ASR - 12 months after exposure	94
2.2.a. ASR – 12 months after exposure to 0.063 Gy.....	94
2.2.b. ASR – 12 months after exposure to 0.125 Gy	95
2.2.c. ASR – 12 months after exposure to 0.5 Gy.....	96
2.3. ASR - 18 months after exposure	97
2.3.a. ASR – 18 months after exposure to 0.063 Gy	97
2.3.b. ASR – 18 months after exposure to 0.125 Gy	98
2.3.c. ASR – 18 months after exposure to 0.5 Gy.....	99
3.Social discrimination (SD).....	100
3.1. SD – 4 months after exposure	100
3.1.a. SD – 4 months after exposure to 0.063 Gy	100
3.1.b. SD – 4 months after exposure to 0.125 Gy	101
3.1.c. SD – 4 months after exposure to 0.5 Gy.....	102
3.2. SD – 12 months after exposure	103
3.2.a. SD – 12 months after exposure to 0.063 Gy	103
3.2.b. SD – 12 months after exposure to 0.125 Gy	104
3.2.c. SD – 12 months after exposure to 0.5 Gy.....	105
3.3. SD – 18 months after exposure	106
3.3.a. SD – 18 months after exposure to 0.063 Gy	106

3.3.b. SD – 18 months after exposure to 0.125 Gy	107
3.3.c. SD – 18 months after exposure to 0.5 Gy.....	108
C. Linear Model with random intercept (LM)	109
1. General radiation effect.....	109
2. Dose-dependent radiation effects at 4 months after exposure	110
3. Dose-dependent radiation effects at 12 months after exposure	111
4. Dose-dependent radiation effects at 18 months after exposure	112
5. Genotype-dose effect at 18 months after exposure	113
D. Immunohistochemistry.....	115
1. Neuronal and glial density in the hippocampus 24 months following radiation exposure to 0, 0.063, 0.125 or 0.5 Gy in wt and <i>Ercc2</i> ^{S737P} het mice, males and females pooled	115
2. Quantification of Iba1+ microglia in the hippocampus 12, 18 and 24 months following radiation exposure to 0, 0.063, 0.125 or 0.5 Gy in wt mice, males and females pooled	116
2.1. Quantification of Iba1+ microglia in the hippocampus 12 months following radiation exposure to 0, 0.063, 0.125 or 0.5 Gy in wt mice, males and females pooled	116
2.2. Quantification of Iba1+ microglia in the hippocampus 18 months following radiation exposure to 0, 0.063, 0.125 or 0.5 Gy in wt mice, males and females pooled	117
2.3. Quantification of Iba1+ microglia in the hippocampus 24 months following radiation exposure to 0, 0.063, 0.125 or 0.5 Gy in wt mice, males and females pooled	118
2.4. Quantification of Iba1+ microglia in the hippocampus 12 months following radiation exposure to 0, 0.063, 0.125 or 0.5 Gy in <i>Ercc2</i> ^{S737P} het mice, males and females pooled	119
2.5. Quantification of Iba1+ microglia in the hippocampus 18 months following radiation exposure to 0, 0.063, 0.125 or 0.5 Gy in <i>Ercc2</i> ^{S737P} het mice, males and females pooled	120
2.6. Quantification of Iba1+ microglia in the hippocampus 24 months following radiation exposure 0, 0.063, 0.125 or 0.5 Gy in <i>Ercc2</i> ^{S737P} het mice, males and females pooled ..	121
2.7. Linear Model Analysis: Iba1	122
2.8. Morphological analysis of hippocampal microglial cells 24 months after exposure to ionizing radiation.....	124

3. Quantification of GFAP+ astrocytes in the hippocampus of wt and Ercc2 ^{S737P} het mice, 12, 18 or 24 months following radiation exposure to 0; 0.063; 0.125 or 0.5 Gy, males and females pooled.....	129
3.1. Quantification of GFAP+ astrocytes in the hippocampus of wt mice, males and females pooled, 12 months after radiation exposure to 0; 0.063; 0.125 or 0.5 Gy.....	129
3.2. Quantification of GFAP+ astrocytes in the hippocampus of wt mice, males and females pooled, at 18 months after radiation exposure to 0; 0.063; 0.125 or 0.5 Gy.....	130
3.3. Quantification of GFAP+ astrocytes in the hippocampus of wt mice, males and females pooled, at 24 months after radiation exposure to 0; 0.063; 0.125 or 0.5 Gy.....	131
3.4. Quantification of GFAP+ astrocytes in the hippocampus of Ercc2 ^{S737P} het mice, males and females pooled, at 12 months after radiation exposure to 0; 0.063; 0.125 or 0.5 Gy	131
3.5. Quantification of GFAP+ astrocytes in the hippocampus of Ercc2 ^{S737P} het mice, males and females pooled, at 18 months after radiation exposure to 0; 0.063; 0.125 or 0.5 Gy	132
3.6. Quantification of GFAP+ astrocytes in the hippocampus of Ercc2 ^{S737P} het mice, males and females pooled, at 24 months after radiation exposure to 0; 0.063; 0.125 or 0.5 Gy	133
3.7. Linear Model Analysis: GFAP.....	134
3.8. Morphological analysis of hippocampal astrocyte cells 24 months after exposure to ionizing radiation.....	136
V. Discussion	141
1.Main findings	142
2.Early and delayed radiation effects	143
3.Dose-dependent effects	143
4.Neuroinflammation	144
5.Effect of the Ercc2 ^{S737P} mutation at older age	147
6.Health consequences following low-dose radiation exposure	147
7.Limitations in the techniques used to determine radiation damages.....	148
8.Limitations of the study	149
9.Conclusions and outlook.....	149

Bibliography	151
Acknowledgements	159

List of figures

Fig.2.1.a. NHEJ and HR pathways for the repair of DSBs.	25
Fig.4.2. Possible dose-reponse relationships after low dose radiation exposure	28
Fig. 3. Experimental design – Behavior	40
Fig.5.4.a. A representative Nissl-stained mouse brain hippocampal region	45
Fig.5.4.b. A representative photomicrograph showing Iba1+ cells in the hippocampus	46
Fig 5.4.c. A representative photomicrograph of GFAP+ cells in the hippocampus	46
Fig.5.5 Stereology parameters used to calculate the total of positive-stained cells in one brain	48
Fig. A.1.1.a. 1) Spontaneous locomotion at 4 months post-irradiation with 0.063 Gy	52
Fig. A.1.1.a. 2) Explorative behavior and anxiety at 4 months post-irradiation with 0.063 Gy	53
Fig. A.1.1.b.1) Spontaneous locomotion at 4 months post-irradiation with 0.125 Gy	53
Fig. A.1.1.b.2). Explorative behavior and anxiety at 4 months post-irradiation with 0.125 Gy	54
Fig. A.1.1.c.1) Spontaneous locomotion at 4 months post-irradiation with 0.5 Gy	54
Fig. A.1.1.c.2) Explorative behavior and anxiety at 4 months post-irradiation with 0.5 Gy	55
Fig. A.1.2.a.1) Spontaneous locomotion at 12 months post-irradiation with 0.063 Gy	55
Fig. A.1.2.a.2) Explorative behavior and anxiety at 12 months post-irradiation with 0.063 Gy	56
Fig. A.1.2.b.1) Spontaneous locomotion at 12 months post-irradiation with 0.125 Gy	56
Fig. A.1.2.b.2) Explorative behavior and anxiety at 12 months post-irradiation with 0.125 Gy	57
Fig. A.1.2.c.1) Spontaneous locomotion at 12 months post-irradiation with 0.5 Gy	57
Fig. A.1.2.c.2) Explorative behavior and anxiety at 12 months post-irradiation with 0.5 Gy	58
Fig. A.1.3.a.1) Spontaneous locomotion at 18 months post-irradiation with 0.063 Gy	58
Fig. A.1.3.a.2) Explorative behavior and anxiety at 18 months post-irradiation with 0.063 Gy	59
Fig. A.1.3.b.1) Spontaneous locomotion at 18 months post-irradiation with 0.125 Gy	59
Fig. A.1.3.b.2) Explorative behavior and anxiety at 18 months post-irradiation with 0.125	60
Fig. A.1.3.c.1) Spontaneous locomotion at 18 months post-irradiation with 0.5 Gy	60
Fig. A.1.3.c.2) Explorative behavior and anxiety at 18 months post-irradiation with 0.5 Gy	61
Fig.A.2.1.a.1) ASR – 4 months after exposure to 0.063 Gy	63
Fig. A.2.1.a.2) PPI – 4 months after exposure to 0.063 Gy	63
Fig. A. 2.1.b.1) ASR – 4 months after exposure to 0.125 Gy	64
Fig. A.2.1.b.2) PPI – 4 months after exposure to 0.125 Gy	64

Fig. A. 2.1.c.1) ASR – 4 months after exposure to 0.5 Gy	65
Fig.A.2.1.c.2) PPI – 4 months after exposure to 0.5 Gy	65
Fig.A.2.2.a.1) ASR – 12 months after exposure to 0.063 Gy	66
Fig.A.2.2.a.2) PPI – 12 months after exposure to 0.063 Gy	66
Fig. A.2.2.b.1) ASR – 12 months after exposure to 0.125 Gy	67
Fig.A.2.2.b.2) PPI – 12 months after exposure to 0.125 Gy	67
Fig. A.2.2.c.1) ASR – 12 months after exposure to 0.5 Gy.....	68
Fig.A.2.2.c.2) PPI – 12 months after exposure to 0.5 Gy.....	68
Fig.A.2.3.a.1) ASR – 18 months after exposure to 0.063 Gy	69
Fig.A.2.3.a.2) PPI – 18 months after exposure to 0.063 Gy	69
Fig.A.2.3.b.1) ASR – 18 months after exposure to 0.125 Gy	69
Fig.A.2.3.b.2) PPI – 18 months after exposure to 0.125 Gy	70
Fig. A.2.3.c.1) ASR – 18 months after exposure to 0.5 Gy.....	71
Fig. A.2.3.c.2) PPI – 18 months after exposure to 0.5 Gy	71
Fig. A.3.1.a. SD - 4 months after exposure to 0.063 Gy	73
Fig. A.3.1.b. SD – 4 months after exposure to 0.125 Gy.....	73
Fig.A.3.1.c. SD - 4 months after exposure to 0.5 Gy	75
Fig. A.3.2.a. SD – 12 months after exposure to 0.063 Gy.....	76
Fig. A.3.2.b. SD – 12 months after exposure to 0.125 Gy	77
Fig.A.3.2.c. SD – 12 months after exposure to 0.5 Gy.....	78
Fig.A.3.3.a. SD – 18 months after exposure to 0.063 Gy.....	79
Fig. A.3.3.b. SD – 18 months after exposure to 0.125 Gy	80
Fig.A.3.3.c. SD – 18 months after exposure to 0.5 Gy.....	81
Fig. B.1.1.a. 1) Spontaneous locomotion at 4 months post-irradiation with 0.063 Gy	82
Fig. B.1.1.a. 2) Explorative behavior and anxiety at 4 months post-irradiation with 0.063 Gy	82
Fig. B.1.1.b.1) Spontaneous locomotion at 4 months post-irradiation with 0.125 Gy	83
Fig. B.1.1.b.2). Explorative behavior and anxiety at 4 months post-irradiation with 0.125 Gy	83
Fig. B.1.1.c.1) Spontaneous locomotion at 4 months post-irradiation with 0.5 Gy	84
Fig. B.1.1.c.2) Explorative behavior and anxiety at 4 months post-irradiation with 0.5 Gy	84
Fig. B.1.2.a.1) Spontaneous locomotion at 12 months post-irradiation with 0.063 Gy	85

Fig. B.1.2.a.2) Explorative behavior and anxiety at 12 months post-irradiation with 0.063 Gy	85
Fig. B.1.2.b.1) Spontaneous locomotion at 12 months post-irradiation with 0.125 Gy	86
Fig. B.1.2.b.2) Explorative behavior and anxiety at 12 months post-irradiation with 0.125 Gy	86
Fig. B.1.2.c.1) Spontaneous locomotion at 12 months post-irradiation with 0.5 Gy	87
Fig. B.1.2.c.2) Explorative behavior and anxiety at 12 months post-irradiation with 0.5 Gy	87
Fig. B.1.3.a.1) Spontaneous locomotion at 18 months post-irradiation with 0.063 Gy	88
Fig. B.1.3.a.2) Explorative behavior and anxiety at 18 months post-irradiation with 0.063 Gy	88
Fig. B.1.3.b.1) Spontaneous locomotion at 18 months post-irradiation with 0.125 Gy	89
Fig. B.1.3.b.2) Explorative behavior and anxiety at 18 months post-irradiation with 0.125 Gy	89
Fig. B.1.3.c.1) Spontaneous locomotion at 18 months post-irradiation with 0.5 Gy	90
Fig. B.1.3.c.2) Explorative behavior and anxiety at 18 months post-irradiation with 0.5 Gy	90
Fig. B.2.1.a.1) ASR – 4 months after exposure to 0.063 Gy	91
Fig. B.2.1.a.2) PPI – 4 months after exposure to 0.063 Gy.....	91
Fig. B. 2.1.b.1) ASR – 4 months after exposure to 0.125 Gy	92
Fig. B.2.1.b.2) PPI – 4 months after exposure to 0.125 Gy.....	92
Fig. B. 2.1.c.1) ASR – 4 months after exposure to 0.5 Gy	93
Fig. B.2.1.c.2) PPI – 4 months after exposure to 0.5 Gy	93
Fig. B.2.2.a.1) ASR – 12 months after exposure to 0.063 Gy.....	94
Fig. B.2.2.a.2) PPI – 12 months after exposure to 0.063 Gy.....	94
Fig. B.2.2.b.1) ASR – 12 months after exposure to 0.125 Gy	95
Fig. B.2.2.b.2) PPI – 12 months after exposure to 0.125 Gy	95
Fig. B.2.2.c.1) ASR – 12 months after exposure to 0.5 Gy.....	96
Fig. B.2.2.c.2) PPI – 12 months after exposure to 0.5 Gy	96
Fig. B.2.3.a.1) ASR – 18 months after exposure to 0.063 Gy.....	97
Fig. B.2.3.a.2) PPI – 18 months after exposure to 0.063 Gy.....	97
Fig.B.2.3.b.1) ASR – 18 months after exposure to 0.125 Gy	98
Fig.B.2.3.b.2) PPI – 18 months after exposure to 0.125 Gy	98
Fig. B.2.3.c.1) ASR – 18 months after exposure to 0.5 Gy.....	99
Fig. B.2.3.c.2) PPI – 18 months after exposure to 0.5 Gy	99
Fig. B.3.1.a. SD - 4 months after exposure to 0.063 Gy	100

Fig. B.3.1.b. SD – 4 months after exposure to 0.125 Gy.....	101
Fig.B.3.1.c. SD - 4 months after exposure to 0.5 Gy.....	102
Fig. B.3.2.a. SD – 12 months after exposure to 0.063 Gy.....	103
Fig. B.3.2.b. SD – 12 months after exposure to 0.125 Gy.....	104
Fig.B.3.2.c. SD – 12 months after exposure to 0.5 Gy.....	105
Fig.B.3.3.a. SD – 18 months after exposure to 0.063 Gy.....	106
Fig. B.3.3.b. SD – 18 months after exposure to 0.125 Gy.....	107
Fig.B.3.3.c. SD – 18 months after exposure to 0.5 Gy.....	108
Fig. C.1. Radiation effect over time	109
Fig. C.2 Dose-dependent radiation effects at 4 months after exposure	110
Fig. C.3 Dose-dependent radiation effects at 12 months after exposure	111
Fig. C.4 Dose-dependent radiation effects at 18 months after exposure	112
Fig.C.5.a. Genotype-dose interaction at 18 months	113
Fig.C.5.b. Genotype differences in age-related changes in non-irradiated mice	114
Fig. D.1.a Nissl 24 months after exposure, males and females pooled, wt.....	115
Fig. D.1.b. Nissl 24 months after exposure, males and females pooled, <i>Ercc2</i> ^{S73P} het	116
Fig.D.2.1. Quantification of Iba1+ microglia in in the hippocampus of wt mice at 12 months after exposure to ionizing radiation (0; 0.063; 0.125 and 0.5 Gy)	117
Fig.D.2.2. Quantification of Iba1+ microglia in the hippocampus of wt mice, 18 months after exposure to ionizing radiation (0; 0.063; 0.125 and 0.5 Gy).....	118
Fig.D.2.3. Quantification of Iba1+ microglia in the hippocampus of wt mice, 24 months after exposure to ionizing radiation (0; 0.063; 0.125 and 0.5 Gy).....	119
Fig.D.2.4. Quantification of Iba1+ microglia in the hippocampus of <i>Ercc2</i> ^{S73P} het mice, 12 months after exposure to ionizing radiation (0; 0.063; 0.125 and 0.5 Gy)	120
Fig.D.2.5. Quantification of Iba1+ microglia in the hippocampus of <i>Ercc2</i> ^{S73P} het mice, 18 months after exposure to ionizing radiation (0; 0.063; 0.125 and 0.5 Gy)	121
Fig.D.2.6. Quantification of Iba1+ microglia in the hippocampus of <i>Ercc2</i> ^{S73P} het mice, 24 months after exposure to ionizing radiation (0; 0.063; 0.125 and 0.5 Gy)	122
Fig.D.2.7. Linear Model Analysis: Iba1	123
Fig. D.2.8.a. Dose-dependent effects of radiation on microglial morphology	125
Fig. D.2.8.b. Sholl-analysis of microglial cells	126

Fig. D.2.8.c. 3D-traced structures of exemplary hippocampal microglia of sham-, 0.063 Gy-, 0.125 Gy- and 0.5 Gy-irradiated animals 24 months after exposure.	126
Fig. D.3.1. Quantification of GFAP+ astrocytes in the hippocampus of wt mice, males and females pooled, at 12 months after radiation exposure to 0; 0.063; 0.125 or 0.5 Gy	129
Fig.D.3.2 Quantification of GFAP+ astrocytes in the hippocampus of wt mice, males and females pooled, at 18 months after radiation exposure to 0; 0.063; 0.125 or 0.5 Gy	130
Fig.D.3.3. Quantification of GFAP+ astrocytes in the hippocampus of wt mice, males and females pooled, at 24 months after radiation exposure to 0; 0.063; 0.125 or 0.5 Gy.	131
Fig.D.3.4. Quantification of GFAP+ astrocytes in the hippocampus of <i>Ercc2</i> ^{S737P} het mice, males and females pooled, at 12 months after radiation exposure to 0; 0.063; 0.125 or 0.5 Gy	132
Fig. D.3.5. Quantification of GFAP+ astrocytes in the hippocampus of <i>Ercc2</i> ^{S737P} het mice, males and females pooled, at 18 months after radiation exposure to 0; 0.063; 0.125 or 0.5 Gy	133
Fig. D.3.6. Quantification of GFAP+ astrocytes in the hippocampus of <i>Ercc2</i> ^{S737P} het mice, males and females pooled, at 24 months after radiation exposure to 0; 0.063; 0.125 or 0.5 Gy	134
Fig.D.3.7. Linear Model Analysis: GFAP	135
Fig.D.3.8.a. Dose-dependent radiation effects on astrocyte branching complexity	137
Fig.D.3.8.b. Sholl-analysis of astrocytes	138
Fig.D.3.8.c. 3D-traced structures of exemplary hippocampal astrocytes of sham-, 0.063 Gy-, 0.125 Gy- and 0.5 Gy- irradiated animals 24 months after exposure.	138

List of tables

Table 5.2 List of consumables for immunohistochemistry	43
Table 5.3 List of technical equipments	44
Table 5.5. Stereology parameters	48
Tables D.2.8. Dose-dependent radiation effects on microglial branching complexity.....	127
Table D.3.8. Dose-dependent radiation effects on astrocytic branching complexity	139

Abbreviations

ASR Acoustic Startle Response

ASR/BW Acoustic Startle Response Averaged To Body Weight

⁶⁰Co Cobalt-60

CA Cornus Ammonis

cNHEJ classical non-homologous end joining

DAB 3-3'diaminobenzidine

DCX Doublecortin

DG Dentate Gyrus

DNA deoxyribonucleic acid

DSBs DNA Double Strands Breaks

dB Decibel

ENU N-ethyl-N-nitrosourea

Ercc2 Excision Repair Cross-Complementing Rodent Repair Deficiency, Complementation Group 2

GMC German Mouse Clinic

GFAP Glial Fibrillary Acidic Protein

Gy Gray

het heterozygous

HR homologous recombination

hom homozygous

Iba1 Ionized Calcium-Binding Adapter Molecule 1

INSTRA Integrative Langzeitstudie Zur Wirkung Niedriger Strahlendosen In Der Maus

ICRP International Commission for Radiological Protection

mSv Millisievert

NeuN Neuronal Nuclear Antigen

NHEJ Non-Homologous End-Joining

ns not significant

OF Open Field

PCNA Proliferating Cell Nuclear Antigen

PFA Paraformaldehyde

PPI Prepulse Inhibition

PFC Prefrontal Cortex

RBE Relative Biological Effectiveness

ROS Reactive Oxygen Species

SD Social Discrimination

SSBs single strands breaks

SVZ Subventricular Zone

Sv Sievert

UNSCEAR United Nations Scientific Committee on the Effects of Atomic Radiation

wt wildtype

W_T Tissue Weighting Factor

γ gamma

γ H2AX H2A histone family member X

Abstract

Radiation is naturally present in our environment. Emitted from the soil, from stones, from the sky, humans learned to use this source of energy to produce electricity, to see the structures of our bodies and to treat cancer. While what happens to a human body after exposure to high doses of radiation is well-documented, scientists are still unsure of the health effects of low dose radiation.

To answer this question, the INSTRA project was launched in 2013. This joint research activity studied the late health effects in mice that had received a low dose gamma (γ) radiation exposure early in life. A broad spectrum of investigations was performed, on the molecular (genomics, transcriptomics, proteomics), microscopic (cells and cellular structures) and macroscopic scales (tissues, whole organs and behavior). At the adult age of 10 weeks male and female mice (C57BL/6 x C3HF1) were whole-body irradiated with a range of low doses of γ radiation (0, 0.063, 0.125 and 0.5 Gray, (Gy)) from a Cobalt-60 (^{60}Co) source. Behavioral tests were performed on animals after 4, 12 or 18 months after exposure to check for radiation effects on sensorimotor reflex, spontaneous locomotion, anxiety, olfaction and social memory. In parallel, pathological examinations and organ collection were performed at the corresponding time points to investigate the incidence of tumors and to provide biological samples for study.

To investigate the contribution of genetic predisposition on the consequences of exposure to low dose ionizing radiation, heterozygous (het) mice carrying a recessive mutation (c.2209T>C) in the Excision Repair Cross-Complementing Rodent Repair Deficiency, Complementation Group 2 (*Ercc2*) gene were compared to wildtype (wt) mice. *Ercc2* has a DNA helicase activity and is involved in transcription and DNA repair via its transcribed protein XPD. It had been previously shown that 6 hours after exposure with 1 Gy, lymphocytes from het *Ercc2*^{S737P} mice presented increased H2A histone family member X (γ H2AX) foci compared to the ones from wt mice. Based on that observation, these mice were considered more susceptible to radiation effects and included in the study.

The aim of this thesis was to assess if a single low dose exposure to ionizing radiation in adult mice had any consequences on the behavior and on the cell populations in the brain. Behavioral features were tested at 3 different time points using the open field (OF), the acoustic startle response/prepulse inhibition (ASR/PPI) test and the social discrimination (SD) tests. Animals were sacrificed 24 months after the radiation exposure and their brains collected for immunohistochemistry. The single low dose of ionizing radiation affected adult mouse behavior in the long term. A decrease in ASR at 110 dB (decibels) was visible already at 4 months after exposure whereas decreases in spontaneous locomotor activity and explorative behavior appeared at 12 months after exposure. Whereas a dose of 0.5 Gy

induced decreased performances in ASR, spontaneous locomotion and rearing, a dose of 0.063 Gy induced an increase in ASR and rearing at 18 months post-irradiation, compared to sham-irradiated mice of the same age.

The radiation exposure modified the distribution of neuronal and glial cell populations in the hippocampus. In particular, changes in the different sub-categories of glia were investigated. Quantitative changes in microglial and astrocytic cell number occurred in the dentate gyrus and CA1 of mice at 18 and 24 months after exposure to ionizing radiation.

Surprisingly, a general reduction in microglia with age was observed in all parts of the hippocampus, independent of exposure. A morphological analysis of the microglia at 24 months after exposure indicated that with a dose of 0.063 Gy, microglia showed an increased number of endings, nodes, intersections and length whereas a dose of 0.5 Gy decreased significantly all these parameters. Similarly, a decreased number of endings and nodes and a decreased branch length were observed at 24 months in astrocytes after exposure to 0.125 Gy.

In conclusion, dose-dependent changes in the behavior of adult mice were documented after a single low dose radiation exposure, with some changes seen at a dose as low as 0.063 Gy. The radiation impacted both the neuronal and glial cell populations in the hippocampus, as well as glial morphology, also in a dose-dependent manner. These results are a valuable starting point for future studies addressing different aspects in more detail, such as the long-term molecular changes in the brain after low dose ionizing radiation and the biological differences between exposures to high or low dose radiation.

Zusammenfassung

Strahlung ist in unserer Umwelt natürlich vorhanden. Die Menschen lernten diese Energiequelle zu nutzen, um Elektrizität zu erzeugen, die Strukturen unseres Körpers zu erkennen und Krankheiten zu heilen. Die Wissenschaftler sind sich noch nicht sicher, wie sich Strahlung mit niedriger Dosis auswirkt.

Das Projekt *Integrative Langzeitstudie Zur Wirkung Niedriger Strahlendosen In Der Maus* (INSTRA) widmete sich dieser Frage. Es untersuchte ein breites Spektrum von Geweben, Zellsystemen, biologischen Merkmalen, Genen, Transkripten, Proteinen und Zellstrukturen bis hin zu Organen und Verhaltensänderungen. Im Erwachsenenalter von 10 Wochen wurden männliche und weibliche Mäuse (C57BL/6 × C3H F1) unter einer Co^{60} -Quelle mit niedrigen Dosen von γ -ionisierender Strahlung (0, 0.063, 0.125 und 0.5 Gy) am ganzen Körper bestrahlt. Verhaltenstests wurden 4, 12 und 18 Monate nach Exposition durchgeführt, um die mittel- bis langfristigen Auswirkungen von niedrigen Strahlendosen auf die sensorimotorische Integrationsleistung, Spontanaktivität, Emotionalität, Geruchssinn und Gedächtnisleistung zu betrachten. Zur Untersuchung der zugrunde liegenden Mechanismen strahleninduzierter Effekte fanden zu verschiedenen Zeitpunkten (12, 18 und 24 Monate nach Exposition) pathologische Untersuchungen und Organentnahmen statt.

Um eine potentielle Interaktion von Genotyp und Strahlung zu berücksichtigen, wurden Mäuse mit einer genetisch bedingt erhöhten Suszeptibilität gegenüber Strahlenwirkungen in die Studie eingeschlossen. Diese Mäuse trugen eine rezessive Mutation im *Ercc2*-Gen (c.2209T> C), die zu einem Ser737Pro-Austausch führte. *Ercc2* besitzt eine DNA-Helikase-Aktivität und ist über sein transkribiertes Protein XPD an der allgemeinen Transkription und DNA-Reparatur beteiligt. Lymphozyten von heterozygoten *Ercc2*S737P-Mäusen wiesen 6 Stunden nach Exposition mit 1 Gy *in vitro* im Vergleich zu denen von wt-Mäusen eine erhöhte Anzahl von Strahlenschäden gemessen an γ H2AX-Herden auf. Basierend auf dieser Beobachtung wurden diese Mäuse in die Studie einbezogen.

Ziel dieser Doktorarbeit war es, zu beurteilen, ob eine niedrige Strahlendosis bei erwachsenen Mäusen langfristige Auswirkungen auf das Verhalten und ausgewählte Zellpopulationen des Gehirns hat. Die Mäuse wurden zu 3 verschiedenen Zeitpunkten mit dem Open Field (OF), dem Acoustic Startle Response / Prepulse Inhibition (ASR / PPI) -Test und dem Social Discrimination (SD) -Test getestet. Sie wurden 24 Monate nach Exposition getötet und ihre Gehirne für immunhistochemische Analysen gesammelt. Eine niedrig dosierte ionisierende Strahlung beeinflusste Gehirn und Verhalten auf lange Sicht. Eine dosis-abhängige (0.5 Gy) Abnahme der ASR bei 110 dB war bereits 4 Monate nach Exposition sichtbar, während eine dosisabhängige (0.5 Gy) Abnahme der Spontanaktivität erst 12 Monate nach Exposition auftrat. Interessanterweise hatte die Dosis von 0.063 Gy einen späten positiven Effekt, da sie 18 Monate nach Exposition der natürlichen altersbedingten Abnahme von ASR und Spontanaktivität entgegen wirkte.

In Bezug auf das Gehirn veränderte Strahlung die Anzahl der Neuronen- und Gliazellpopulationen im Hippocampus 24 Monate nach der Exposition. Die Verteilung der verschiedenen Arten von Glia wurde untersucht.

Im Hippocampus (Gyrus Dentatus und CA1-Region des Cornus Ammonis) wurden 18 und 24 Monaten nach der Exposition geringfügige Unterschiede, dosis-abhängigen Veränderungen der Mikroglia- oder Astrozyten-Zellzahlen festgestellt.

Überraschenderweise zeigte sich unabhängig von der Exposition eine Abnahme der Mikroglia mit zunehmendem Alter. Eine morphologische Analyse der Mikroglia ergab, dass Mikroglia nach einer Dosis von 0.063 Gy eine erhöhte Anzahl von Enden, Knoten, Kreuzungen und Länge aufwies, während eine Dosis von 0.5 Gy alle diese Parameter signifikant verringerte. Gleichfalls, ergab eine morphologische Analyse der Astrozyten, dass Astrozyten nach einer Dosis von 0.125 Gy eine signifikant verringerte Anzahl von Enden, Knoten und Länge.

Zusammenfassend, eine einmalige Strahlenexposition mit einer Dosis ab 0.063 Gy das Verhalten erwachsener Mäuse langfristig verändern kann. Nachweisend, Strahlung hat einen quantitativen Einfluss auf die Neuronen- und Glia-Zellpopulationen im Gehirn sowie auf die Mikroglia- und Astrozyte- Morphologie hat. Diese Ergebnisse sind ein wertvoller Ausgangspunkt für künftige Studien, die sich eingehender mit verschiedenen Aspekten befassen, z. B. den langfristigen molekularen Veränderungen im Gehirn nach niedrig dosierter ionisierender Strahlung und den biologischen Unterschieden zwischen hoch oder niedrig dosierter Strahlung.

I. Introduction

1. Exposure to ionizing radiation

1.1. What is ionizing radiation?

Radiation is the emission of energy in the form of electromagnetic waves or moving subatomic particles. At high energies the radiation can interact with atomic nuclei to remove electrons, causing ionization. Ionized atoms have lost electrons of their outer shell and are therefore temporarily positively charged. This allows them to enter into chemical reactions otherwise prohibited by their regular atomic state (Bundesamt für Strahlenschutz).

Among these chemical reactions, radioactive decay is the process of transformation of atomic nuclei into other nuclei while emitting radiation. Radioactivity creates decay products, which could be stable or unstable. These radioactive decay products can further disintegrate. Radioactive substances continue emitting radiation until the last radionuclide has decayed (Bundesamt für Strahlenschutz).

There are four major types of radiation: α -, β -, γ - and neutron radiations, with different origins and properties.

1.2. Where is ionizing radiation present?

Radiation is naturally emitted by radionuclides, which are radioactive atomic nuclei, naturally present in the soil as part of the composition of the Earth's crust. Their presence in the soil also led to radioactive traces in our food (principally isotopes of potassium, uranium, thorium, radium and lead). The decay of organic soil material also produces radioactive radon gas. Radon is an undetectable gas (no colour, odor or flavor) which is released from the ground into the air. Outside Earth, astronauts are affected by cosmic rays emitted by celestial bodies. Most of these cosmic rays nuclei are composed of hydrogen or helium (Bundesamt für Strahlenschutz).

1.3. How ionizing radiation is measured?

Radiation energy can be expressed in Gray (Gy) and Sieverts (Sv).

The Gray (Gy) is used to measure the absorbed dose, which is the energy deposited per unit mass. The absorbed dose provides information on the amount of energy absorbed by an organ or a tissue. 1 Gy is defined as the absorption of one joule of energy per kilogram of matter (J/kg) (IRCP, 2019).

The Sievert (Sv) is used to measure the equivalent dose and the effective dose. The equivalent dose is calculated for individual organs. It is based on the absorbed dose to an organ, adjusted to account for the effectiveness of the type of radiation. The effective dose is calculated for the whole body, after performing the addition of equivalent doses to all organs, each adjusted to account for the sensitivity of the organs to radiation. The Sv

represents the biological effect of the deposition of a joule of radiation energy in a kilogram of human tissue (IRCP, 2019).

The conversion from Gy to Sv requires information on the biological effect of the different radiation forms. The conversion therefore takes into account the type of tissue irradiated and the type of radiation energy. Information on the type of tissue irradiated is included on the tissue weighting factor W_T , which is the fraction of the overall health risk, resulting from uniform whole body irradiation, attributable to specific tissue T. The different types of radiation energy (α -, β -, γ - and neutron) penetrate differently into biological tissues and lead to different biological risks (IRCP, 2010).

Other factors important for measurements are the dose rate, which is the delivered dose divided by the time of exposure (Gy/min), and the cumulative dose, which is a total dose resulting from repeated or continuous exposures to ionizing radiation.

The main factors influencing biological response are total absorbed dose and dose rate. Other factors include distribution of the radiation sources and structure and dimensions of the biological targets (Vaiserman et al., 2018). One indicator of the biological effect of radiation is the relative biological effectiveness (RBE). It is defined as the ratio of biological effectiveness of one type of ionizing radiation relative to another, given the same amount of absorbed energy. Values of the RBE vary with the dose, dose rate, and biological endpoint considered (IRCP, 2003).

1.4. What is a low-dose radiation?

It is known that exposure to “high”-dose or “low”-dose ionizing radiation causes different biological effects and therefore leads to different health consequences. The meaning of “high” or “low”-dose does not only refer to the actual given number, but also the intensity of the biological effect caused by the exposure to this dose. Estimation and classification of the biological effects provoked by “low”-dose exposure is difficult and does not lead so far to a clear definition.

A comparison of the effects of different dose ranges of ionizing radiation could be found on the website of the United Nations Scientific Committee on the Effects of Atomic Radiation (UNSCEAR). It mentions at doses below 10 mGy, no direct evidence of human health effects (including on an unborn child) has been found. This precision about the effect of radiation on fetuses refers to the fact that children are known to be more vulnerable than adults to ionizing radiation (Bakmutsky et al., 2014; Casciati et al., 2016). This vulnerability is correlated with the increased number of progenitor cells present in developing tissues, where the less condensed DNA is more vulnerable to cellular aggression (Fukuda et al., 2005).

At exposures of between 10 mGy and 1 Gy, no acute effects have been found but increased incidence of certain cancers was observed in exposed populations at higher doses. Between

1 and 10 Gy, irradiated subjects start to suffer from radiation sickness, with the risk of death and increased incidence of certain cancers in exposed populations appears (UNSCEAR, 2017). So for the UNSCEAR, doses below 10 mGy would be considered as very low doses, because of the lack of evidence of human health effects. Low doses would start above 10 mGy.

The previous information can be compared with the ones provided by the German Commission on Radiation Protection (SSK). This commission has adopted a level of below 100 mGy as being a low dose range for purposes of cancer risk (SSK, 2007). Legislation suggests low doses are in the order of 10 to 100 mGy (Ruhm et al., 2018). Doses below 10 mGy were shown to induce merely background effects (Shimura and Kojima, 2018). The doses used in this study are ranging from 0 to 500 mGy, which classify them in the low-to-moderate dose range.

To provide an order of magnitude, for natural sources, annual dose vary from 0.2 to 1 mGy from terrestrial and ingested sources as well as cosmic rays and up to 10 mGy from radon gas. From external sources, a subject would be exposed to 0.03 mGy during a 10-hours airplane flight, 0.05 mGy during a chest X-ray and up to 10 mGy during a computer tomography scan (CT). As a reference, the annual limit for professional exposure in Europe is 20 mGy.

2. Damages caused by ionizing radiation

2.1. Direct damages

2.1.a. Double strands breaks (DSBs)

As mentioned earlier, ionizing radiation can penetrate biological tissues. The energy it carries induces local ionization of large target molecules such as DNA and the generation of reactive oxygen species (ROS) when the predominant cellular constituent, water, is hit (Desouky et al., 2015). DNA ionization lead to the disruption of the DNA strands by damage to the bases at the phosphate backbone, which induces DNA damage. DNA damage, in particular double strands breaks (DSBs) can lead to cell death but in unrepaired surviving cells can also lead to carcinogenesis. Direct collision between a high-energy particle or photon and a strand of DNA breaks the phosphodiester backbone and creates DSBs. (Cannan and Pederson, 2016).

DSBs will be recognized by sensors such as Ku, MRE11 complex and Parp1, leading to a signal transduction sent by the protein ATM in order to elicit either DNA repair, cell cycle arrest, apoptosis or senescence. The number of DSBs tends to decrease over time, as they are repaired by DSBs repair mechanisms, such as classical non-homologous end joining (cNHEJ) and homologous recombination (HR) (Nickoloff et al., 2017).

Briefly, cNHEJ joins DNA ends by ligation and does not require a homologous repair template. DSBs are recognized by Ku70-80. The binding of the ends is performed by the MRE11 complex, DNA-PK, 53BP1 and γ H2AX and additional DNA damage repair factors. The protein Artemis finalizes the end processing with additional nucleases and polymerases such as XRCC4-Ligase IV-XLF (Deriano and Roth, 2013). cNHEJ may occur in all cell-cycle phases (Willers et al., 2004).

A contrario, a complete template molecule with a homologous DNA sequence is necessary for the repair of DSBs by HR. It is usually present on the sister chromatid in the S and G2 phases of the cell cycle, and therefore restricts the execution of HR to these phases. The MRN complex resesects the broken DNA ends with the help of proteins and exonucleases, generating single-strand DNA. The tail is coated by a replication protein, which is then replaced by RAD51 via the mediation of BRCA2. The formed nucleoprotein filament will search for the homologous sequence on the sister chromatid. The DNA strand is then extended using the complete sequence as template. After restoration of the lost sequence information, junctions are resolved (Brandsma and Gent, 2012). HR is a critical pathway of DSBs repair after exposure to ionizing radiation as it is virtually error-free.

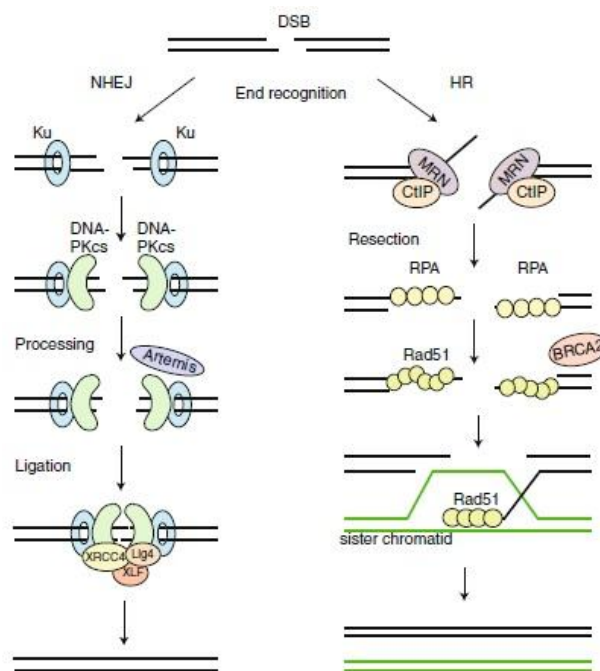


Fig.2.1.a. NHEJ and HR pathways for the repair of DSB. DSB: Double Strands Breaks, NHEJ: Non-Homologous End Joining, HR: Homologous recombination, DNA-PKcs: DNA dependent protein kinase, XRCC4: X-Ray Repair Cross Complementing Protein 4, Lig4: DNA Ligase 4, XLF: XRCC4-Like Factor, MRN (complex): Mre11+Rad50+Nbs1, RPA: Replication Protein A, BRCA2: Breast Cancer type 2 susceptibility protein. Adapted from Brandsma and Gent, 2012.

2.1.b. Reactive oxygen species

Another type of damage occurs when radiation hits the water molecules present in the cellular cell components, producing reactive oxygen species (ROS), also called free radicals. The impaired electron in their structure is especially reactive and can interact with DNA molecules to induce structural damages. For example, reactive oxygen species such as $O_2^{\bullet-}$, $^{\bullet}OH$, H_2O_2 , RO_2 , and $ROOH$ can induce lipid peroxidation and protein inactivation (Azzam et al., 2012).

Through the excess production of ROS and the consecutive alteration of the cellular redox environment, ionizing radiation can disrupt mitochondrial functions, causing mutations of the mitochondrial DNA and interferences in the signaling pathways (Leach et al., 2001; Spitz et al., 2004).

Protective mechanisms against reactive oxygen species include intracellular antioxidant enzymes, in particular the manganese superoxide dismutase (MnSOD)(Sun et al., 1998). Other protective molecules are scavengers, which are a group of antioxidant substances reacting with reactive oxygen species and thus deactivating them (Múčka et al., 2018).

Radiation-induced oxidative stress may spread from targeted cells to non-targeted bystander cells through intercellular communication mechanisms (Burdak-Rothkamm and Rothkamm, 2018).

2.2. Indirect damages

Radiation is also known to cause so-called bystander effects. Neighboring non-irradiated cells around the irradiated target zone start to show effects as a result of the signals received by the irradiated cells. These non-irradiated cells may respond with changes in process of translation, gene expression, cell proliferation, apoptosis and cell death. Bystander effects include free radicals, immune system factors, expression changes of some genes involved in inflammation pathway and epigenetic factors (Najafi et al., 2014).

In particular, the authors relate bystander effects in non-irradiated tissues to production in lymphocytes and macrophages of elevated levels of cytokines (IL-1, 2, 6, 8, $TNF\alpha$, $TGF\beta$) which lead on one side to production of nitric oxide and consecutive oxidative stress response and in the other side to mutations and chromosomal damages. They also theorize that bystander effects could have a radioprotective goal as it triggers mechanisms leading to the removal of cells indirectly affected by irradiation, preventing carcinogenesis.

3. Effects of unrepaired damages consecutive to exposure to ionizing radiation

Cellular aggression by DNA damage and ROS consecutive to radiation exposure can lead to cancer and non-cancer health effects. Non-cancer health effects differ greatly in the shape of the dose–response curve, latency, persistency, recurrence, curability, fatality and impact on quality of life (Hamada and Fujimichi, 2014). Such diverse effects were divided by the International Commission on Radiological Protection (ICRP) into stochastic effects (cancer and heritable effects) and tissues reaction (formerly termed deterministic effects).

3.1. Stochastic effects

“stochastic” is a term meaning “of a random or statistical nature”. Stochastic effects occur by chance and may occur without a dose. Their probability is proportional to the dose and their severity is independent of the dose. Cancer and hereditary effects are assigned to this category. Stochastic effects have been supposed to result from DNA damage to a single cell or small number of cells (Hamada and Fujimichi, 2014) followed by a clonal expansion of cells with a growth advantage.

From the Life Span Study of survivors of the atomic bombings in Japan in 1949 and long-term following of cohorts of radiation workers exposed to prolonged low-dose exposure, there are epidemiological evidences of increased cancer risk after exposure to low-dose radiation. Authorities consider that there is an increase in risk to health proportionate to the radiation dose received down to the very lowest levels. This consideration led to the conception of the Linear Non-Threshold Model (LNT).

A series of developments from 1954 through 1972 marked the transition to adoption of the LNT model as a predictive model of radiation injury in exposed populations (Kate-Louis D. Gottfried and Gary Penn, 1996). The base for the LNT model is assuming that there is no lower threshold for the start of stochastic effects and that the dose-response relationship between dose and stochastic health risk is linear. In other words, the LNT model assumes that radiation has the potential to cause harm at any dose level. In addition, it assimilates the stochastic health effect of cumulative exposures to the risk caused by a single exposure with equal absorbed dose value.

But one can question if extrapolating low-dose risk from high-dose risk model is appropriate. Over the years, several studies showed that molecular and cellular mechanisms after low dose radiation exposure actually differ from the ones observed at high doses.

Notably, the existence of protective pathways against deleterious effects of DNA damages after irradiation was brought up, such DNA repair pathway, cell cycle control, apoptosis and a transcriptional response. Dysfunction of the detection and the repair system by these pathways after excessive DNA damage could either lead to programmed cell death and proliferation or to accumulated genetic damage which is one factor of carcinogenesis (Mullenders et al., 2009).

3.2. Non-stochastic/deterministic effects/tissues reaction

Non-stochastic effects can be defined as effects which whose severity is proportional to dose but where there is a threshold. These effects are damages resulting from the collective injury of cells in affected tissues. The dose at which these damages occur depends on the sensitivity of methods for detecting the damage. The time at which this non-stochastic effect can be detected depends on the evolution of the injury through time, which varies with the speed of repair or injury progression (Hamada and Fujimichi, 2014).

Based on the fact that radiation-induced apoptosis is a stochastic process, the term ‘non-stochastic effects’ was deemed unsuitable for injuries resulting from the death of a large number of cells. It was further thought that although the initial cellular killing is random, the large number of cells involved in the initiation of a clinically observable non-stochastic effect gives the effect a deterministic character. Thus, ‘non-stochastic’ was replaced with ‘deterministic’, defined to mean causally determined by preceding events (Hamada and Fujimichi, 2014).

Deterministic effects are more recently referred to as tissue reactions because these effects are not determined at the time of irradiation and can be altered by the use of various biological response modifiers. Tissue reactions were defined as injury in populations of cells characterized by a threshold dose and an increase in the severity of the reaction as the dose is increased further (Hamada and Fujimichi, 2014).

In non-stochastic effects can be included cataracts, non-malignant skin damage (erythema), hematologic syndrome, gastro-intestinal syndrome (involved in radiation sickness) and effects on the central nervous system (Bolus, 2017).

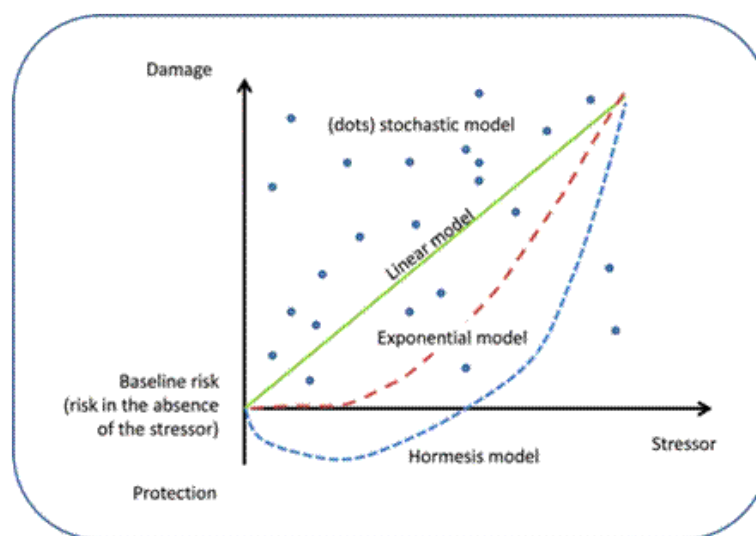


Fig.3.2. Possible dose-response relationships for biological risks after low-dose radiation exposure (adapted from *Eur Heart J*, Volume 33, Issue 3, February 2012, Pages 292–295)

Non-stochastic effects occur seconds, minutes or hours after exposure whereas stochastic effects such as cancer can occur years or decades after exposure and have long-lasting consequences, notably on the offspring. If non-stochastic effects can be directly traced to ionizing radiation exposure, it is more difficult to evaluate the role played by this exposure in the apparition of cancer since genetic predisposition and environmental factors are also important risk factors (Barnett et al., 2009).

For low doses, between 10 and 100 mGy, scientific evidences identify a possible threshold for biological effects and a possible adaptive response after exposure.

4. Threshold for biological effects

Thresholds for biological risks caused by ionizing radiation are updated regularly by the International Commission on Radiological Protection (ICRP). As an overview, the ICRP Publication 118 published in 2012 stated that the absorbed dose threshold for the lens and for circulatory disease (concerning the heart or the brain) is now 0.5 Gy. This dose is also the acute threshold dose for depression of haematopoiesis. 0.5 Gy may lead to approximately 1% of exposed individuals developing cardiovascular or neurological diseases, more than 10 years after exposure. The acute threshold dose is higher for intestinal irradiation and lung diseases, namely 6 Gy and 6.5 Gy. The threshold dose for the human kidney is approximately 7–8 Gy acute dose.

To sum up, the acute thresholds for each organ are very different. This can be related to the different cellular compositions and structures of the tissues of each organ and their variable sensitivities to ionizing radiation. In addition, it is unclear from available evidence whether or not the threshold is the same for acute, fractionated, and chronic exposures.

5. Adaptive responses

As an environmental stressor, radiation can trigger adaptive responses. Following a first dose of radiation (prime dose), reduced biological effects can be observed when a second higher dose of radiation is administered. The mechanisms behind this adaptive response are transcriptional modulation (which involves reactive oxygen species) of specific gene sets (Tapio and Jacob, 2007). It is important to note that adaptive responses are showing a high degree of inter- and intra- individual variability and the role of each factor involved in the trigger, control and efficacy of this response is still unclear.

As we saw, several cellular and molecular mechanisms are observed after radiation exposure but so far no evidence allows us to decide which model is actually more faithful to reality. Cellular in-vitro studies and transgenic mouse models allowed us identify key proteins and genes involved in this response. However, providing a complete explanation for complex biological changes observed after radiation exposure such as cognitive decline is especially challenging. Cognition involves multiple pathways, ranging from molecular mechanisms at synaptic level to cellular neurotransmission. The only way to reach a satisfying answer would be to investigate the effects of radiation on each of these elements.

6. Effects of unrepaired damages caused by ionizing radiation on the brain

6.1. Brain development and neurogenesis

Radiation is particularly damaging for mitotic cells between G2 and S phase (Betlazar et al., 2016) because during these phases of the cellular cycle, the DNA is decondensed and therefore more susceptible to be damaged. The brain was considered relatively resistant to radiation because of its low mitotic activity. Tissue weighting factor W_T , used to calculate biological risk, is 0.01 for the brain, which is much lower for example than for the proliferative bone marrow (0.12), which is a tissue with a high mitotic activity.

Mitotic activity in the adult brain, where neurogenesis happens, is mostly present in the subventricular zone and the dentate gyrus of the hippocampus. It is called “adult neurogenesis” to distinguish it from embryonic neurogenesis, which occurs at high levels during early development (Eriksson et al., 1998; Gage, 2000). In spite of its low levels, the rate of adult neurogenesis influences emotionality, learning and memory, supports repair processes and brain plasticity and is sensitive towards ionizing radiation (Mizumatsu et al., 2003). Damage inflicted to adult neurons going through neurogenesis by ionizing radiation exposure can therefore induce long-term consequences.

It was shown in recent studies that the brain is indeed sensitive to irradiation. Patients treated with cranial radiation therapy reported cognitive decline, memory deficits and fatigue as undesirable effects (Makale et al., 2016). Extent and severity of these effects on the brain depends on the dose.

6.2. Brain regions

It was shown that in the brain, radiation effects are age-, brain region-, and sex-specific (Koturbash et al., 2011; Hua et al., 2012; Casciati et al., 2016). Among the brain regions, the prefrontal cortex (PFC) and the hippocampus are considered the most sensitive to irradiation. The reasons for these observations is that the hippocampus is one of the 2 active sites of neurogenesis in the adult mammalian brain, the other one being the olfactory bulb (Gage, 2000). The proliferation of neuronal precursors in the subgranular zone of the dentate gyrus generates cells that migrate further to the granule cell layer and differentiate into mature neuronal and glial phenotypes. Adult neurogenesis is well-known to support learning and memory processes. As mitotic cells are particularly sensitive to radiation, damages to the dentate gyrus after exposure can be counted as possible reasons for behavioural changes. The PFC is a key regulatory region that collects inputs from all other cortical regions and then plans and directs an array of motor, cognitive, and social

behaviours (Kovalchuk and Kolb, 2017). In the same way as for the hippocampus, damages to the PFC after exposure could possibly lead to behavioural changes.

6.3. Behavior

6.3.a. Acoustic Startle Response

The ASR is defined as a quick contraction of the muscles of the body and the face after an unexpected and intense acoustic stimulus. It is reported to exist in many species mammals and is probably a protective mechanism. An amplitude greater to 80 dB is necessary to elicit ASR in the mouse. It has a brief latency (5-10 ms). The circuit mediating the ASR starts in the cochlea and travel through the auditory nerve to the ventral cochlear nucleus, the dorsal nucleus of the lateral lemniscus, the caudal pontine reticular nucleus, spinal interneurons and spinal motor neurons. These elements were identified through lesions studies in rodents (Hammond, 1973; Leitner et al., 1980).

If a non-startling stimulus is presented 30 to 500 ms before the occurrence of the ASR, the amplitude of the startle pulse decreases. This phenomenon is named prepulse inhibition (PPI) and is considered an example of sensorimotor gating. The logic behind the PPI is that the repetition of an auditory stimulus reduces its value as a signal for a potential threat so the body reaction towards this stimulus will decrease in intensity as there is no justified need for a fight-or-flight response. If the PPI does not occur, or at a reduced level compared to the wildtype control, this might be indicative of a deficit in central nervous system gating mechanisms which are involved in processing of sensory informations (Koch and Schnitzler, 1997). Alterations of the PPI were found in patients suffering from neuropsychiatric disorders (Braff et al., 1978; Swerdlow et al., 1994).

Radiation exposure was shown to induce alterations of the ASR. A study in 1989 showed that rats exposed to a partial fractionated brain irradiation of 13 Gy during the first 16 days post partum presented a 91% reduction of granule cells in the hippocampal dentate gyrus as well as a consistently higher startle response amplitude. These animals with hippocampal damage failed to habituate to the startle stimulus and under certain circumstances showed potentiated startle responses after many tone presentations (Mickley and Ferguson, 1989).

More recently, in a study in 2002, C57BL/6 mice, 8 weeks of age, were exposed, either with or without 15-g/cm² aluminum shielding, to 0-, 3-, or 4-Gy proton irradiation, mimicking features of a solar particle event. Short-term habituation of the acoustic startle response exhibited a dose-related reduction in magnitude, which was observable during the 1st week of startle testing (Pecaut et al., 2002).

A study in 2012 characterized the effects of gamma and proton irradiation on acoustic startle in mice exposed to 0 to 5 Gy- partial brain irradiation, and assessed these effects 2 days later. Radiation reduced the startle response at 2 and 5 Gy. Following a 2-Gy exposure, the response reached a minimum at the 2-day point. Proton and gamma ray exposures did not differ in their impact on startle. No effects of radiation on pre-pulse inhibition of the startle response were observed (Haerich et al., 2012)

6.3.b. Open field test

The open field test evaluates spontaneous locomotor activity and spontaneous exploration as well as anxiety. This test is based on conflicting innate tendencies of avoidance of bright light and open spaces (that ethologically mimic a situation of predator risk) and of exploring novel environment.

Radiation exposure was shown to induce alterations in the parameters of the open field test. A study in 2013 investigated the short-term impact of low-dose ionizing radiation on mouse behaviour and neuro-immunity using male CD-1 mice whole-body irradiated with 0.5 Gy or 2 Gy of gamma or proton radiation. Gamma radiation was found to reduce spontaneous locomotor activity by 35% and 36%, respectively, 6 h post irradiation. In contrast, the motivated behaviour of social exploration was not impacted by gamma radiation (York et al., 2012). The study described earlier by Pecaut et al. 2002 showed that long-term (>2 weeks) indirect deficits in open-field activity appeared in mice after exposure to 3- or 4- proton radiation.

6.3.c. Social discrimination test

This test evaluates olfaction and social recognition memory. Both functions are complementary in rodents, since mice rely on the sense of olfaction to recognize social and mating partners (Zou et al., 2015). Current studies on social olfactory behavior in rodents after radiation exposure do not agree on the results. A study in 2014 showed that male Long-Evans rats exposed to head-only X-ray radiation (2.3 Gy at a dose rate of 1.9 Gy/min) did not show a significant alteration of the social odor recognition memory (Davis et al., 2014).

Another study in 2018 tested social recognition memory 3 months after a single dose of 5 Gy of X-rays at a rate of approximately 110 cGy/minute with an energy beam of 160 kVp/25 mA in male and female mice at 4 weeks of age. Long-term radiation-induced impairment in odor recognition memory was observed. Sex-differences were present, with males showing greater exploration of social odors than females. General exploration was not affected by irradiation. Irradiated males had impaired odor recognition memory in adulthood, compared to controls. Female olfactory recognition memory was dependent on estrus stage. Histological evaluation of olfactory neurogenesis suggested a reduction after radiation

exposure versus control and imaging analyses showed that the majority of brain regions were reduced in volume after exposure but more specifically, the amygdala and the piriform cortex, in males but not females, paralleling olfactory recognition findings (Perez et al., 2018).

6.4. Effect of high-dose radiation exposure on the brain

It was shown that acute radiation of the brain of humans and animals led to apoptosis, brain inflammation, loss of oligodendrocyte precursor cells and of myelin sheaths, and to irreversible damage of neuronal stem cells with long-term consequences on adult neurogenesis (Marazziti et al., 2012). Thus, ionizing radiation can potentially affect mood, learning, repair, plasticity, memory and olfaction, which in turn are biomarkers for early stages of neurodegenerative diseases.

The main responses of the central nervous system to high doses of ionizing radiation are excess production of ROS, oxidative stress damage and neuroinflammation (Betlazar, 2012). High doses of ionizing radiation (>1 Gy) can reduce also the number of newly differentiated cells by increasing DNA damage and promoting cell cycle arrest (Mizumatsu et al., 2003). On the molecular level, exposure to high dose ionizing radiation was shown to increase the production of key apoptotic proteins such as cytochrome-c, caspase-3 and to decrease expression of anti-apoptotic Bcl-2 (Saeed et al., 2014). Pro-inflammatory cytokines such as TNF- α , IL-1 β and IL-6 and lipid peroxidation markers were also upregulated. Deng et al. (2012) demonstrated the importance of the MAPK MEK/ERK1/2 signalling cascade in mediating the responses of microglia after high dose irradiation (Deng et al., 2012). High doses also promote apoptosis of endothelial cells in the brain, thereby causing microvascular damage and possibly disruption of the blood brain barrier (d'Avella et al., 1992). Cognitive decline in patients after clinical exposure to high dose irradiation (e.g in the context of brain radiotherapy) has led to a research focus on the hippocampal microenvironment and its population of mature cells and proliferating progenitor cells in the subgranular zone of the dentate gyrus (Makale et al., 2016).

6.5. Effect of low-dose radiation exposure on the brain

If the impact of high dose ionizing radiation on the brain is clear, the impact of low dose ionizing radiation on the brain is more complex. The ambiguity on the effects of low dose ionizing radiation has been acknowledged in recent reviews (Betlazar et al., 2016; Tharmalingam et al., 2019).

Results from transcriptomics studies performed on mouse brain tissue after whole body irradiation showed that an exposure to 0.1 Gy does not induce the same genes than an exposure to 2 Gy. These pathways contained mostly down-regulated genes involving ion

channels, long-term potentiation and depression, vascular damage. Nine neural signaling pathways were identified in both low-dose irradiated mouse brain tissue, unirradiated aging human brain and brain tissue from patients with Alzheimer's disease (Lowe et al., 2009).

The effects of chronic low-dose radiation were also studied on cultured human neural progenitor cells (hNPCs). After irradiation with 31 mGy, alterations were observed on interferon signaling and cell junction pathways, related to inflammatory processes. After 124 mGy, the researchers observed effects on DNA repair and cell adhesion molecules. By 496 mGy, changes on DNA synthesis, apoptosis, metabolism and neural differentiation were present (Katsura et al., 2016). So the effects of chronic low-dose radiation are variable in intensity and variety with the dose.

So in principle, exposure to even low radiation doses in adulthood could increase the risk for the development of neurodegenerative diseases in the long term, potentially by inducing neuroinflammation, oxidative stress and mitochondrial dysfunction, which are all considered contributing factors to neurodegenerative diseases (Mosley et al., 2006; Verri et al., 2012; Kempf et al., 2014).

If deleterious effects of chronic low-dose exposures have been shown, low dose ionizing radiation has also been found to stimulate molecular and cellular protective mechanisms such as antioxidant activity (Yamaoka et al., 1994) and enhanced immune system (Cui et al., 2017). Radioadaptive dosing was observed, where a first exposure to a low dose can reduce vulnerability to higher ones (Otsuka et al., 2006). The ambiguity on the effects of low-dose radiation exposure therefore remains and needs to be elucidated.

7. Ercc2^{S737P} biology

An important factor to take in consideration for biological risk evaluation after radiation exposure is the genetic background. Impaired DNA replication and greater sensitivity to ionizing radiation can occur through genetic mutations affecting components of the HR pathway (Thompson and Schild, 2001; Powell and Kachnic, 2003). Other genes could be also involved, such as ERCC2/XPD (Kunze et al., 2015). ERCC2 is well known as DNA helicase and involved in DNA repair (Fuss and Tainer, 2011). This gene belongs to the family of genes whose mutations lead in homozygotes to various forms of Xeroderma pigmentosum, here complementation group D. This well-known clinical trait is characterized by major UV-sensitivity of the skin; UV irradiation leads frequently to skin cancer. The study by Kunze et al. in 2015 showed that lymphocytes of heterozygous ERCC2 mice showed higher number of H2AX foci 6 hours after exposure to 1 Gy, showing that ERCC2 could be considered as potential candidate for gene-related radiation sensitivity.

8. Importance of the research

A clear definition of low doses and of their long-term consequences on health is necessary. Between 1987 and 2006 in the United States, medical radiation exposure almost doubled. The same tendency occurred in Europe. In Germany in 2008, medical radiation represented half of the total average public radiation exposure (Abbott, 2015). This increased exposure is due to the improvement of X-ray technologies, making them the first tools for diagnostics. In addition, cancer is now the second leading cause of death globally and is responsible for an estimated 9.6 million deaths in 2018 (World Health Organization, 2018). Most cancer patients will go through radiotherapy and it is necessary to research the consequences of long term exposure to design safer and more efficient treatments. A number of professionals such as radiologists, interventional cardiologists and flight attendants are exposed daily to ionizing radiation (Sanchez et al., 2014; Alvarez et al., 2016; Mohammadi et al., 2017) and this can impact their health at an older age.

Nuclear reactors are used since the last 50 years as a source of electrical power. Some countries rely heavily on this technology, making research important to guarantee the health safety of the workers. Some countries decided to stop its usage, raising the question of decontamination. After the Fukushima Daiichi nuclear disaster in 2011, former residents decided to return to live in the surroundings. Studies on the effects of the remaining radiation on the population, especially on children, are directly relevant to understand the long term health effects of low dose ionizing radiation (Matsuo et al., 2019).

Since the second half of the 20th century, plane travel became part of our daily life. Each journey involves exposure to low dose ionizing radiation, from X-rays security control to cosmic rays. Studies have been done on frequent flyers (Alvarez et al., 2016). Multiple studies on the health effects of cosmic rays on astronauts are currently running because of the high expectations connected with Martian exploration (Arena et al., 2014; Acharya et al., 2017; Krukowski et al., 2018). Researching the effects of low dose ionizing radiation is important because it is present in several aspects of our daily life and its effects on health are not yet clearly understood.

Low dose rate radiation exposure is also especially important in the context of public radiation protection. Epidemiologic studies failed to show consistent biological effects under 100 mSv but it is not sufficient to conclude that these doses are harmless. Some areas in the world such as Ramsar in Iran, Kerala in India, Yangjian in China and Guarapari in Brazil have natural high level of background radiation (in some cases higher than 100 mSv/year) and it is unclear how this exposure affects the health of the inhabitants on the long-term (Hendry et al., 2009). Closer to us, Bavaria is one of the regions of Germany with high level of radon gas. Studies are still running on the long-term effects of indoor radon exposure, in particular increased lung cancer (Stanley et al., 2019).

9. Unresolved questions

The effects of low dose ionizing radiation are not clearly defined yet. First of all, there is evidence that shows the existence of a dose marking the limit between harmless and detrimental effects (Chien et al., 2015). Interestingly, scientists showed that high doses and low doses of radiation do not activate the same molecular pathways (Lowe et al., 2009). But so far, there is no clear number defining this dose.

The genetic background of the irradiated subject and the dose rate of the radiation can influence the biological results (Kunze et al., 2015; Ruhm et al., 2018). Genetic mutations impacting players of the HR pathways such as ATM or XRCC2 can act as a sensitizing factor to ionizing radiation. Dose-rate of the radiation exposure is an important factor for risk calculation since acute or chronic exposure will not induce the same consequences.

It is also unclear how low-dose radiation is affecting each of our organs. If some tissues with high mitotic contents such as the bone marrow or the gonads are known to be particularly vulnerable to radiation, the question remains for other vital organs. Are the mechanisms of action and the threshold dose similar for each organ or do they vary? How are the possible variations related to the function of each organ? Epidemiological studies are trying to answer these questions (Azizova et al., 2019) but no study has so far assessed the effect of low-dose radiation in its globality.

In particular, for studies researching the effect of low-dose radiation on the brain, rodent studies have been conducted either with young animals, when mitotic activity and therefore radiation sensitivity is higher due to ongoing developmental processes, or with moderate instead of low doses, and the period of observation for delayed radiation effects on brain or behavior was at maximum 6 or 12 months. A study with an adult animal model, using a comparative range of low doses of ionizing radiation and assessing the behavioral, cellular and molecular changes during the remaining lifetime of the irradiated animal, is therefore needed.

II. Aims of the study

1. Research questions

This project addresses the lack of clarity about the definition of low dose ionizing radiation and its effects on health. A collaborator previously assessed cognitive defects in neonatally irradiated mice and studied the molecular mechanisms behind these changes (Kempf et al., 2014). As a next step, it was planned to study the effect of low dose ionizing radiation on young adults in a mouse model. The aim of this thesis was to understand the impact of low dose radiation exposure on brain and behavior in adult mice and whether it causes alterations that could increase the risk for developing neurodegenerative diseases.

2. Objectives

The first objective of this thesis was to assess if exposure to low dose ionizing radiation was affecting adult mouse behavior or not. If changes were visible after exposure, it was important to determine which behavioral parameters were affected, at which dose level and how it interacted with factors such as genotype, sex and time after exposure. The second objective of this thesis was to investigate cellular changes after exposure, using mouse brain samples (1 hemisphere/animal). The samples were treated to be used for immunohistochemistry analyses. The final objective was to reflect on the connection between behavioral and cellular changes, in order to provide a possible explanation for the changes observed after exposure.

3. Hypotheses

It was hypothesized that low dose radiation at levels below those actually recommended for occupationally exposed individuals (<20 mGy/year) would be able to provoke long-lasting cellular changes in the brain that would be sufficient to influence behavior. The second work hypothesis was that an heterozygous point mutation of the ERCC2 gene would enhance the brain response to low-dose radiation exposure.

III. Materials and Methods

1. Animals

1.1. F1 hybrid C57/C3H mice

F1 hybrids of C57BL/6JG female and a C3HeB/FeJ male mice were used as wildtype; F1 hybrids of a wild-type C57BL/6JG mother and a homozygous *Ercc2*^{S737P} father on C3HeB/FeJ background (Kunze et al., 2015) were used as heterozygous *Ercc2*[±] mutants. This breeding schedule was chosen because the recessive *Ercc2*^{S737P} mutation on the C3H strain background suffers from a recessive retinal degeneration caused by a mutation in the *Pde6b* gene (Pittler and Baehr, 1991). Importantly, these mice are also het for the two parental strains (F1 hybrids), thus keeping the genetic background comparable. 560 mice were used in total, 280 wt and 280 mutant mice.

Mice were maintained under specific pathogen-free conditions at the Helmholtz Center Munich and housed in the German Mouse Clinic, under controlled light, temperature and diet. The use of animals was in strict accordance with the German Law of Animal Protection and the tenets of the Declaration of Helsinki. The study was approved by the Government of Upper Bavaria (Az. 55.2-1-54-2532-161-12).

1.2. *Ercc2*^{S737P} heterozygous mice

The *Ercc2*^{S737P} mouse mutation was identified during a *N*-ethyl-*N*-nitrosourea (ENU)-mutagenesis screen in the German Mouse Clinic (GMC; Munich, Germany). For further detailed information, see Kunze et al. 2015. The mutation is recessive. Homozygous mutant animals show reduced coat, small eyes, lamellar cataract and females are sterile. The mutation was mapped to chromosome 7 between the markers 116J6.1 and D7Mit294. Using exome sequencing, c.2209T>C point mutation was identified in the *Xpd/Ercc2* gene leading to a Ser737Pro exchange (Kunze et al., 2015). *Ercc2* is a DNA helicase involved in nucleotide excision repair (NER). Mutations of the ERCC2 gene in humans, responsible for the transcription of the XPD protein, are associated with a spectrum of diseases characterized by increased photosensitivity due to impaired DNA repair mechanisms, and in some cases developmental and cognitive deficiencies (Manuguerra et al., 2006). Cataracts were observed only in homozygous animals. For linkage analysis, genotyping of a genome-wide mapping panel consisting of 153 single nucleotide polymorphisms (SNP) was performed using MassExtend, a MALDI-TOF (matrix-assisted laser/desorption ionization, time of flight analyzer) mass spectrometry high-throughput genotyping system supplied by Sequenom (San Diego, CA, USA) (Klaften and Hrabé de Angelis, 2005).

2. Irradiation

At the age of 10 weeks (\pm 10 days), groups of 16-20 mice (littermates, 7-12 wt and het, male and female) were whole-body irradiated by doses of 0, 0.063, 0.125 and 0.5 Gy (dose rate 0.063 Gy/min; ^{60}Co source, Eldorado 78 teletherapy irradiator, AECL, Canada); the sham-irradiated animals (0 Gy) had the same treatment but without dose (sham radiation).

3. Behavioral tests

Three behavioral tests were performed at 4, 12 and 18 months after exposure: the open field test, the acoustic startle test, the social discrimination test. All three tests are widely used tests for assessing behavior in mice. The methodology presented here are established methods used in the German Mouse Clinic (GMC) in Munich.

These three tests were performed successively over a timespan of three weeks for each of the mentioned time points. After 24 months (from the irradiation), the experiment was terminated and four mice of each group were taken for organ sampling. To obtain data at earlier time points, additional groups of 16 males and females, wt and mutant were irradiated; 4 mice of each group were killed at two different time points (12 and 18 months after radiation). The different cohorts were prepared between May 2013 and February 2016; a half of the cohort was composed of sham-irradiated animals to minimize possible seasonal effects. All behavioral testing groups included an equal number of males and females, wt and mutant, irradiated and non-irradiated animals. Each tested animal was coded, to avoid bias in the data analysis. The same experimenter (J. Einicke) performed all testing rounds (1 testing round included all 3 tests and lasted 3 weeks).

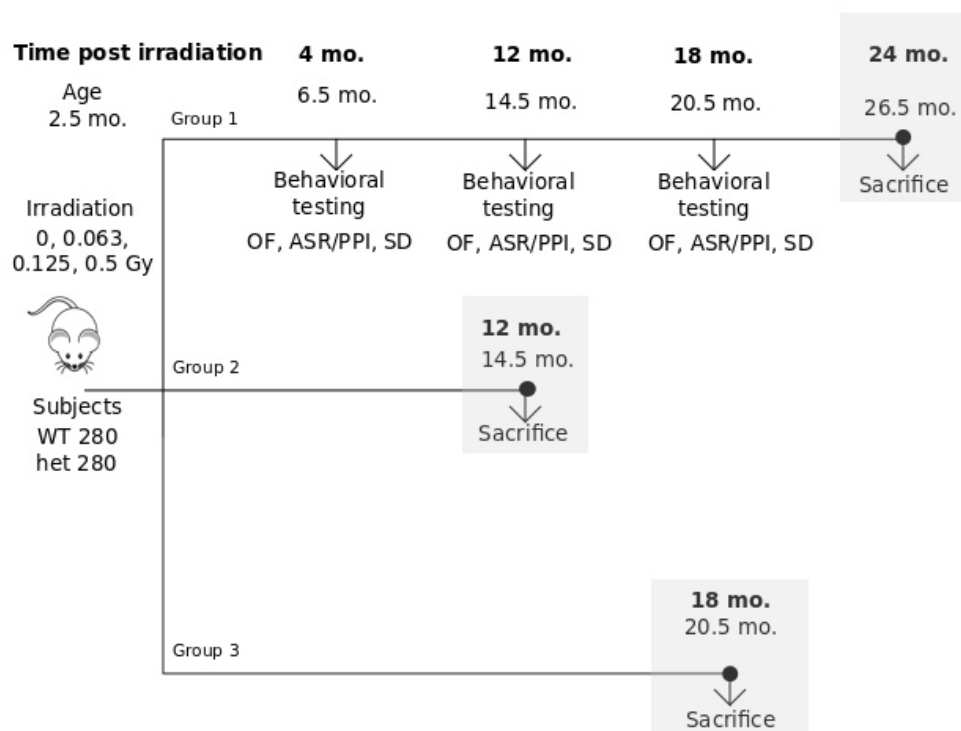


Fig.3. Experimental design – Behavior At the age of 10 weeks/2.5 months (2.5 mo.), wt (wt) and heterozygous (het) *Ercc2*^{S737P} mice were irradiated with ⁶⁰Co (dose rate 0.063 Gy/min) with doses ranging from 0 to 0.5 Gy. One group (“24-months” animals) was successively tested in the open field (OF), the acoustic startle/prepulse inhibition test (ASR/PPI) and the social discrimination test (SD) at precise time points. This group was then sacrificed at the end of the testing pipeline, 2 years later. In parallel, two other groups of mice (“12-months” and “18 months” animals) were irradiated in the same conditions but not tested and sacrificed at the precise time points of 12 and 18 months.

3.1. Open field test (OF)

The testing device is composed of a square arena (45 cm x 45 cm x 45 cm) constructed of transparent plastic and metal frame equipped with infrared beam detectors to automatically monitor motor activity of the test animal as well as its location. Among the recorded parameters (using the ActiMot software, TSE Systems) are the total distance traveled (in cm), average speed (cm/sec), and rearing as parameters of exploratory behavior and time spent in the center of the arena (in sec) as a measure of anxiety (Holter et al., 2015a).

3.2. Acoustic startle/Prepulse Inhibition test (ASR/PPI)

The testing device is composed of a large soundproof cubicle that isolates the animal in the presence of background noise (65 dB). A loudspeaker is located in the upper part of this chamber. A cylinder encloses the animal in the chamber and is installed on a piezoelectric motion sensor platform that transduces movements of the animal into electrical signals that are recorded and analyzed. Each session began with an initial stimulus-free (except for background noise), acclimation period of 5 min followed by 5 repetitions of the startle stimulus alone (110 dB) trials. The following trial types for ASR and PPI were arranged in a pseudo-random order and organized in 10 blocks, each presented 10 times. ASR trial types consisted of acoustic stimulus levels of 70, 80, 85, 90, 100, 110, and 120 dB. PPI was assessed for a startle stimulus level of 110 dB with prepulse levels of 67, 69, 73, and 81 dB preceding the startle pulse at an inter-stimulus interval of 50 ms. A value called “PPI global” is calculated by summing up each of the individual PPI values assessed previously, averaged by the total value.

3.3. Social discrimination (SD)

During a 4 minutes sampling session, a known ovariectomized female mouse (“familiar subject”) is presented to the tested subject. A fixed retention interval (2 hours) where the tested subject is left isolated then follows. During the 4 minutes test session, the test subject is re-exposed to the familiar subject together with a mouse previously not encountered (also an ovariectomized female mouse, termed the “unknown subject”). The time spent by the test subject with the familiar and the unknown subjects are recorded by a human observer with a handheld device in both sampling and test sessions, to evaluate the recognition index (calculated as time spent investigating the unknown subject/ sum of time spent investigating both subjects), which is used as an indicator of social memory.

4. Tissue sampling procedure

Mice were sacrificed with carbon dioxide (CO₂). After dissection, brain samples were removed and incubated overnight with 4% paraformaldehyde (PFA) and stored in 30% sucrose (without PFA) at 4°C. Before use, brains hemispheres were snap-frozen for 5 minutes on dry ice and conserved in a freezer at -20°C. They were sectioned sagittally in 40 µm slices on a cryostat (Leica CM3050S) and sections were stored in storage solution at -20°C. For each staining, one-in-six serial sections were used. The slides from each series were coded to ensure that the observer was blind to the experimental group until after the analysis.

5. Immunohistochemistry

5.1. Reagents and solutions

Deionized, distilled water was used in all recipes (unless otherwise mentioned).

Basic solvent for solution is phosphate-buffered saline (PBS; 0.1 M, pH 7.4), made of 1 liter of deionized, distilled H₂O, 80 g NaCl, 2.0 g KCl, 21.7 g Na₂HPO₄ · 7H₂O and 2.59 g KH₂PO₄. It can be stored up to 1 year at room temperature.

If 500 ml of 0.1 M phosphate-buffered saline is combined to 1.2 ml Triton X-100, the final result is named PBS-T and is used as basic solvent for immunohistochemistry. It can be stored up to 1 month at room temperature.

If 50 ml fetal bovine serum (FBS) are added up to 500 mL of PBS-T, the final result is named PBS++ and is also used as basic solvent for immunohistochemistry. It can be stored up to 1 week at 4°C.

Basic storage solution for freshly cryostat-cut tissues is composed of 250 ml of glycerin, 250 ml of ethylene glycol and 500 ml of 0.1 M PBS. It can be stored up to 1 year at room temperature.

Sodium citrate buffer is used to weaken the membrane of the cells composing some tissues in order to allow recognition of the target protein by the corresponding antibody. Dissolved 2.94 g trisodium citrate is mixed with 1 liter H₂O. pH is adjusted to 6.0 with 1 N HCl. It can be stored up to 3 months at room temperature or up to 6 months at 4°C.

ABC Elite Solution (VECTASTAIN ABC Kit, Vector Labs) is used for Avidin/Biotin immunohistochemistry staining procedure and is prepared by mixing 0.1 M phosphate-buffered saline with 1:300 dilution of reagent A and 1:300 dilution of reagent B. It has to be incubated 30 min at 4°C before use and can be stored up to 3 days at 4°C.

The DAB solution (3,3'-Diaminobenzidine) is a classic staining technique of immunohistochemistry known for its characteristic long-lasting brownish colour. It is composed of 1 ml of DAB in Tris-Cl, pH 7.5, 19 ml phosphate-buffered saline and 15 µl of 30% H₂O₂, this last element is added immediately prior to use. It has to be prepared fresh before each use. Due to its toxicity and carcinogenic properties, the solution should be disposed of carefully after use according to laboratory safety guidelines.

The hydrogen peroxide (H₂O₂) at 0.3% concentration is prepared by adding 500 µl of 30% H₂O₂ to 50 ml of 0.1 M phosphate-buffered saline. To keep its properties, it has to be prepared fresh.

FD Rapid Golgi Staining Kit from FD Technologies allows the user to perform long-lasting staining of neurons in brain tissue. Freshly harvested brain tissues have to be soaked in impregnation solution which is made of equal volume of solution A and solution B (present in the kit). The impregnation solution should be prepared at least 24 hr prior to use and left unstirred. The staining procedure itself employs a working solution prepared with one volume of solution D, one volume of solution E (from the basic kit) and two volumes of deionized, distilled H₂O at room temperature. It has be prepared fresh before use.

5.2. Consumables

Table 5.2. List of consumables

Name	Specification	Manufacturer
Cell culture plates	6-well tissue culture plate	Thermofisher Scientific; Waltham, MA, USA
Cell stainer	100 μ m nylon cell strainer	Sigma-Aldrich
Eppendorf tubes	1.5 mL	Eppendorf
Microscope slides	Charged microscope slides, Superfrost	Thermofisher Scientific; Waltham, MA, USA
Coverslips for microscope slides	24 \times 60–mm coverslips	Thermofisher Scientific; Waltham, MA, USA
Pasteur pipettes	3 MI	VWR; Darmstadt, Germany
Ethanol	100%, 95%, and 70% (v/v)	
Xylo		
Pertex	Mounting medium	Medite

5.3. Technical equipment

Table 5.3. List of technical equipments

Name	Specification	Manufacturer
Acoustic Startle device		TSE Systems, Berlin
Open field device		TSE Systems, Berlin
Platform shaker	Rotamax 120	Heidolph Instruments
Zeiss Axioplan2 microscope	equiped with a motorized stage, a CCD color camera	Zeiss
Cryostat	Leica CM3050 S	Leica Biosystem
Stereoinvestigator software	Stereo Investigator 11.03, NeuroLucida	MFB Biosciences
Platform shaker	Rotamax 120	Heidolph Instruments
NeuroLucida	Version 2018	MBF biosciences, Williston, VT, USA.
NeuroLucida Explorer 2018		MBF biosciences, Williston, VT, USA

5.4. Nissl, Iba1 and GFAP staining

For Nissl staining of 24 months old brain sections, the brains are sliced on cryostat and stored in storage solution. After rinsing the free-floating tissue sections three times, with PBS 0.1M, pH 7.4 at room temperature on shaker, the 40 μ M brain slices were mounted on slides using a brush. The mounted sections are left to dry in the dark for at least 12 hours. The slides are then immersed in cresyl violet. The longer the immersion time, the stronger the staining intensity. Here the immersion time was 10 minutes. The slides are then rinsed once with PBS 0.1M, pH 7.4 at room temperature. The stained and rinsed slides are left to dry in the dark at least for 12 hours. Then the sections were dehydrated in 70%, 90% and 100% ethanol and xylol. The dehydrated slides were then coverslipped using mounting medium.

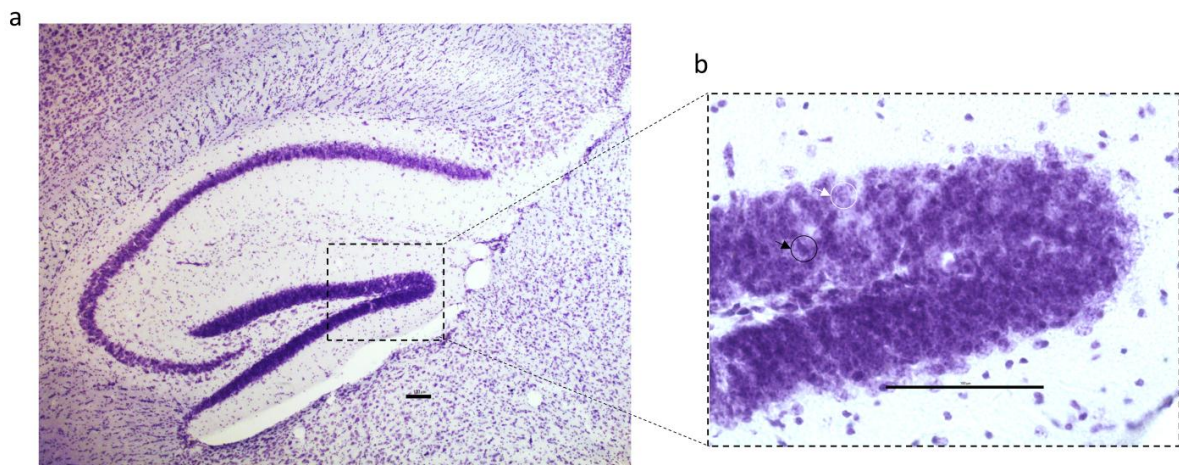


Fig.5.4.a. a. A representative Nissl-stained mouse brain hippocampal region. Objective 5x. Scale bar 100 μ M. b. Higher magnification photomicrograph of the dentate gyrus. Objective 40x. Scale bar 100 μ M. Nissl stain distinguishes neurons (white arrow, white circle) from glial cells (black arrow, black circle).

Iba1 stain of 12, 18 and 24 months old brain sections was performed with a primary monoclonal anti-Iba1 antibody, against goat, from Abcam, Cambridge, UK; order number ab5076, with a 1:200 concentration. A secondary biotin antibody (Biotin-SP AffiniPure) developed in rabbit against goat IgG von Jackson ImmunoResearch Inc., USA with 1:300 concentration in combination with ABC Elite Solution (VECTASTAIN ABC Kit, Vector Labs) and DAB solution was used for revelation of the staining.

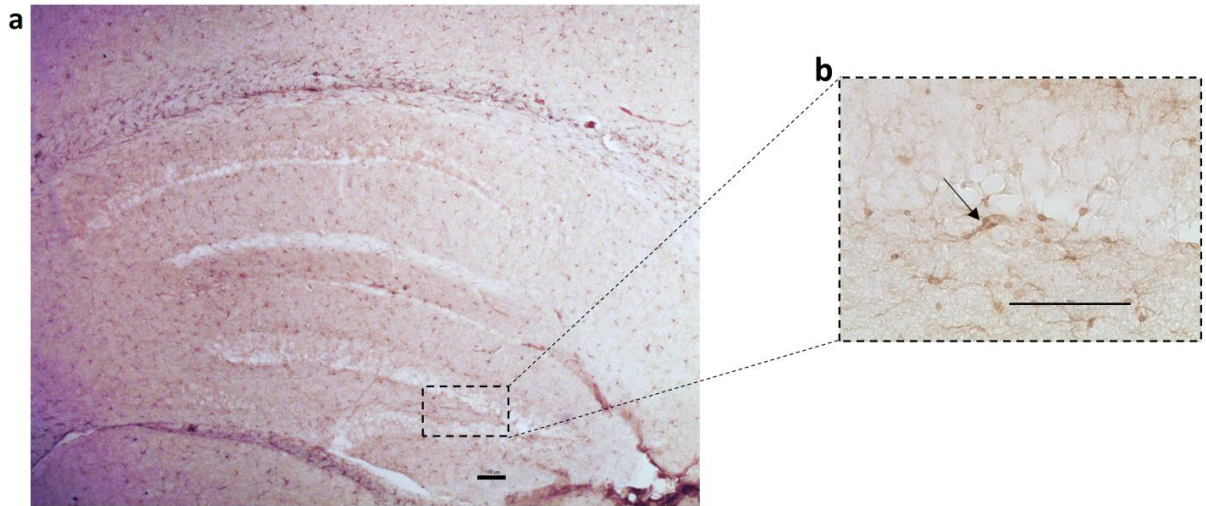


Fig.5.4.b. a. A representative photomicrograph showing Iba1+ cells in the hippocampus. Objective 5x. Scale bar 100μM. **b. A higher magnification image of Iba1+ microglia in the dentate gyrus.** Objective 40x. Scale bar 100 μM. Pointed by the arrow, an Iba1-positive microglia.

GFAP stain of 12, 18 and 24 months old brain sections was performed with a primary monoclonal anti-GFAP antibody, against rabbit, from Abcam, Cambridge, UK; order number ab4648, with a 1:5000 concentration. A secondary biotin antibody (Biotin-SP AffiniPure) developed in goat against rabbit IgG von Jackson ImmunoResearch Inc., USA with 1:300 concentration in combination with ABC Elite Solution (VECTASTAIN ABC Kit, Vector Labs) and DAB solution was used for revelation of the staining.

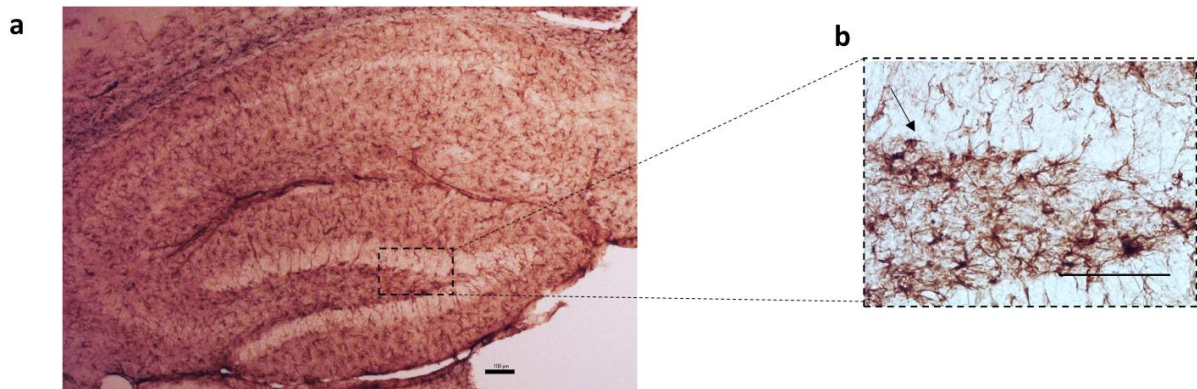


Fig 5.4.c. a. A representative photomicrograph of GFAP+ cells in the hippocampus. Objective 5x. Scale bar 100μM. **b.A higher magnification image of the dentate gyrus region.** Objective 40x. Scale bar 100 μM. Pointed by the arrow, a GFAP-positive astrocyte.

The immunostaining procedure of 12, 18 and 24 months old brain sections for Iba1 and GFAP was carried out as described: the free-floating cryostat sectioned 40 μ M brain sections were rinsed three times 10 minutes with 0.1M PBS, pH 7.4 at room temperature on shaker in 6 well plates with an inserted cell strainer. The sections were then quenched with endogenous peroxidase with 0.03% H₂O₂ for 30 minutes at room temperature. The sections were then rinsed three times 10 minutes with PBS and blocked with PBS++ for an hour at room temperature on shaker. The primary antibody was then added and the sections incubated in 2 mL Eppendorf tubes overnight at -4 degrees.

The next day, the sections were transferred into cell strainers inserted in 6-well plates and rinsed three times 10 minutes with 0.1M PBS, pH 7.4 at room temperature on shaker. They were blocked with PBS++ for an hour at room temperature on shaker. The biotinylated secondary antibody was then added and the sections were incubated in the secondary antibody solution for 2 hours at room temperature on shaker. The sections were then rinsed three times 10 minutes with PBS and incubated 2 hours in ABC solution. The sections were then rinsed three times 10 minutes with PBS. Revelation of the staining was performed with DAB chromogene. Intensity of the stain was defined manually by the user by adjusting the incubation time with DAB (in average 5 minutes). The stained sections were then rinsed 3 times 10 minutes in PBS and mounted on slides using a brush and dried in the dark for at least 12 hours. Then the sections were dehydrated in 70%, 90% and 100% ethanol and xylol. The dehydrated slides were then coverslipped using mounting medium.

5.6. Cell quantification (stereology)

Iba1-, GFAP- and Nissl- stained sections were analyzed with a Zeiss Axioplan2 microscope equipped with a motorized stage, a CCD color camera and the Stereo Investigator software. Anatomical levels of each brain section and regions of interest were assessed with the Mouse Brain Atlas with stereotaxic coordinates by Paxinos and Franklin (Keith Franklin George Paxinos, 2019). Four sections were analyzed per animal. Using the 5x objective, the dorsal hippocampal dentate gyrus, the dorsal hippocampal CA1 and CA2/3 regions were contoured using the software. Our three regions of interest were analyzed between the lateral boundaries of 2.40 to 1.08 mm according to the atlas. All cells within the contours were counted by scanning through the tissue in the x-y plane using the software and a \times 20 objective.

Stereology is a technique of quantitative histology which was used here to determine the number of Nissl+, Iba1+ or GFAP+ cells stained by the corresponding antibody in a specific brain region, here the hippocampus and its sub-regions, CA1, 2 and 3.

Important information was first provided manually to the software: section thickness, mounted thickness of the tissue section (tissue tends to shrink after embedding in medium), the depth of stained tissue (or optical dissector height, variable according to the penetration of the stain into the tissue), the size of the counting grid and of the counting frame (adjusted to the type of staining performed), the section sampling interval (the order of each section in the brain, in the rostro-caudal axis) and the value of the error coefficient (which varies with the size of the counting frame and the counting grid, the amount of stained cells and the number of sections available).

Table 5.6. Stereology parameters used in this study

Stereology parameter	Value
Mounted thickness	35 μM
Optical dissector height	25 μm
Grid size	100 \times 100 μm
Counting frame	100 μm
Section sampling interval	6
Section thickness	40 μm
Error coefficient	<0.1

The user then indicates manually using the software the number of positive cells in each counting frame in the selected brain region for each available brain section containing this brain region.

From this manual count and the information provided earlier by the user, the software uses a formula to calculate the total amount of positive cells present in this brain region.

$$N = \sum Q^- * \frac{\bar{t}_Q^-}{h} * \frac{1}{asf} * \frac{1}{ssf}$$

$$\text{for } \bar{t}_Q^- = \frac{\sum_i (t_i q_i)}{\sum_i q_i}$$

Figure 5.6. Important parameters and formula used to calculate the total number N of positive-stained cells

in one brain. \bar{t}_Q^- is the number-weighted mean section thickness, h is the height of the disector, asf is the area sampling fraction, ssf is the section sampling fraction and t_i is the section thickness in the i-th counting frame with a cell count of q_i^- in the dissector. Modified from (Olesen et al., 2017).

5.7. Golgi staining

A classic method to stain and analyze neuronal morphology is the Golgi staining, developed by Camillo Golgi in 1873. Described here is the procedure for implementing the commercially available Rapid Golgi technique (FD Technologies, Rapid Golgi kit) used in conjunction with the Neurolucida neuronal tracing software (MBF Bioscience).

The intact brain is first immersed for a day in 5 mL of impregnation solution. The solution is replaced by fresh impregnation solution the next day and the brain is left to soak for 2 weeks in the dark. The brain is then transferred to 5 mL of solution C (provided in the FD Rapid Golgi kit) for a day. The solution is replaced by fresh solution C the next day and left to soak for 3 days. Until sectioning, the brain is stored in solution C. Sectioning and mounting of the brain on microscope slides was performed with a cryostat. Section thickness was 100 μM . Each slide was soaked in solution and the excess solution gently removed. The slides were then dried flat in the dark for 2 days. The slides were then rinsed two times, each time with 60 ml ddH₂O for 4 min at room temperature, covered with the working solution supplied in the kit and incubated in the dark for 10 min at room temperature. The slides were then rinsed twice in ddH₂O for 4 min and dehydrated in 70%, 96%, and 100% ethanol and Xylol for 4 min each. The slides were finally coverslipped with mounting medium and dried overnight prior to imaging.

5.8. Analysis of Microglial and Astrocytic Morphology

The analysis of the morphology of the Iba1-stained and the GFAP-stained sections was done with a Zeiss Axio Imager M2 microscope and the software Neurolucida. On 100x-level 10 microglia cells per animal in the region of the dentate gyrus were traced. Therefore, the cell body of each selected cell was contoured in the software at the z-stage-level where it showed the largest area in focus. The branches were traced via the Dendrite function always keeping them in focus and also adapting the thickness of the respective branch using the Thickness tracing function of the software. The traced 3D-cell structures were analyzed afterwards in Neurolucida Explorer software using Sholl Analysis (radius 5 μm) and the Branched Structure Analysis function.

The Sholl Analysis is a classical method used to analyze neuronal morphology, providing information on the morphological complexity. From the cell body, concentric circles are traced with a regular user-defined radius until the end of each dendrite. The software is then able to provide information on the morphological aspect of the neuron through parameters such as branch length, number of nodes on each branch, number of endings per branch, etc (Binley et al., 2014).

6. Statistical analyses

Numerical analysis was performed using GraphPad Prism 7 version 7.03 for Windows (GraphPad Software, La Jolla, California, USA, www.graphpad.com), SAS and R version 3.0.2. For normal distribution, a one-way ANOVA was performed to test treatment effect and a two-way ANOVA was performed to check interactions of genotype-treatment and sex-treatment. If the interactions were not significant, genotypes or sexes were pooled together. When significant interactions were detected, a post hoc (Tukey's multiple comparisons) test was used to determine differences between groups.

In a more global way, the complete behavioral dataset available for all 560 mice used in the study (OF, ASR and SD parameters at 4, 12 and 18 months post-exposure to 0; 0.063; 0.125 and 0.5 Gy) was also analyzed using the statistical software SAS (Version 9.3) with a linear model with random intercept with the help of the statistician Dr. Peter Reitmeir to assess the influence of dose, sex, genotype and time post exposure and their interactions on the different measured behavioral parameters.

This analysis was deemed appropriate because of the high number of animals (560 mice) and the repeated measurements (the same group of animals "24-months animals" was tested successively at 4, 12 and 18 months after exposure).

The investigation focused on dose-dependent radiation effects over all three time points, as well as on potential sex-specific or genotype-specific radiation effects.

Behavioral data was first organized in an Excel file for each test (OF, ASR, SD) with time (4, 12 or 18 months) and behavioral parameters (e.g. for OF: total distance travelled, average speed, centre time, rearing; for ASR: ASR/BW, PPI; for SD: recognition index, test phase, sample phase) as titles of columns. Lines titles were the ID number of each mouse. For each test, it was first verified if each parameter could be analyzed with linear model with random intercept. Validation analysis was performed by Dr. P. Reitmeir and returned $Pr > ChiSq < .0001$ if the parameter was valid for analysis with the linear model with random intercept and a $Pr > ChiSq > .0001$ if the parameter was not valid for analysis.

The model was valid ($Pr > ChiSq < .0001$) for the analysis of OF parameters (total distance travelled, rearing, percentage of total center time, whole average speed) and for the analysis of ASR/PPI parameters (ASR/BW 110, percentage of PPI global). The model was not valid for the analysis of the recognition index in the SD test ($Pr > ChiSq = 0.761$) but was valid for the analysis of the investigation time during the sample and test phases with the familiar subject and the test phase with the unknown subject ($Pr > ChiSq < .0001$).

The stereological data was analyzed with 1-way ANOVA with GraphPad Prism 7. The overall morphology data per group was analyzed with a one-way-ANOVA of the averaged individual parametric values (branch length, number of nodes on each branch, number of endings per branch). For multiple comparisons, the Tukey's test was used. For the Sholl-analysis data, a

repeated measures (RM) ANOVA (genotype as between subject factor and distance from soma as within subject factor) with post-hoc Sidak's test was performed. The Spearman's test was performed to detect correlations between the tested parameters. For all tests, a p value <0.05 was used as the level of significance and data are presented as means +/- SEM.

IV. Results

A. Wildtype animals

1. Open field testing

For open field testing, the effects of ionizing radiation exposure on spontaneous locomotion (total distance and average speed), explorative behavior (rearing) and anxiety (center time) were analyzed separately for wt and mutant and for males and females, always sham (control-irradiated) versus irradiated animals.

Each graph represents the performance of each group for one of the mentioned parameters. Each symbol represents the performance of one individual. Sham animals are represented by empty circles, 0.063 Gy-irradiated animals are represented by filled lozenges, 0.125 Gy-irradiated animals are represented by crosses and 0.5 Gy-irradiated animals are represented by filled stars. For each graph, on the left side of the graph, male sham animals are compared to irradiated male animals and the right side of the graph female sham animals are compared to irradiated female.

1.1. OF – 4 months after exposure

1.1.a. OF – 4 months after exposure to 0.063 Gy

No significant differences between wt sham and wt 0.063 Gy-irradiated animals were observed 4 months after exposure for spontaneous locomotion, explorative behavior or anxiety, for wt males and female animals.

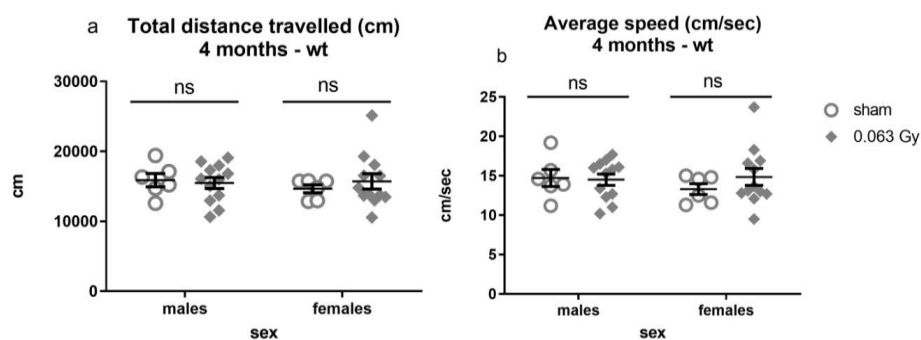


Fig. A.1.1.a. 1) Spontaneous locomotion at 4 months post-irradiation with 0.063 Gy. Total distance travelled and average speed were analyzed with 2-way ANOVA and Sidak's multiple comparisons test to decipher the effect of treatment on both sexes and to detect potential sex-specific treatment effects (i.e. treatment x sex interaction). No significant differences were observed in total distance (a, treatment $F(1,32)=0.09929$; $p=0.7547$) and average speed (b, treatment $F(1,32)=0.4239$; $p=0.5196$). Data is presented as a scatter plot +/- SEM. n=6-12 animals.

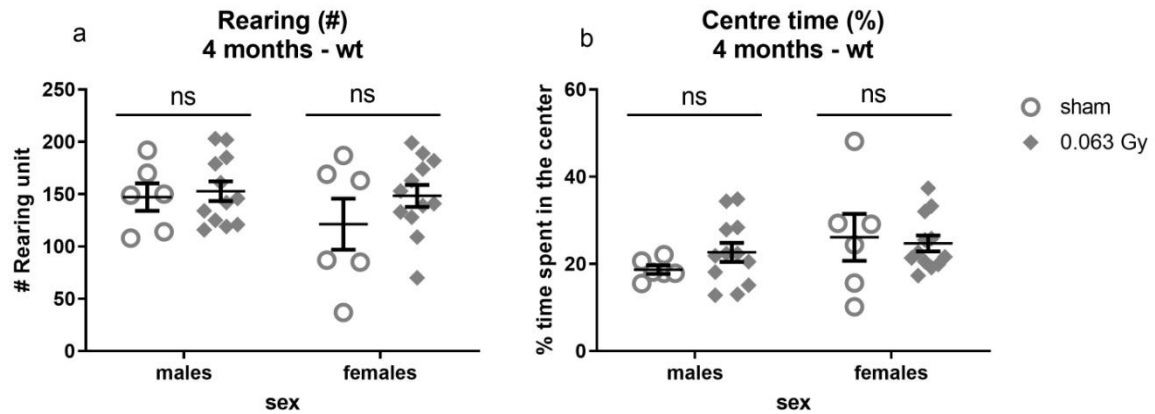


Fig. A.1.1.a. 2) Explorative behavior and anxiety at 4 months post-irradiation with 0.063 Gy. Rearing and centre time were analyzed with 2-way ANOVA and Sidak's multiple comparisons test to decipher the effect of treatment on both sexes and to detect potential sex-specific treatment effects (i.e. treatment x sex interaction). No significant differences were observed in rearing (a, treatment $F(1, 32)=1.377$; $p=0.2493$) and centre time (b, treatment $F(1,32)=0.2124$; $p=0.6480$). Data is presented as a scatter plot +/- SEM. $n=6-12$ animals.

1.1.b. OF – 4 months after exposure to 0.125 Gy

No significant differences between wt sham and wt 0.125 Gy-irradiated animals were observed 4 months after exposure for spontaneous locomotion, explorative behavior or anxiety, for wt male and female animals.

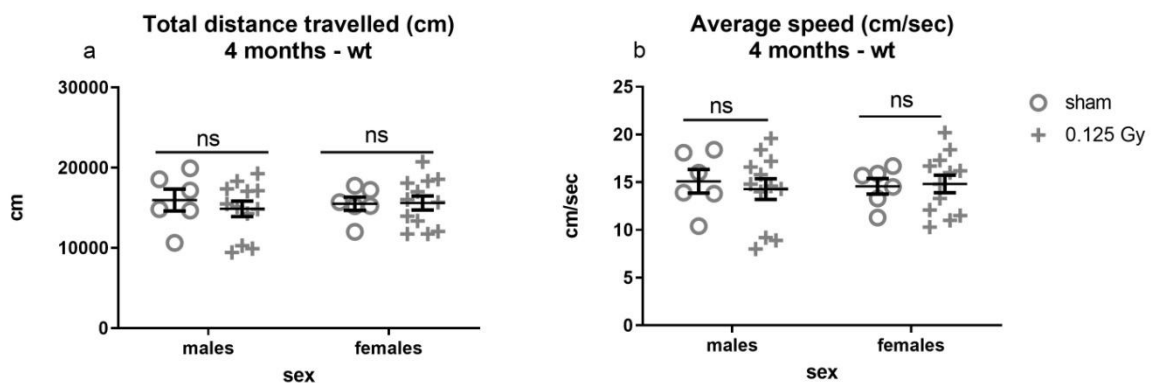


Fig. A.1.1.b.1) Spontaneous locomotion at 4 months post-irradiation with 0.125 Gy. Total distance travelled, and average speed were analyzed with 2-way ANOVA and Sidak's multiple comparisons test to decipher the effect of treatment on both sexes and to detect potential sex-specific treatment effects (i.e. treatment x sex interaction). No significant differences were observed in total distance (a, treatment $F(1, 32) = 0.2146$; $p=0.6463$) and average speed (b, treatment $F(1, 32) = 0.06182$; $p=0.8052$). Data is presented as a scatter plot +/- SEM, $n=6-12$ animals.

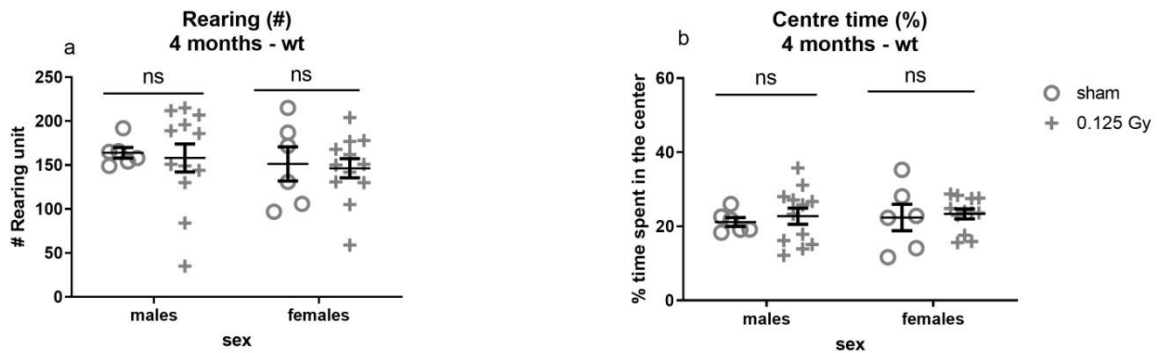


Fig. A.1.1.b.2). Explorative behavior and anxiety at 4 months post-irradiation with 0.125 Gy. Rearing and centre time were analyzed with 2-way ANOVA and Sidak's multiple comparisons test to decipher the effect of treatment on both sexes and to detect potential sex-specific treatment effects (i.e. treatment x sex interaction). No significant differences were observed in rearing (a, treatment $F(1, 32) = 0.1199$; $p = 0.7314$) and centre time (b, treatment $F(1, 32) = 0.3264$; $p = 0.5718$). Data is presented as a scatter plot +/- SEM, $n = 6-12$ animals.

1.1.c. OF – 4 months after exposure to 0.5 Gy

No significant differences between wt sham and wt 0.5 Gy-irradiated animals were observed 4 months after exposure for spontaneous locomotion, explorative behavior or anxiety, for males and female wt animals.

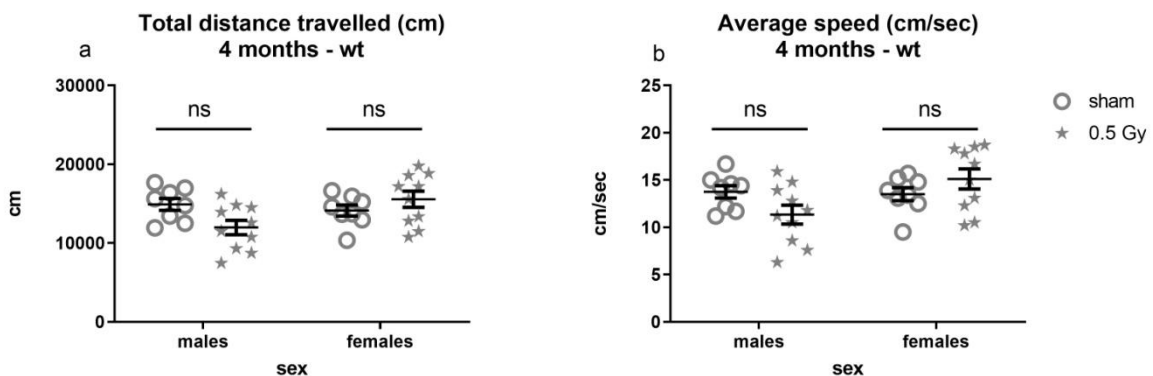


Fig. A.1.1.c.1) Spontaneous locomotion at 4 months post-irradiation with 0.5 Gy. Total distance travelled and average speed were analyzed with 2-way ANOVA and Sidak's multiple comparisons test to decipher the effect of treatment on both sexes and to detect potential sex-specific treatment effects (i.e. treatment x sex interaction). No significant differences were observed in total distance (a, treatment $F(1, 32) = 0.7165$; $p = 0.4036$) and average speed (b, treatment $F(1, 32) = 0.1937$; $p = 0.6628$). Data is presented as a scatter plot +/- SEM. $n = 8-10$ animals.

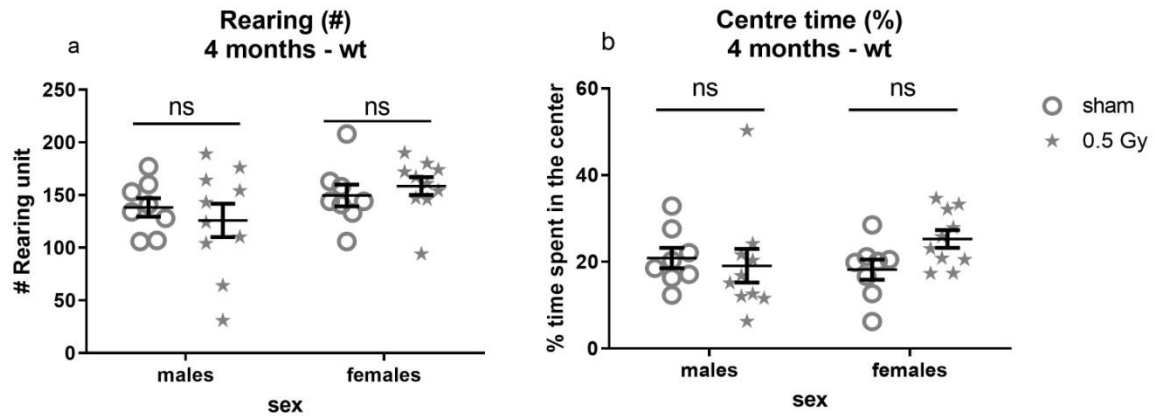


Fig. A.1.1.c.2) Explorative behavior and anxiety at 4 months post-irradiation with 0.5 Gy. Rearing and centre time were analyzed with 2-way ANOVA and Sidak's multiple comparisons test to decipher the effect of treatment on both sexes and to detect potential sex-specific treatment effects (i.e. treatment x sex interaction). No significant differences were observed in rearing (a, treatment $F(1, 32) = 0.02183$; $p = 0.8835$) or centre time (b, treatment $F(1, 32) = 0.8444$; $p = 0.3650$). Data is presented as a scatter plot +/- SEM. $n = 8-10$ animals.

1.2. OF – 12 months after exposure

1.2.a. OF – 12 months after exposure to 0.063 Gy

No significant differences between wt sham and wt 0.063 Gy-irradiated animals were observed 12 months after exposure for spontaneous locomotion, explorative behavior or anxiety, for wt males and female animals.

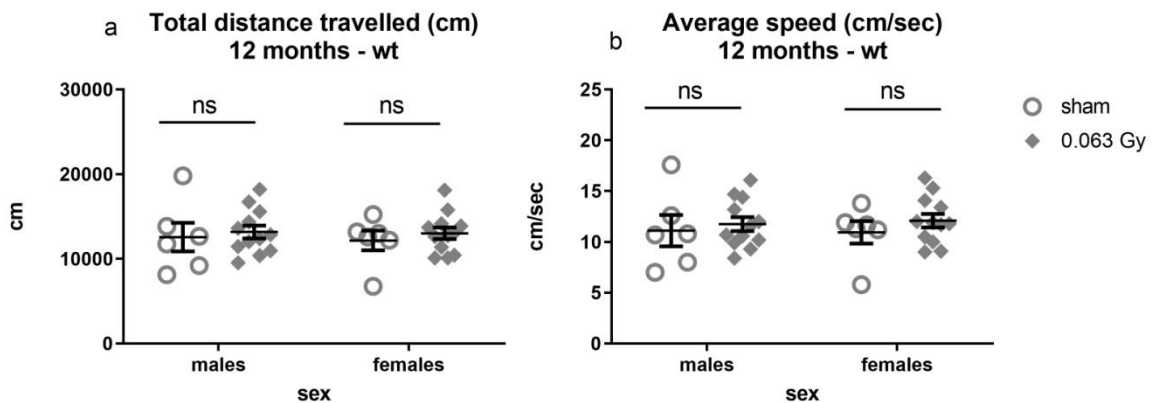


Fig. A.1.2.a.1) Spontaneous locomotion at 12 months post-irradiation with 0.063 Gy. Total distance travelled and average speed were analyzed with 2-way ANOVA and Sidak's multiple comparisons test to decipher the effect of treatment on both sexes and to detect potential sex-specific treatment effects (i.e. treatment x sex interaction). No significant differences were observed for total distance travelled (a, treatment $F(1, 32) = 0.5109$; $p = 0.4799$) or average speed (b, treatment $F(1, 32) = 0.8880$; $p = 0.3531$). Data is presented as a scatter plot +/- SEM. $n = 6-12$ animals.

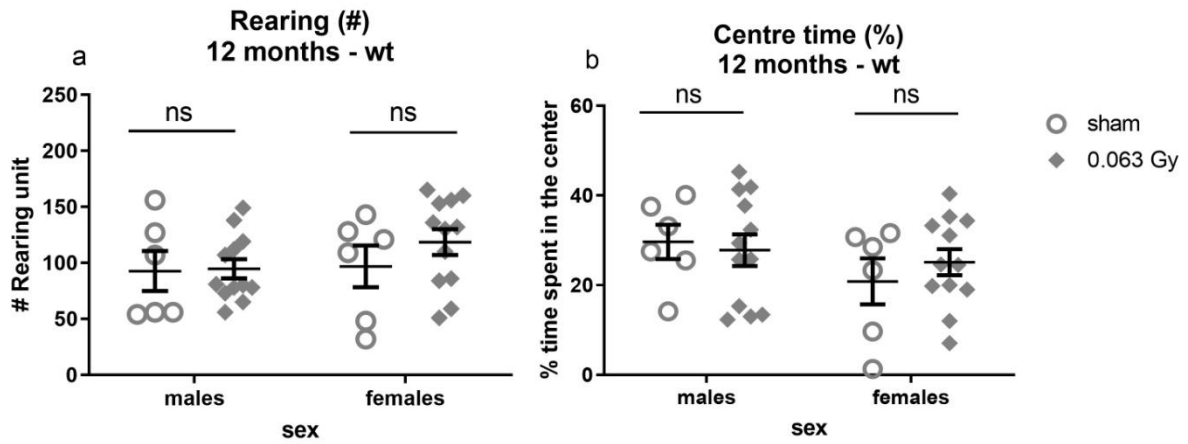


Fig. A.1.2.a.2) Explorative behavior and anxiety at 12 months post-irradiation with 0.063 Gy. Rearing and centre time were analyzed with 2-way ANOVA and Sidak's multiple comparisons test to decipher the effect of treatment on both sexes and to detect potential sex-specific treatment effects (i.e. treatment x sex interaction). No significant differences were observed in rearing (a, treatment $F(1, 32) = 0.7595$; $p=0.3900$) or centre time (b, treatment $F(1, 32) = 0.09444$; $p=0.7606$). Data is presented as a scatter plot +/- SEM. n=6-12 animals.

1.2.b. OF – 12 months after exposure to 0.125 Gy

No significant differences between wt sham and wt 0.125 Gy-irradiated animals were observed 12 months after exposure for spontaneous locomotion, explorative behavior or anxiety, for wt males and female animals.

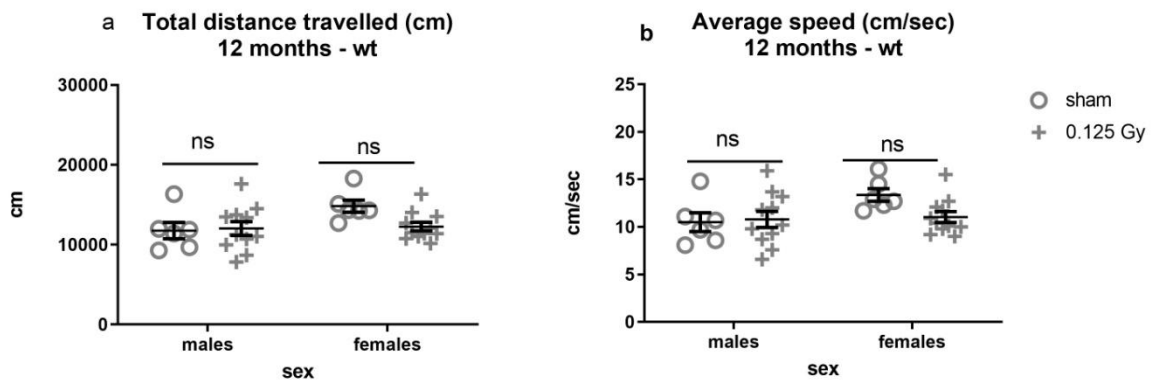


Fig. A.1.2.b.1) Spontaneous locomotion at 12 months post-irradiation with 0.125 Gy. Total distance travelled and average speed were analyzed with 2-way ANOVA and Sidak's multiple comparisons test to decipher the effect of treatment on both sexes and to detect potential sex-specific treatment effects (i.e. treatment x sex interaction). No significant differences were observed for total distance travelled (a, treatment $F(1, 30) = 1.925$; $p=0.1756$) or average speed (b, treatment $F(1, 30) = 1.534$; $p=0.2250$). Data is presented as a scatter plot +/- SEM. n=6-12 animals.

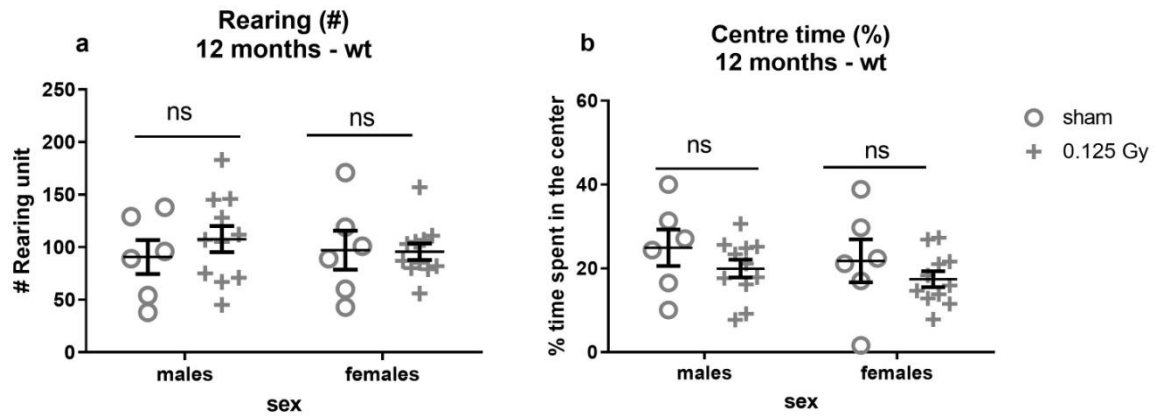


Fig. A.1.2.b.2) Explorative behavior and anxiety at 12 months post-irradiation with 0.125 Gy. Rearing and centre time were analyzed with 2-way ANOVA and Sidak's multiple comparisons test to decipher the effect of treatment on both sexes and to detect potential sex-specific treatment effects (i.e. treatment x sex interaction). No significant differences were observed in rearing (a, treatment $F(1, 30) = 0.3314$; $p=0.5692$) or centre time (b, treatment $F(1, 30) = 2.266$; $p=0.1427$) Data is presented as a scatter plot +/- SEM. $n=6-12$ animals.

1.2.c. OF – 12 months after exposure to 0.5 Gy

No significant differences between wt sham and wt 0.5 Gy-irradiated animals were observed 12 months after exposure for spontaneous locomotion, explorative behavior or anxiety, for wt male and female animals.

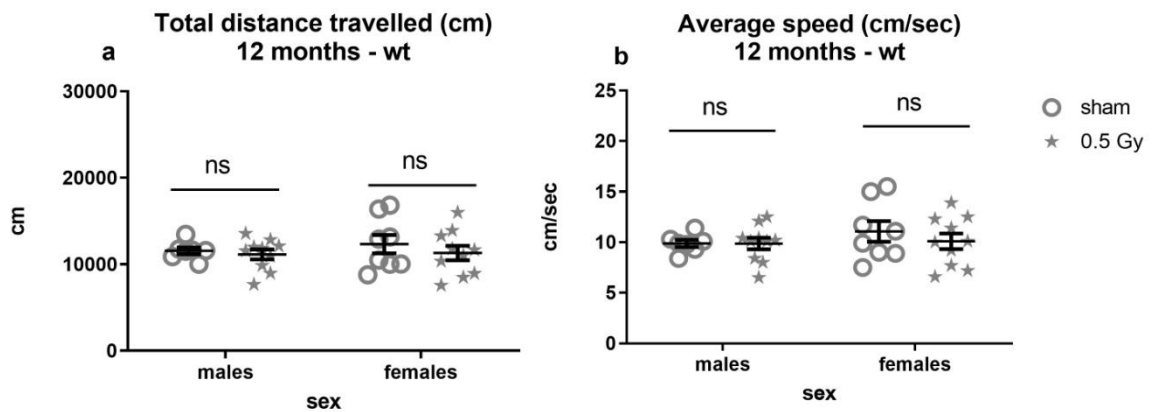


Fig. A.1.2.c.1) Spontaneous locomotion at 12 months post-irradiation with 0.5 Gy. Total distance travelled and average speed were analyzed with 2-way ANOVA and Sidak's multiple comparisons test to decipher the effect of treatment on both sexes and to detect potential sex-specific treatment effects (i.e. treatment x sex interaction). No significant differences were observed for total distance travelled (a, treatment $F(1, 31) = 0.8526$; $p=0.3629$) or average speed (b, treatment $F(1, 31) = 0.4505$; $p=0.5071$). Data is presented as a scatter plot +/- SEM. $n=6-12$ animals.

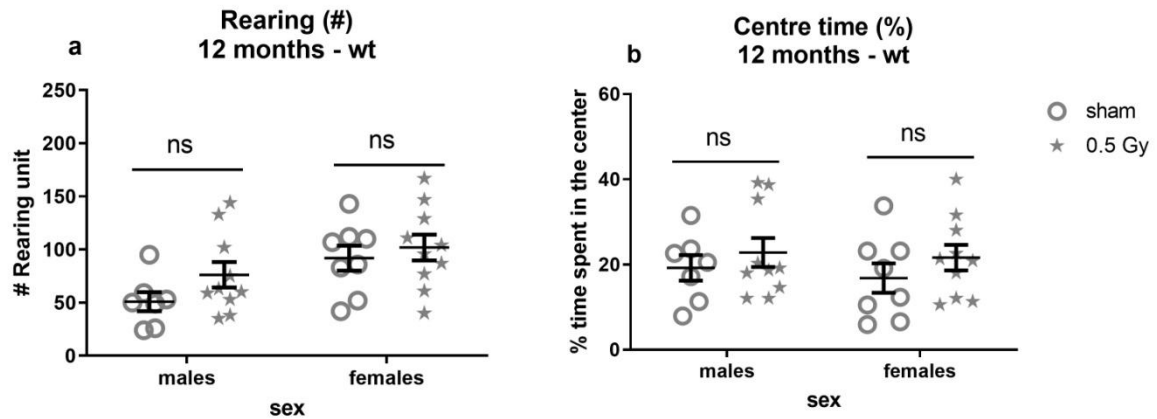


Fig. A.1.2.c.2) Explorative behavior and anxiety at 12 months post-irradiation with 0.5 Gy. Rearing and centre time were analyzed with 2-way ANOVA and Sidak's multiple comparisons test to decipher the effect of treatment on both sexes and to detect potential sex-specific treatment effects (i.e. treatment x sex interaction). No significant differences were observed in rearing (a, treatment $F(1, 31) = 2.209$; $p=0.1473$) or centre time (b, treatment $F(1, 31) = 1.621$; $p=0.2124$). Data is presented as a scatter plot +/- SEM. $n=6-12$ animals.

1.3. OF – 18 months after exposure

At 18 months after exposure, after 0.063 Gy, a treatment effect was observed for rearing in females wt mice (treatment $F(1, 28) = 7.441$, $p=0.0109$). After 0.5 Gy, a treatment effect was observed for center time in female wt mice (treatment $F(1, 27) = 5.5$, $p=0.0266$).

1.3.a. OF – 18 months after exposure to 0.063 Gy

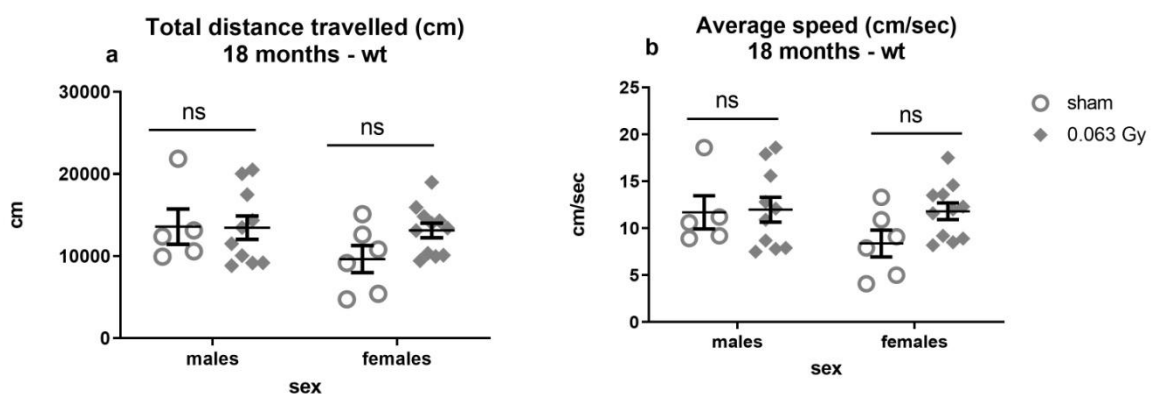


Fig. A.1.3.a.1) Spontaneous locomotion at 18 months post-irradiation with 0.063 Gy. Total distance travelled and average speed were analyzed with 2-way ANOVA and Sidak's multiple comparisons test to decipher the effect of treatment on both sexes and to detect potential sex-specific treatment effects (i.e. treatment x sex interaction). No significant differences were observed on total distance (a, treatment $F(1, 28) = 1.277$; $p=0.2681$) and average speed (b, treatment $F(1, 28) = 1.870$; $p=0.1824$). $n=6-12$ animals.

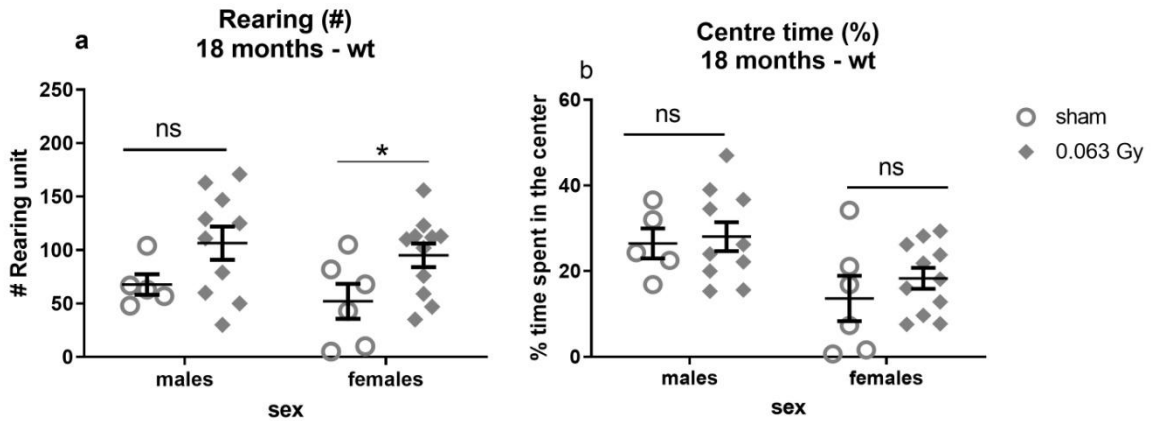


Fig. A.1.3.a.2) Explorative behavior and anxiety at 18 months post-irradiation with 0.063 Gy. Rearing and centre time were analyzed with 2-way ANOVA and Sidak's multiple comparisons test to decipher the effect of treatment on both sexes and to detect potential sex-specific treatment effects (i.e. treatment x sex interaction). No significant difference was observed on center time (b, treatment $F(1, 28) = 0.7126$; $p = 0.4057$). A treatment effect is observed for explorative behavior in females wt mice (a, treatment $F(1, 28) = 7.441$; $p = 0.0109$, post-hoc $p = 0.0439$). Data are presented as scatter plots +/- SEM. Results of the post-hoc tests are indicated on the graphs by * $p < 0.05$. $n = 6-12$ animals.

1.3.b OF – 18 months after exposure to 0.125 Gy

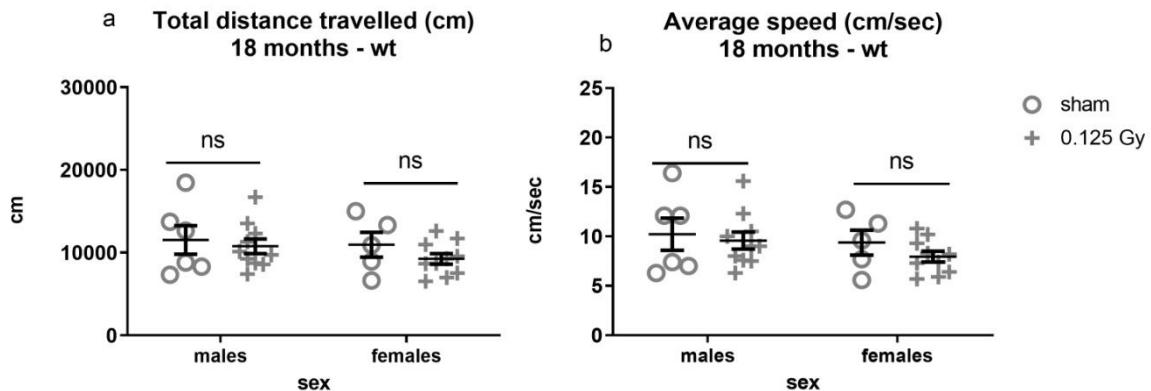


Fig. A.1.3.b.1) Spontaneous locomotion at 18 months post-irradiation with 0.125 Gy. Total distance travelled and average speed were analyzed with 2-way ANOVA and Sidak's multiple comparisons test to decipher the effect of treatment on both sexes and to detect potential sex-specific treatment effects (i.e. treatment x sex interaction). No significant differences were observed on total distance (a, treatment $F(1, 27) = 1.218$; $p = 0.2796$) and average speed (b, treatment $F(1, 27) = 0.9916$; $p = 0.3282$). Data are presented as scatter plots +/- SEM. $n = 6-12$ animals.

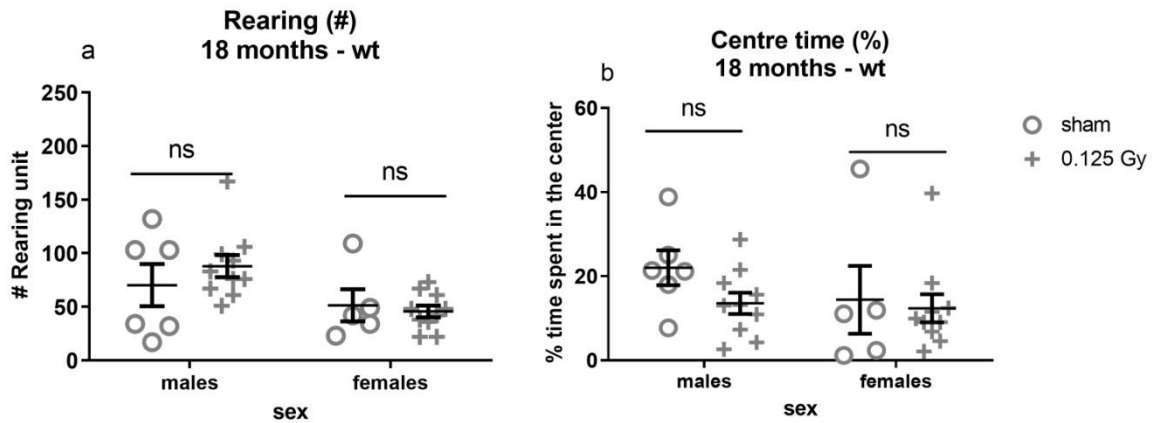


Fig. A.1.3.b.2) Explorative behavior and anxiety at 18 months post-irradiation with 0.125 Gy. Rearing and centre time were analyzed with 2-way ANOVA and Sidak's multiple comparisons test to decipher the effect of treatment on both sexes and to detect potential sex-specific treatment effects (i.e. treatment x sex interaction). No significant difference was observed on rearing (a, treatment $F(1, 27) = 0.2430$; $p=0.626$) or center time (b, treatment $F(1, 27) = 1.558$; $p=0.2227$). Data are presented as scatter plots +/- SEM. $n=6-12$ animals.

1.3.c OF – 18 months after exposure to 0.5 Gy.

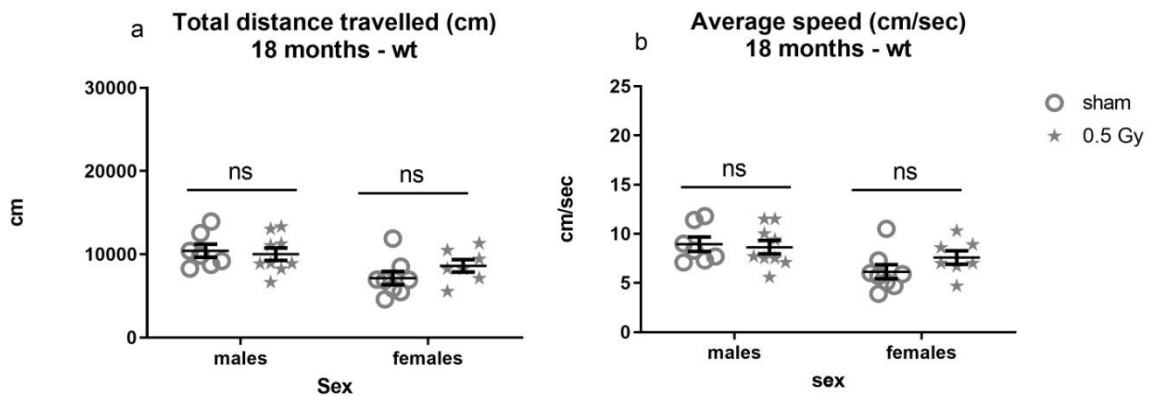


Fig. A.1.3.c.1) Spontaneous locomotion at 18 months post-irradiation with 0.5 Gy. Total distance travelled and average speed were analyzed with 2-way ANOVA and Sidak's multiple comparisons test to decipher the effect of treatment on both sexes and to detect potential sex-specific treatment effects (i.e. treatment x sex interaction). No significant differences were observed on total distance (a, treatment, $F(1, 27) = 0.4847$; $p=0.4923$) and average speed (b, treatment, $F(1, 27) = 0.6687$; $p=0.4207$). Data are presented as scatter plots +/- SEM. $n=6-12$ animals.

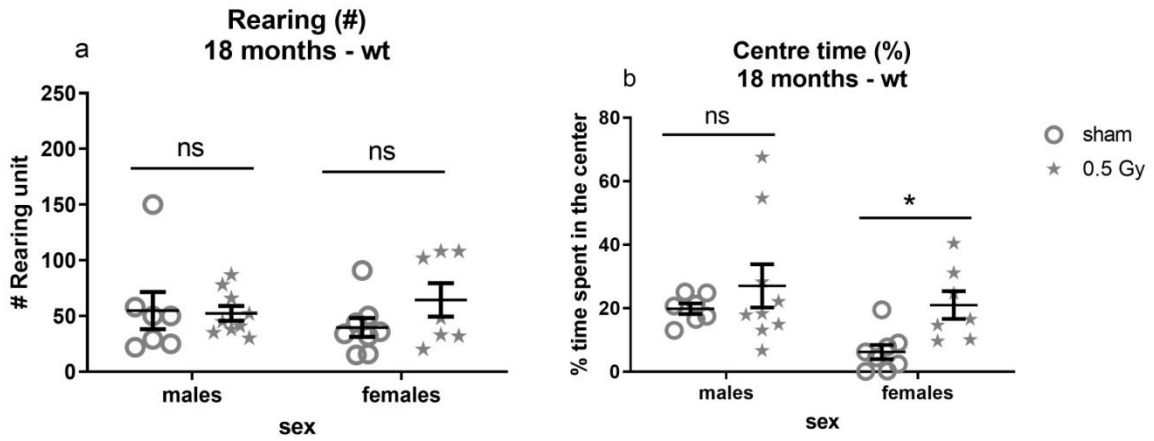


Fig. A.1.3.c.2) Explorative behavior and anxiety at 18 months post-irradiation with 0.5 Gy. Rearing and centre time were analyzed with 2-way ANOVA and Sidak's multiple comparisons test to decipher the effect of treatment on both sexes and to detect potential sex-specific treatment effects (i.e. treatment x sex interaction). No significant difference was observed on rearing (a, treatment $F(1, 27) = 0.8998$; $p=0.3512$). A treatment effect is observed for female wt mice on center time (b, $F(1, 27) = 5.500$; $p=0.0266$, post-hoc $p=0.0365$). Data are presented as scatter plots +/- SEM. Results of the post-hoc tests are indicated on the graphs by * $p<0.05$. $n=6-12$ animals.

2. Acoustic startle test (ASR)

For acoustic startle testing, the effects of ionizing radiation exposure on acoustic startle normalized by body weight (ASR/BW) and prepulse inhibition (PPI) filtering were analyzed separately for wt and mutant and for male and females, always sham versus irradiated animals.

For the acoustic startle, for each graph, on the x axis are scaled the different acoustic stimulations applied to the animal (ranging from background noise (BN) to 120 dB) and on the y axis is scaled the corresponding acoustic startle response averaged by body weight in arbitrary units. Each symbol represents the mean value of all irradiated or all sham animals for this acoustic stimulation value.

For the prepulse inhibition, for each graph, on the x axis is scaled the prepulse intensity above background (ranging from 2 to 16 dB) and on the y axis is scaled the prepulse inhibition in %. As for acoustic startle, each symbol represents the mean value of all irradiated or all sham animals for this prepulse intensity.

Sham animals are represented by empty circles, 0.063 Gy-irradiated animals are represented by filled lozenges, 0.125 Gy-irradiated animals are represented by crosses and 0.5 Gy-irradiated animals are represented by filled stars.

Data were analyzed with 2-way RM ANOVA, analyzing the interaction of stimulus intensity with treatment, stimulus intensity, treatment and subject variability. Only the interaction of stimulus intensity with treatment and treatment were of interest in this study. Mean value ASR/BW or PPI of all irradiated animals was compared to the mean value of all sham animals, for each acoustic stimulation/prepulse intensity. Post-hoc tests were performed with the Sidak's multiple comparisons test.

2.1. ASR - 4 months after exposure

2.1.a. ASR – 4 months after exposure to 0.063 Gy

At 4 months after exposure, after 0.063 Gy, ASR/BW decreased in wt males at 120 dB (treatment $F(1, 16) = 5.152$, $p=0.0374$). No significant differences were observed for females ASR/BW or PPI for both sexes.

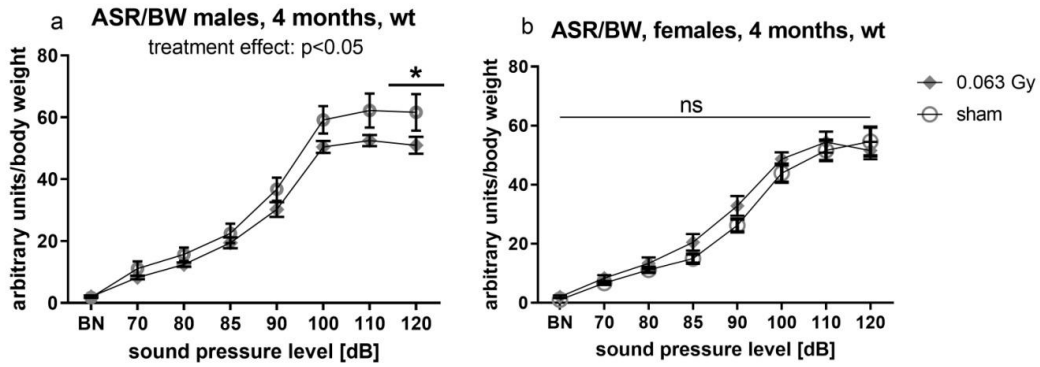


Fig.A.2.1.a.1) ASR – 4 months after exposure to 0.063 Gy. ASR/BW decreased in wt males at 120 dB after 0.063 Gy (a, treatment $F(1, 16) = 5.152$; $p = 0.0374$). No significant differences were observed for ASR/BW in females wt mice (b, treatment $F(1, 16) = 0.7854$; $p = 0.3886$). Data are presented as means \pm SEM. Results of the post-hoc tests are indicated on the graphs by * $p < 0.05$. For each group, $n = 8-10$.

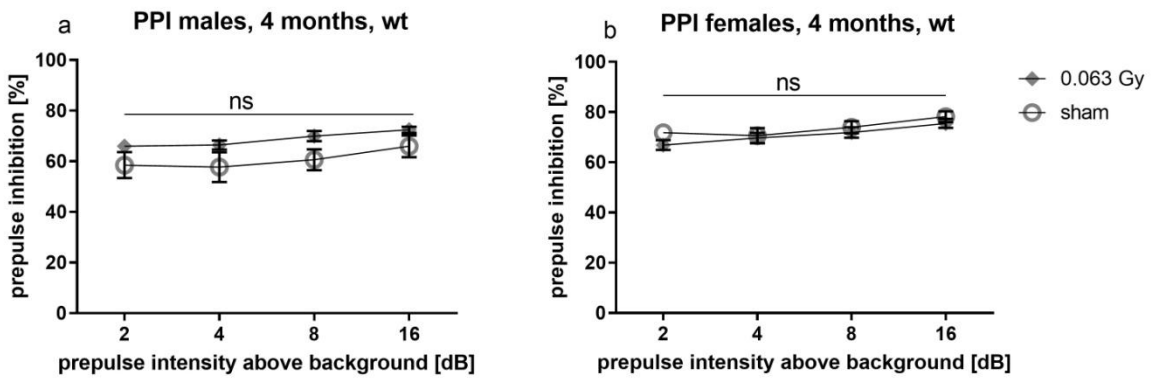


Fig. A.2.1.a.2) PPI – 4 months after exposure to 0.063 Gy. No significance difference were observed after exposure for PPI in wt males (a, treatment $F(1, 16) = 4.363$; $p = 0.0531$) or for PPI in wt females (b, treatment $F(1, 16) = 0.7333$; $p = 0.4045$). Data are presented as means \pm SEM. For each group, $n = 8-10$.

2.1.b. ASR – 4 months after exposure to 0.125 Gy

No significant differences were observed on ASR/BW or PPI, 4 months after exposure to 0.125 Gy, either for wildtype male or female mice.

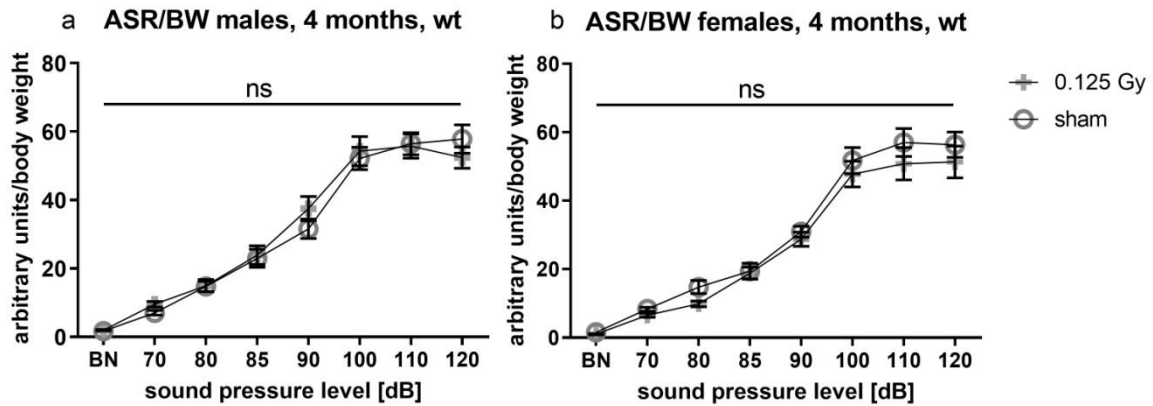


Fig. A.2.1.b.1) ASR – 4 months after exposure to 0.125 Gy. No significant differences were observed on ASR/BW for wt male mice (treatment $F(1, 16) = 0.04777$; $p=0.8298$) or for ASR/BW for wt females mice (treatment $F(1, 16) = 1.025$; $p=0.3264$) 4 months after exposure to 0.125 Gy. Data are presented as means \pm SEM. For each group, $n=8-10$.

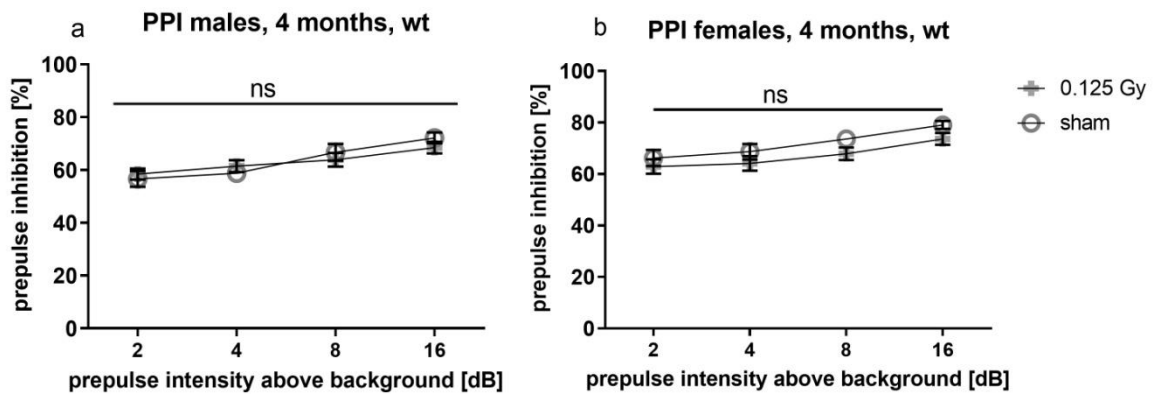


Fig. A.2.1.b.2) PPI – 4 months after exposure to 0.125 Gy. No significant differences were observed for PPI for wt male mice ($F(1, 16) = 0.02603$; $p=0.8739$) and for PPI in wt female mice (treatment $F(1, 16) = 1.548$; $p=0.2313$) 4 months after exposure to 0.125 Gy. Data are presented as means \pm SEM. For each group, $n=8-10$.

2.1.c. ASR – 4 months after exposure to 0.5 Gy

No significant differences were observed on ASR/BW or PPI, 4 months after exposure to 0.5 Gy, either for wildtype male or female mice.

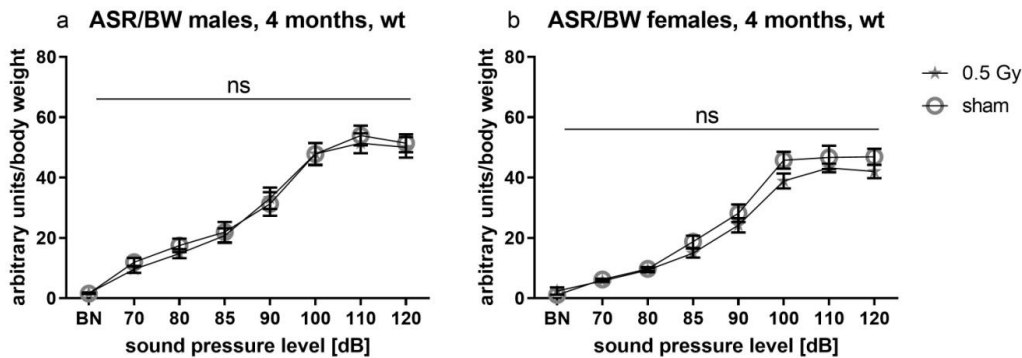


Fig.A.2.1.c.1) ASR – 4 months after exposure to 0.5 Gy. No significant differences were observed for ASR/BW in wt male mice (a, treatment F (1, 16) = 0.1103; p=0.7441) or for ASR/BW in females wt mice (b, treatment F (1, 16) = 2.112; p=0.1654). Data are presented as means +/- SEM. For each group, n=8-10.

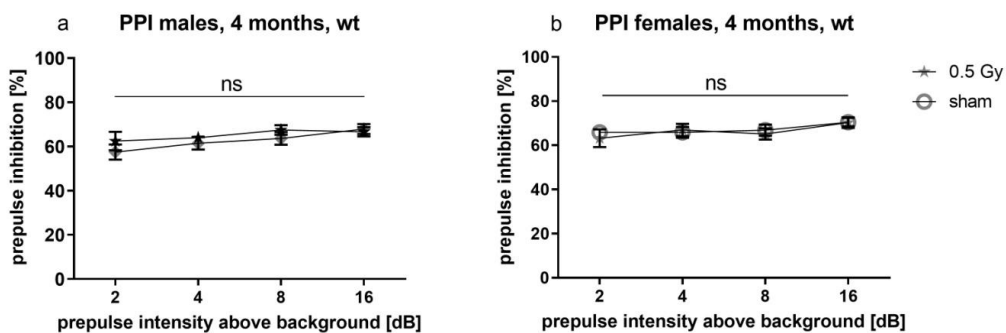


Fig.A.2.1.c.2) PPI – 4 months after exposure to 0.5 Gy. No significant differences were observed for PPI in wt male mice (a, treatment F (1, 16) = 0.4782; p=0.4992) and for PPI in females wt mice (b, treatment F (1, 16) = 0.05539; p=0.8169). Data are presented as means +/- SEM. For each group, n=8-10.

2.2. ASR - 12 months after exposure

2.2.a. ASR – 12 months after exposure to 0.063 Gy

At 12 months after exposure to 0.063 Gy, ASR/BW decreased in wt male mice, particularly at high intensities (interaction F (7, 112) = 3.523, p=0.0019, treatment F (1, 16) = 7.469, p=0.0147). ASR/BW increased in wt female mice (treatment F (1, 16) = 5.054, p=0.0390). No differences were observed in PPI after exposure in wt male or female mice.

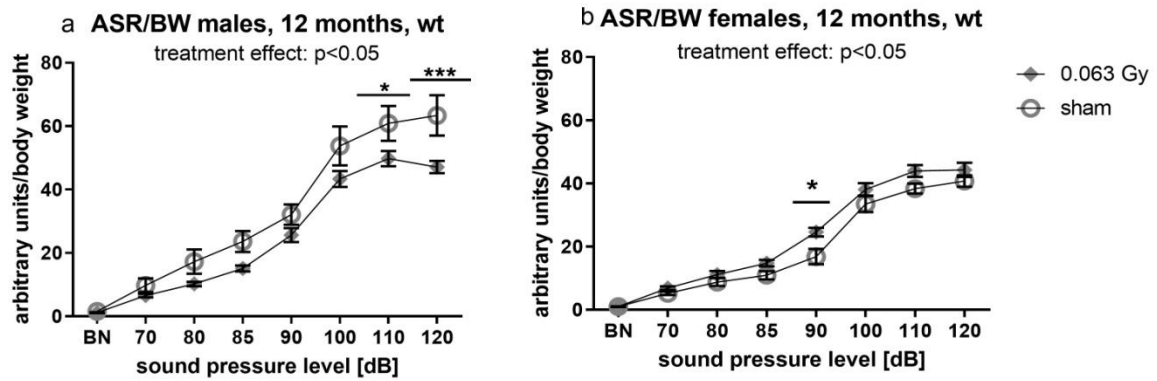


Fig.A.2.2.a.1). ASR – 12 months after exposure to 0.063 Gy. ASR/BW was affected at high intensities (90, 110, 120 dB) after 0.063 Gy in male and female wt mice (a, treatment $F(1, 16) = 7.469$; $p = 0.0147$; b, treatment $F(1, 16) = 5.054$; $p = 0.0390$). Data are presented as means \pm SEM. Results of the post-hoc tests are indicated on the graphs by * $p < 0.05$, *** $p < 0.001$. For each group, $n = 8-10$.

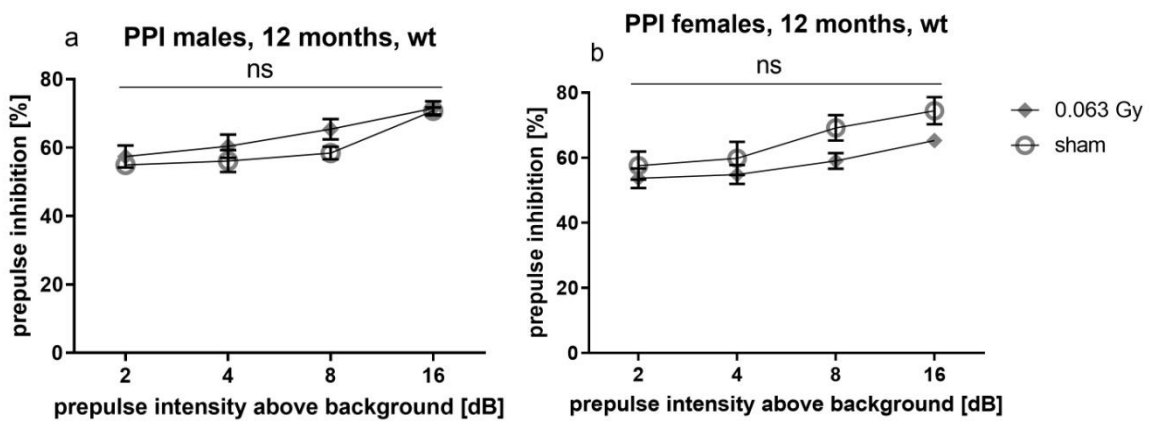


Fig.A.2.2.a.2) PPI – 12 months after exposure to 0.063 Gy. No significant differences were observed after exposure in PPI for wt males (a, treatment $F(1, 16) = 0.7922$; $p = 0.3866$) or wt females (b, treatment $F(1, 16) = 2.487$; $p = 0.1343$). Data are presented as means \pm SEM. For each group, $n = 8-10$.

2.2.b. ASR – 12 months after exposure to 0.125 Gy

No significant differences were observed in ASR/BW or PPI 12 months after exposure to 0.125 Gy in wt male or in female mice.

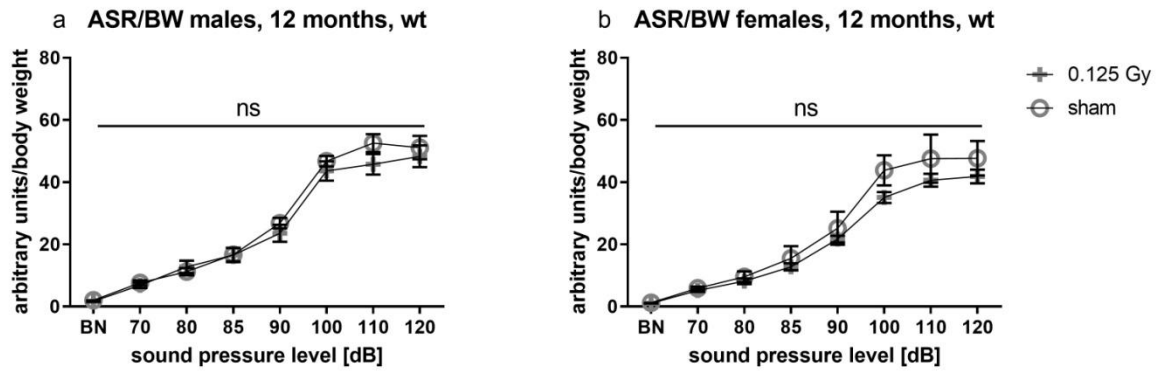


Fig. A.2.2.b.1) ASR – 12 months after exposure to 0.125 Gy. No significant differences were observed for ASR/BW for male wt mice (a, treatment F (1, 15) = 0.4763; p=0.5006), for ASR/BW for females wt mice (b, treatment F (1, 15) = 1.736; p=0.2074) Data are presented as means +/- SEM. For each group, n=8-10.

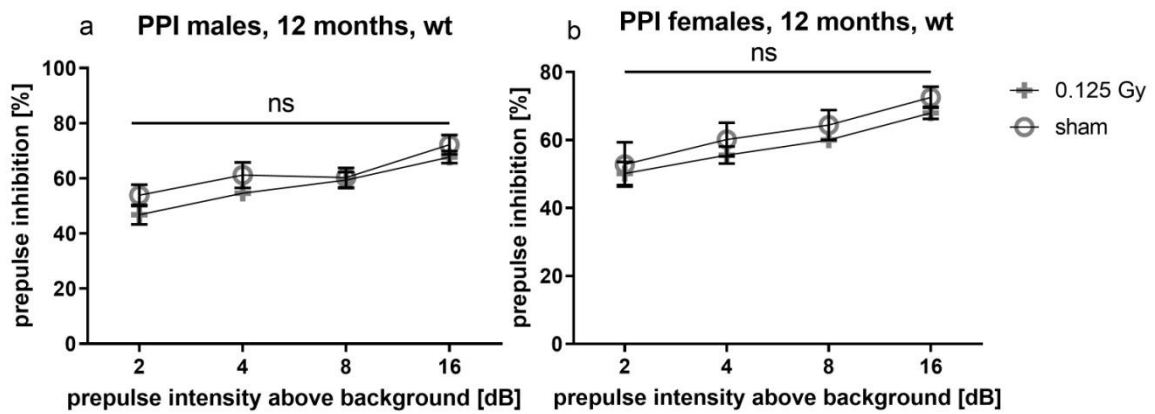


Fig.A.2.2.b.2). PPI – 12 months after exposure to 0.125 Gy. No significant differences were observed for PPI in wt male mice (a, treatment F (1, 15) = 1.105; p=0.3098) and for PPI in females wt mice (b, treatment F (1, 15) = 0.8039; p=0.3841). Data are presented as means +/- SEM. For each group, n=8-10.

2.2.c. ASR – 12 months after exposure to 0.5 Gy

No significant differences were observed in ASR/BW or PPI 12 months after exposure to 0.5 Gy in male or in female mice.

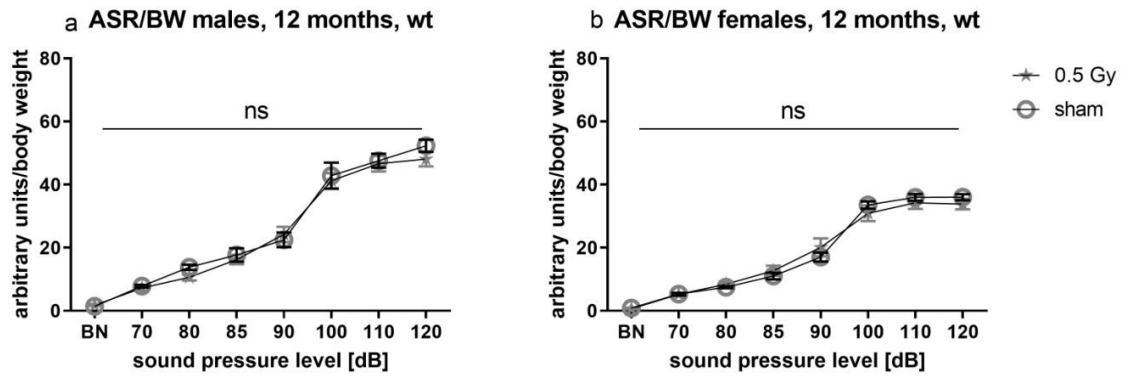


Fig. A.2.2.c.1) ASR – 12 months after exposure to 0.5 Gy. No significant differences were observed for ASR/BW for males wt mice (a, treatment $F(1, 15) = 0.4850$; $p=0.4968$) and for ASR/BW for females wt mice (b, treatment $F(1, 16) = 0.008539$; $p=0.9275$). Data are presented as means \pm SEM. For each group, $n=8-10$.

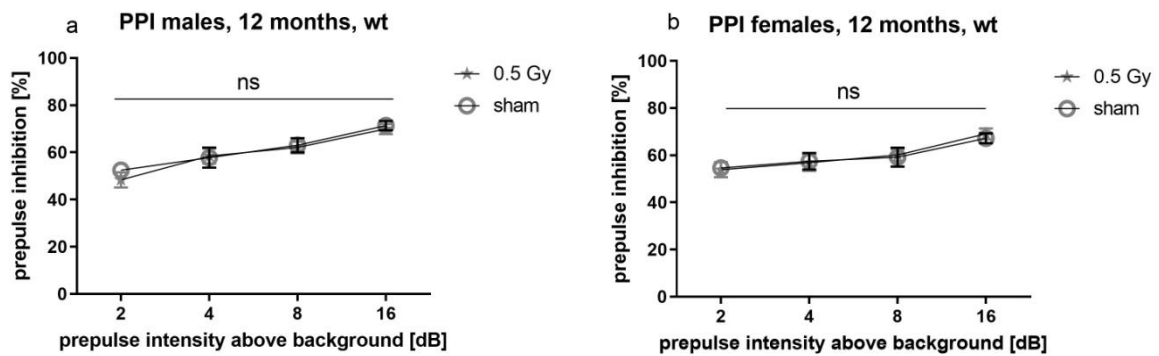


Fig.A.2.2.c.2). PPI – 12 months after exposure to 0.5 Gy. No significant differences were observed for PPI in males wt mice (a, treatment $F(1, 15) = 0.1573$; $p=0.6972$) and for PPI in females wt mice (b, treatment $F(1, 16) = 0.008024$; $p=0.9297$). Data are presented as means \pm SEM. For each group, $n=8-10$.

2.3. ASR - 18 months after exposure

2.3.a. ASR – 18 months after exposure to 0.063 Gy

At 18 months after exposure, after 0.063 Gy, PPI decreased in wt females (treatment $F(1, 15) = 9.857$, $p=0.0067$). After 0.125 Gy, ASR/BW decreased in wt females (interaction $F(7, 91) = 2.739$, $p=0.0126$, treatment $F(1, 13) = 11.01$, $p=0.0055$). After 0.5 Gy, no significant differences were observed.

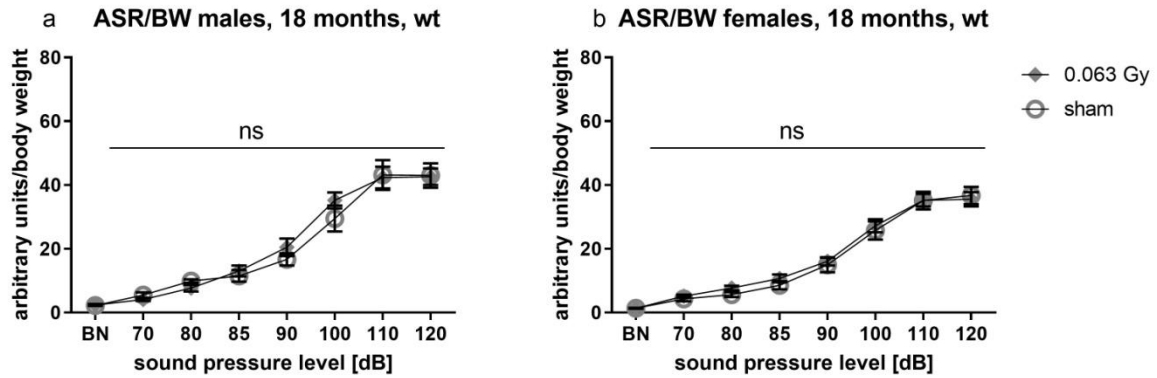


Fig.A.2.3.a.1) ASR – 18 months after exposure to 0.063 Gy. No significant differences were observed in ASR/BW in males wt mice (a, treatment $F(1, 13) = 0.09015$; $p=0.7687$) and in ASR/BW in females wt mice (b, treatment $F(1, 15) = 0.1958$; $p=0.6644$). Data are presented as means \pm SEM. For each group, $n=8-10$.

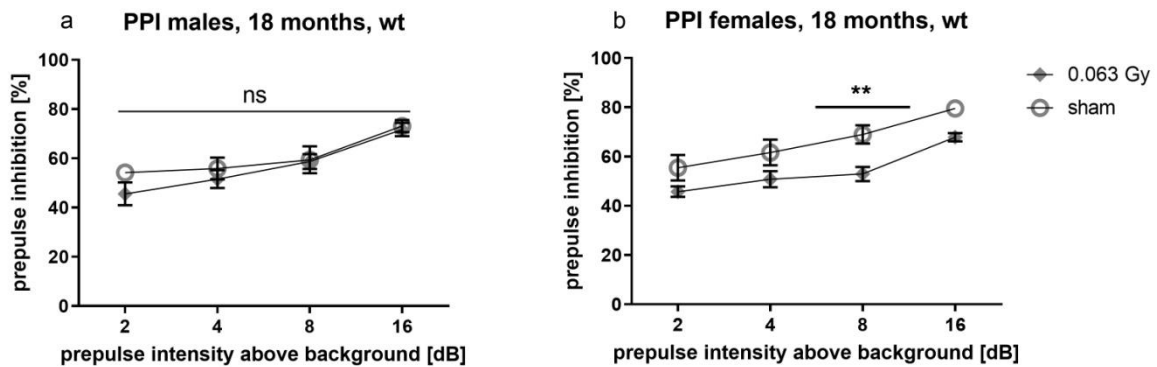


Fig.A.2.3.a.2) PPI – 18 months after exposure to 0.063 Gy. PPI decreased after 0.063 Gy in wt females at 8 dB (b, treatment $F(1, 15) = 9.857$; $p=0.0067$). No significant differences were observed for PPI in wt male mice (a, treatment $F(1, 13) = 0.5628$; $p=0.4665$). Data are presented as means \pm SEM. Results of the post-hoc tests are indicated on the graphs by ** $p<0.01$. For each group, $n=8-10$.

2.3.b. ASR – 18 months after exposure to 0.125 Gy

ASR/BW decreased after 0.125 Gy in wt females at 90 and 100 dB (treatment $F(1, 13) = 11.01$; $p=0.0055$). No significant differences were observed 18 months after exposure to 0.125 Gy in ASR/BW or in PPI in male mice and in PPI in both male and female wt mice.

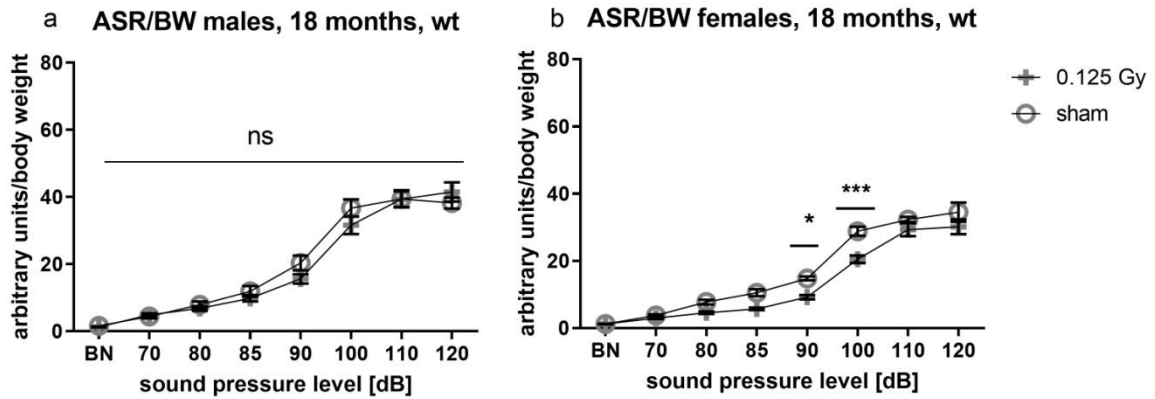


Fig.A.2.3.b.1) ASR – 18 months after exposure to 0.125 Gy. ASR/BW decreased after 0.125 Gy in wt females at 90 and 100 dB (b, treatment $F(1, 13) = 11.01$; $p = 0.0055$). No significant differences were observed in ASR/BW in wt male mice (a, treatment $F(1, 14) = 0.4191$; $p = 0.5278$). Data are presented as means \pm SEM. Results of the post-hoc tests are indicated on the graphs by * $p < 0.05$, *** $p < 0.001$. For each group, $n = 8-10$.

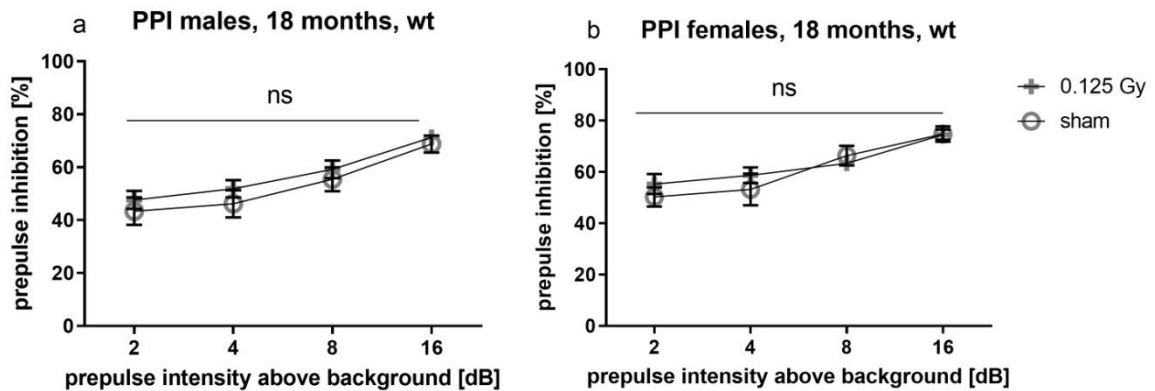


Fig.A.2.3.b.2) PPI – 18 months after exposure to 0.125 Gy. No significant differences were observed 18 months after exposure in PPI in wt male mice (a, treatment $F(1, 14) = 0.6639$; $p = 0.4288$) or in PPI in females wt mice (b, treatment $F(1, 13) = 0.1521$; $p = 0.7028$). Data are presented as means \pm SEM. For each group, $n = 8-10$.

2.3.c. ASR – 18 months after exposure to 0.5 Gy

No significant differences were observed 18 months after exposure to 0.5 Gy in ASR/BW or in PPI for both male and female wt mice.

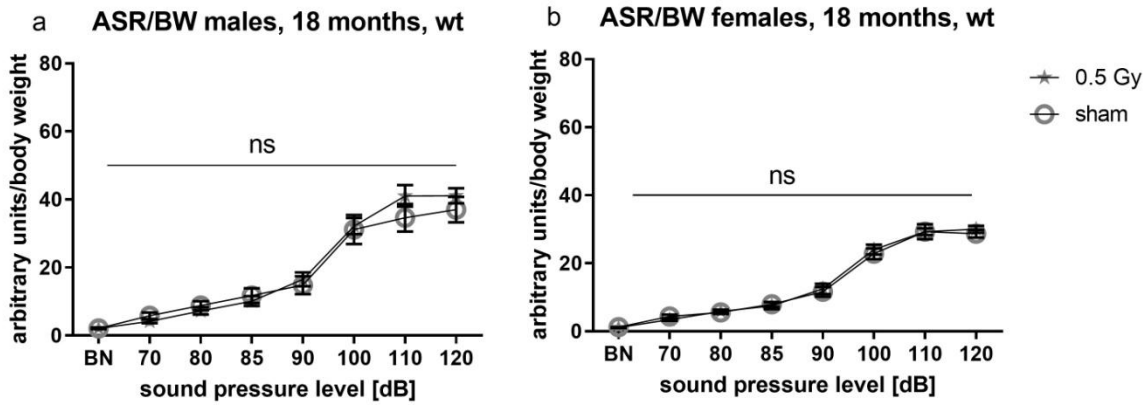


Fig. A.2.3.c.1) ASR – 18 months after exposure to 0.5 Gy. Data are presented as means +/- SEM. For each group, n=8-10. No significant differences were observed in ASR/BW in wt male mice (a, treatment F (1, 16) = 0.1103; p=0.7441) or in ASR/BW in wt female mice (b, treatment F (1, 16) = 2.112; p=0.1654).

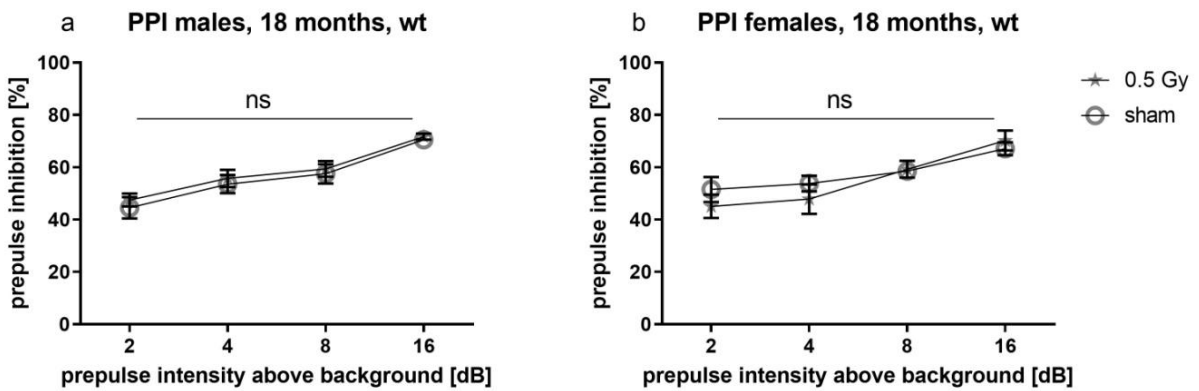


Fig. A.2.3.c.2) PPI – 18 months after exposure to 0.5 Gy. No significant differences were observed 18 months after exposure to 0.125 Gy in PPI for wt male mice (a, treatment F (1, 16) = 0.4782; p=0.4992) or in PPI for female wt mice (b, treatment F (1, 16) = 0.05539; p=0.8169).

3. Social discrimination (SD)

This test evaluates olfactory capacities and social interest. From the investigation time (in seconds) measured in the sample phase and in the test phase, a recognition index is calculated by dividing the time spent investigating the unknown subject by sum of time spent investigating both unknown and familiar subjects.

Wildtype and heterozygous animals were analyzed separately, as well as male and females, always comparing sham versus irradiated animals.

Each graph represented the performance of each group for one of the mentioned parameters. Each symbol represents the performance of one individual. Sham animals are represented by empty circles, 0.063 Gy-irradiated animals are represented by filled lozenges, 0.125 Gy-irradiated animals are represented by crosses and 0.5 Gy-irradiated animals are represented by filled stars.

For each graph, on the left side of the graph, male sham animals are compared to irradiated male animals and the right side of the graph female sham animals are compared to irradiated female.

Results were analyzed with 2-way ANOVA to look at the effect of sex, treatment and their interaction. Post-hoc analyses were performed with Sidak's multiple comparisons test.

3.1. SD – 4 months after exposure

At 4 months after exposure, recognition index decreased in wt males after 0.5 Gy (interaction $F(1, 32) = 12.97$, $p=0.0011$, treatment $F(1, 32) = 4.639$, $p=0.0389$). No significant differences were observed in any of the other groups.

3.1.a. SD – 4 months after exposure to 0.063 Gy

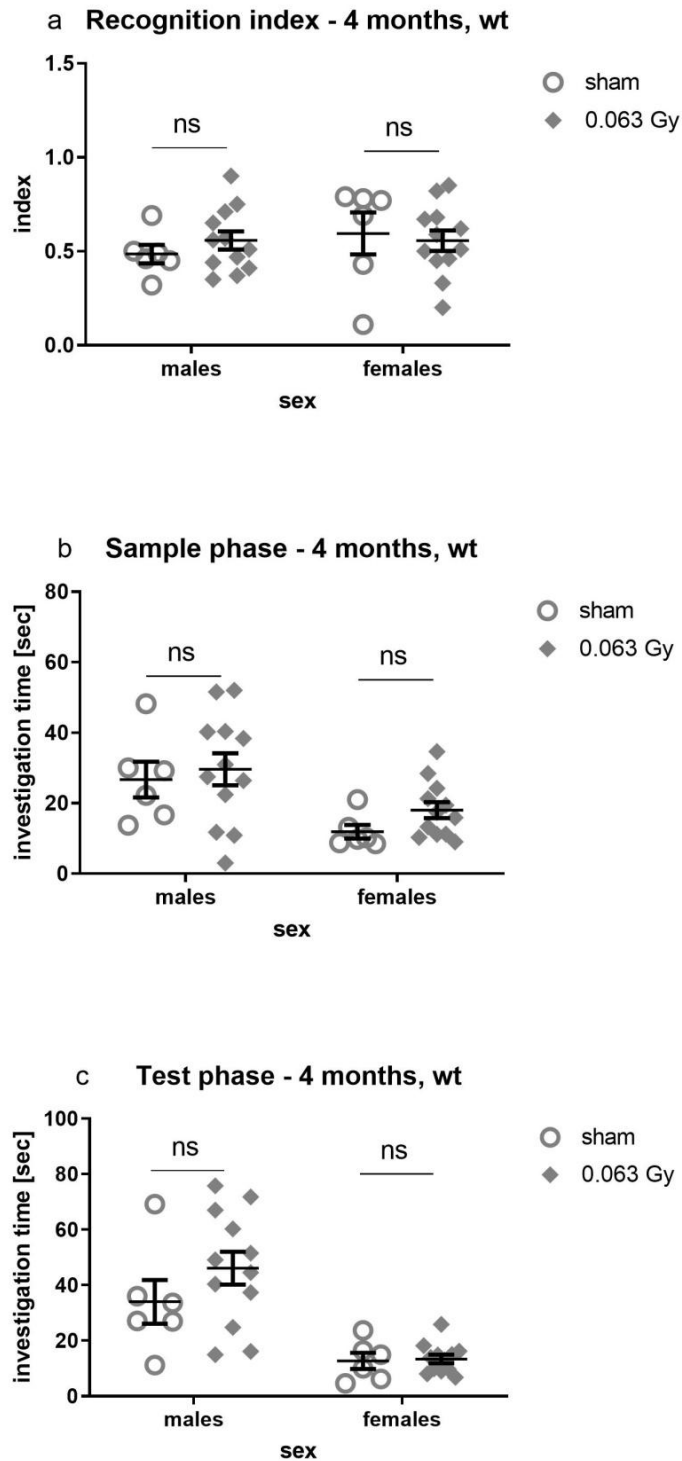


Fig. A.3.1.a. SD – 4 months after exposure to 0.063 Gy. No significant differences were observed in recognition index (a, treatment $F(1, 32) = 0.06502$; $p=0.8004$), in sample phase (b, treatment $F(1, 32) = 1.222$; $p=0.2772$) or in test phase (c, treatment $F(1, 32) = 1.496$; $p=0.2302$) in wt animals. Data is presented as a scatter plot +/- SEM. $n=6-12$ animals.

3.1.b. SD – 4 months after exposure to 0.125 Gy

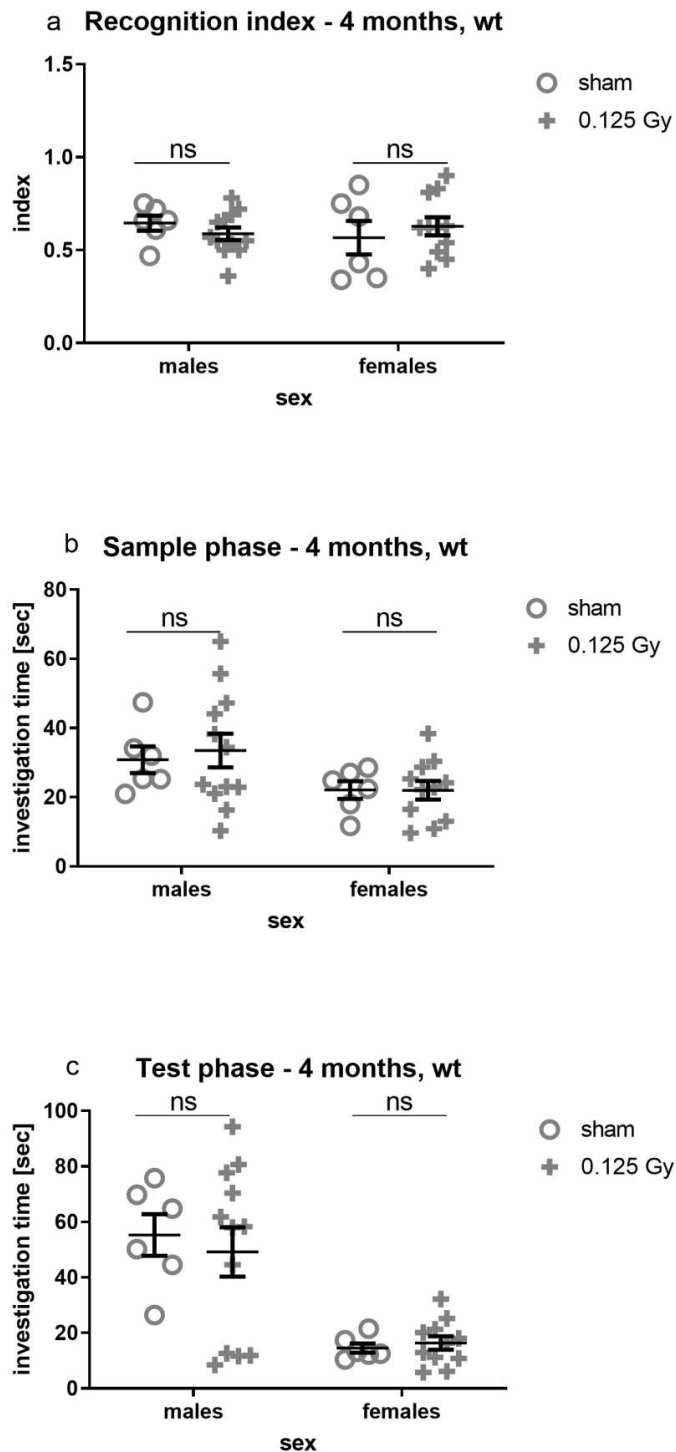


Fig. A.3.1.b. SD – 4 months after exposure to 0.125 Gy. No significant differences were observed in recognition index (a, treatment $F(1, 31) = 0.002054$; $p = 0.9641$), sample phase (b, treatment $F(1, 31) = 0.08779$; $p = 0.7690$) and test phase (c, treatment $F(1, 31) = 0.08589$; $p = 0.7714$). Data is presented as a scatter plot +/- SEM. $n = 6-12$ animals.

3.1.b. SD – 4 months after exposure to 0.5 Gy

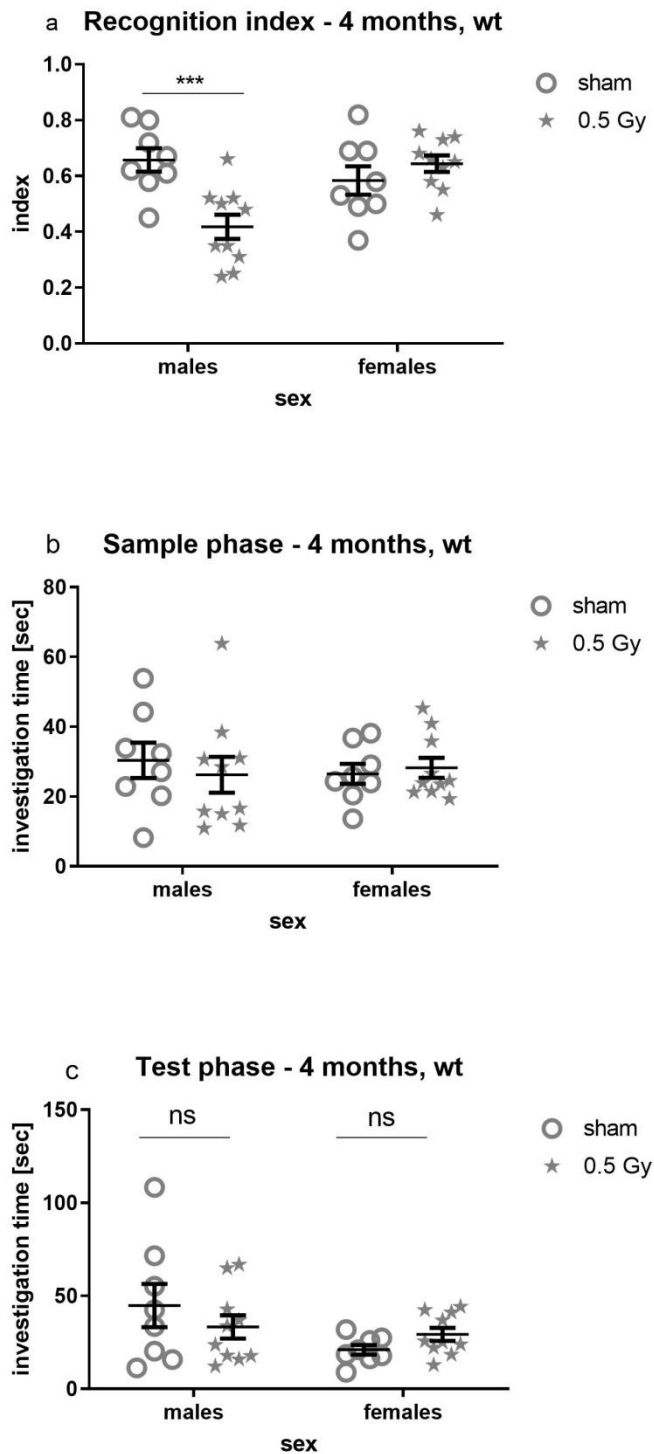


Fig.A.3.1.c. SD - 4 months after exposure to 0.5 Gy. Recognition index decreased in wt males (a, treatment $F(1, 32) = 4.639$; $p=0.0389$; interaction $F(1, 32) = 12.97$; $p=0.0011$). No significant differences were observed in sample phase (b, treatment $F(1, 32) = 0.08178$; $p=0.7767$) and in test phase (c, treatment $F(1, 32) = 0.06108$; $p=0.8064$). Data is presented as a scatter plot +/- SEM. Results of the post-hoc test are indicated on the graph by *** $p<0.001$. $n=8-10$ animals.

3.2. SD – 12 months after exposure

Any significant effects of radiation exposure were observed at 12 months after exposure in any of the irradiated groups.

3.2.a. SD – 12 months after exposure to 0.063 Gy

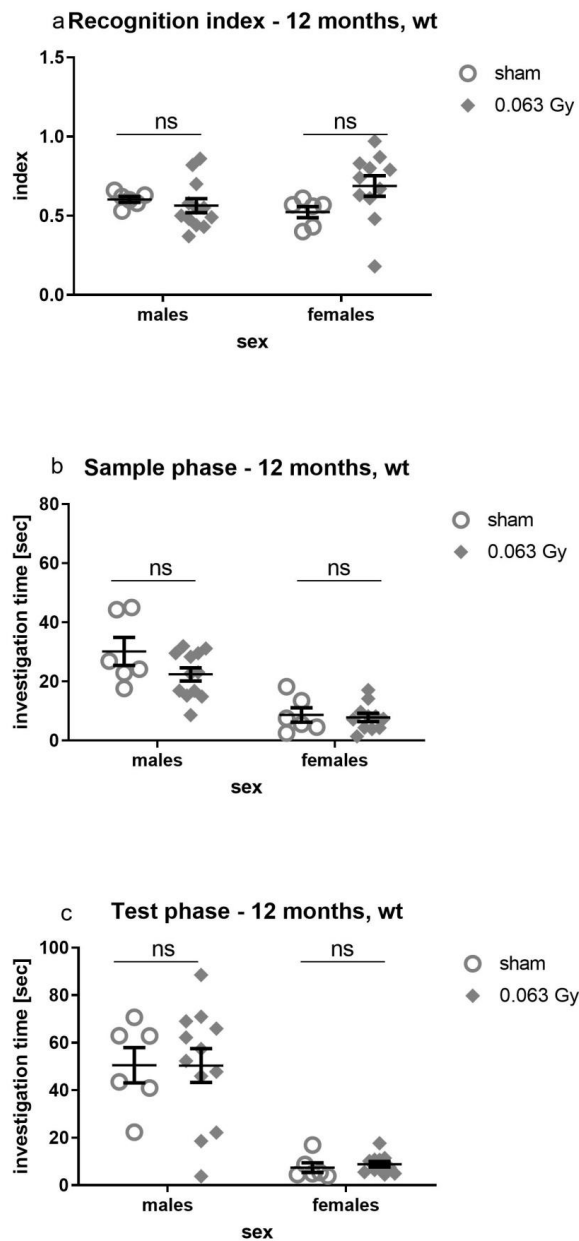


Fig. A.3.2.a. SD – 12 months after exposure to 0.063 Gy. No significant differences were observed in recognition index (a, treatment $F(1, 31) = 1.242$; $p=0.273$), sample phase (b, treatment $F(1, 31) = 2.602$; $p=0.1169$) and test phase (c, treatment $F(1, 31) = 0.01211$; $p=0.9131$). Data is presented as a scatter plot +/- SEM. $n=6-12$ animals.

3.2.b. SD – 12 months after exposure to 0.125 Gy

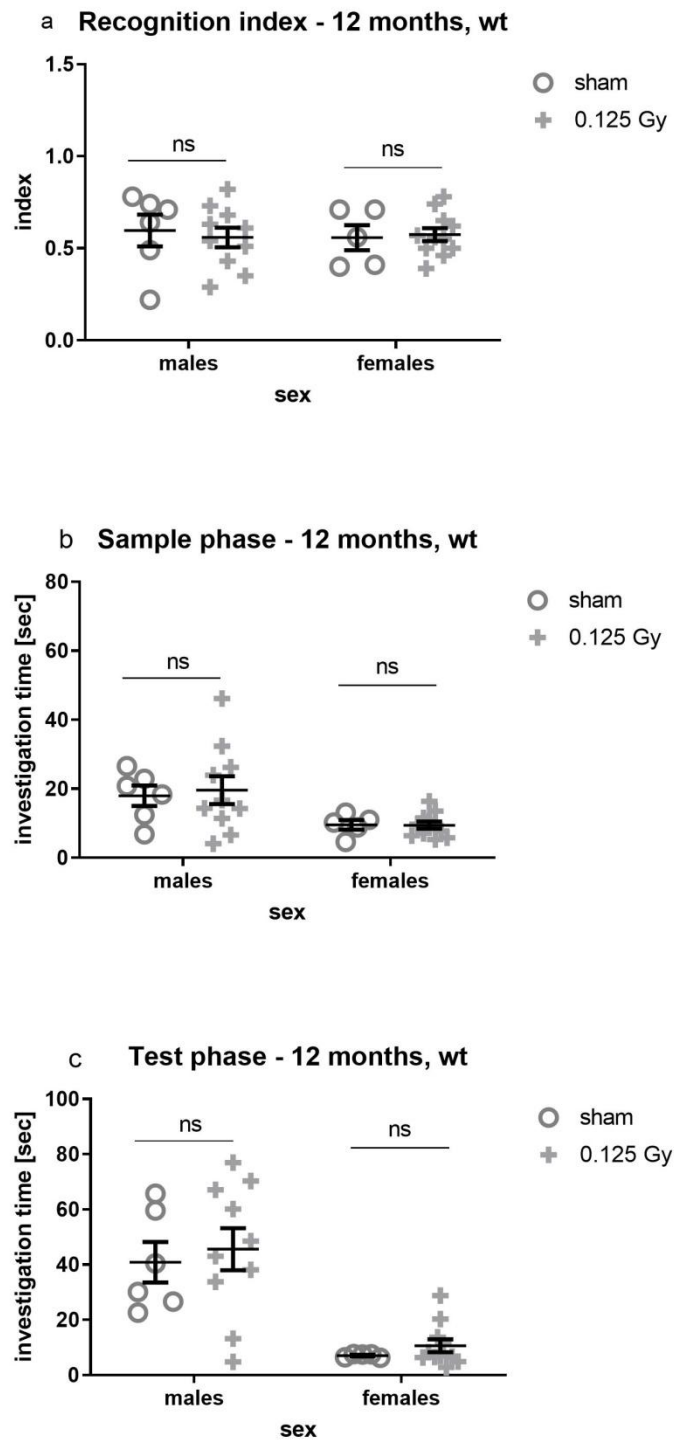


Fig. A.3.2.b. SD – 12 months after exposure to 0.125 Gy. No significant differences were observed in recognition index (a, treatment $F(1, 28) = 0.03170$; $p = 0.8600$), sample phase (b, treatment $F(1, 28) = 0.06301$; $p = 0.8036$) and test phase (c, treatment $F(1, 28) = 0.4632$; $p = 0.5017$) in wt mice. Data is presented as a scatter plot \pm SEM. $n = 6-12$ animals.

3.2.c. SD – 12 months after exposure to 0.5 Gy

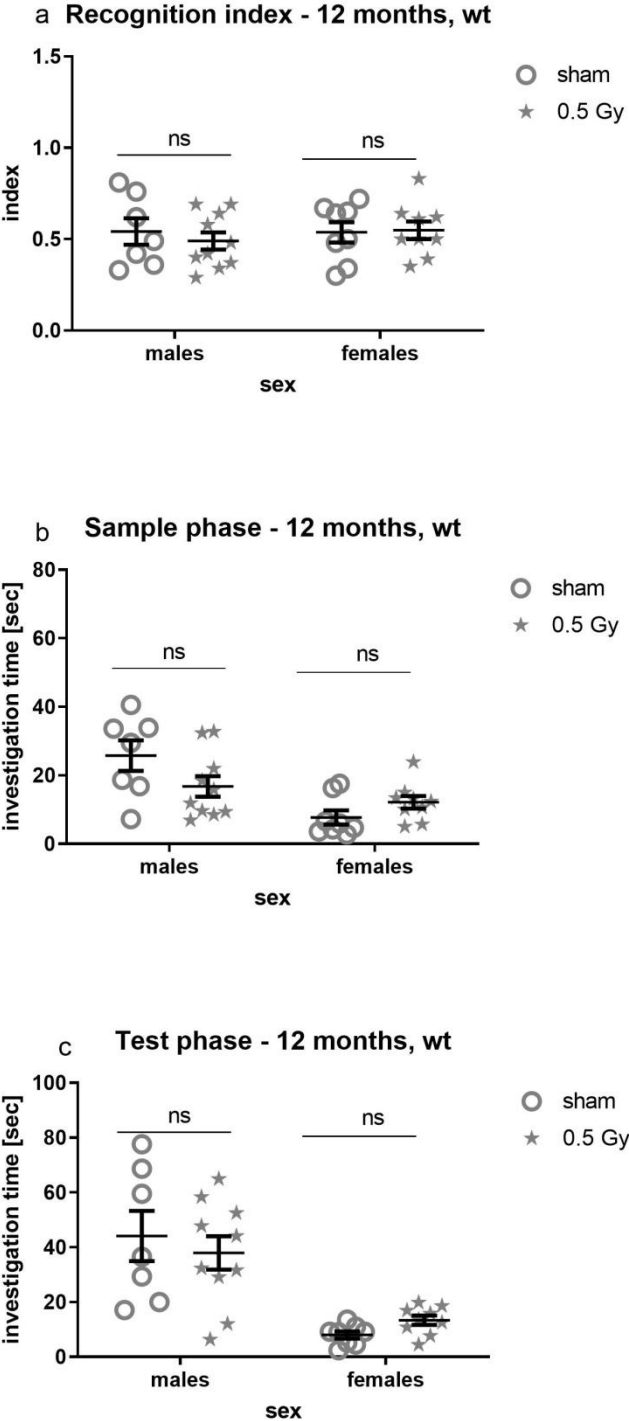


Fig.A.3.2.c. SD – 12 months after exposure to 0.5 Gy. No significant differences were observed in recognition index (a, treatment F (1, 30) = 0.1314; p=0.7195), sample phase (b, treatment F (1, 30) = 0.6113; p=0.4404) or test phase (c, treatment F (1, 30) = 0.005974; p=0.9389) in wt mice. Data is presented as a scatter plot +/- SEM. n=8-10 animals.

3.3. SD – 18 months after exposure

At 18 months after exposure to 0.5 Gy, investigation time decreased during the sample phase in wt males after exposure to 0.5 Gy (treatment $F(1, 27) = 6.993$; $p=0.0135$; interaction $F(1, 27) = 8.337$; $p=0.0076$) and during the test phase as well (treatment $F(1, 27) = 4.798$; $p=0.0373$). No significant differences were observed for any of the other groups.

3.3.a. SD – 18 months after exposure to 0.063 Gy

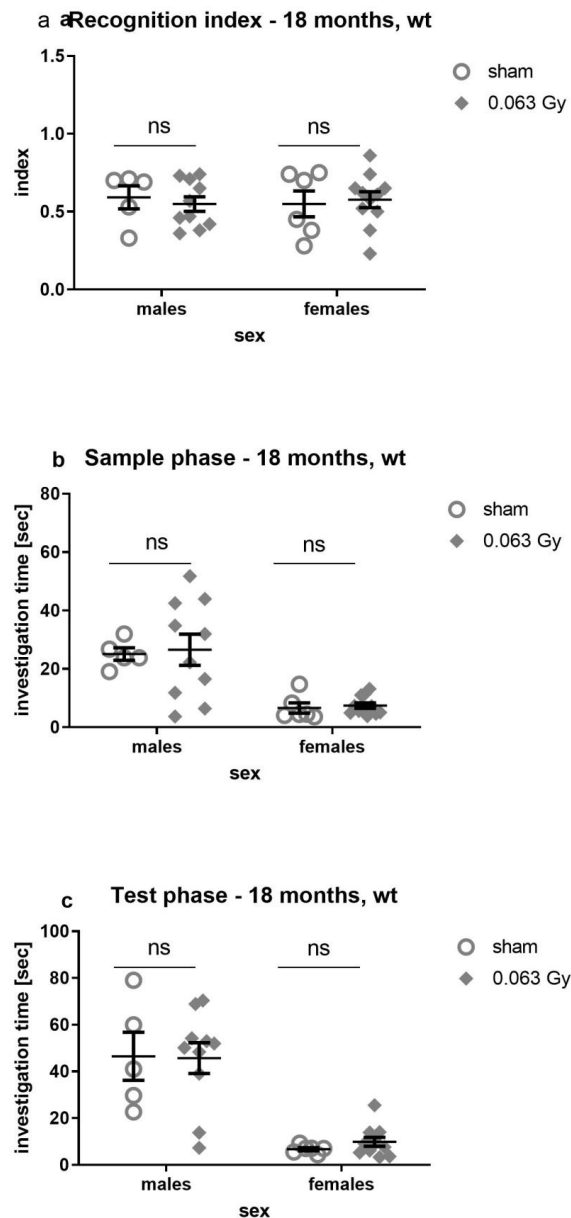


Fig.A.3.3.a.SD – 18 months after exposure to 0.063 Gy. No significant differences were observed in recognition index (a, treatment $F(1, 28) = 0.01332$; $p=0.9089$), sample phase (b, treatment $F(1, 28) = 0.09348$; $p=0.7621$) or test phase (c, treatment $F(1, 28) = 0.04173$; $p=0.8396$). Data is presented as a scatter plot +/- SEM. $n=6-11$ animals.

3.3.b. SD – 18 months after exposure to 0.125 Gy

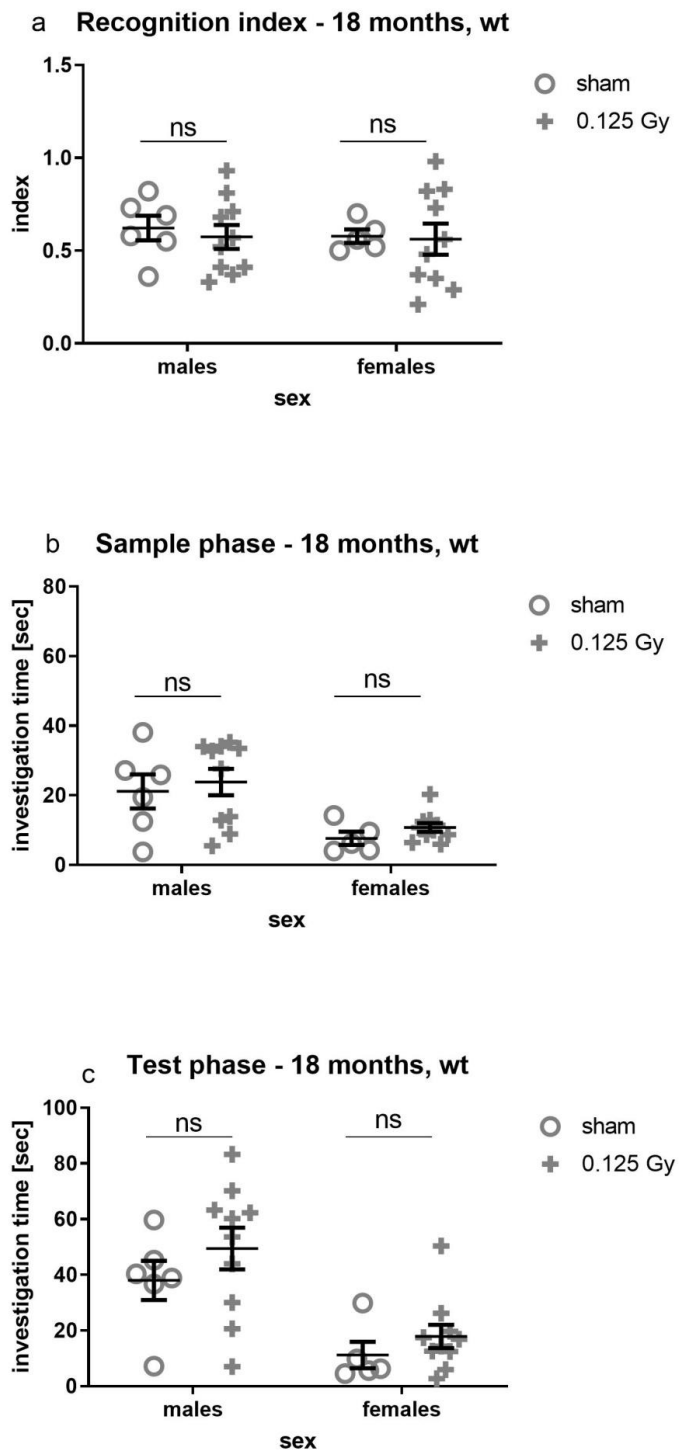


Fig.A.3.3.b. SD – 18 months after exposure to 0.125 Gy. No significant differences were observed in investigation time (a, treatment $F(1, 27) = 0.1673$; $p=0.6858$), sample phase (b, treatment $F(1, 27) = 0.7097$; $p=0.4070$) and test phase (c, treatment $F(1, 27) = 1.805$; $p=0.1902$). Data is presented as a scatter plot +/- SEM. n=6-11 animals

3.3.c. SD – 18 months after exposure to 0.5 Gy

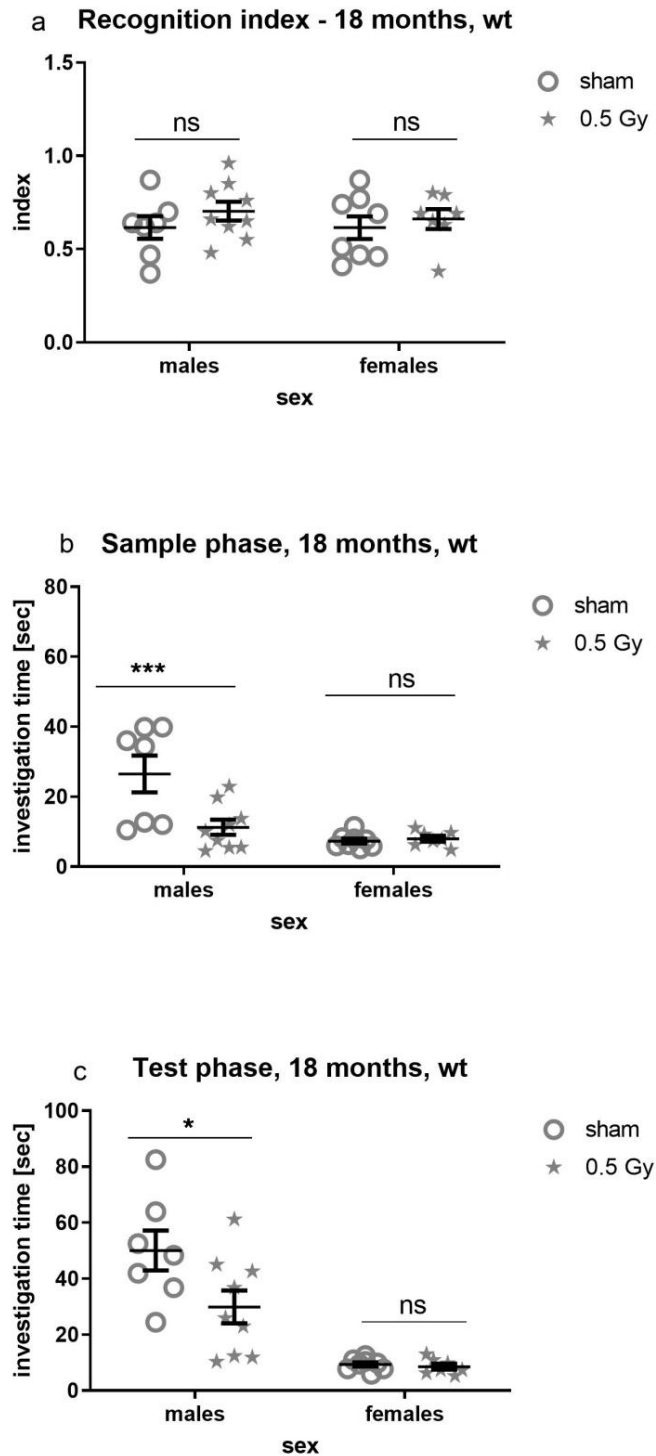


Fig.A.3.3.c. SD – 18 months after exposure to 0.5 Gy. No significant differences were observed on recognition index (a, treatment $F(1, 27) = 1.397$; $p=0.2476$). Investigation time decreased during the sample phase in wt males after exposure to 0.5 Gy (b, treatment $F(1, 27) = 6.993$; $p=0.0135$; interaction $F(1, 27) = 8.337$; $p=0.0076$). Investigation time decreased during the test phase in wt males after 0.5 Gy (c, treatment $F(1, 27) = 4.798$; $p=0.0373$). Data are presented as scatter plots +/- SEM. Results of the post-hoc tests are indicated on the graphs by * $p<0.05$, *** $p<0.001$. $n=6-11$ animals.

B. Heterozygous *Ercc2*^{S737P} mice

1. Open field (OF)

1. 1. OF – 4 months after exposure

1. 1.a. OF – 4 months after exposure to 0.063 Gy

No significant effects on spontaneous locomotion, explorative behavior and anxiety were observed 4 months after exposure to 0.063 Gy, for both sexes.

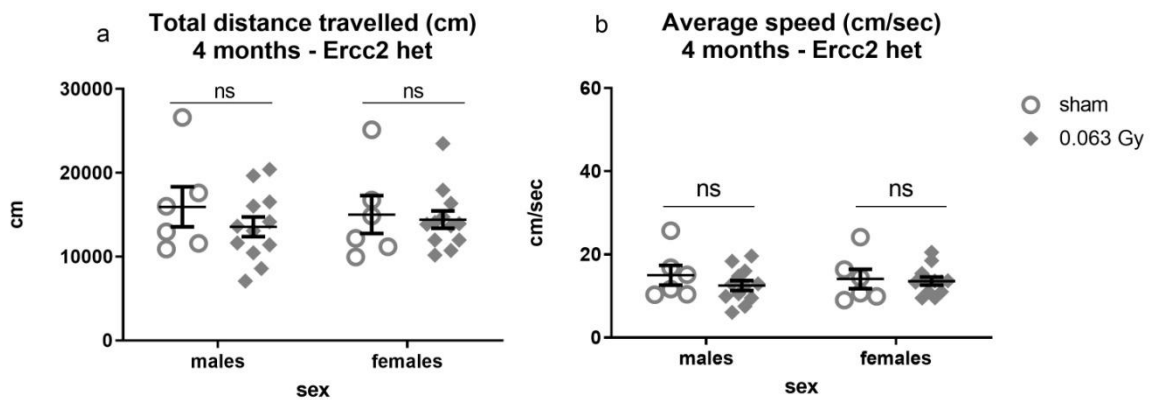


Fig. B.1.1.a.1) Spontaneous locomotion at 4 months post-irradiation with 0.063 Gy. Total distance travelled and average speed were analyzed with 2-way ANOVA and Sidak's multiple comparisons test to decipher the effect of treatment on both sexes and to detect potential sex-specific treatment effects (i.e. treatment x sex interaction). No significant differences were observed in total distance (a, treatment $F(1, 32) = 0.8783$; $p = 0.3557$) and average speed (b, treatment $F(1, 32) = 0.8738$; $p = 0.3569$). Data is presented as a scatter plot +/- SEM, $n = 6-12$ animals.

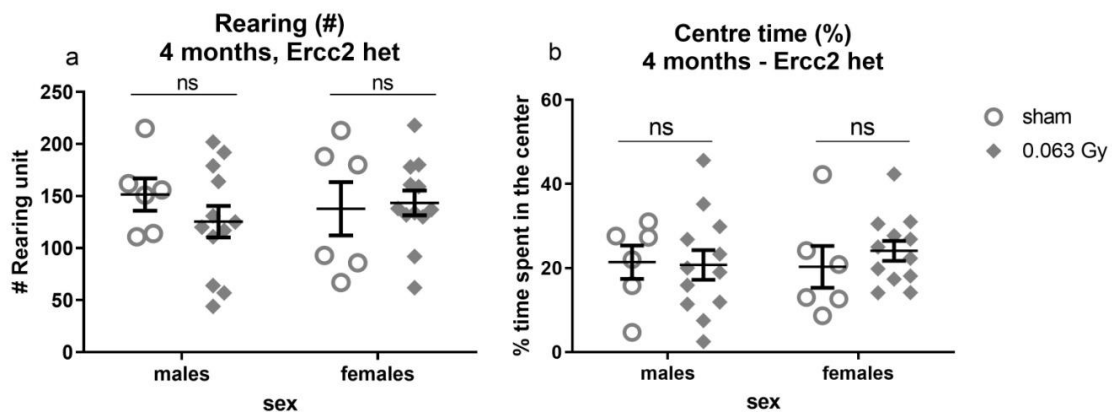


Fig. B.1.1.a.2) Explorative behavior and anxiety at 4 months post-irradiation with 0.063 Gy. Rearing and centre time were analyzed with 2-way ANOVA and Sidak's multiple comparisons test to decipher the effect of treatment on both sexes and to detect potential sex-specific treatment effects (i.e. treatment x sex interaction). No significant differences were observed in rearing (a, treatment $F(1, 32) = 0.3541$; $p = 0.5560$) and centre time (b, treatment $F(1, 32) = 0.1772$; $p = 0.6766$). Data is presented as a scatter plot +/- SEM, $n = 6-12$ animals.

1.b. OF – 4 months after exposure to 0.125 Gy

No significant effects on spontaneous locomotion, explorative behavior and anxiety were observed 4 months after exposure to 0.125 Gy, for both sexes.

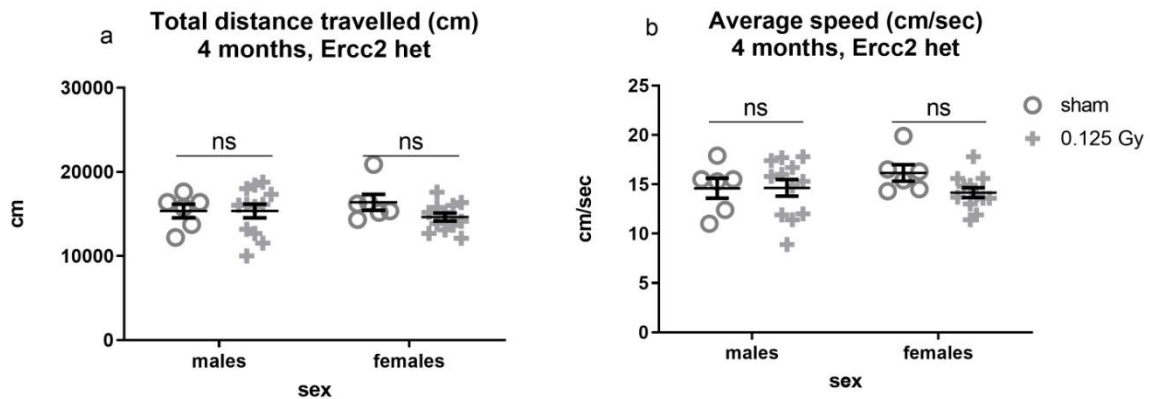


Fig. B.1.1.b.1) Spontaneous locomotion at 4 months post-irradiation with 0.125 Gy. Total distance travelled and average speed were analyzed with 2-way ANOVA and Sidak's multiple comparisons test to decipher the effect of treatment on both sexes and to detect potential sex-specific treatment effects (i.e. treatment x sex interaction). No significant differences were observed in total distance (a, treatment $F(1, 32) = 1.197$; $p = 0.2821$) and average speed (b, treatment $F(1, 32) = 1.380$; $p = 0.487$). Data is presented as a scatter plot +/- SEM, $n = 6-12$ animals.

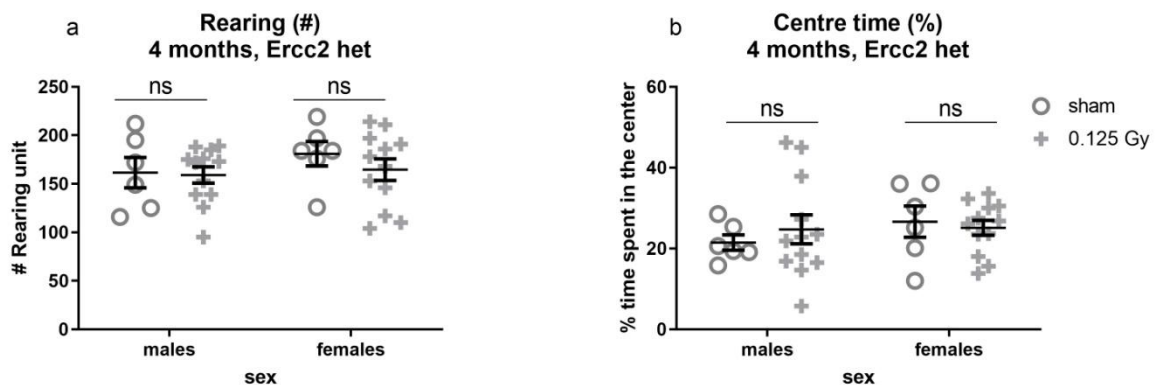


Fig. B.1.1.b.2) Explorative behavior and anxiety at 4 months post-irradiation with 0.125 Gy in *Ercc2*^{S737P} heterozygous animals. Rearing and centre time were analyzed with 2-way ANOVA and Sidak's multiple comparisons test to decipher the effect of treatment on both sexes and to detect potential sex-specific treatment effects (i.e. treatment x sex interaction). No significant differences were observed in rearing (a, treatment $F(1, 32) = 0.5945$; $p = 0.4463$) and centre time (b, treatment $F(1, 32) = 0.07303$; $p = 0.7887$). Data is presented as a scatter plot +/- SEM, $n = 6-12$ animals.

1.c. OF – 4 months after exposure with 0.5 Gy

No significant effects on spontaneous locomotion, explorative behavior and anxiety were observed 4 months after exposure to 0.5 Gy, for both sexes.

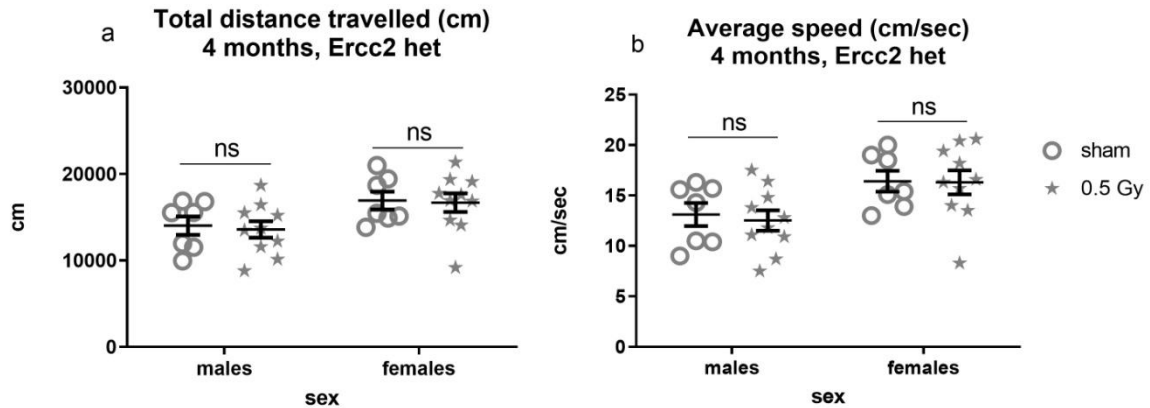


Fig. B.1.1.c.1) Spontaneous locomotion at 4 months post-irradiation with 0.5 Gy. Total distance travelled and average speed were analyzed with 2-way ANOVA and Sidak's multiple comparisons test to decipher the effect of treatment on both sexes and to detect potential sex-specific treatment effects (i.e. treatment x sex interaction). No significant differences were observed in total distance (a, treatment $F(1, 30) = 0.1031$; $p = 0.7503$) and average speed (b, treatment $F(1, 30) = 0.09478$; $p = 0.7603$). Data is presented as a scatter plot +/- SEM, $n = 8-10$ animals.

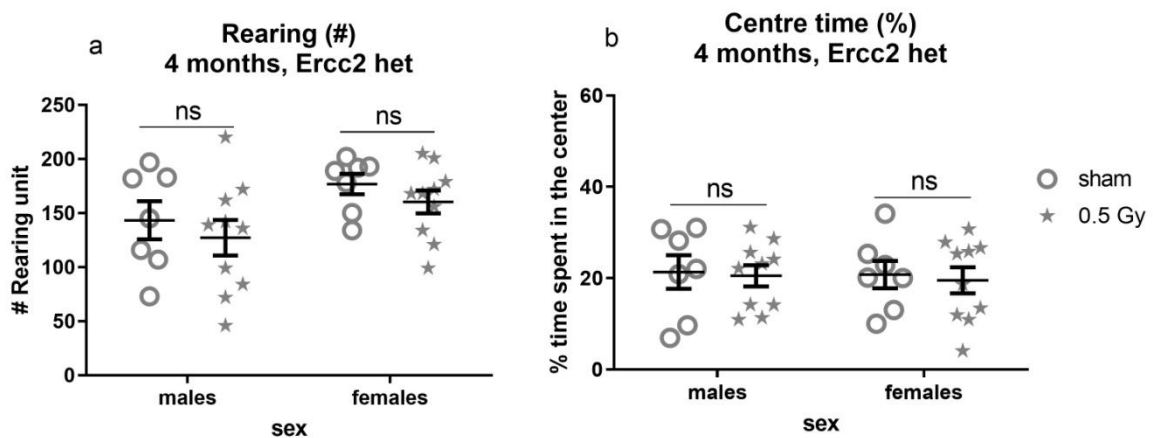


Fig. B.1.1.c.2) Explorative behavior and anxiety at 4 months post-irradiation with 0.5 Gy. Rearing and centre time were analyzed with 2-way ANOVA and Sidak's multiple comparisons test to decipher the effect of treatment on both sexes and to detect potential sex-specific treatment effects (i.e. treatment x sex interaction). No significant differences were observed in rearing (a, treatment $F(1, 30) = 1.275$; $p = 0.2678$) and centre time (b, treatment $F(1, 30) = 0.1240$; $p = 0.7272$). Data is presented as a scatter plot +/- SEM, $n = 8-10$ animals.

1. 2. OF – 12 months after exposure
1. 2. a. OF – 12 months after exposure with 0.063 Gy

No significant effects on spontaneous locomotion, explorative behavior and anxiety were observed 12 months after exposure to 0.063 Gy, for both sexes.

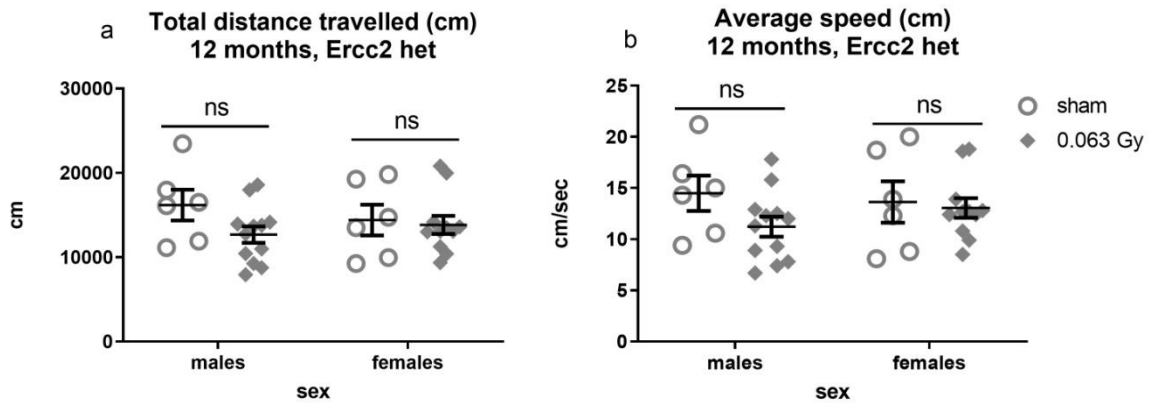


Fig. B.1.2.a.1) Spontaneous locomotion at 12 months post-irradiation with 0.063 Gy. Total distance travelled and average speed were analyzed with 2-way ANOVA and Sidak's multiple comparisons test to decipher the effect of treatment on both sexes and to detect potential sex-specific treatment effects (i.e. treatment x sex interaction). No significant differences were observed in total distance (a, treatment $F(1, 31) = 2.229$; $p = 0.1456$) and average speed (b, treatment $F(1, 31) = 2.054$; $p = 0.1618$). Data is presented as a scatter plot +/- SEM. $n = 6-12$ animals.

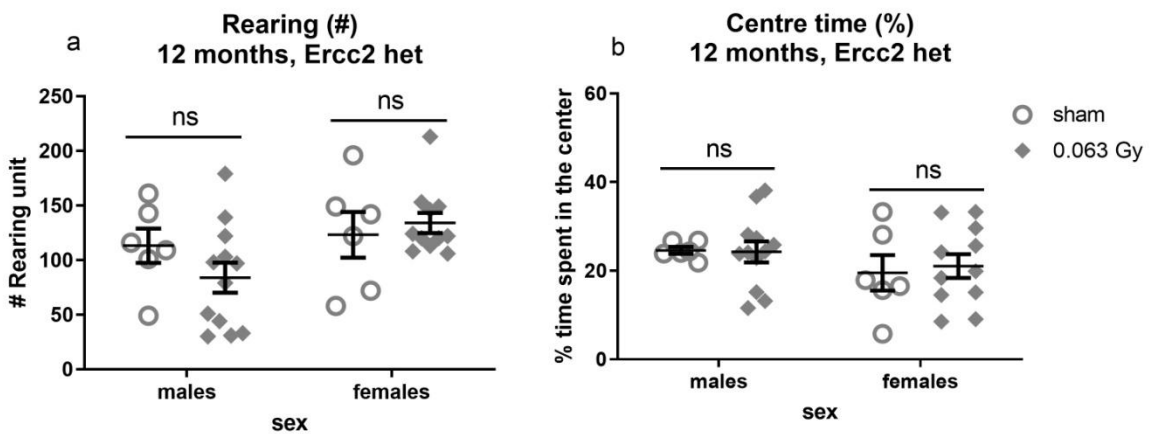


Fig. B.1.2.a.2). Explorative behavior and anxiety at 12 months post-irradiation with 0.063 Gy. Rearing and centre time were analyzed with 2-way ANOVA and Sidak's multiple comparisons test to decipher the effect of treatment on both sexes and to detect potential sex-specific treatment effects (i.e. treatment x sex interaction). No significant differences were observed in rearing (a, treatment $F(1, 31) = 0.3771$; $p = 0.5436$) and centre time (b, treatment $F(1, 31) = 0.04067$; $p = 0.8415$). Data is presented as a scatter plot +/- SEM, $n = 6-12$ animals.

1.2.b. OF – 12 months after exposure with 0.125 Gy

No significant effects on spontaneous locomotion, explorative behavior and anxiety were observed 12 months after exposure to 0.125 Gy, for both sexes.

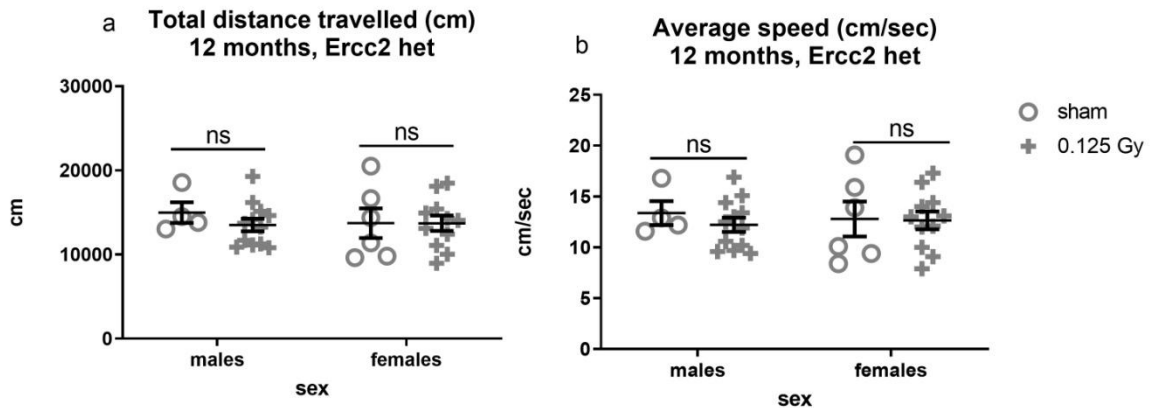


Fig. B.1.2.b.1) Spontaneous locomotion at 12 months post-irradiation with 0.125 Gy. Total distance travelled and average speed were analyzed with 2-way ANOVA and Sidak's multiple comparisons test to decipher the effect of treatment on both sexes and to detect potential sex-specific treatment effects (i.e. treatment x sex interaction). No significant differences were observed in total distance (a, treatment $F(1, 29) = 0.3906$; $p = 0.536$) and average speed (b, treatment $F(1, 29) = 0.3197$; $p = 0.5761$). Data is presented as a scatter plot +/- SEM, $n = 6-11$ animals.

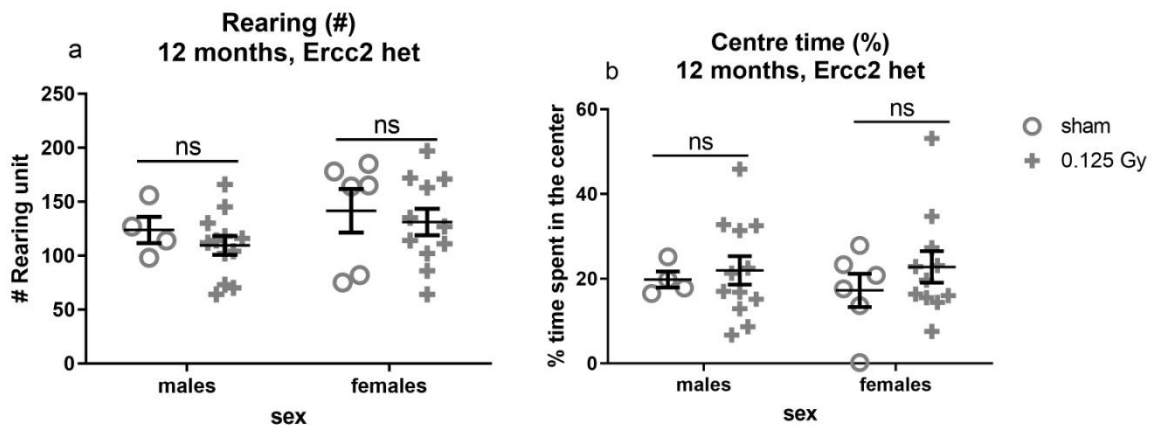


Fig. B.1.2.b.2) Explorative behavior and anxiety at 12 months post-irradiation with 0.125 Gy in het animals. Rearing and centre time were analyzed with 2-way ANOVA and Sidak's multiple comparisons test to decipher the effect of treatment on both sexes and to detect potential sex-specific treatment effects (i.e. treatment x sex interaction). No significant differences were observed in rearing (a, treatment $F(1, 29) = 0.7305$; $p = 0.3997$) and centre time (b, treatment $F(1, 29) = 0.8244$; $p = 0.3714$). Data is presented as a scatter plot +/- SEM, $n = 6-12$ animals.

1.2.c. OF – 12 months after exposure with 0.5 Gy

No significant effects on spontaneous locomotion, explorative behavior and anxiety were observed 12 months after exposure to 0.5 Gy, for both sexes.

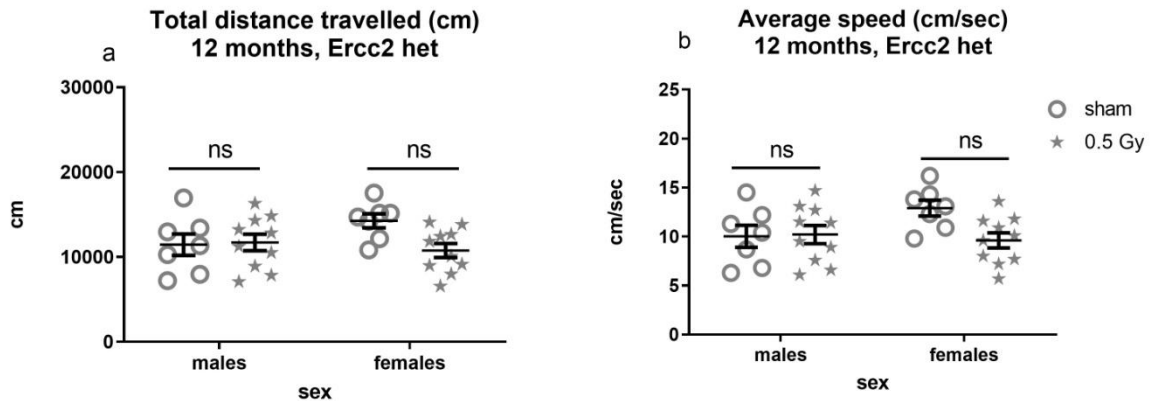


Fig. B.1.2.c.1) Spontaneous locomotion at 12 months post-irradiation with 0.5 Gy. Total distance travelled and average speed were analyzed with 2-way ANOVA and Sidak's multiple comparisons test to decipher the effect of treatment on both sexes and to detect potential sex-specific treatment effects (i.e. treatment x sex interaction). No significant differences were observed in total distance (a, treatment $F(1, 30) = 2.646$; $p = 0.1143$) and average speed (b, treatment $F(1, 30) = 2.838$; $p = 0.1024$). Data is presented as a scatter plot +/- SEM. $n = 8-10$ animals.

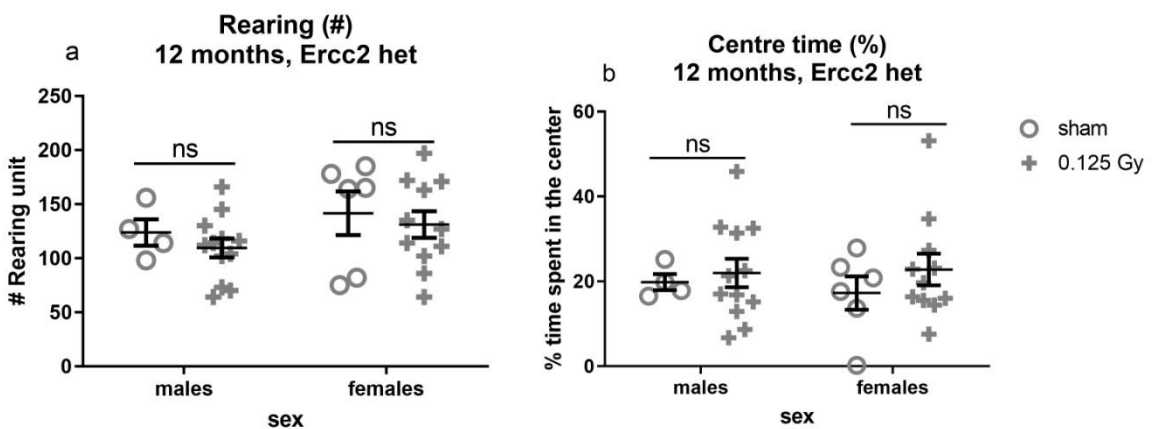


Fig. B.1.2.c.2) Explorative behavior and anxiety at 12 months post-irradiation with 0.5 Gy. Rearing and centre time were analyzed with 2-way ANOVA and Sidak's multiple comparisons test to decipher the effect of treatment on both sexes and to detect potential sex-specific treatment effects (i.e. treatment x sex interaction). No significant differences were observed in rearing (a, treatment $F(1, 30) = 2.215$; $p = 0.1471$) and centre time (b, treatment $F(1, 30) = 0.1590$; $p = 0.6929$). Data is presented as a scatter plot +/- SEM. $n = 6-12$ animals.

1.3. OF – 18 months after exposure

18 months after exposure to ionizing radiation, decreased center time (increased anxiety) has been detected in 0.125 Gy-irradiated male mice, and significant treatment effect on spontaneous locomotion has been observed on 0.5 Gy-irradiated mice.

1.3.a. OF – 18 months after exposure with 0.063 Gy

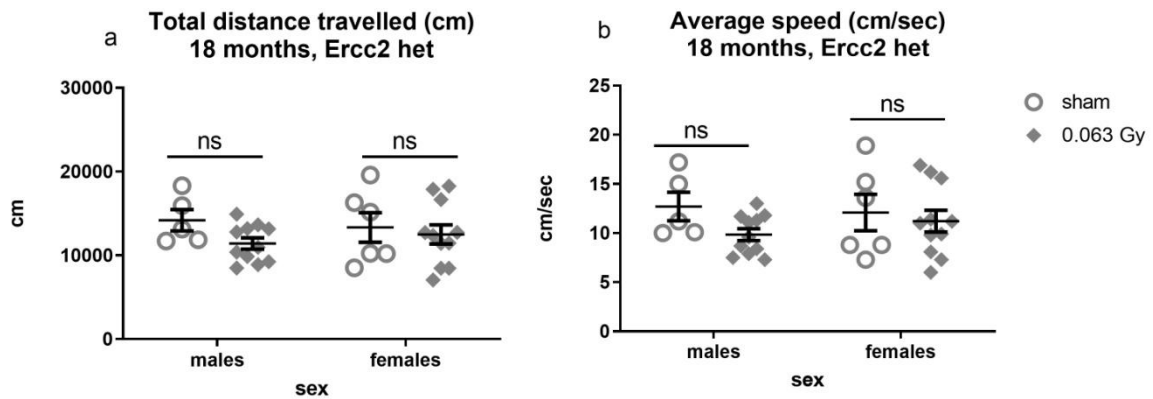


Fig. B.1.3.a.1) Spontaneous locomotion at 18 months post-irradiation with 0.063 Gy. Total distance travelled and average speed were analyzed with 2-way ANOVA and Sidak's multiple comparisons test to decipher the effect of treatment on both sexes and to detect potential sex-specific treatment effects (i.e. treatment x sex interaction). No significant differences were observed in total distance (a, treatment $F(1, 29) = 2.173$; $p=0.1513$) and average speed (b, treatment $F(1, 29) = 2.326$; $p=0.1381$). Data is presented as a scatter plot +/- SEM. $n=6-11$ animals

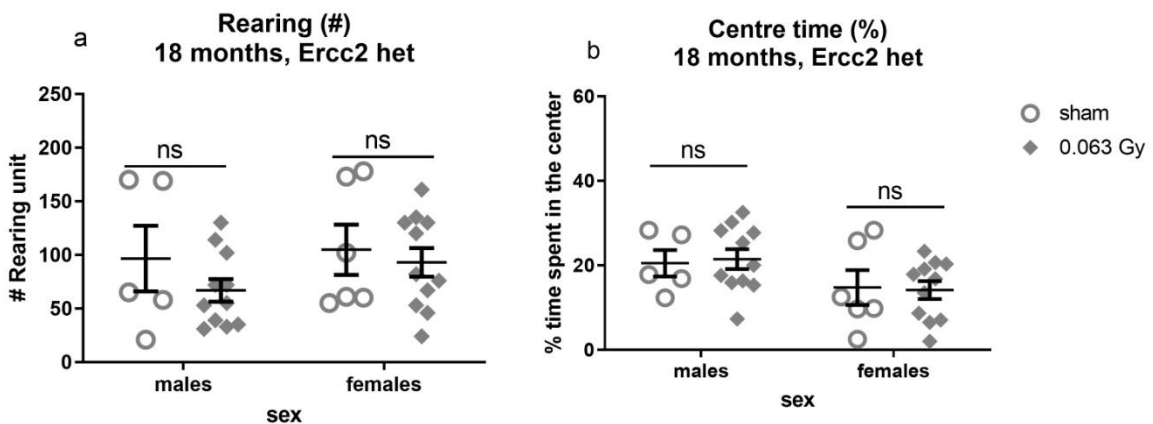


Fig. B.1.3.a.2) Explorative behavior and anxiety at 18 months post-irradiation with 0.063 Gy. Rearing and centre time were analyzed with 2-way ANOVA and Sidak's multiple comparisons test to decipher the effect of treatment on both sexes and to detect potential sex-specific treatment effects (i.e. treatment x sex interaction). No significant differences were observed in rearing (a, treatment $F(1, 29) = 1.358$; $p=0.2533$) and centre time (b, treatment $F(1, 29) = 0.004600$; $p=0.9464$). Data is presented as a scatter plot +/- SEM. $n=6-12$ animals.

1.3.b. OF – 18 months after exposure with 0.125 Gy

Decreased center time (increased anxiety) has been detected in 0.125 Gy-irradiated male mice, 18 months after exposure.

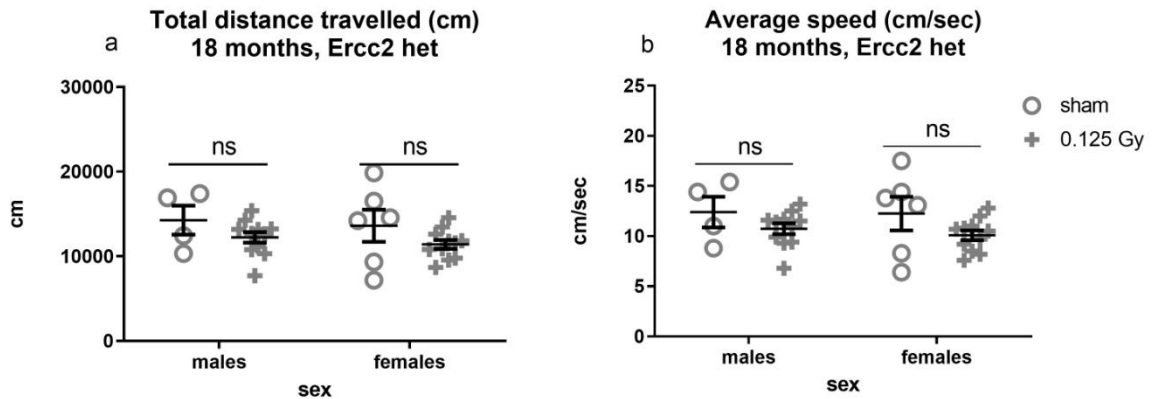


Fig. B.1.3.b.1) Spontaneous locomotion at 18 months post-irradiation with 0.125 Gy. Total distance travelled and average speed were analyzed with 2-way ANOVA and Sidak's multiple comparisons test to decipher the effect of treatment on both sexes and to detect potential sex-specific treatment effects (i.e. treatment x sex interaction). No significant differences were observed in total distance (a, treatment $F(1, 28) = 3.837$; $p=0.0602$) and average speed (b, treatment $F(1, 28) = 3.977$; $p=0.0560$). Data is presented as a scatter plot +/- SEM. $n=4-11$ animals.

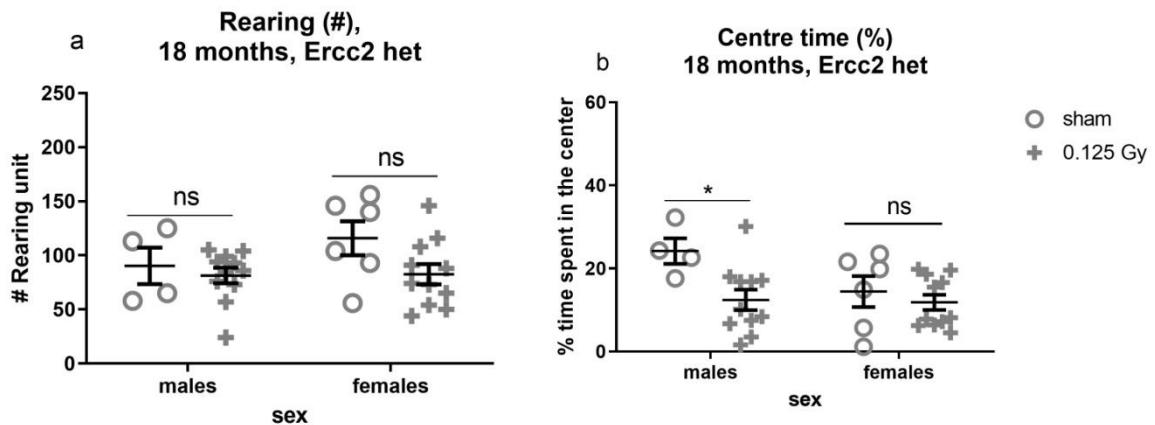


Fig. B.1.3.b.2) Exploratory behavior and anxiety at 18 months post-irradiation with 0.125 Gy. Rearing and centre time were analyzed with 2-way ANOVA and Sidak's multiple comparisons test to decipher the effect of treatment on both sexes and to detect potential sex-specific treatment effects (i.e. treatment x sex interaction). No significant differences were observed in rearing (a, treatment $F(1, 28) = 3.166$; $p=0.0860$). Centre time was decreased after 0.125 Gy irradiation in Ercc2 het male mice 18 months after exposure (b, treatment $F(1, 28) = 6.123$; $p=0.0197$) but not in Ercc2 het females. Data is presented as a scatter plot +/- SEM. Results of the post-hoc tests are indicated on the graphs by * $p<0.05$. $n=4-12$ animals.

1.3.c. OF – 18 months after exposure with 0.5 Gy

18 months after exposure to ionizing radiation, significant treatment effect on spontaneous locomotion (total distance travelled and average speed) has been observed on 0.5 Gy-irradiated mice.

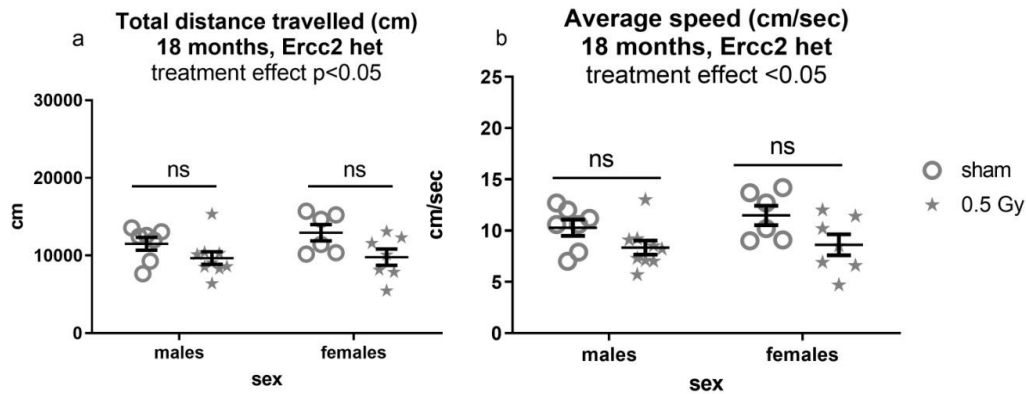


Fig. B.1.3.c.1) Spontaneous locomotion at 18 months post-irradiation with 0.5 Gy. Total distance travelled and average speed were analyzed with 2-way ANOVA and Sidak's multiple comparisons test to decipher the effect of treatment on both sexes and to detect potential sex-specific treatment effects (i.e. treatment x sex interaction). A significant treatment effect was observed in total distance (a, treatment effect $F(1, 25) = 7.067$; $p = 0.0135$) and average speed (b, treatment $(1, 25) = 7.772$; $p = 0.0100$). Post-hoc tests were not significant. Data is presented as a scatter plot +/- SEM. $n = 4-11$ animals

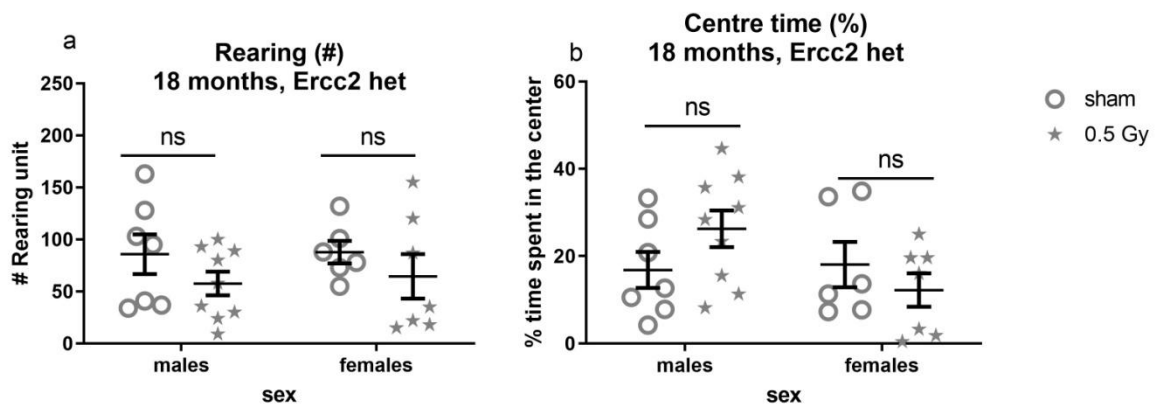


Fig. B.1.3.c.2) Explorative behavior and anxiety at 18 months post-irradiation with 0.5 Gy. Rearing and centre time were analyzed with 2-way ANOVA and Sidak's multiple comparisons test to decipher the effect of treatment on both sexes and to detect potential sex-specific treatment effects (i.e. treatment x sex interaction). No significant differences were observed in rearing (a, treatment $F(1, 25) = 2.497$; $p = 0.1266$) and centre time (b, treatment $F(1, 25) = 0.1658$; $p = 0.6874$). Data is presented as a scatter plot +/- SEM. $n = 6-12$

2. Acoustic startle test (ASR)

2.1. Acoustic startle test (ASR), 4 months after exposure

2.1.a. Acoustic startle test (ASR), 4 months after exposure to 0.063 Gy

No significant effects on acoustic startle/body weight or prepulse inhibition were observed 4 months after exposure to 0.063 Gy, for both sexes.

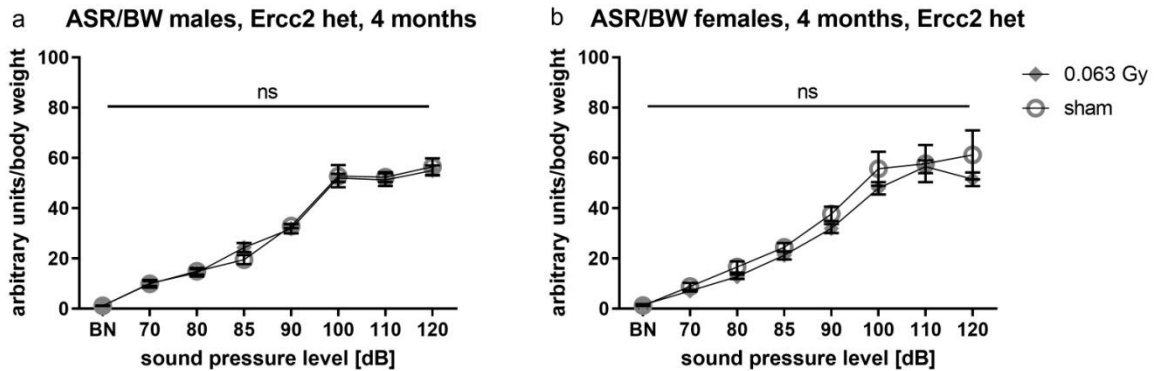


Fig.B.2.1.a.1) ASR – 4 months after exposure to 0.063 Gy. No significant differences were observed for ASR/BW for *Ercc2*^{S737P} heterozygous males (a, treatment F (1, 16) = 3.754e-005; p=0.9952) or female (b, treatment F (1, 15) = 1.669; p=0.2159) 18 months after exposure to 0.063 Gy. Data are presented as means +/- SEM. For each group, n=8-10.

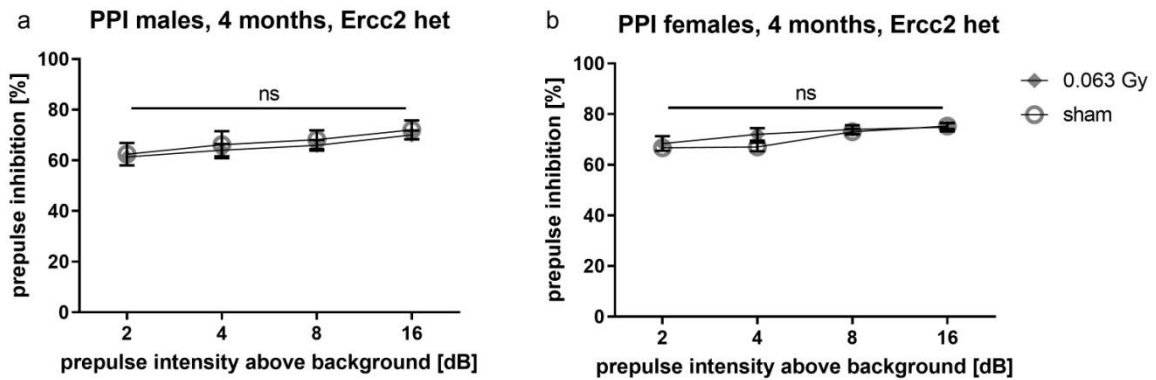


Fig.B.2.1.a.2) PPI – 4 months after exposure to 0.063 Gy. No significant differences were observed 4 months after exposure to 0.063 Gy in PPI for *Ercc2*^{S737P} heterozygous male mice (a, treatment F (1, 16) = 0.2322; p=0.6364) or in PPI for female mice (b, treatment F (1, 15) = 0.3875; p=0.5430). Data are presented as means +/- SEM. For each group, n=8-10.

2.1.b Acoustic startle test (ASR), 4 months with 0.125 Gy

No significant differences were observed on ASR/BW or PPI, 4 months after exposure to 0.125 Gy, either for male or female mice.

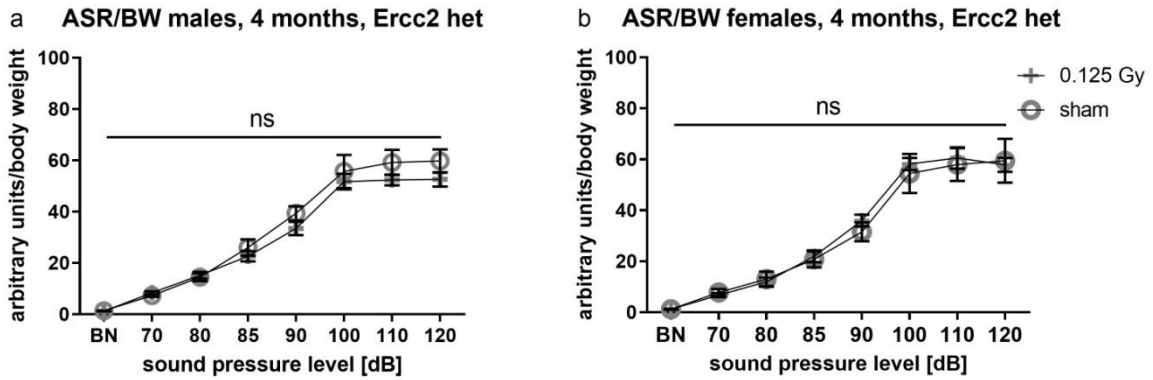


Fig.B.2.1.b.1) ASR – 4 months after exposure to 0.125 Gy. No significant differences were observed for ASR/BW for *Ercc2*^{S737P} heterozygous males (a, treatment F (1, 16) = 1.336; p=0.2647) or female (b, treatment F (1, 16) = 0.08969; p=0.7684) mice 4 months after exposure to 0.125 Gy. Data are presented as means +/- SEM. For each group, n=8-10.

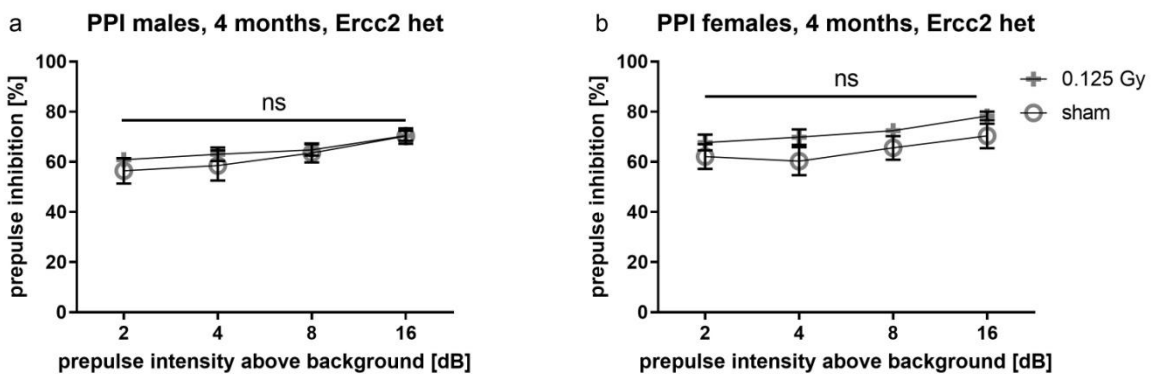


Fig.B.2.1.b.2) PPI – 4 months after exposure to 0.125 Gy. No significant differences were observed 4 months after exposure to 0.125 Gy in PPI for *Ercc2*^{S737P} heterozygous male mice (a, treatment F (1, 16) = 0.4080; p=0.5320) or in PPI for female *Ercc2*^{S737P} heterozygous mice (b, treatment F (1, 16) = 2.523; p=0.1318). Data are presented as means +/- SEM. For each group, n=8-10.

2.1.c. Acoustic startle test (ASR), 4 months with 0.5 Gy

4 months after exposure to 0.5 Gy, ASR/BW increased in females *Ercc2*^{S737P} het mice after 110 dB.

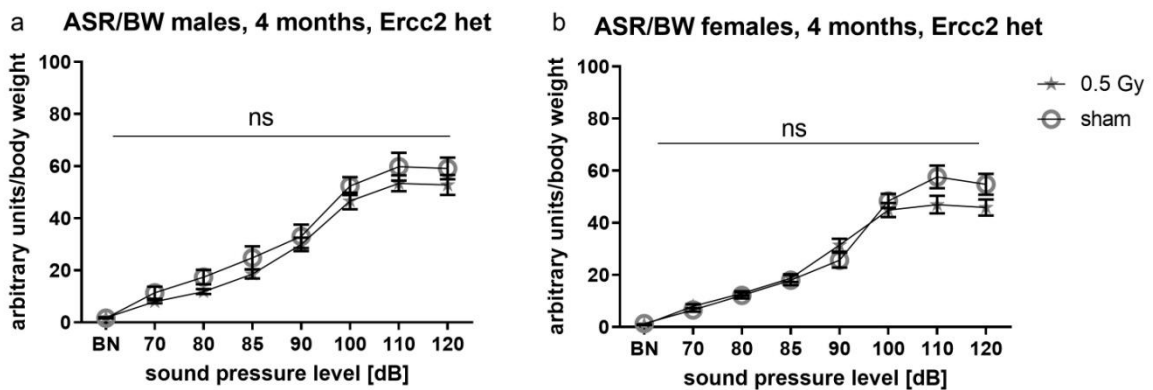


Fig.B.2.1.c.1) ASR – 4 months after exposure to 0.5 Gy. No significant differences were observed for ASR/BW for *Ercc2*^{S737P} het males (a, treatment F (1, 15) = 2.147; p=0.1635) or female (b, treatment F (1, 15) = 0.5950; p=0.4525) mice 4 months after exposure to 0.5 Gy. Data are presented as means +/- SEM. For each group, n=8-10.

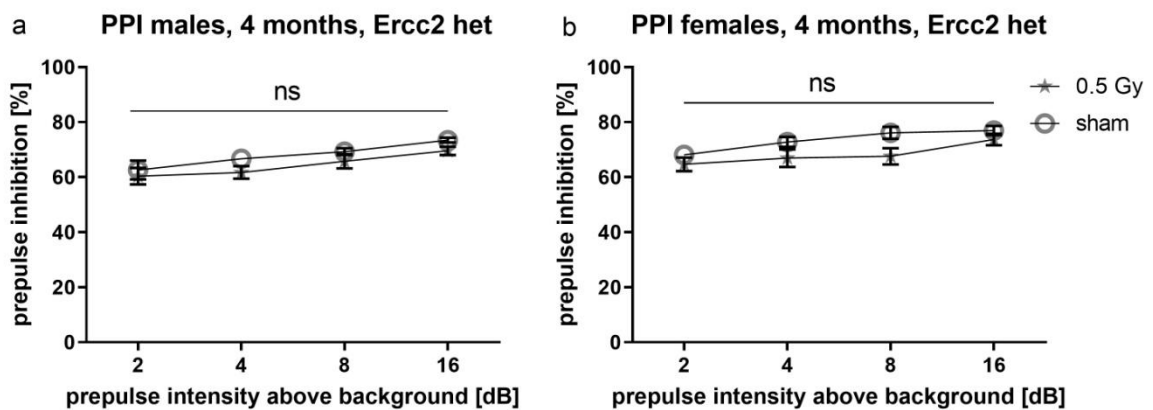


Fig.B.2.1.c.2) PPI - 4 months after exposure to 0.5 Gy. No significant differences were observed 4 months after exposure to 0.5 Gy in PPI for *Ercc2*^{S737P} het male mice (a, treatment F (1, 15) = 1.877; p=0.1908) or in PPI for female *Ercc2*^{S737P} het mice (b, treatment F (1, 15) = 2.523; p=0.1331). Data are presented as means +/- SEM. For each group, n=8-10.

2.2. Acoustic startle test (ASR), 12 months after exposure

2.2.b. Acoustic startle test (ASR), 12 months after exposure to 0.063 Gy

12 months after exposure to 0.063 Gy, no significant differences were observed on ASR/BW in *Ercc2*^{S737P} het male mice but ASR/BW at 90 dB decreased in female *Ercc2*^{S737P} het mice. No significant differences were observed on PPI after exposure, either on male or on female mice.

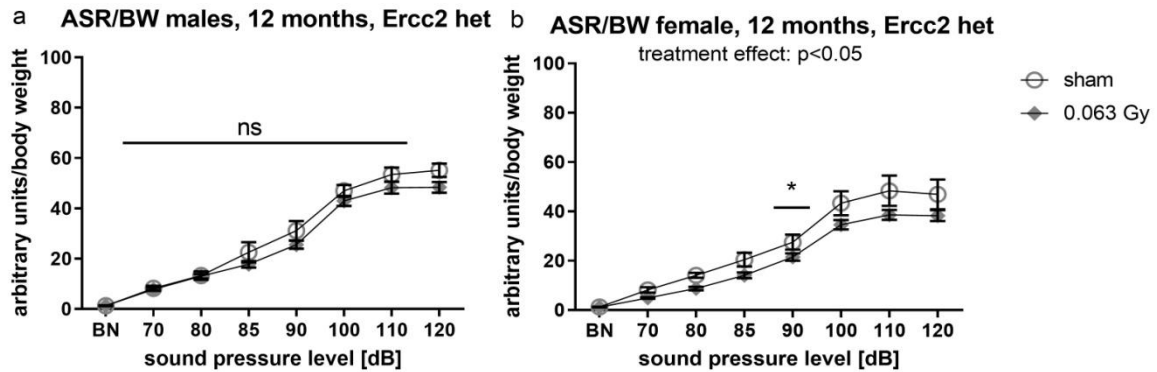


Fig. B.2.2.b.1) ASR – 12 months after exposure to 0.063 Gy. No significant differences were observed for ASR/BW for *Ercc2*^{S737P} het males (a, treatment $F(1, 16) = 3.224$; $p = 0.0915$). For female *Ercc2*^{S737P} het mice, ASR/BW decreased at 90 dB (b, treatment $F(1, 15) = 5.954$; $p = 0.0276$) 12 months after exposure to 0.063 Gy. Data are presented as means \pm SEM. For each group, $n = 8-10$. Results of the post-hoc test are indicated on the graphs by * $p < 0.05$.

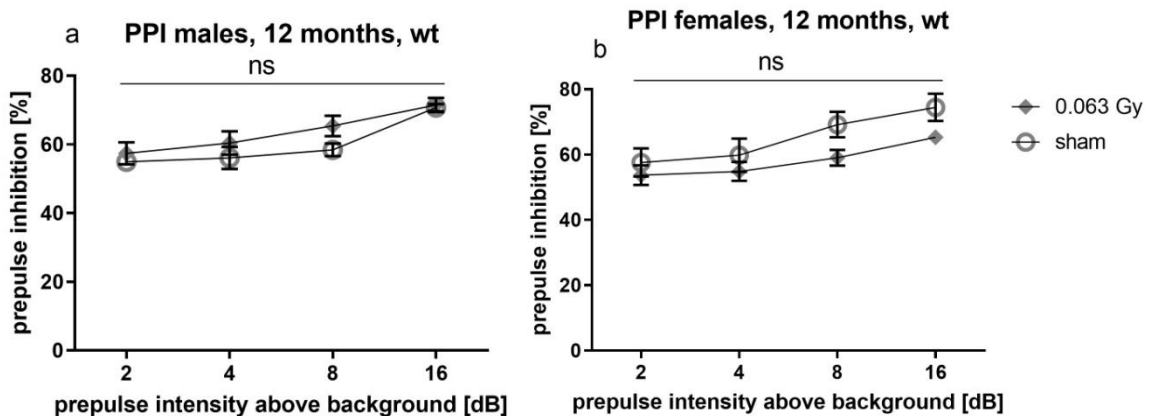


Fig. B.2.2.b.2) PPI – 12 months after exposure to 0.063 Gy. No significant differences were observed 12 months after exposure to 0.063 Gy in PPI for *Ercc2*^{S737P} het male mice (a, treatment $F(1, 16) = 0.009956$; $p = 0.9218$) or in PPI for female *Ercc2*^{S737P} het mice (b, treatment $F(1, 15) = 0.3759$; $p = 0.5490$). Data are presented as means \pm SEM. For each group, $n = 8-10$.

2.2.b. Acoustic startle test (ASR), 12 months with 0.125 Gy

No significant differences were observed on ASR/BW or PPI, 12 months after exposure to 0.125 Gy, either for male or female mice.

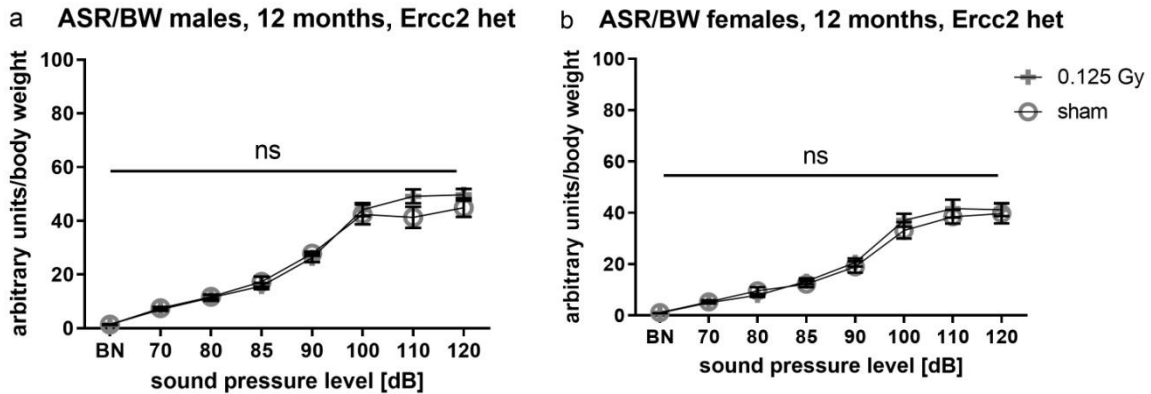


Fig. B.2.2.b.1) ASR – 12 months after exposure to 0.125 Gy. No significant differences were observed for ASR/BW for Ercc2^{S737P} het males (a, treatment F (1, 14) = 0.3406; p=0.5688) and female (treatment F (1, 15) = 0.3124; p=0.5845) mice. Data are presented as means +/- SEM. For each group, n=8-10.

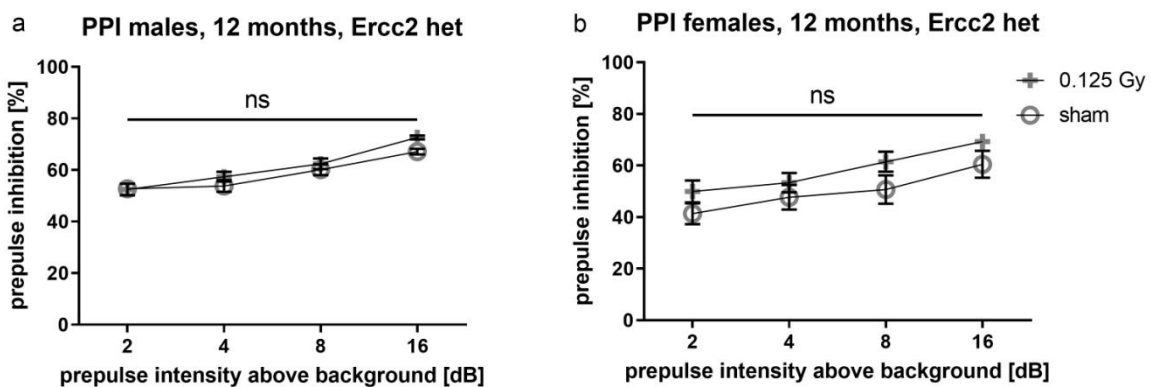


Fig. B.2.2.b.2) PPI – Ercc2 het, 12 months after exposure to 0.125 Gy. No significant differences were observed 12 months after exposure to 0.125 Gy in PPI for Ercc2^{S737P} het male mice (a, treatment F (1, 14) = 1.170; p=0.2977) or in PPI for female Ercc2^{S737P} het mice (b, treatment F (1, 15) = 2.123; p=0.1657). Data are presented as means +/- SEM. For each group, n=8-10.

2.2.c. Acoustic startle test (ASR), 12 months after exposure to 0.5 Gy

At 12 months after exposure to 0.5 Gy, significant treatment effect on ASR/BW was observed in Ercc2^{S737P} het male mice but not in females. Post-results did not confirm this significance. No significant effect was observed on PPI for both males and females after exposure.

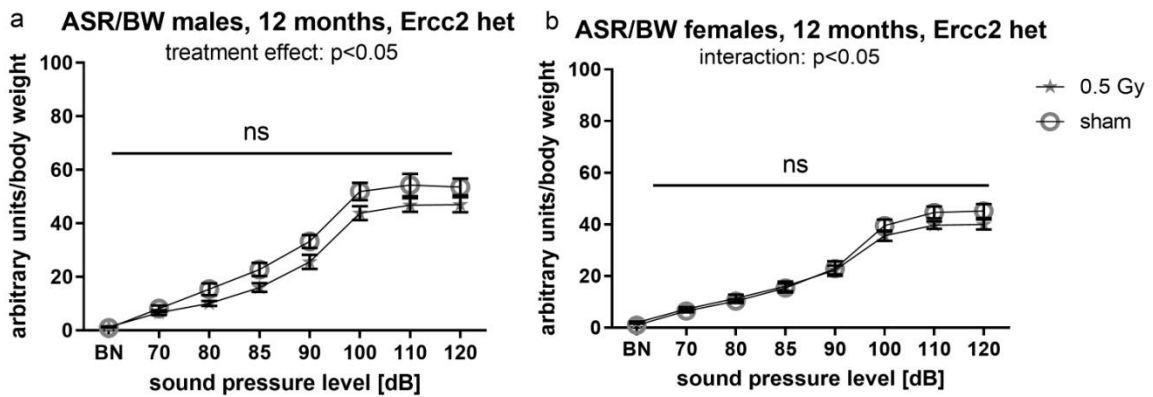


Fig.B.2.2.c.1) ASR – 12 months after exposure to 0.5 Gy. A significant treatment effect was observed for ASR/BW for *Ercc2*^{S737P} het males (a, treatment effect $F(1, 15) = 4.613$; $p = 0.0485$) but not for female (b, treatment $F(1, 15) = 0.6757$; $p = 0.4240$) mice. Post hoc test did not confirm this significance for ASR/BW in *Ercc2* het males. Data are presented as means \pm SEM. For each group, $n = 8-10$.

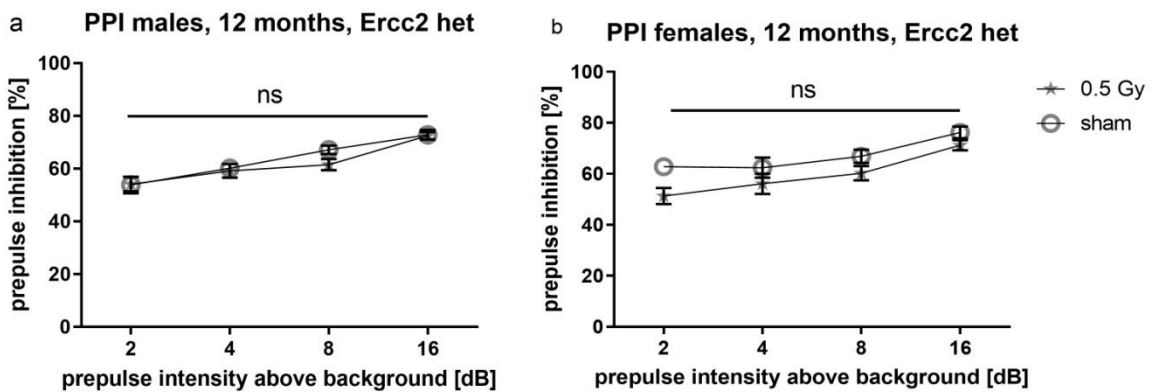


Fig.B.2.2.c.2) PPI – 12 months after exposure to 0.5 Gy. No significant differences were observed 12 months after exposure to 0.5 Gy in PPI for *Ercc2*^{S737P} het male mice (a, treatment $F(1, 15) = 0.3788$; $p = 0.5475$) or in PPI for female *Ercc2*^{S737P} het mice (b, treatment $F(1, 15) = 4.046$; $p = 0.0626$). Data are presented as means \pm SEM. For each group, $n = 8-10$.

2.3. Acoustic startle test (ASR), 18 months after exposure

2.3.a. Acoustic startle test (ASR), 18 months after exposure to 0.063 Gy

At 18 months after exposure to 0.063 Gy, decreased PPI at 2 dB was observed in female *Ercc2*^{S737P} het mice. Decreased ASR/BW was observed at 90, 100 and 110 dB after exposure to 0.5 Gy in *Ercc2* het male mice.

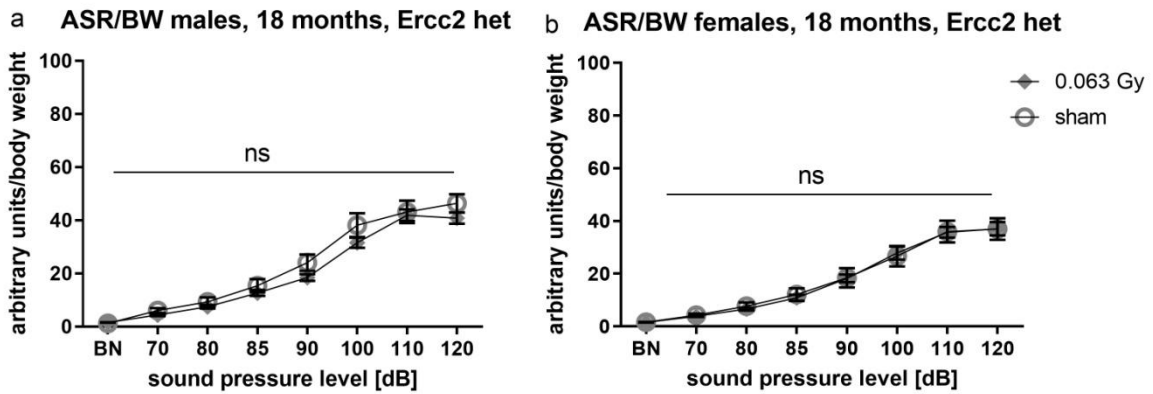


Fig.B.2.3.a.1) ASR – 18 months after exposure to 0.063 Gy. No significant differences were observed for ASR/BW for Ercc2 het males (treatment F (1, 14) = 2.092; $p=0.1701$) and female (treatment F (1, 15) = 0.01124; $p=0.9170$) mice. Data are presented as means +/- SEM. For each group, n=8-10.

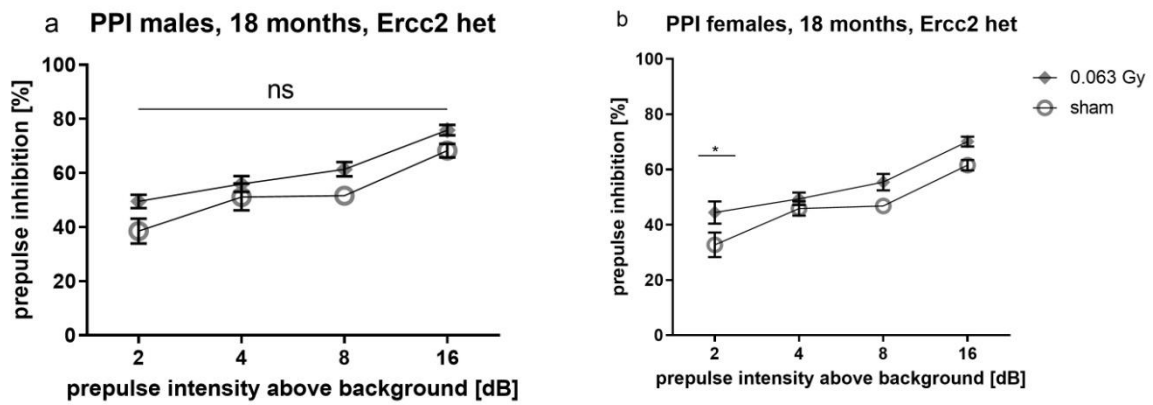


Fig.B.2.3.a.2) PPI – 18 months after exposure to 0.063 Gy. No significant differences were observed 18 months after exposure to 0.063 Gy in PPI for Ercc2^{S737P} het male mice (a, treatment F (1, 14) = 4.350; $p=0.0558$). For female Ercc2^{S737P} het mice, an increased PPI at 2 dB was observed 18 months after exposure to 0.063 Gy (b, treatment F (1, 28) = 7.441; $p=0.0109$). Data are presented as means +/- SEM. For each group, n=8-10. Results of the post hoc test are presented as * $p<0.05$.

2.3.b. Acoustic startle test (ASR), 18 months after exposure to 0.125 Gy

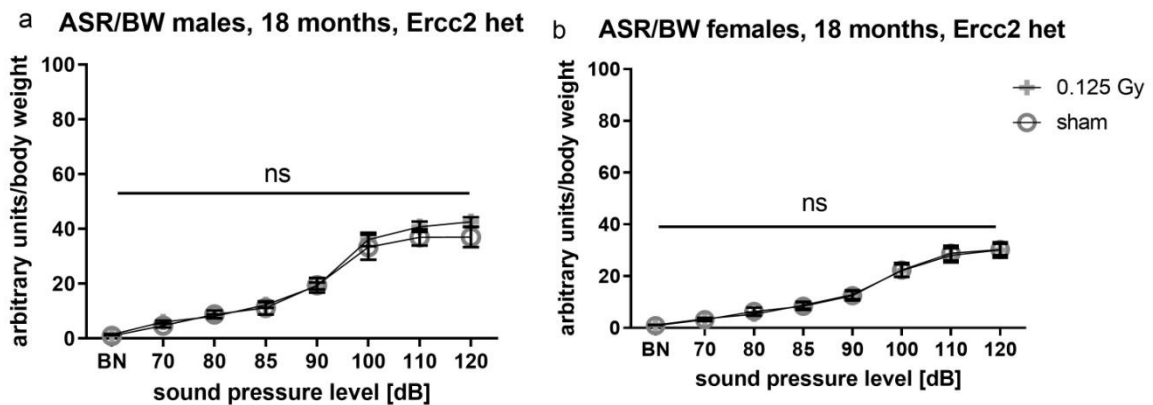


Fig.B.2.3.b.1) ASR – 18 months after exposure to 0.125 Gy. No significant differences were observed for ASR/BW for Ercc2^{S737P} het males (a, treatment F (1, 13) = 0.7845; p=0.3919) and female (b, treatment F (1, 15) = 0.002723; p=0.9591) mice. Data are presented as means +/- SEM. For each group, n=8-10.

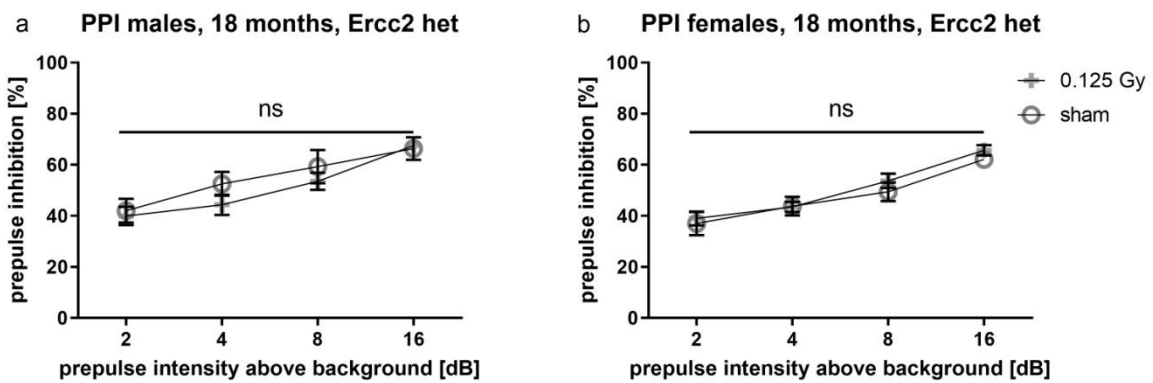


Fig.B.2.3.b.2) PPI – 18 months after exposure to 0.125 Gy. No significant differences were observed 18 months after exposure to 0.125 Gy in PPI for Ercc2^{S737P} het male mice (a, treatment F (1, 13) = 0.4067; p=0.5347) or in PPI for female Ercc2 het mice (b, treatment F (1, 15) = 0.5435; p=0.4723). Data are presented as means +/- SEM. For each group, n=8-10.

2.3.c. Acoustic startle test (ASR), 18 months after exposure to 0.5 Gy

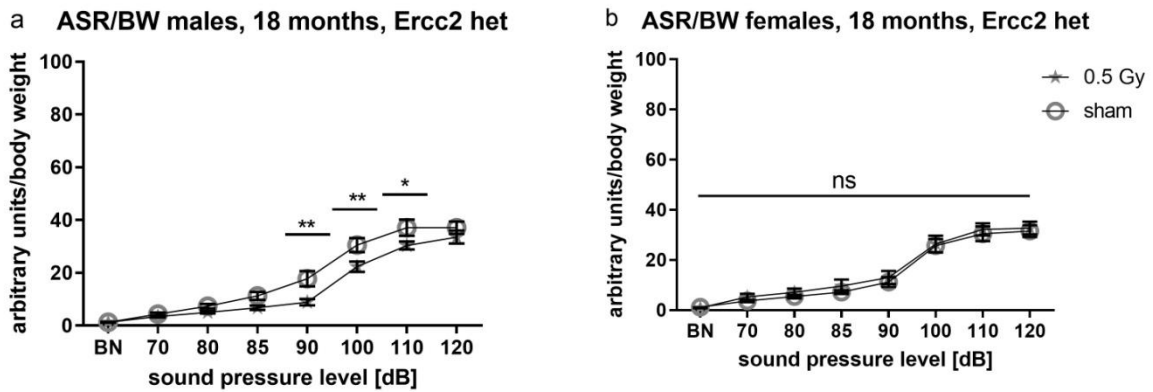


Fig.B.2.3.c.1) ASR – 18 months after exposure to 0.5 Gy. Significant decreases in ASR/BW at 90, 100 and 110 dB were observed for *Ercc2*^{S737P} het males (a, treatment F (1, 14) = 7.584; p=0.0155) but not for *Ercc2*^{S737P} het female mice (b, treatment F (1, 11) = 0.3512; p=0.5654). Data are presented as means +/- SEM. For each group, n=8-10. Results of the post-hoc tests are presented on the graph as * p<0.05, ** p<0.01.

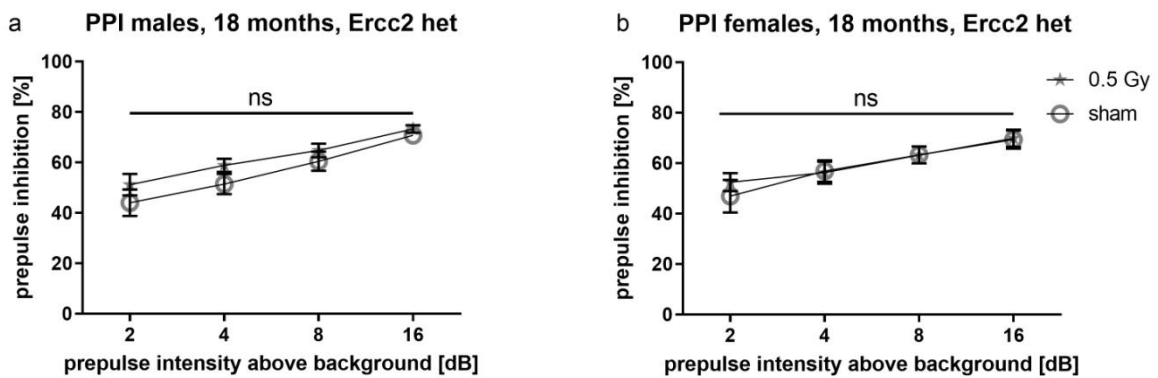


Fig. B.2.3.c.2) PPI – 18 months after exposure to 0.5 Gy. No significant differences were observed 18 months after exposure to 0.5 Gy in PPI for *Ercc2*^{S737P} het male mice (a, treatment F (1, 14) = 1.780; p=0.203) or in PPI for female *Ercc2* het mice (b, treatment F (1, 11) = 0.06275; p=0.8068). Data are presented as means +/- SEM. For each group, n=8-10.

3. Social discrimination test (SD)

3.1. Social discrimination test (SD), 4 months after exposure

3.1.a. Social discrimination test (SD), 4 months after exposure to 0.063 Gy

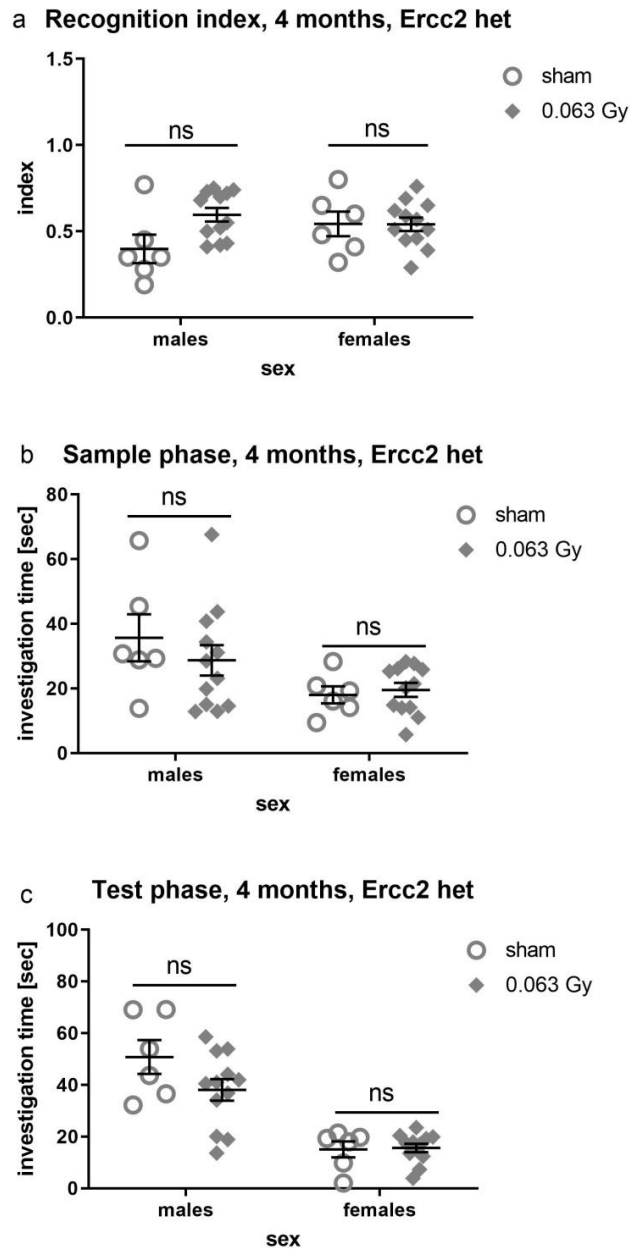


Fig. B.3.1.a. SD – 4 months after exposure to 0.063 Gy. No significant differences were observed in recognition index (a, treatment $F(1, 32) = 3.223$; $p=0.0820$), in sample phase (b, treatment $F(1, 32) = 8.650$; $p=0.0060$) or in test phase (c, treatment $F(1, 32) = 2.256$; $p=0.1429$) in het animals. Data is presented as a scatter plot +/- SEM. $n=6-12$ animals.

3.1.b. Social discrimination test (SD), 4 months after exposure to 0.125 Gy

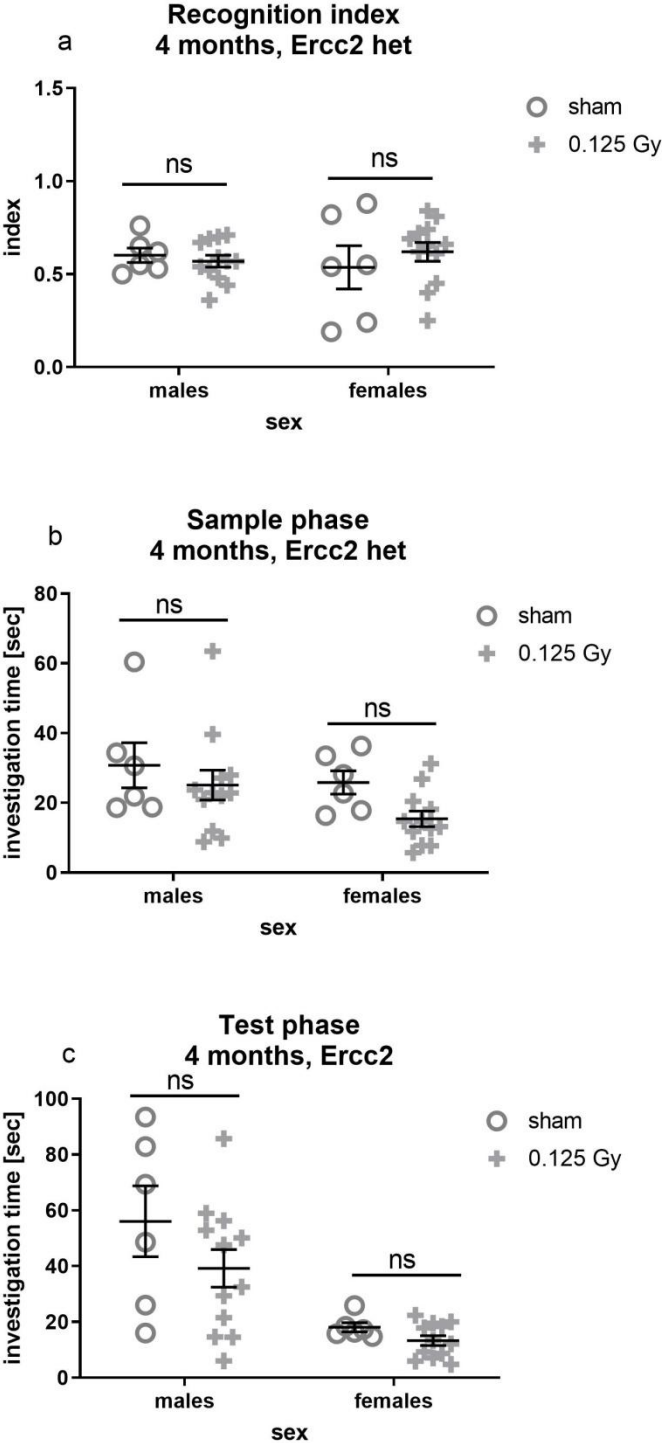


Fig.B.3.1 b. SD – 4 months after exposure to 0.125 Gy. No significant differences were observed in recognition index (a, treatment $F(1, 32) = 0.1863$; $p=0.6689$), in sample phase (b, treatment $F(1, 32) = 3.561$; $p=0.0683$) or in test phase (c, treatment $F(1, 32) = 2.653$; $p=0.1132$) in het animals. Data is presented as a scatter plot +/- SEM. $n=6-12$ animals.

3.1.c. Social discrimination test (SD), 4 months after exposure to 0.5 Gy

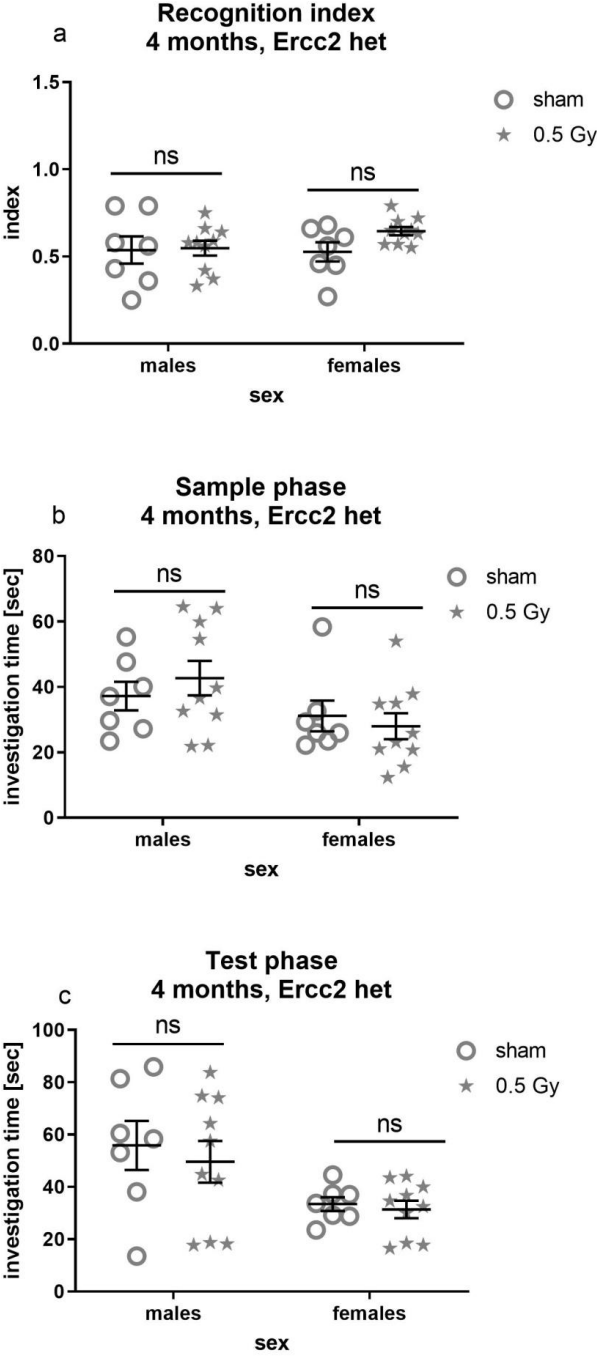


Fig.B.3.1. c. SD – 4 months after exposure to 0.5 Gy. No significant differences were observed in recognition index (a, treatment $F(1, 30) = 1.753$; $p=0.1955$), in sample phase (b, treatment $F(1, 30) = 0.06107$; $p=0.8065$) or in test phase (c, treatment $F(1, 30) = 0.4018$; $p=0.5310$) in het animals. Data is presented as a scatter plot +/- SEM. $n=6-12$ animals.

3.2. Social discrimination test (SD), 12 months after exposure

3.2.a. Social discrimination test (SD), 12 months after exposure to 0.063 Gy

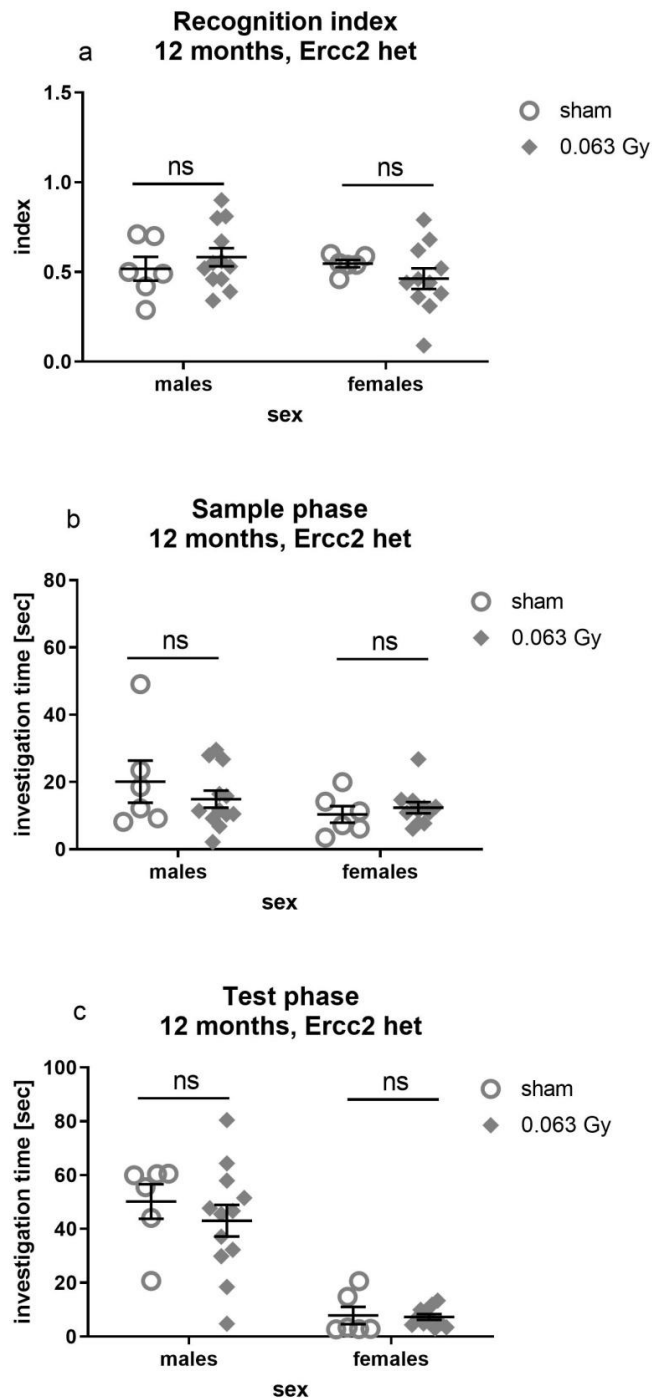


Fig.B.3.2 a. SD – 12 months after exposure to 0.063 Gy. No significant differences were observed in recognition index (a, treatment $F(1, 31) = 0.02810$; $p = 0.8680$), in sample phase (b, treatment $F(1, 31) = 0.2511$; $p = 0.6198$) or in test phase (c, treatment $F(1, 31) = 0.5839$; $p = 0.4506$) in het animals. Data is presented as a scatter plot +/- SEM. $n = 6-12$ animals.

3.2.b. Social discrimination test (SD), 12 months after exposure to 0.125 Gy

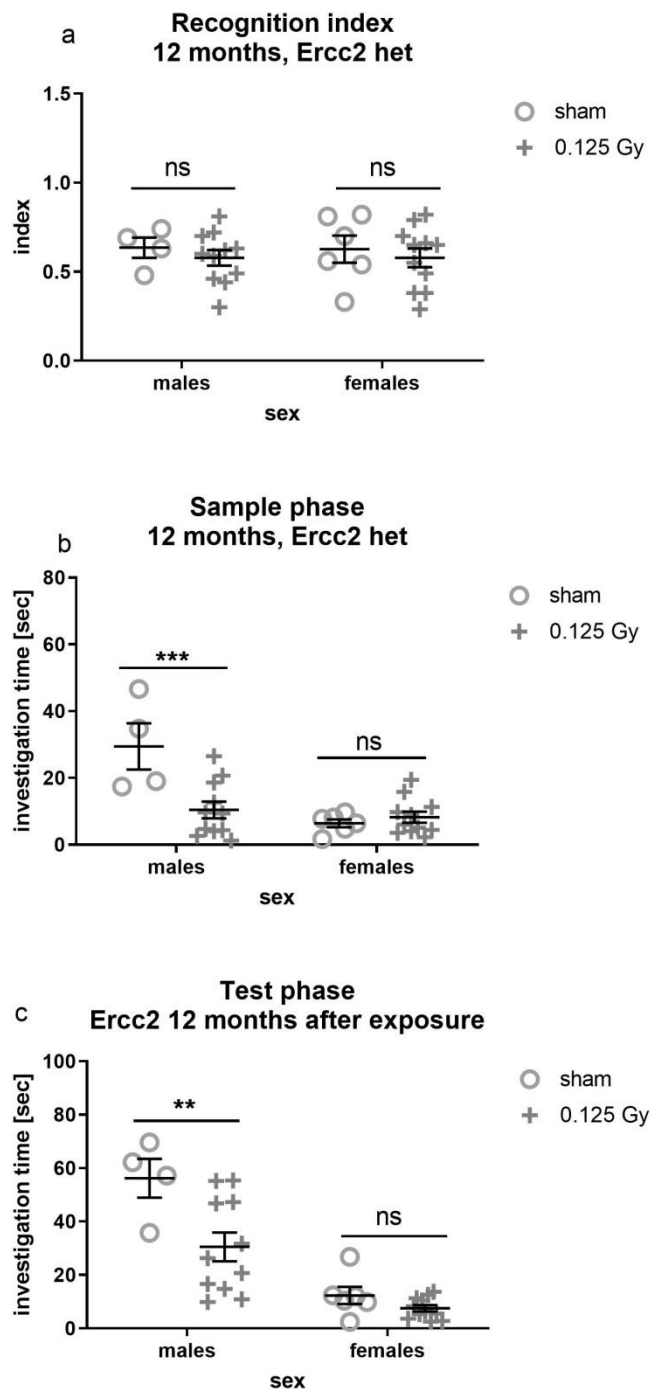


Fig.B.3.2. b. SD – 12 months after exposure to 0.125 Gy. No significant differences were observed in recognition index (a, treatment $F(1, 28) = 0.7090$; $p=0.4069$) but both sample phase (b, treatment $F(1, 28) = 8.615$; $p=0.0066$; interaction $F(1, 28) = 12.63$; $p=0.0014$) and test phase (c, (treatment $F(1, 28) = 10.25$; $p=0.0034$; interaction $F(1, 28) = 4.794$; $p=0.0371$) decreased in $Ercc2^{5737P}$ male het animals. Data is presented as a scatter plot +/- SEM. $n=6-12$ animals.

3.2.c. Social discrimination test (SD), 12 months after exposure to 0.5 Gy

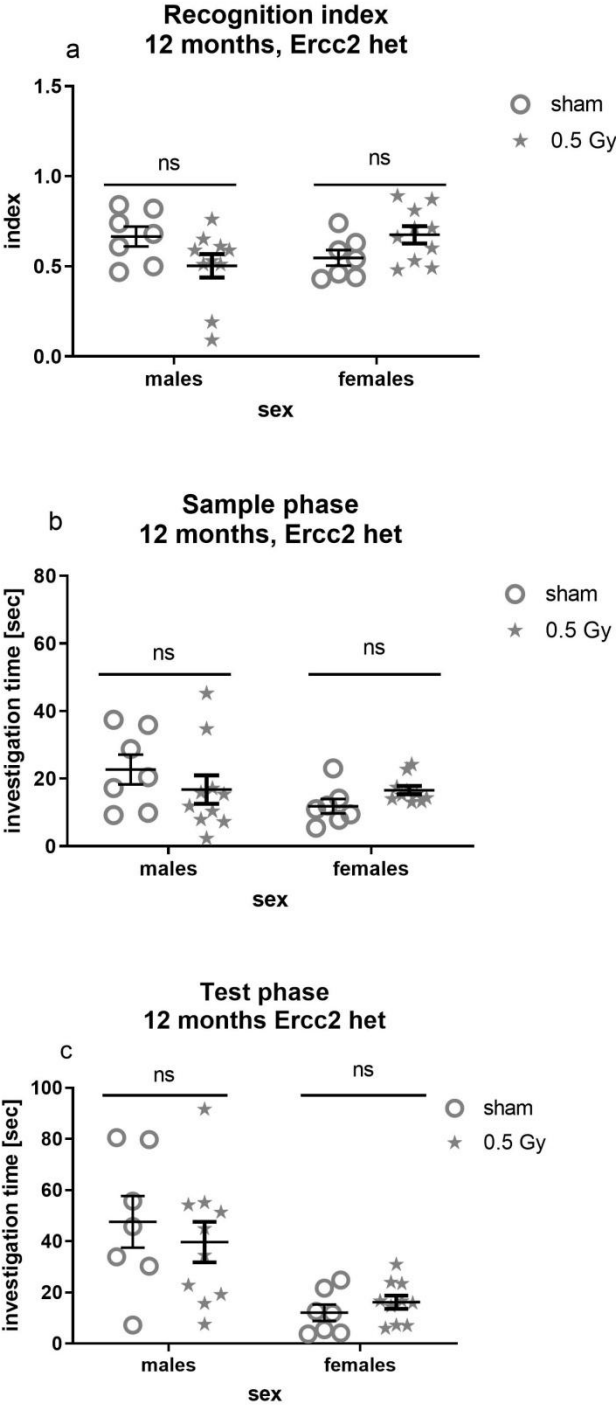


Fig.B.3.2 c. SD – 12 months after exposure to 0.5 Gy. No significant differences were observed in recognition index (a, treatment $F(1, 30) = 0.09438$; $p=0.7608$) in sample phase (b, treatment $F(1, 30) = 0.03006$; $p=0.8635$) and test phase (c, treatment $F(1, 30) = 0.07983$; $p=0.7795$) in $Ercc2^{S737P}$ male het animals. Data is presented as a scatter plot +/- SEM. $n=6-12$ animals.

3.3. Social discrimination test (SD), 18 months after exposure

3.3.a. Social discrimination test (SD), 18 months after exposure to 0.063 Gy

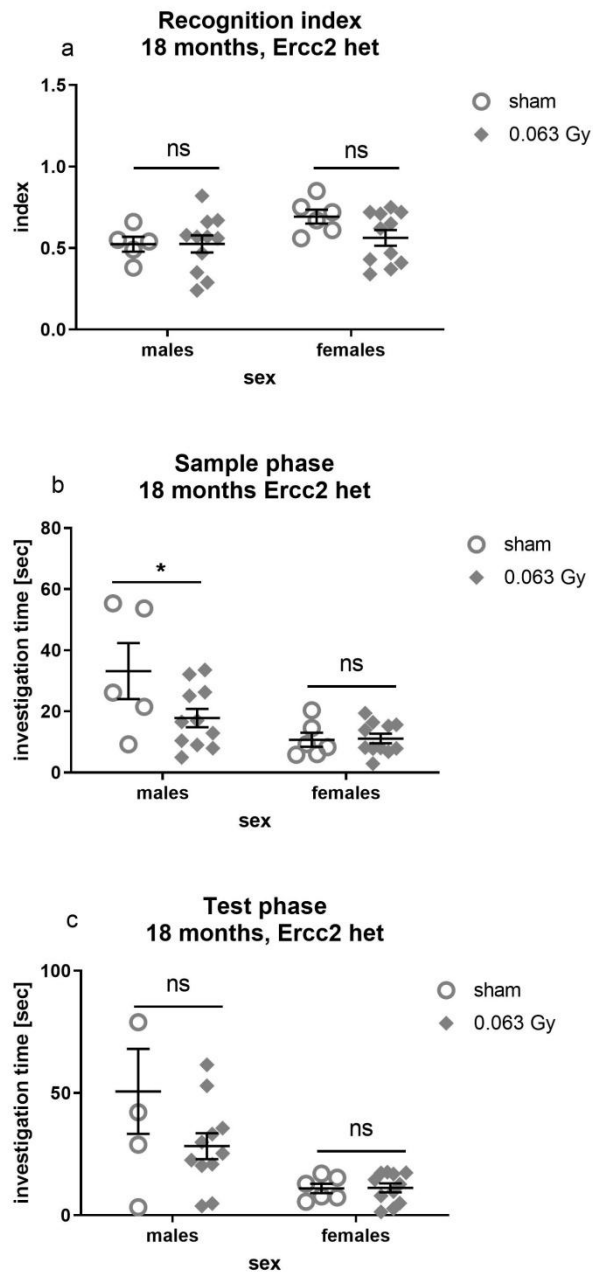


Fig.B.3.3.a. SD – 18 months after exposure to 0.063 Gy. No significant differences were observed in recognition index (a, treatment $F(1, 29) = 1.350$; $p=0.2547$) and test phase (c, treatment $F(1, 29) = 2.697$; $p=0.2547$). Sample phase decreased in $Ercc2^{S737P}$ het male mice (b, treatment $F(1, 29) = 3.833$; $p=0.0599$; interaction $F(1, 29) = 4.235$; $p=0.0487$). Data is presented as a scatter plot \pm SEM. $n=6-12$ animals. Results of the post-hoc tests are presented on the graph as * $p<0.05$.

3.3.b. Social discrimination test (SD), 18 months after exposure to 0.125 Gy

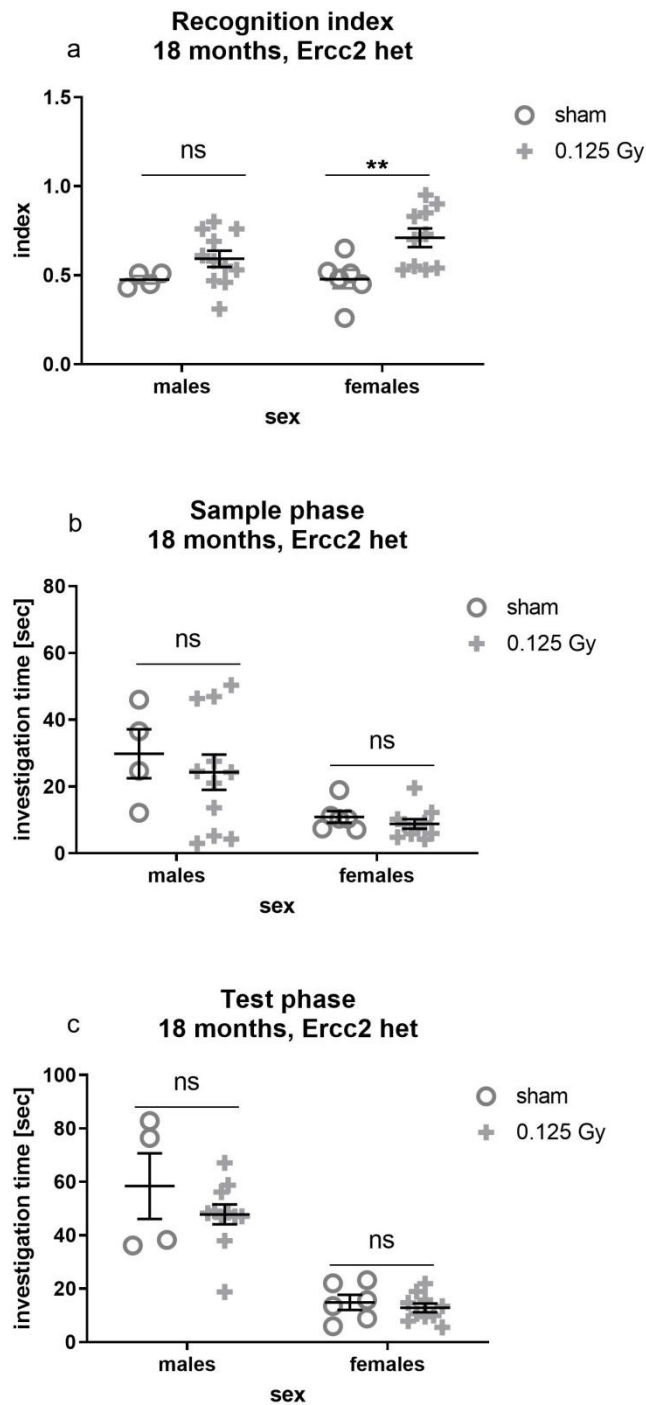


Fig.B.3.3. b. SD – 18 months after exposure to 0.125 Gy. Increased recognition index was observed in female het *Ercc2*^{S737P} mice 18 months after exposure to 0.125 Gy (a, treatment $F(1, 27) = 9.734$; $p = 0.0043$). No significant effects were observed on sample phase (b, treatment $F(1, 27) = 0.6556$; $p = 0.4252$) or on test phase (c, treatment $F(1, 27) = 1.879$; $p = 0.1817$). Data is presented as a scatter plot +/- SEM. $n = 6-12$ animals. Results of the post-hoc tests are presented on the graph as ** $p < 0.01$.

3.3.c. Social discrimination test (SD), 18 months after exposure to 0.5 Gy

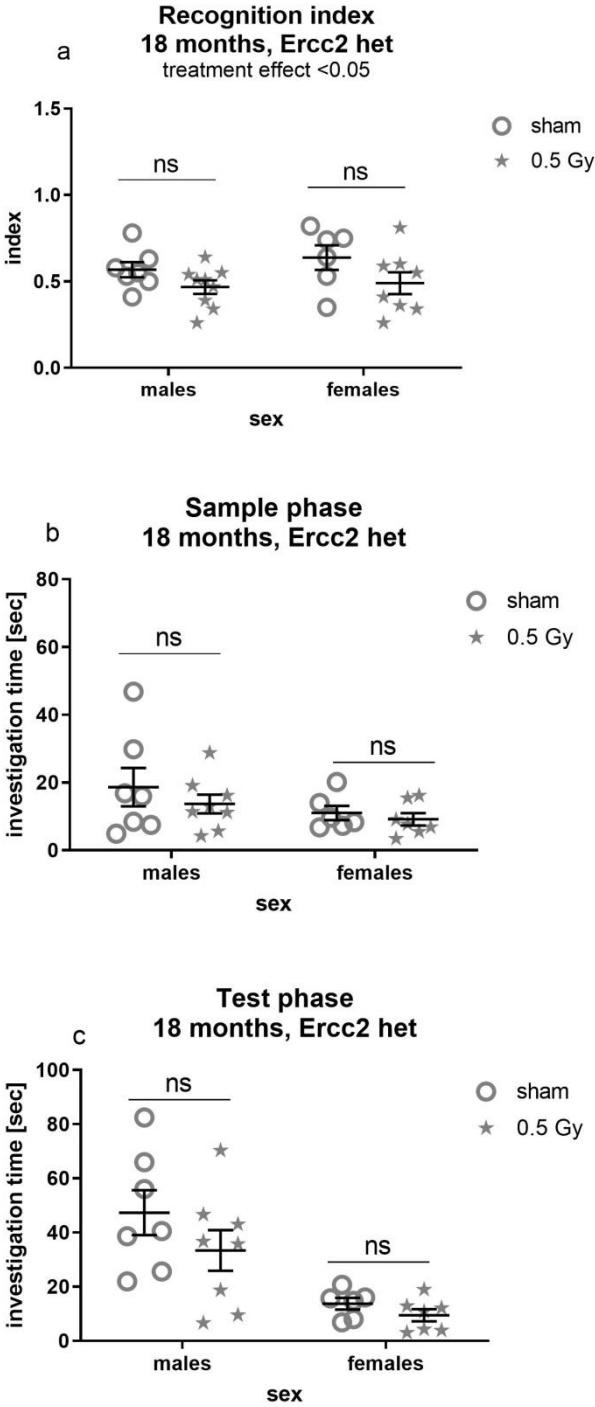


Fig.B.3.3.c. SD – 18 months after exposure to 0.5 Gy. A significant treatment effect was observed on recognition index but not confirmed by post-hoc test (a, significant treatment effect $F(1, 26) = 5.202$; $p=0.0310$). No significant effects were observed on sample phase (b, treatment $F(1, 24) = 0.9440$; $p=0.3409$) or on test phase (c, treatment $F(1, 24) = 2.149$; $p=0.1556$). Data is presented as a scatter plot +/- SEM. n=6-12 animals.

C. Linear model with random intercept (LM): behavioral results

1. General radiation effects

The objective of the analysis performed with linear model with random intercept is to identify dose-dependent radiation effects over all three time points, as well as identify potential sex-specific or genotype-specific radiation effects.

Dose effect was significant for total distance travelled ($F(3,196) = 4.32$; $p=0.0057$), whole average speed ($F(3,196) = 3.74$; $p=0.0121$) and ASR/BW 110 dB ($F(3,197) = 4.2$; $p=0.0066$). Time effect was significant for all parameters ($p<0.0001$). Treatment-genotype interaction was significant for rearing ($F(3,196) = 4.08$; $p=0.0077$) and whole average speed ($F(3,196) = 2.89$; $p=0.0365$).

Data was later on analyzed with difference of least square means as a post-hoc test. After 0.5 Gy radiation, total distance (Fig.C.1; a), whole average speed (b), rearing (c) and ASR/BW 110 dB (d) all decreased, indicating a significant effect of the highest radiation dose on these behavioral parameters over the course of the study.

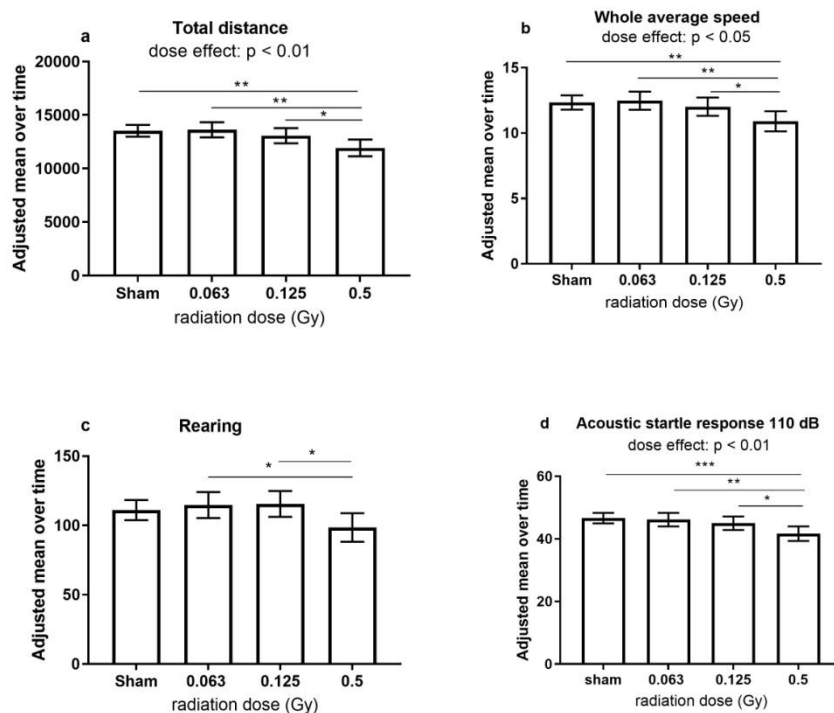


Fig.C.1. Radiation effect over time (pooled behavioral data collected after 4, 12 and 18 months after exposure from the same animals, tested successively at these time points) (a) Total distance decreased after 0.5 Gy compared to sham-, 0.063 Gy- and 0.125 Gy-irradiated mice. (b) Whole average speed decreased after 0.5 Gy compared to sham-, 0.063 Gy- and 0.125 Gy-irradiated mice. (c) Rearing decreased after 0.5 Gy compared to 0.063 Gy- and 0.125 Gy-irradiated mice. (d) Acoustic startle decreased after 0.5 Gy compared to sham-, to 0.063 Gy- and 0.125 Gy-irradiated mice. Results of post-hoc tests are indicated on the graphs by * $p<0.05$, ** $p<0.01$ *** $p<0.001$. Data are presented as adjusted means over time +/- Errors bars indicate the highest/lowest value.

2. Dose-dependent radiation effects at 4 months after exposure

Since the behavior was assessed at 3 different time points after exposure, it was possible to narrow down the onset of the changes, by analyzing each time point separately. At 4 months after exposure, results of the linear model indicated that dose effect was significant only for ASR/BW 110 dB ($F(3,197) = 3.86$; $p = 0.0103$). Already at 4 months after exposure, ASR/BW 110 dB was significantly decreased after 0.5 Gy (Fig C.2; d). No differences were observed for total distance travelled, whole average speed or rearing, at this time point.

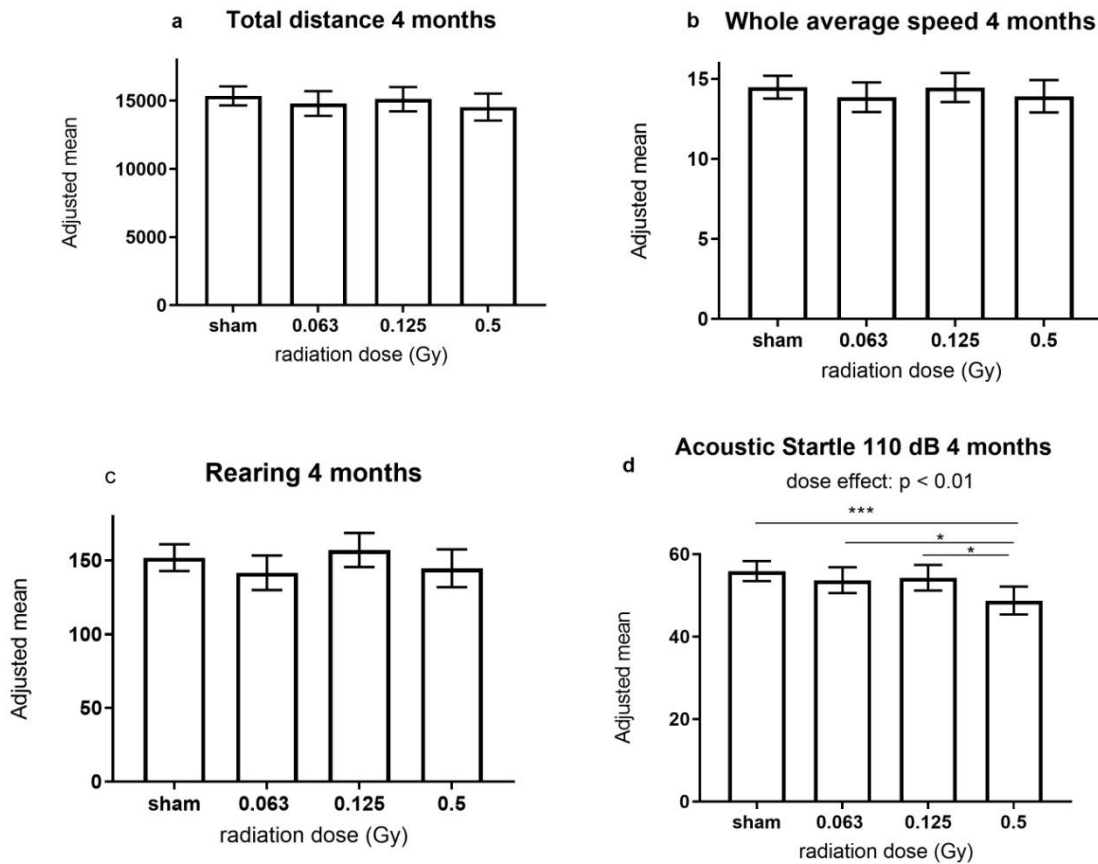


Fig.C.2. Dose-dependent radiation effects at 4 months after exposure. (a-c) Total distance, whole average speed and rearing did not show significant differences at 4 months after exposure. (d) Acoustic startle was already decreased at 4 months after exposure to 0.5 Gy compared to sham-irradiated mice but also compared to 0.063 Gy- and 0.125 Gy-irradiated mice. Results of post-hoc tests are indicated on the graphs by * $p < 0.05$, *** $p < 0.001$. Data are presented as adjusted means +/- error bars indicating highest/lowest value.

3. Dose-dependent radiation effects at 12 months after exposure

At 12 months after exposure, results of the linear analysis indicated that dose effect was significant for ASR/BW 110 dB ($F(3,191) = 2.87$; $p = 0.0375$) but also for total distance travelled ($F(3,190) = 4.37$; $p = 0.0053$), rearing ($F(3,190) = 3.96$; $p = 0.0091$) and whole average speed ($F(3,190) = 4.82$; $p = 0.003$). Decreased total distance, whole average speed, rearing and ASR/BW at 110 dB were observed after exposure to 0.5 Gy.

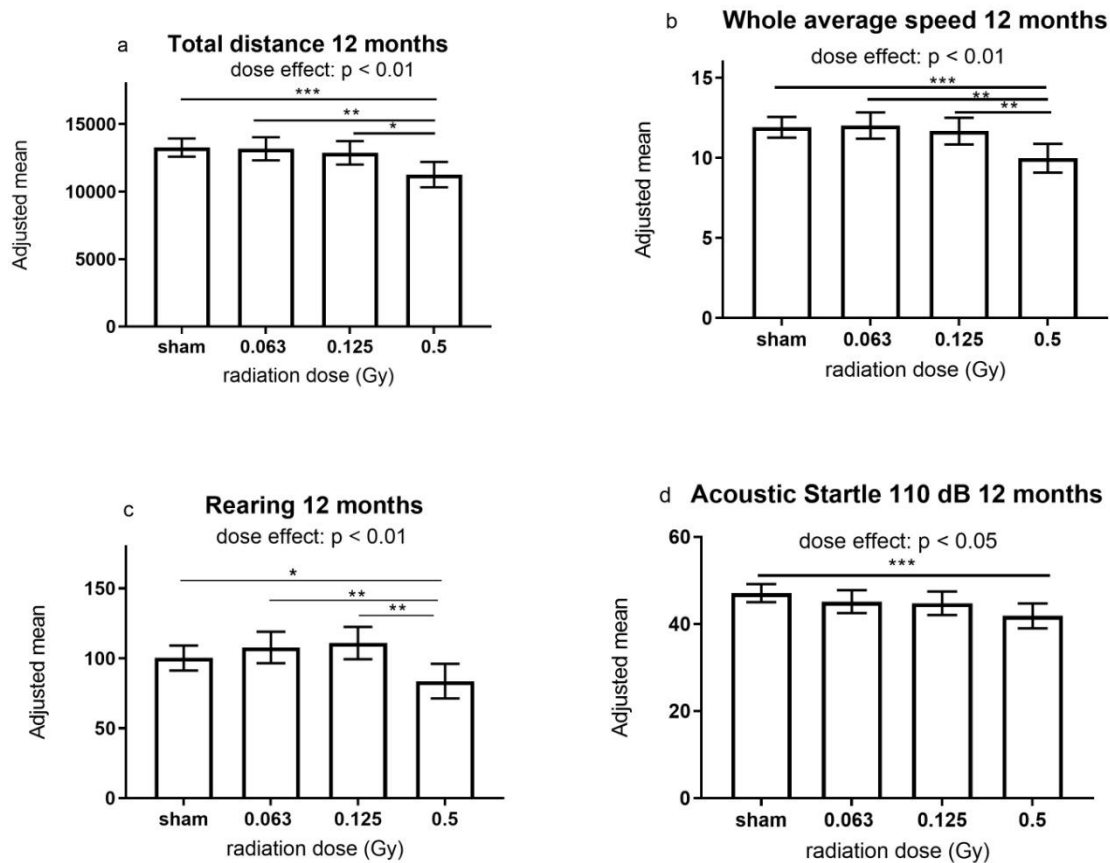


Fig.C.3. Dose-dependent radiation effects at 12 months after exposure. (a) Total distance decreased after 0.5 Gy at 12 months compared to sham-, to 0.063 Gy- and to 0.125 Gy- irradiated mice. (b) Whole average speed decreased after 0.5 Gy at 12 months compared to sham-, to 0.063 Gy- and to 0.125 Gy-irradiated mice. (c) Rearing decreased after 0.5 Gy at 12 months compared to sham-, to 0.063 Gy- and to 0.125 Gy-irradiated mice. (d) Acoustic startle decreased after 0.5 Gy at 12 months compared to sham- irradiated mice. Results of post-hoc tests are indicated on the graphs by * $p < 0.05$, ** $p < 0.01$ *** $p < 0.001$. Data are presented as adjusted means +/- error bars indicating highest/lowest value.

4. Dose-dependent effects at 18 months after exposure

At 18 months after exposure, results of the linear analysis showed that dose effect was significant for acoustic startle ($F(3,172) = 3.96$; $p = 0.0093$), total distance ($F(3,172) = 6.84$; $p = 0.0002$), whole average speed ($F(3,171) = 7.07$; $p = 0.0002$) and rearing ($F(3,172) = 4.03$; $p = 0.0084$). Genotype effect ($F(1,172) = 4.01$; $p = 0.0469$) was significant for total distance. Post-hoc analyses showed that compared to sham-irradiated animals, mice exposed to 0.5 Gy showed decreased total distance, speed and rearing at 18 months after exposure. In addition, compared to sham-irradiated mice, 0.063 Gy-irradiated animals showed an increased ASR/BW at 110 dB and increased rearing.

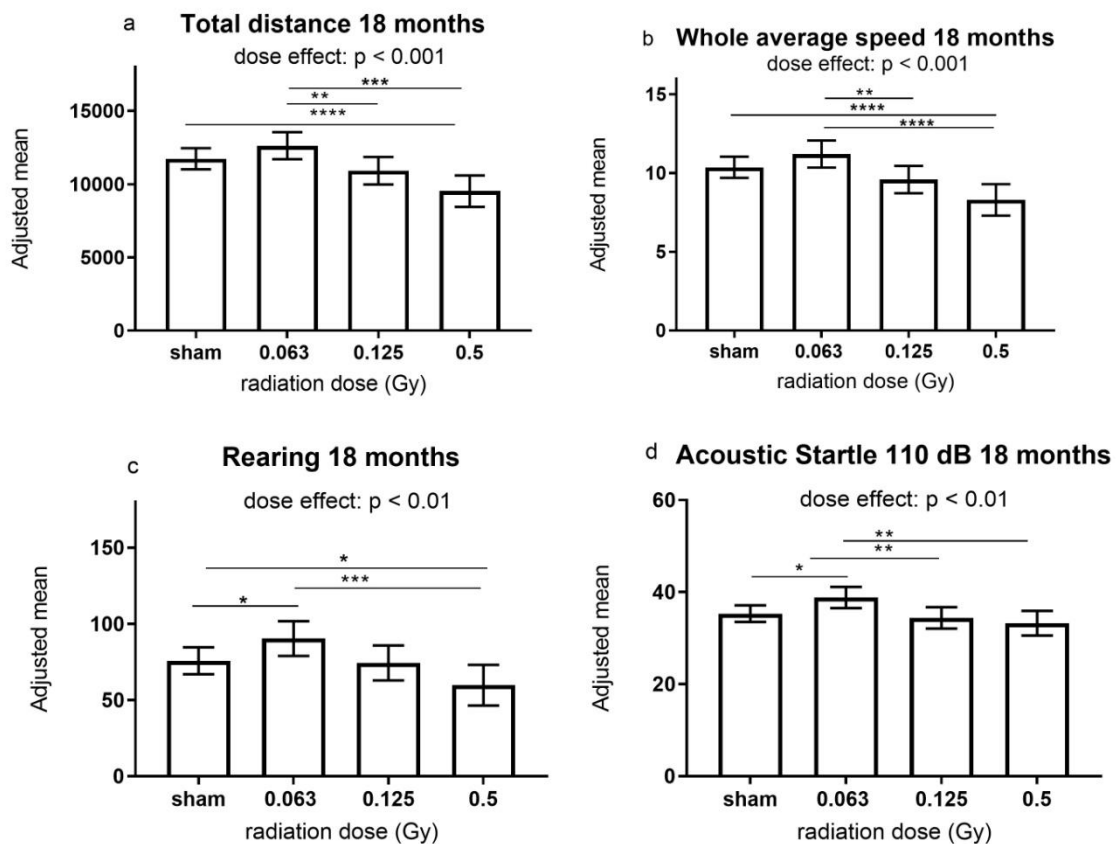


Fig.C.4. Dose-dependent radiation effects at 18 months after exposure (a) Total distance decreased after 0.5 Gy compared to sham-irradiated mice, decreased between 0.063 Gy and 0.125 Gy and between 0.063 Gy and 0.5 Gy. (b) Whole average speed decreased after 0.5 Gy compared to sham-irradiated mice, decreased between 0.063 Gy and 0.125 Gy and between 0.063 Gy and 0.5 Gy. (c) Rearing increased after 0.063 Gy compared to sham-irradiated mice, decreased after 0.5 Gy compared to sham-irradiated mice and decreased between 0.063 and 0.5 Gy. (d) Acoustic startle increased after 0.063 Gy compared to sham-irradiated mice, decreased between 0.063 and 0.125 Gy and between 0.063 Gy and 0.5 Gy. Results of post-hoc tests are indicated on the graphs by * $p < 0.05$, ** $p < 0.01$ *** $p < 0.001$. Data are presented as adjusted means +/- highest/lowest value.

5. Genotype-dose effect at 18 months after exposure

At 18 months after exposure, genotype-dose interactions were significant for total distance ($F(3,172) = 4.5$; $p = 0.0045$), for whole average speed ($F(3,171) = 5.02$; $p = 0.0023$), for rearing ($F(3,172) = 6.36$; $p = 0.0004$) and PPI global ($F(3,172) = 5.91$; $p = 0.0007$). Observation of these parameters at 18 months after exposure showed that sham-irradiated *Ercc2*^{S737P} het mice started on a higher baseline for total distance, speed and rearing at this age compared to sham-irradiated wt mice. They started on a lower baseline for PPI global. Of note, this difference developed over time in non-irradiated mice (see Fig.C.5.b).

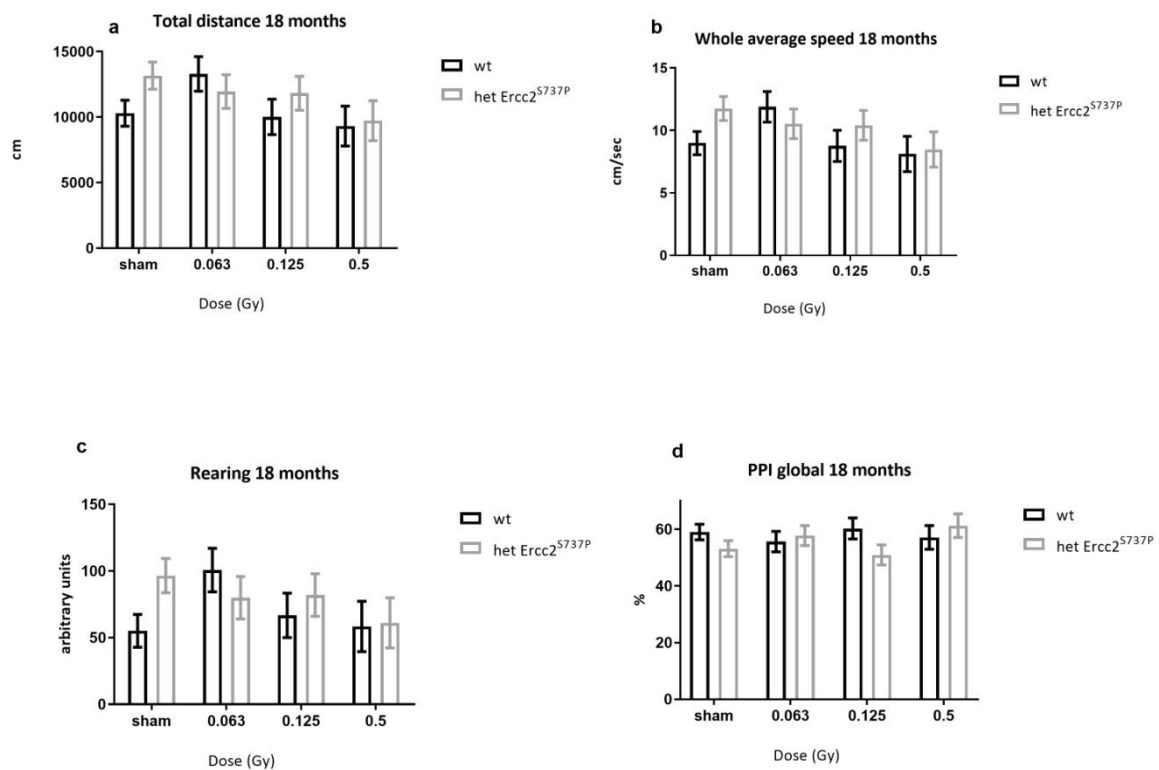


Fig.C.5.a. Genotype-dose interaction at 18 months. At this time point, non-irradiated *Ercc2*^{S737P} het mice demonstrated higher levels of total distance (a), speed (b) and rearing (c) in comparison to non-irradiated wt mice. The inverse trend happened for PPI global (d). Data are presented as means +/- upper/lower limit. Bars represent pooled data of both sexes per group.

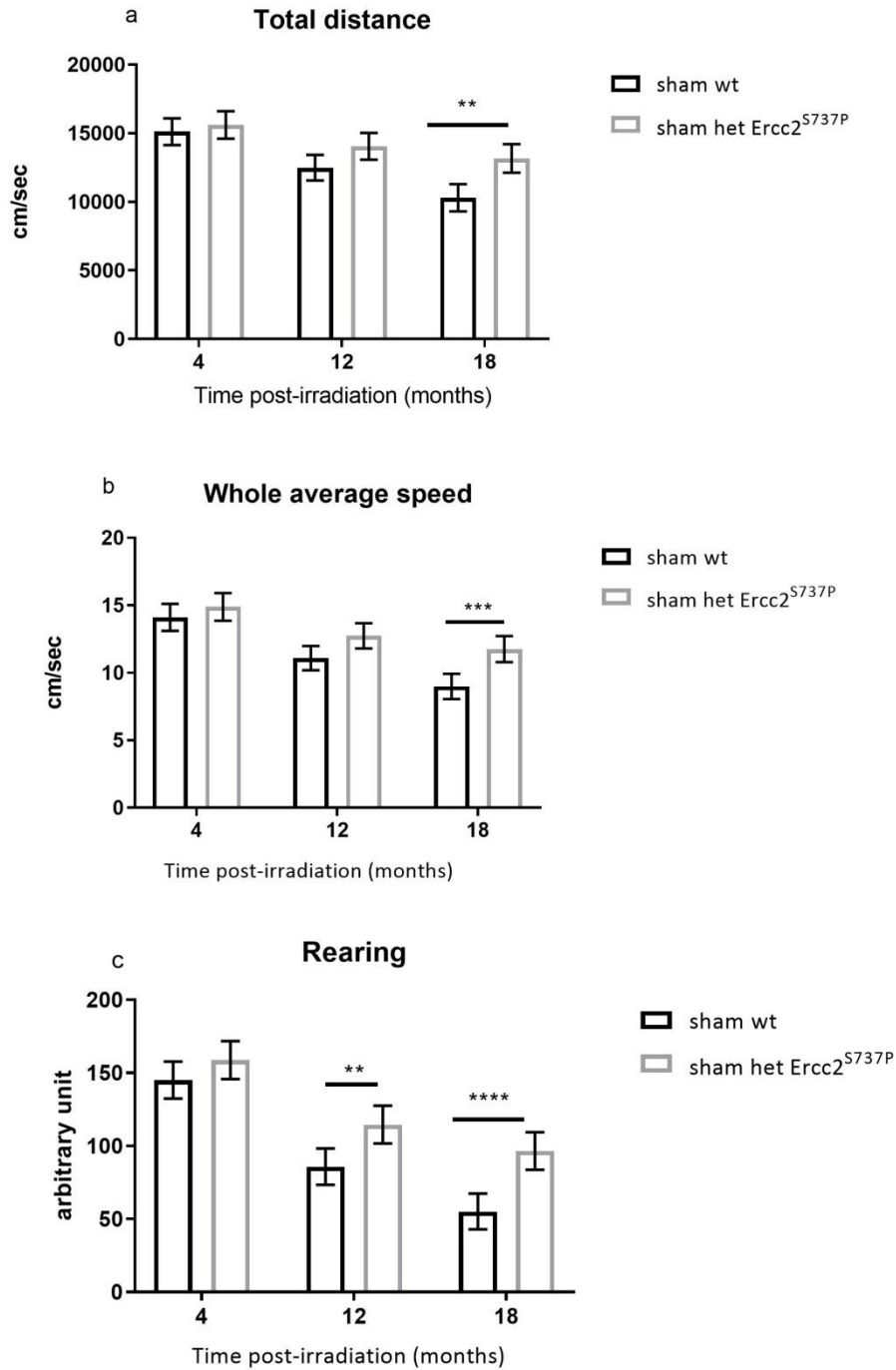


Fig.C.5.b Genotype differences in age-related changes in non-irradiated mice. Data were analyzed with RM ANOVA. (a) Sham-irradiated wt mice showed decreased total distance at 18 months compared to sham-irradiated het mice (interaction $F(2, 138) = 5.43$, $p = 0.0054$, time $F(2, 138) = 43.06$, $p < 0.0001$, genotype $F(1, 69) = 5.893$, $p = 0.0178$). (b) Sham-irradiated wt mice showed decreased average speed at 18 months compared to sham-irradiated het mice (interaction $F(2, 136) = 4.715$, $p = 0.0105$, time $F(2, 136) = 64.97$, $p < 0.0001$, genotype $F(1, 68) = 6.75$, $p = 0.0115$). (c) Sham-irradiated wt mice showed decreased rearing at 12 and 18 months compared to sham-irradiated het mice (interaction $F(2, 138) = 5.439$, $p = 0.0053$, time $F(2, 138) = 154.3$, $p < 0.0001$, genotype $F(1, 69) = 12.14$, $p = 0.0009$). Post-hoc results are indicated on the graphs by ** $p < 0.01$, *** $p < 0.001$, **** $p < 0.0001$. Data are presented as means \pm upper/lower limit. Bars represent pooled data of both sexes per group.

It should also be noted that for all behavioral parameters measured the absolute values declined over time, as evident from the significant time effects for all parameters stated earlier (§C.1). This represents a normal ageing effect that can be also observed in mice.

D. Immunohistochemistry and stereological analysis of mouse brain tissues following low dose radiation exposure

To investigate the molecular changes underlying the behavior observed after radiation, the brain tissues of the mice were processed for immunohistochemistry and stereology. Brain tissues of the mice tested for behavior and sacrificed at the end are the so-called “24 months” tissues. To obtain also tissue data during the experiment, additional groups of 16 males and females were irradiated; 4 mice of each group were killed at different time points aligned with the time points of behavioral assessment (“12 months” and “18 months” tissues).

1. Neuronal and glial density in the hippocampus 24 months following radiation exposure to 0, 0.063, 0.125 or 0.5 Gy in wt and *Ercc2*^{S737P} het mice, males and females

After exposure, brain radiation can potentially affect neurogenesis and induces inflammation (Hladik and Tapio, 2016). Therefore, a first analysis was run on brain tissues collected 24 months after exposure to ionizing radiation, from the animals which had been behaviorally tested, to check those parameters. Using stereology the neuronal and glial populations present in the hippocampal dentate gyrus (DG) in each of the animal groups were quantified. Because of the low number of animals available per group for the analysis of the brain tissues, males and females were pooled.

In wt animals (Fig. D.1.a; a; n=5-9), a lower number of neurons was observed in the DG for 0.063 Gy-irradiated animals compared to 0.125 Gy- and 0.5 Gy- irradiated animals ($F(3, 20) = 4.883$; $p=0.0105$, post-hoc $p=0.0429$ and $p=0.0186$). Number of glia in the DG increased in 0.125 Gy-irradiated animals compared to sham- and 0.063 Gy-irradiated mice (b, $F(3, 20) = 4.746$; $p=0.0117$, post-hoc $p=0.0212$ and $p=0.0180$).

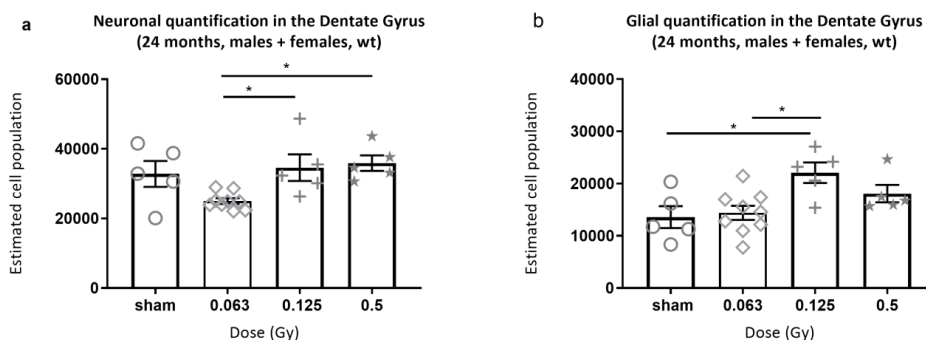


Fig. D.1.a Nissl 24 months after exposure, males and females pooled, wt. (a) A decreased number of neurons was found in the DG of 0.063 Gy-irradiated wt animals compared to 0.125 Gy- and 0.5 Gy wt animals. (b) An increased number of glia was found in the DG of 0.125 Gy-irradiated wt animals compared to sham- and 0.063 Gy-irradiated wt animals.

In het animals (n=5-7), an increased number of neurons in the DG was observed in 0.125 Gy-irradiated mice compared to sham-, to 0.063 Gy- and to 0.5 Gy-irradiated animals (Fig.D.1.b., a, $F(3, 21) = 6.407$; $p=0.0030$, post-hoc: $p=0.0064$; $p=0.0168$ and $p=0.0122$). Number of glia in the DG decreased in 0.063 Gy-irradiated animals compared to 0.125 Gy- and 0.5 Gy irradiated-animals (b; $F(3, 21) = 5.818$; $p=0.004$, post-hoc: $p=0.0269$ and $p=0.0043$).

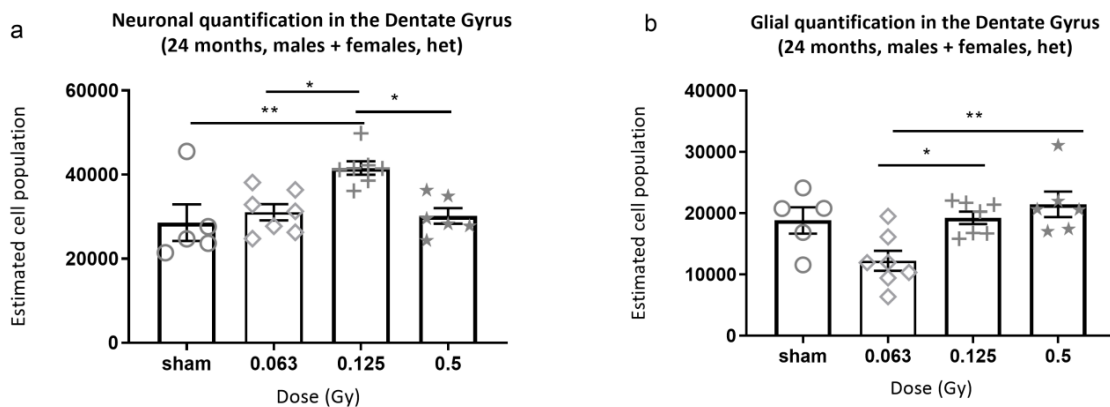


Fig. D.1.b. Nissl 24 months after exposure, males and females pooled, *Ercc2*^{S737P} (a) An increased number of neurons was observed in the DG of 0.125 Gy-irradiated het animals, compared to sham-, 0.063 Gy- and 0.5 Gy-irradiated het animals (b) A decreased number of glia was found in the DG of 0.063 Gy-irradiated het animals compared to 0.125 Gy- and 0.5 Gy-irradiated het animals. Post-hoc tests results are indicated on the graphs by * $p<0.05$, ** $p<0.01$. Data are presented as means +/- SEM.

2. Quantification of Iba1+ microglia in the hippocampus 12, 18 and 24 months following radiation exposure to 0, 0.063, 0.125 or 0.5 Gy in wt and *Ercc2* het mice, males and females

Changes in the number of microglia, one of the main glial constituents of the inflammatory response in the brain after radiation exposure were quantified in the hippocampus in three regions, the dentate gyrus (DG), the Cornus Ammonis 1 and 2/3 (CA1 and CA2/3), after staining them with Iba1.

Because of the low number of animals available per group for the analysis of the brain tissues, males and females were pooled.

2.1. Quantification of Iba1+ microglia in the hippocampus 12 months following radiation exposure to 0, 0.063, 0.125 or 0.5 Gy in wt mice, males and females

For the wt animals (n=2-9), no effects of radiation on the number of microglia in the DG ($F(3, 21) = 0.3884$, $p=0.7625$), CA23 ($F(3, 17) = 0.3476$, $p=0.7913$) and CA1 ($F(3, 17) = 0.2816$, $p=0.8379$) were observed between the treatment groups (Fig.D.2.1, a-c, n=5-9).

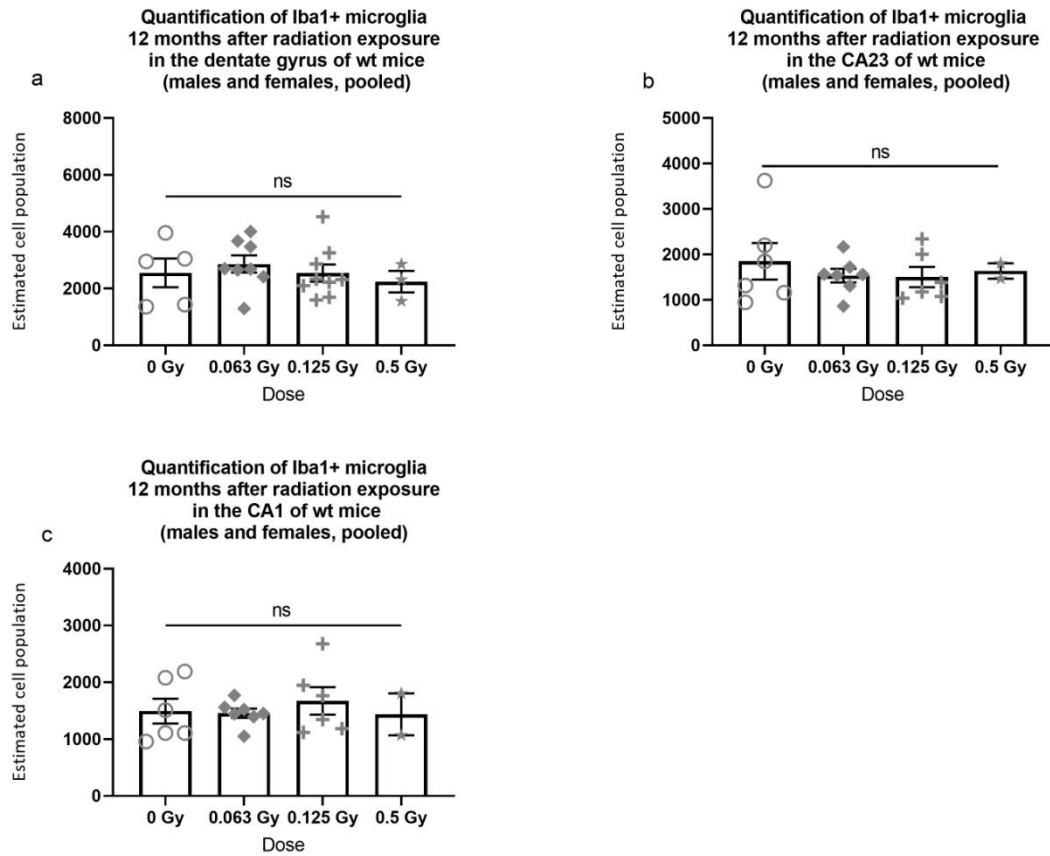


Fig.D.2.1. Quantification of Iba1+ microglia in in the hippocampus of wt mice at 12 months after exposure to ionizing radiation (0; 0.063; 0.125 and 0.5 Gy). Data are presented as scatter plots +/- SEM. n=3-9 animals. No significant differences in Iba1 expression were observed in the DG, the CA23 or in the CA1 of wt animals (a-c).

2.2. Quantification of Iba1+ microglia in the hippocampus 18 months after radiation exposure in wt mice

Because of the low number of animals available per group for the analysis of the brain tissues, males and females were pooled.

For the wt animals (n=6-8), no difference in microglial number in the DG ($F(3, 24) = 1.503$, $p=0.2391$), CA23 ($F(3, 23) = 0.8309$, $p=0.4905$) and CA1 ($F(3, 22) = 0.4682$, $p=0.7074$) were observed between the treatment groups (Fig. D.2.2; a-c).

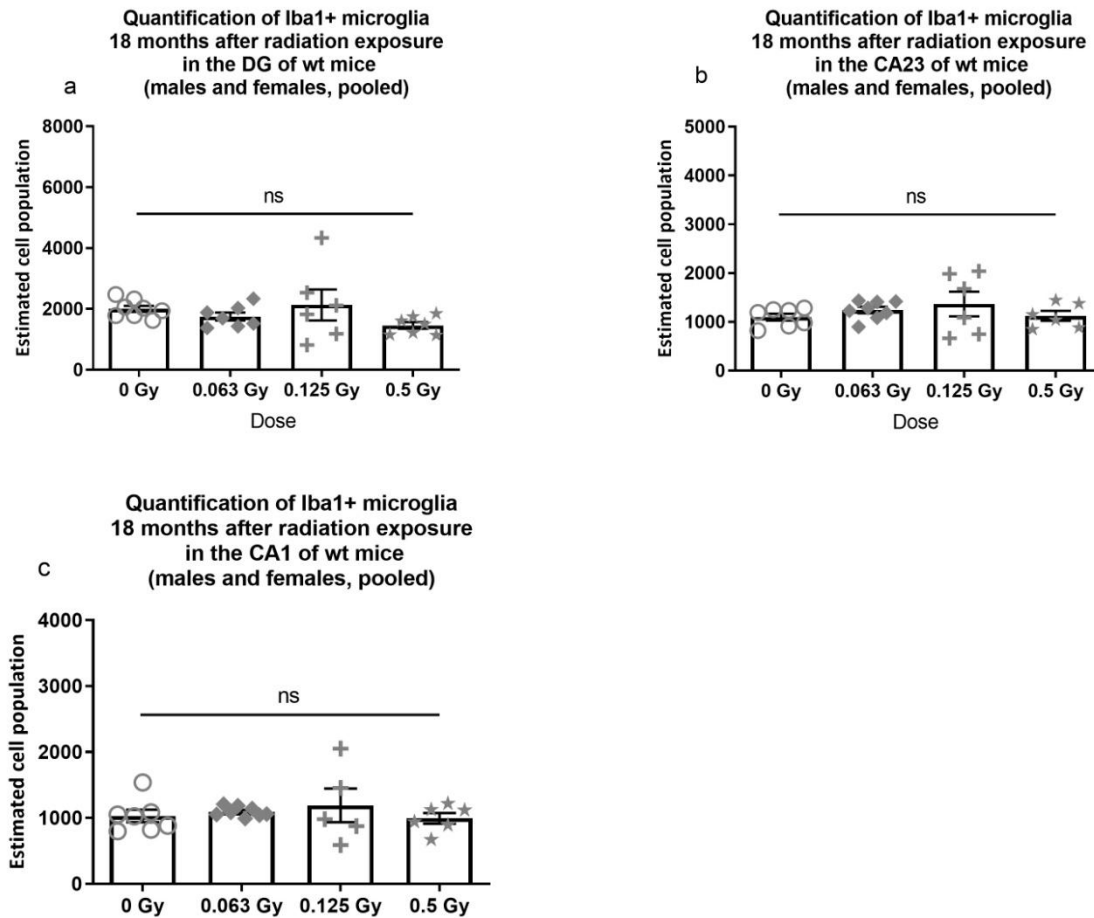


Fig.D.2.2. Quantification of Iba1+ microglia in the hippocampus of wt mice, 18 months after exposure to ionizing radiation (0; 0.063; 0.125 and 0.5 Gy). Data are presented as scatter plots +/- SEM. n=6-8 mice No significant differences in Iba1 expression were observed in DG, in the CA23 and the CA1 of wt animals (a-c).

2.3. Quantification of Iba1+ microglia in the hippocampus 24 months after radiation exposure in wt mice

Because of the low number of animals available per group for the analysis of the brain tissues, males and females were pooled.

For the wt animals (n=1-8), no difference in microglia number in the DG ($F(3, 14) = 1.053$, $p = 0.400$) or in CA23 ($F(3, 14) = 0.5318$, $p = 0.6679$) have been observed. Increased microglial number has been observed in CA1 of 0.063 Gy-irradiated animals compared to sham- and 0.125 Gy-irradiated animals (Fig.D.2.3, c, $F(3, 13) = 6.299$; $p = 0.0071$, post-hoc $p = 0.0288$ and $p = 0.0162$).

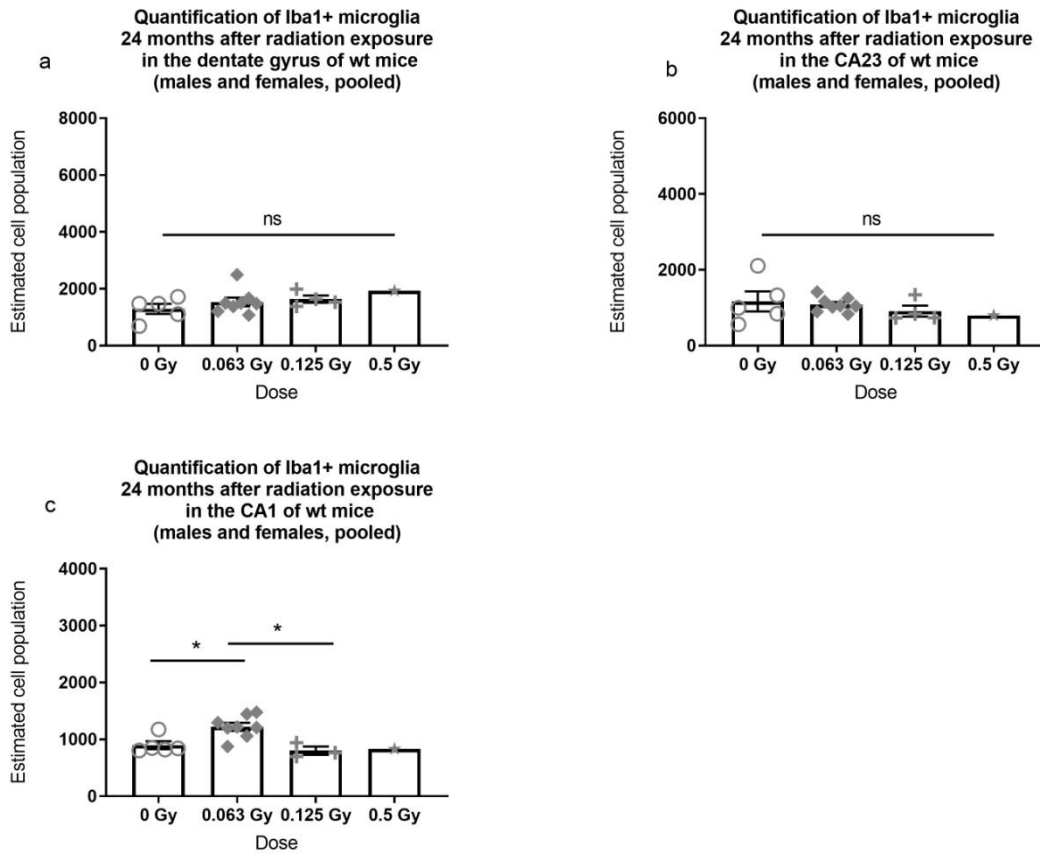


Fig. D.2.3. Quantification of Iba1+ microglia in the hippocampus of wt mice, 24 months after exposure to ionizing radiation (0; 0.063; 0.125 and 0.5 Gy). Results of post-hoc tests are indicated by * $p < 0.05$. Data are presented as scatter plots +/- SEM. $n = 1-8$ animals. No significant differences in Iba1 expression were observed in DG and in CA23 of wt animals (a, b). (c) An increase in Iba1 expression was observed in CA1 of 0.063 Gy-irradiated wt animals compared to sham-irradiated and 0.125 Gy-irradiated animals.

2.4. Quantification of Iba1+ microglia in the hippocampus 12 months after radiation exposure in $Ercc2^{S737P}$ het mice

For the het animals ($n = 4-9$), no significant differences in microglial number in DG ($F(3, 27) = 2.488$, $p = 0.0818$) and CA1 ($F(3, 19) = 2.376$, $p = 0.1021$) were observed between the treatment groups (a, c, $n = 7-9$) but a treatment effect was present for CA23 ($F(3, 21) = 3.182$, $p = 0.0451$).

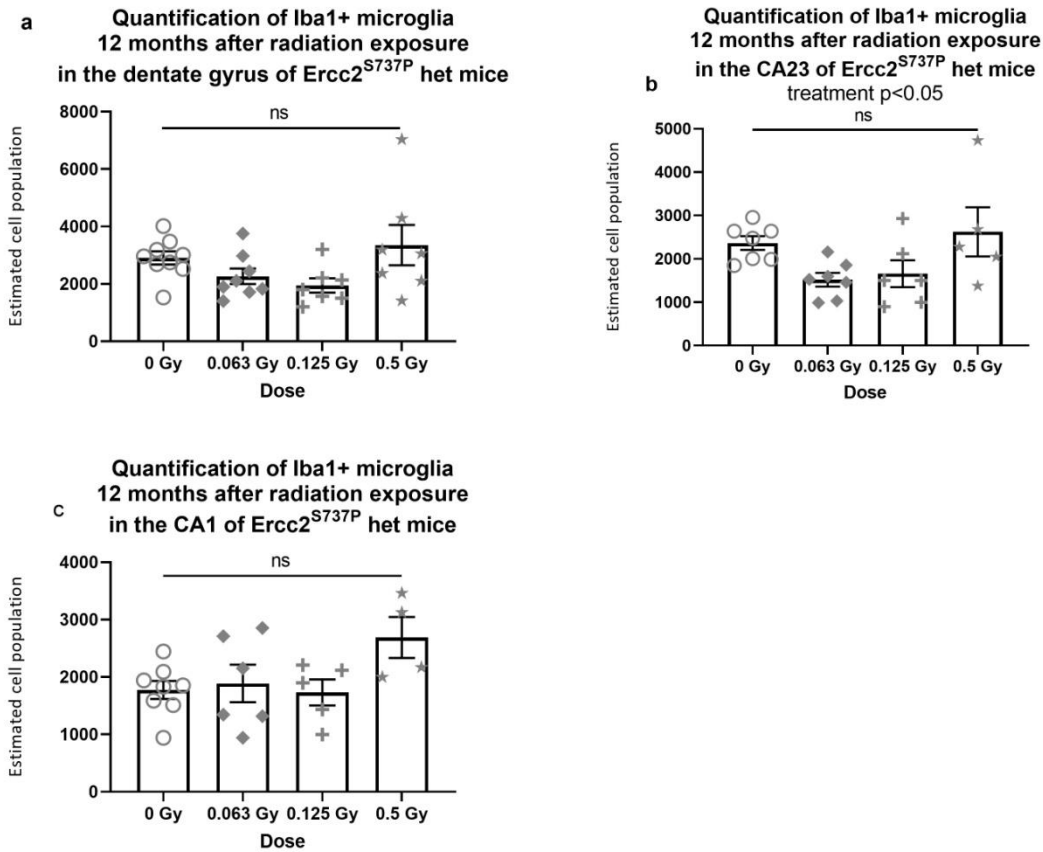


Fig.D.2.4. Quantification of Iba1+ microglia in the hippocampus 12 months after radiation exposure in Ercc2^{S737P} het mice. Data are presented as scatter plots +/- SEM. n=7-9 animals. No significant differences in Iba1 expression were observed in DG and in CA1 of het animals. (a, c). A treatment effect was observed in CA23 of het animals (b).

2.5. Quantification of Iba1+ microglia in the hippocampus 18 months after radiation exposure in Ercc2^{S737P} het mice.

For the het animals (n=2-9), a decrease in microglia in DG was observed after 0.125 Gy compared to sham- and 0.063 Gy-irradiated animals (a, $F(3, 16) = 4.608$; $p=0.0165$, post-hoc $p=0.0269$ and $p=0.0174$). In CA23, a decrease in microglia was observed after 0.125 Gy compared to sham-, 0.063 Gy- and 0.5 Gy-irradiated animals (b, $F(3, 17) = 6.813$; $p=0.0032$, post-hoc $p=0.0180$; $p=0.0018$ and $p=0.0056$). No differences in microglia number were found in CA1 between treatment groups (c, $F(3, 16) = 2.641$, $p=0.0848$).

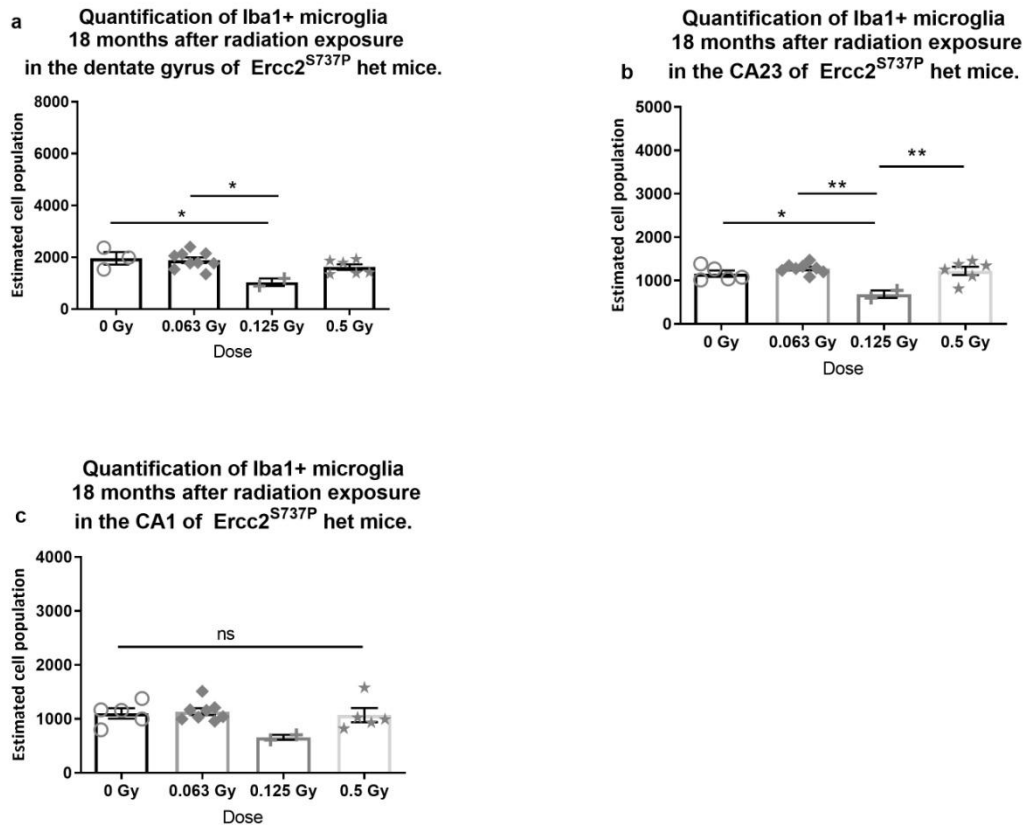


Fig. D.2.5. Quantification of Iba1+ microglia in the hippocampus 18 months after radiation exposure in Ercc2^{S737P} het mice. (a) A decrease in Iba1 expression have been observed in DG of 0.125 Gy-irradiated het animals compared to sham- and 0.063 Gy-irradiated animals. (b) A decrease in Iba1 expression have been observed in CA23 of 0.125 Gy-irradiated het animals compared to sham-irradiated, 0.063 Gy-, and 0.5 Gy-irradiated animals. (c) No significant differences in Iba1 expression have been observed in CA1 of het animals.

2.6. Quantification of Iba1+ microglia in the hippocampus 24 months after radiation exposure in Ercc2^{S737P} het mice.

For the het animals (n=3-8), an increase in Iba1 expression was observed in the DG of 0.5 Gy-irradiated animals compared to 0.063 Gy- and 0.125 Gy-irradiated animals (a, $F(3, 15) = 7.387$, $p=0.0029$, post-hoc $p=0.0114$ and $p=0.0064$). No significant differences were observed in Iba1 expression in CA23 ($F(3, 16) = 0.2301$, $p=0.8741$). A decrease in Iba1 expression was observed in the CA1 of 0.125 Gy-irradiated animals compared to 0.063 Gy- and 0.5 Gy-irradiated animals (c, $F(3, 16) = 4.788$, $p=0.0145$, post-hoc $p=0.0342$ and $p=0.0262$).

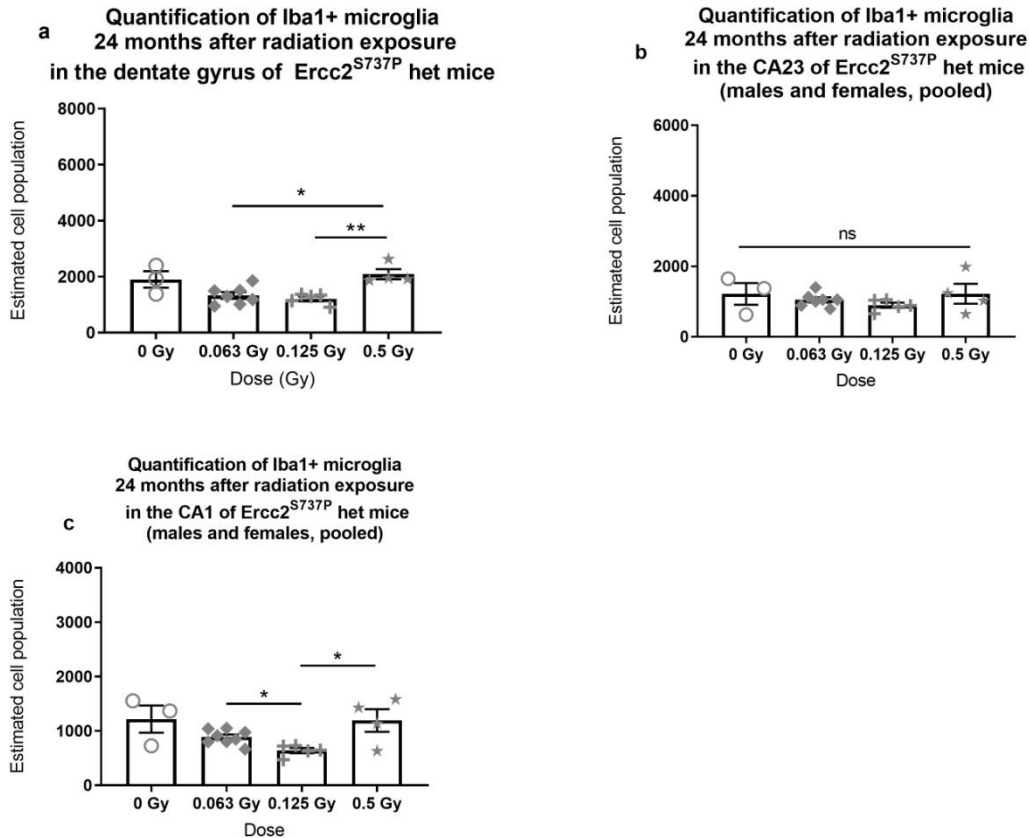


Fig. D.2.6. Quantification of Iba1+ microglia in the hippocampus 24 months after radiation exposure in *Ercc2*^{S737P} het mice. Significant differences in Iba1 expression were observed in DG and in CA1 of het animals (a, c). (c) A decrease in Iba1 expression was observed after 0.125 Gy in CA1 of het animals. 1 animal was excluded for technical reasons.

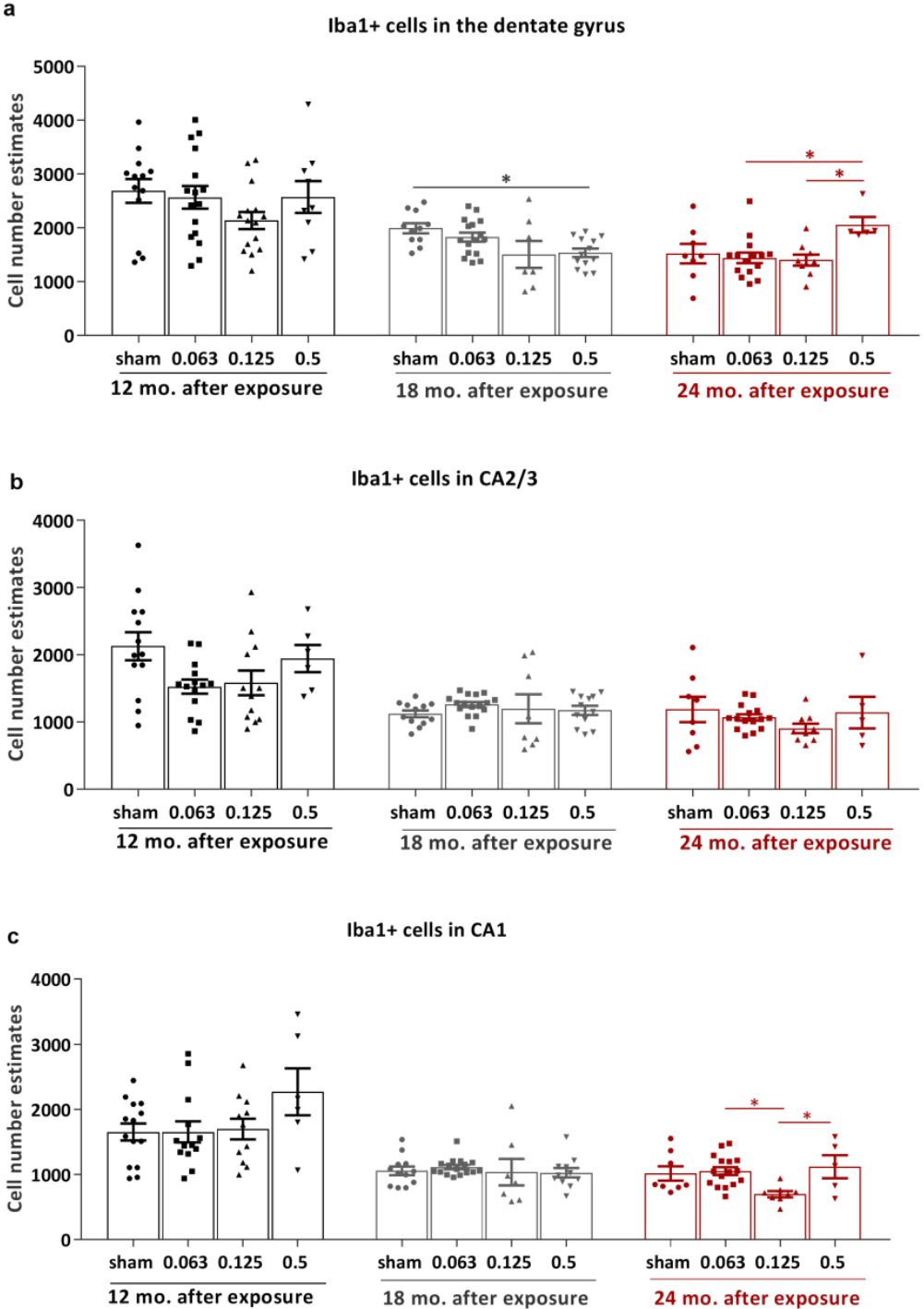
2.7. Linear Model Analysis: Iba1

An overview analysis was performed on all animals, sexes and genotypes pooled, in the continuity of the linear model analysis performed previously on behavioral data (§ Part C).

No consistent effects of the radiation were observed over time. However, a decline of Iba1+ cell number in all 3 hippocampal regions with age was observed, independent of the treatment. Linear model analysis revealed that the effect of time is statistically significant. 12 months was considered as the baseline. Effect of time for DG: $F(7,134) = 4.9$, $p = 6.5e-0.5$; for CA23: $F(7,126) = 2.5$, $p = 0.019$; for CA1: $F(7,125) = 3.2$, $p = 0.004$.

Subtle changes were observed. In the DG, a decrease in Iba1 expression was observed at 18 months after exposure in 0.5 Gy-irradiated animals compared to sham-irradiated animals ($F(3, 43) = 4.061$; $p = 0.0126$). At 24 months after exposure, an increase in Iba1 expression was observed in the DG of 0.5 Gy-irradiated animals, compared to 0.063 Gy- and 0.125 Gy-irradiated animals ($F(3,33) = 3.626$, $p = 0.0229$). No dose-dependent differences were observed in Iba1 expression in the CA23. In the CA1, a decrease in Iba1 expression was observed at 24

months after exposure in 0.125 Gy-irradiated animals compared to 0.063 Gy- and 0.5 Gy-irradiated animals ($F(3,33)=4.023, p=0.0152$).



D.2.7. Linear Model Analysis: Iba1+. Sexes and genotypes were pooled. Results of post-hoc tests are indicated by * $p < 0.05$. Data are presented as scatter plots +/- SEM. (a) A decrease in Iba1+ cell number was observed at 18 months after exposure to 0.5 Gy compared to sham-irradiated mice. An increase in Iba1+ cell number was observed at 24 months after exposure to 0.5 Gy compared to 0.063 Gy- and 0.125 Gy-irradiated mice. (b) No dose-dependent effects of radiation were observed in CA23. (c) A decrease in Iba1+ cell number was observed after 0.125 Gy compared to 0.063 Gy- and 0.5 Gy- irradiated mice in CA1.

2.8. Morphological analysis of microglial cells 24 months after exposure to ionizing radiation

To see if radiation induced long-term effects on inflammation in the hippocampus, microglial morphology was reconstituted in the dentate gyrus of 24-months old wildtype and *Ercc2*^{S737P} heterozygous mice, exposed to doses from 0 to 0.5 Gy. The number of nodes, endings, intersections and branch length of each observed microglia cell was estimated in order to provide information on their possible activation state. Number of endings increased after exposure to 0.063 Gy compared to sham-, 0.125 Gy-, and 0.5 Gy-irradiated animals (Fig. D.2.8, a, $F(3, 28) = 14.35$; $p < 0.0001$; post-hoc $p = 0.0030$; $p = 0.0007$ and $p < 0.0001$). Number of nodes increased after exposure to 0.063 Gy compared to sham-, 0.125 Gy-, and 0.5 Gy-irradiated animals (b, $F(3, 28) = 13.61$; $p < 0.0001$, post-hoc $p = 0.0032$; $p = 0.0032$ and $p < 0.0001$). Branch length increased after exposure to 0.063 Gy compared to sham-, 0.125 Gy-, and 0.5 Gy-irradiated animals (c, $F(3, 28) = 24.54$; $p < 0.0001$; post-hoc $p = 0.0003$; $p < 0.0001$ and $p < 0.0001$).

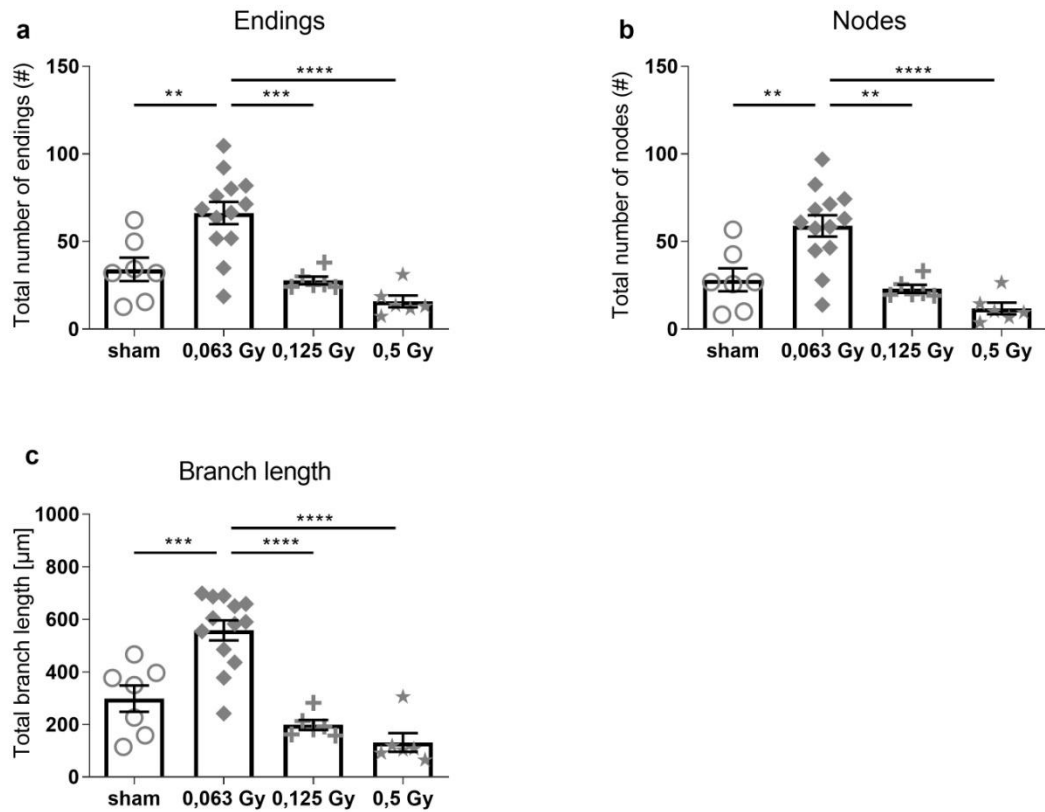


Fig. D.2.8.a. Dose-dependent effects of radiation on microglial morphology. Total numbers of endings (a), nodes (b), and the total branch length showed significant differences between 0.063 Gy-irradiated cells in comparison with all the other groups (c). Data are presented as means \pm SEM. Data were analyzed with 2-way Repeated Measures (RM) ANOVA and post-hoc tests were performed with Sidak's multiple comparisons. 10 cells/animal were traced. $n=6-13$ animals/group. Results of the post-hoc tests are indicated by * $p \leq 0.05$; ** $p \leq 0.01$; *** $p \leq 0.001$; **** $p \leq 0.0001$.

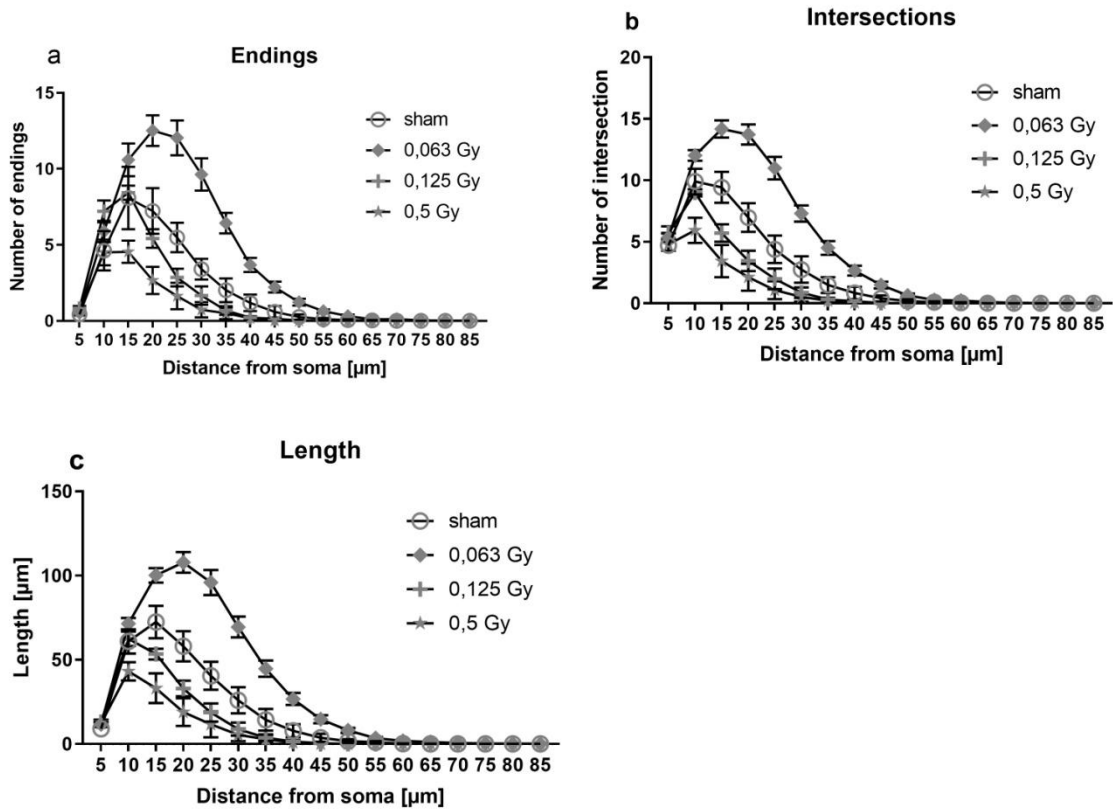


Fig. D.2.8.b. Sholl-analysis of microglial cell endings (a), intersections (b) and branch length (c). Clear hyper-ramification occurred 24 months after 0.063 Gy radiation and de-ramification after 0.5 Gy radiation ($n = 6-13$, $F(48, 448) = 11.85$ (for endings), 10.64 (for nodes) and 21.43 (for length), $p < 0.0001$). See Tables D.2.8.d for Holm-Sidak's *post hoc* test results.

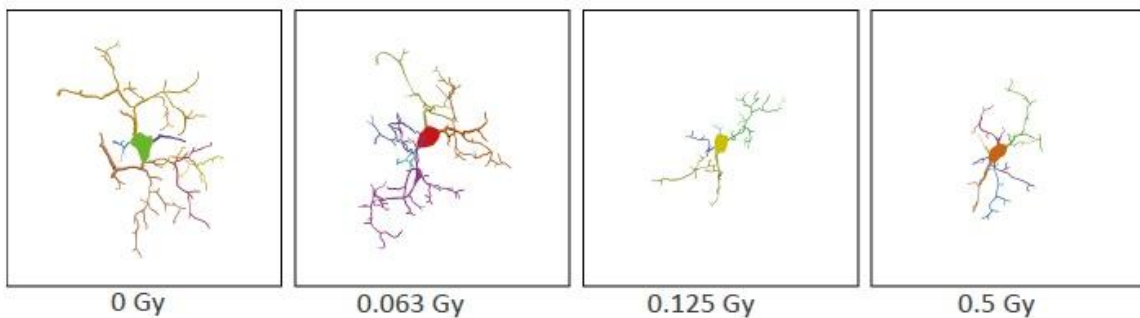


Fig. D.2.8.c. 3D-traced structures of exemplary hippocampal microglia of sham-, 0.063 Gy-, 0.125 Gy- and 0.5 Gy-irradiated animals, 24 months after exposure.

Tables D.2.8. Dose-dependent radiation effects on microglial branching complexity. Data were analyzed with 2-way Repeated Measures (RM) ANOVA and post-hoc tests were performed with Sidak's multiple comparisons. 10 cells/animal were traced. n=6-13 animals/group. * $p \leq 0.05$; ** $p \leq 0.01$; *** $p \leq 0.001$; **** $p \leq 0.0001$

Number of endings									
Radiation dose (Gy)	Distance from Soma [μm]								
	5	10	15	20	25	30	35	40	45
sham vs 0.063 Gy	-	-	*	****	****	****	****	*	-
sham vs 0.125 Gy	-	-	-	-	-	-	-	-	-
sham vs 0.5 Gy	-	-	**	****	***	*	-	-	-
0.063 Gy vs. 0.125 Gy	-	-	-	****	****	****	****	***	-
0.063 Gy vs. 0.5 Gy	-	-	****	****	****	****	****	***	-
0.125 Gy vs. 0.5 Gy	-	-	**	*	-	-	-	-	-

Number of nodes									
Radiation dose (Gy)	Distance from Soma [μm]								
	5	10	15	20	25	30	35	40	45
sham vs 0.063 Gy	-	-	***	****	****	****	***	-	-
sham vs 0.125 Gy	-	-	-	-	-	-	-	-	-
sham vs 0.5 Gy	-	-	****	***	-	-	-	-	-
0.063 Gy vs. 0.125 Gy	-	-	****	****	****	****	****	-	-
0.063 Gy vs. 0.5 Gy	-	****	****	****	****	****	****	*	-
0.125 Gy vs. 0.5 Gy	-	**	*	-	-	-	-	-	-

Branch length									
Radiation dose (Gy)	Distance from Soma [μm]								
	5	10	15	20	25	30	35	40	45
sham vs 0.063 Gy	-	-	****	****	****	****	***	**	-
sham vs 0.125 Gy	-	-	*	***	**	*	-	-	-
sham vs 0.5 Gy	-	*	****	****	****	**	-	-	-
0.063 Gy vs. 0.125 Gy	-	-	****	****	****	****	****	****	-
0.063 Gy vs. 0.5 Gy	-	****	****	****	****	****	****	****	-
0.125 Gy vs. 0.5 Gy	-	*	*	-	-	-	-	-	-

3. Quantification of GFAP+ astrocytes in the hippocampus of wt and Ercc2^{S737P} mice, males and females pooled, at 12, 18 or 24 months after radiation exposure to 0; 0.063; 0.125 or 0.5 Gy.

3.1. Quantification of GFAP+ astrocytes in the hippocampus of wt mice, males and females pooled, at 12 months after radiation exposure to 0; 0.063; 0.125 or 0.5 Gy.

Because of the low number of animals available per group for the analysis of the brain tissues, males and females were pooled.

For the wt animals (n=2-6), no significant differences in astrocytes number in the DG (F(3,13)=2.426, p=0.1123), CA23 (F(3,13)=1.702, p=0.3949) and CA1 (F(3,13)=0.7648, p=0.5338) were observed between the treatment groups.

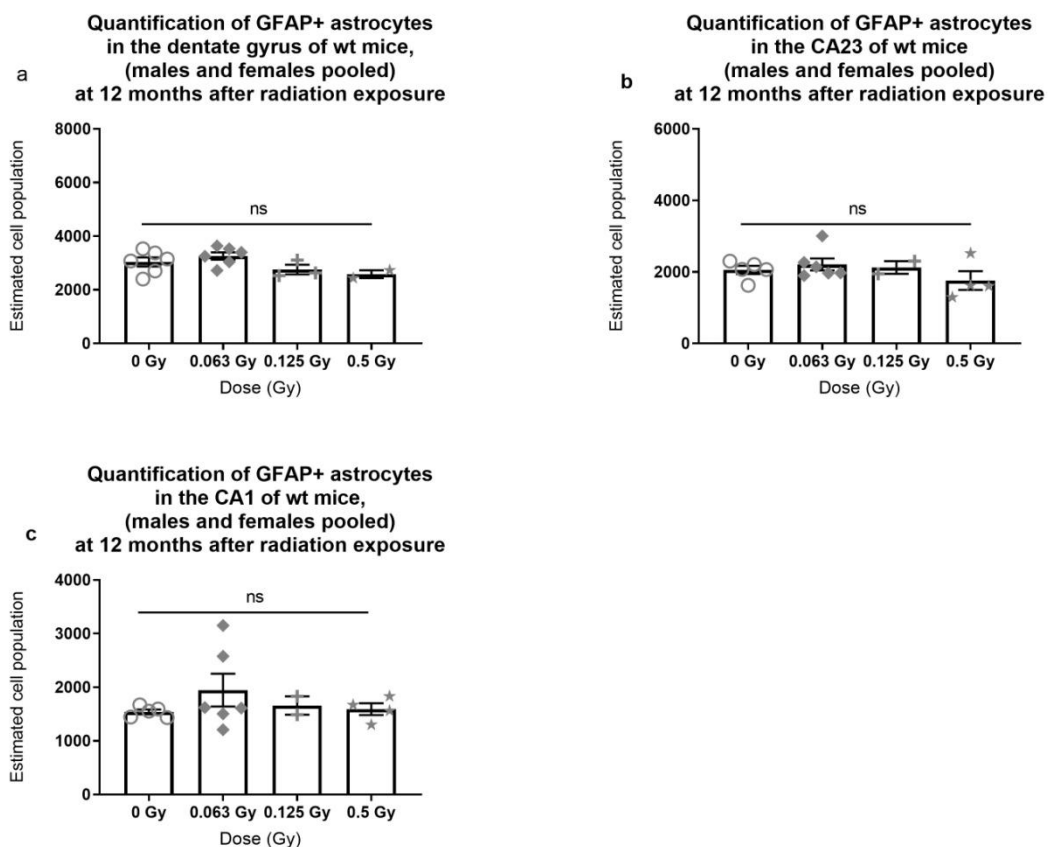


Fig. D.3.1. Quantification of GFAP+ astrocytes in the hippocampus of wt mice, males and females pooled, at 12 months after radiation exposure. Data are presented as scatter plots +/- SEM. n=2-6 animals. No significant differences in GFAP expression were observed in the DG, the CA23 and the CA1 of wt animals (a-c).

3.2. Quantification of GFAP+ astrocytes in the hippocampus of wt mice, males and females pooled, at 18 months after radiation exposure to 0; 0.063; 0.125 or 0.5 Gy.

Because of the low number of animals available per group for the analysis of the brain tissues, males and females were pooled.

For wt animals (n=4-8), an increased astrocyte number was observed in the DG of 0.125 Gy-irradiated animals compared to 0.5 Gy-irradiated animals (Fig.D.3.2, a; $F(3, 23) = 3.972$; $p=0.0204$, post-hoc $p=0.0369$). Increased astrocyte number was also visible in CA23 of 0.125 Gy-irradiated animals compared to sham-, 0.063 Gy- and 0.5 Gy-irradiated animals (b, $F(3, 23) = 7.008$; $p=0.0016$, post-hoc $p=0.0175$; $p=0.0087$ and $p=0.0033$). The same trend was visible in CA1 of 0.125 Gy-irradiated animals, compared to 0.063 Gy- and 0.5 Gy-irradiated animals (c, $F(3, 23) = 7.876$; $p=0.0009$, post-hoc $p=0.0005$ and $p=0.0174$).

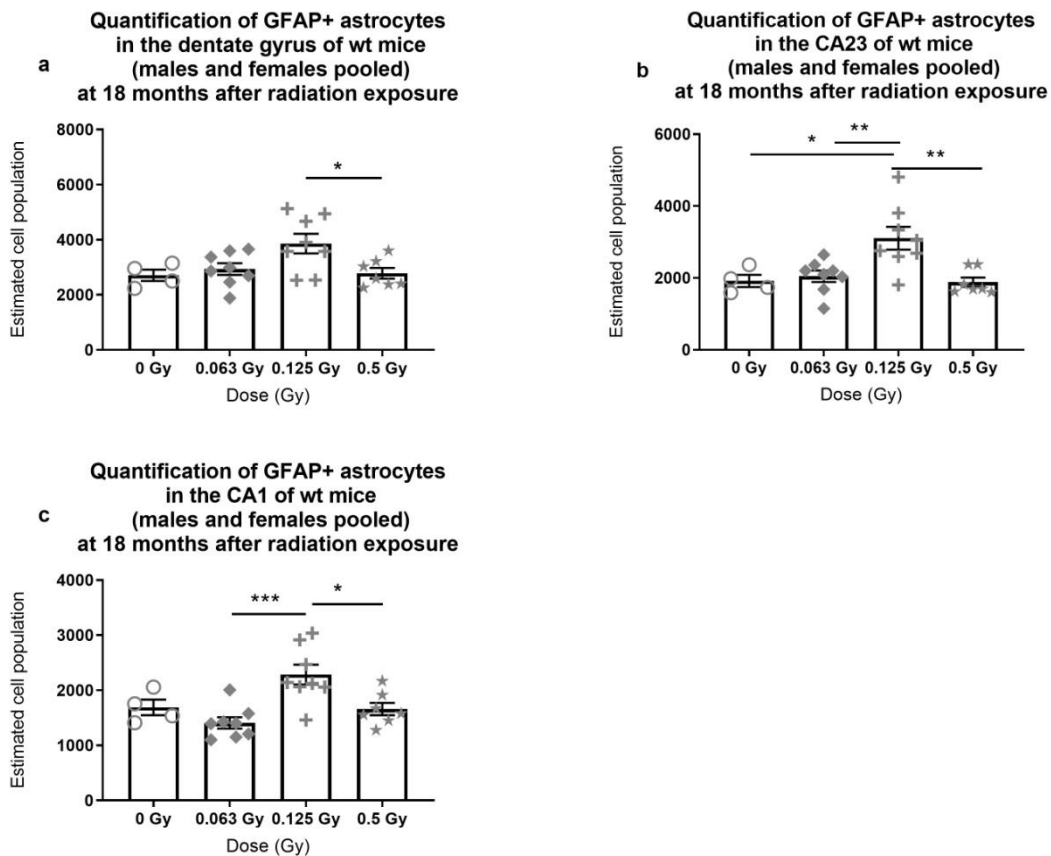


Fig.D.3.2 Quantification of GFAP+ astrocytes in the hippocampus of wt mice, males and females pooled, at 18 months after radiation exposure to 0; 0.063; 0.125 or 0.5 Gy. Results of post-hoc tests are indicated * $p<0.05$, ** $p<0.01$ *** $p<0.001$. Data are presented as scatter plots +/- SEM. n=4-8 animals. (a) An increase in GFAP expression was observed in DG of 0.125 Gy-irradiated wt animals compared to 0.5 Gy-irradiated animals. (b) An increase in GFAP expression was observed in CA23 of 0.125 Gy-irradiated wt animals compared to the other treated groups. (c) An increase in GFAP expression was observed in CA1 of 0.125 Gy-irradiated wt animals compared to 0.063 Gy and 0.5 Gy-irradiated animals.

3.3 Quantification of GFAP+ astrocytes in the hippocampus of wt mice, males and females pooled, at 24 months after radiation exposure to 0; 0.063; 0.125 or 0.5 Gy

Because of the low number of animals available per group for the analysis of the brain tissues, males and females were pooled.

For wt animals (Fig.D.3.3, n=4-7, a-c), no significant differences in astrocyte number were observed in the DG ($F(3, 13) = 2.268, p = 0.1289$), CA23 ($F(3, 14) = 1.382, p = 0.2892$) and CA1 ($F(3, 12) = 3.029, p = 0.0711$) between treatment groups.

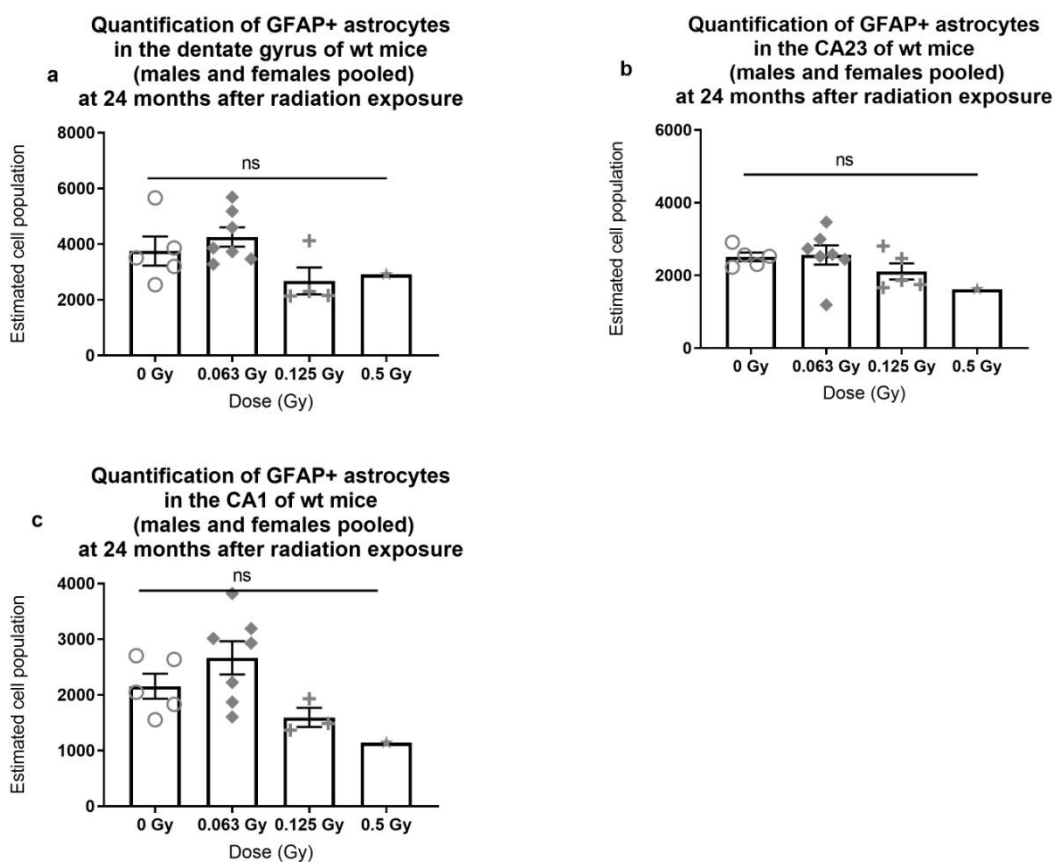


Fig.D.3.3. Quantification of GFAP+ astrocytes in the hippocampus of wt mice, males and females pooled, at 24 months after radiation exposure to 0; 0.063; 0.125 or 0.5 Gy. Data are presented as scatter plots +/- SEM. No significant differences in GFAP expression were observed in the DG, the CA23 and the CA1 of wt animals (a-c).

3.4. Quantification of GFAP+ astrocytes in the hippocampus of *Ercc2*^{S737P} het mice, males and females pooled, 12 months after exposure

For the het animals (n=2-8), no significant differences in astrocytes in the DG ($F(3, 14) = 0.7190, p = 0.5570$) and CA1 ($F(3, 14) = 0.2086, p = 0.8887$) were observed between the

treatment groups. An increased number of astrocytes were observed in CA23 of 0.5 Gy-irradiated het animals compared to sham-, 0.064 Gy- and 0.125 Gy-irradiated animals (Fig.D.3.4; b; $F(3, 13) = 6.709$; $p=0.0056$, post-hoc $p=0.0402$; $p=0.0302$ and $p=0.0072$).

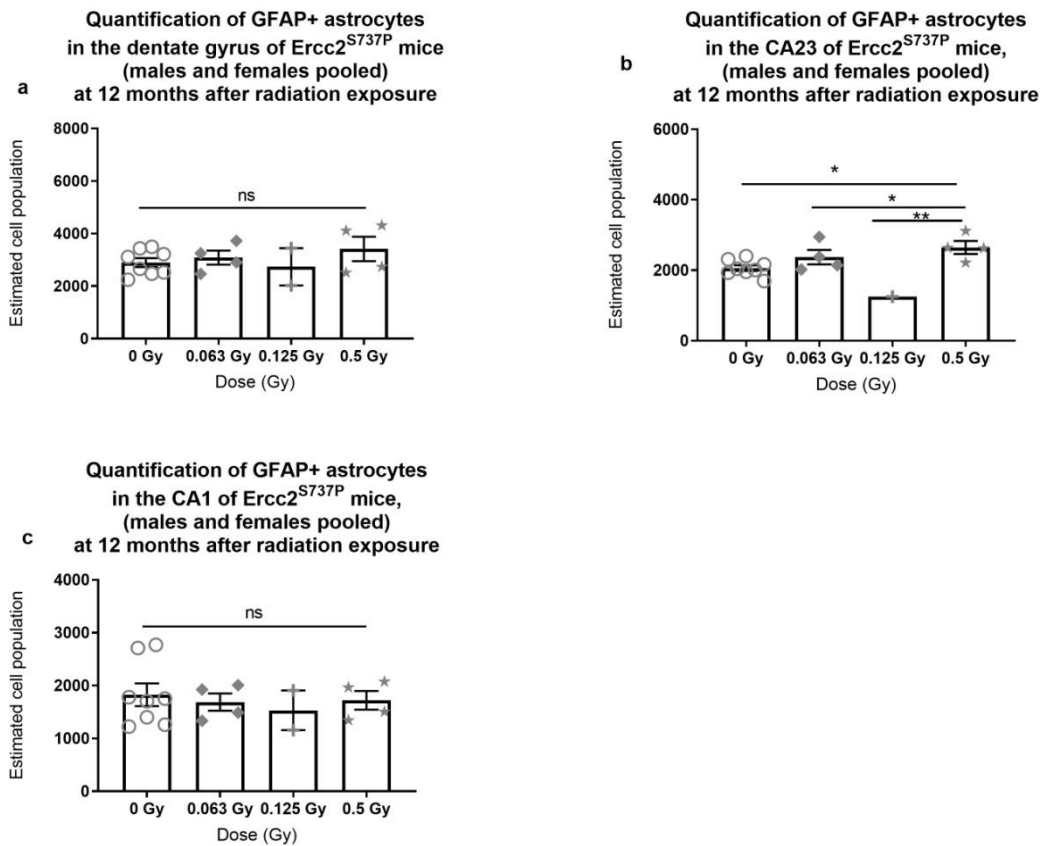


Fig.D.3.4. Quantification of GFAP+ astrocytes in the hippocampus of $Ercc2^{S737P}$ het mice, males and females pooled, at 12 months after radiation exposure to 0; 0.063; 0.125 or 0.5 Gy. (a) No significant differences in GFAP expression were observed in DG of het animals. (b) An increase in GFAP expression was observed in CA23 of 0.5 Gy-irradiated het animals compared to sham-, 0.063 Gy-, and 0.125 Gy-irradiated animals. (c) No significant differences in GFAP expression were been observed in CA1 of het animals. Data are presented as scatter plots +/- SEM. $n=2-8$ animals. Results of the post-tests are indicated on the graph by * $p<0.05$, ** $p<0.01$.

3.5. Quantification of GFAP+ astrocytes in the hippocampus of $Ercc2^{S737P}$ het mice, males and females pooled, at 18 months after radiation exposure to 0; 0.063; 0.125 or 0.5 Gy.

For het animals ($n=4-8$), no significant differences in astrocyte number were observed in GFAP expression in the DG ($F(3, 18) = 0.3059$, $p=0.8207$), CA23 ($F(3, 18) = 0.5991$, $p=0.6238$) and CA1 ($F(3, 18) = 0.4114$, $p=0.7468$) after exposure.

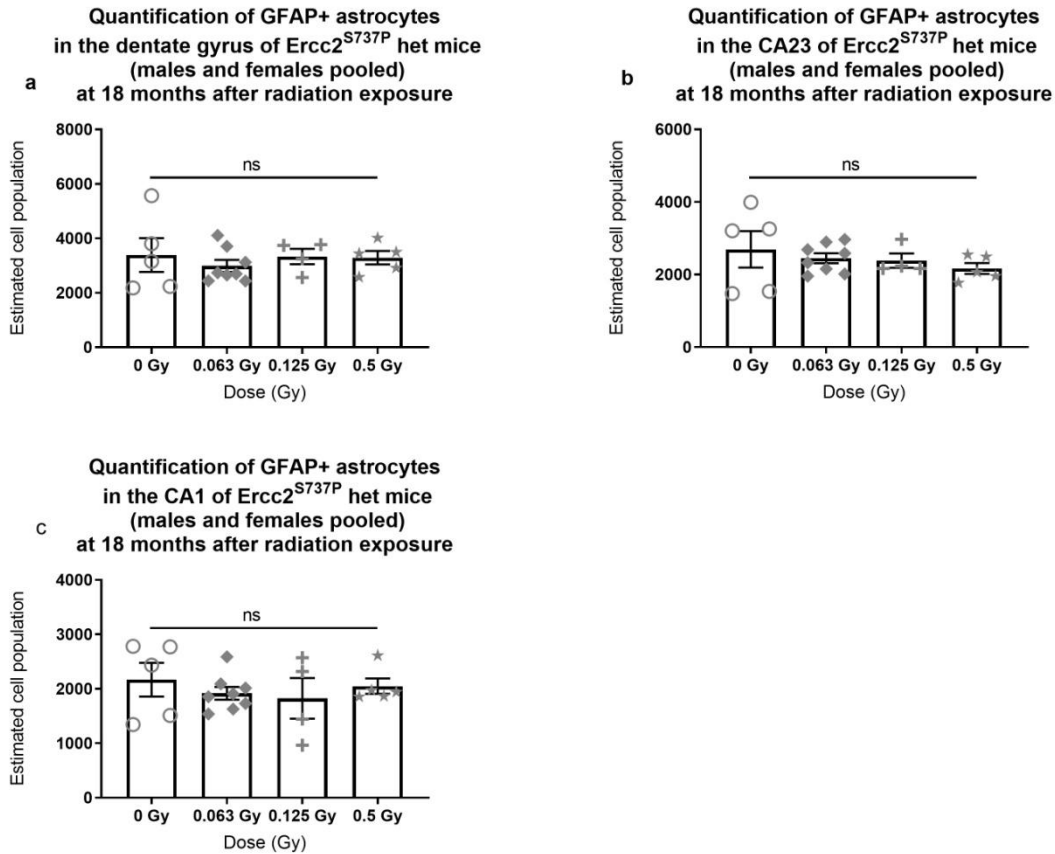


Fig. D.3.5. Quantification of GFAP+ astrocytes in the hippocampus of *Ercc2* het mice, males and females pooled, at 18 months after radiation exposure to 0; 0.063; 0.125 or 0.5 Gy. No significant differences in GFAP expression was observed in the DG, in the CA23 and the CA1 of het animals (a-c). Data are presented as scatter plots +/- SEM. n=4-8 animals.

3.6. Quantification of GFAP+ astrocytes in the hippocampus of *Ercc2* het mice, males and females pooled, at 24 months after radiation exposure to 0; 0.063; 0.125 or 0.5 Gy.

For het animals (a-c, n=4-8), no differences in astrocyte number were observed in the DG ($F(3, 21) = 0.8326$, $p = 0.4909$), CA23 ($F(3, 20) = 0.5515$, $p = 0.6530$) and CA1 ($F(3, 21) = 2.462$, $p = 0.0907$) between treatment groups.

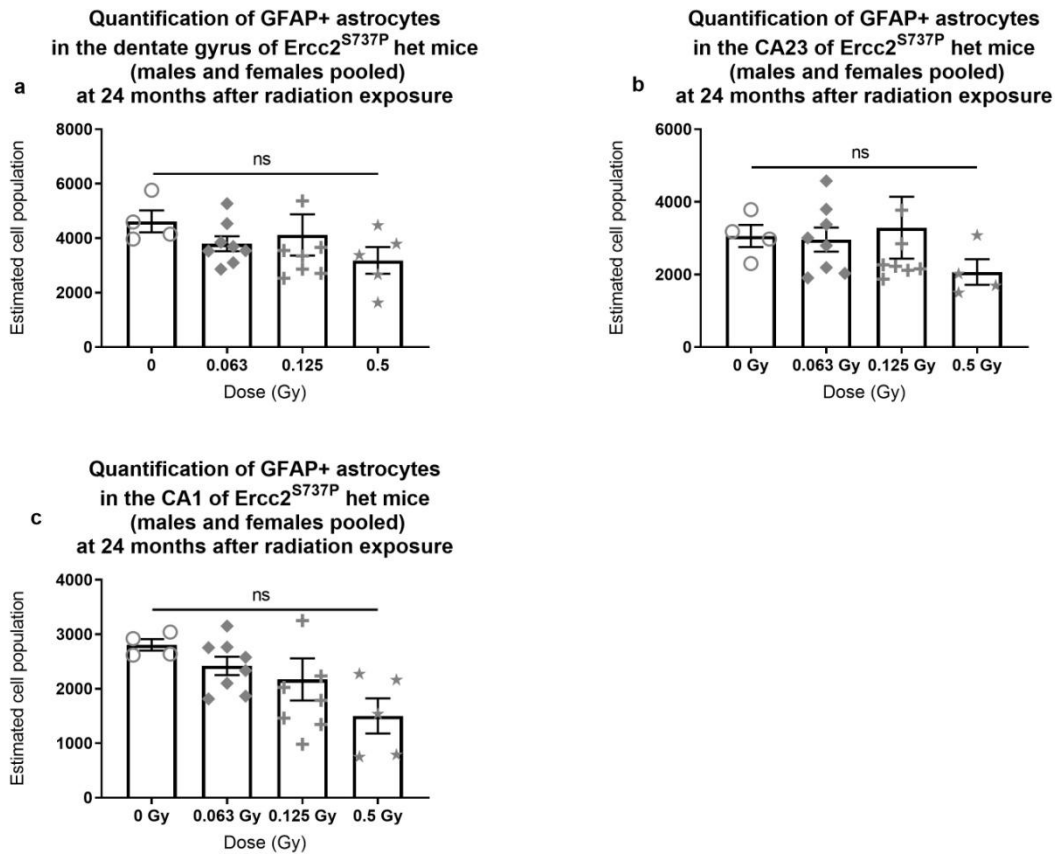


Fig. D.3.6. Quantification of GFAP+ astrocytes in the hippocampus of *Ercc2* het mice, males and females pooled, at 24 months after radiation exposure to 0; 0.063; 0.125 or 0.5 Gy. No significant differences in GFAP expression were observed in the DG, the CA23 and the CA1 of het animals (a-c). Data are presented as scatter plots +/- SEM. n=4-8 animals.

3.7. Linear Model Analysis: GFAP

The following overview analysis was performed on all animals, sexes and genotypes pooled, in the continuity of the linear model analysis performed on the behavioral data (Results, § C).

No consistent effect of radiation on astrocytes was observed over time in the hippocampus. Only at the late time point of 24 months after exposure, there appeared to be a subtle trend towards a dose-dependent radiation effect on astrocyte number in the three hippocampal regions. The only significant effect was a decrease in the CA1 regions as stated in the previous sections. Interestingly, time effect was significant for CA23 ($F(7,133) = 2.6, p = 0.015$) and CA1 ($F(7,134) = 2.8, p = 0.0087$).

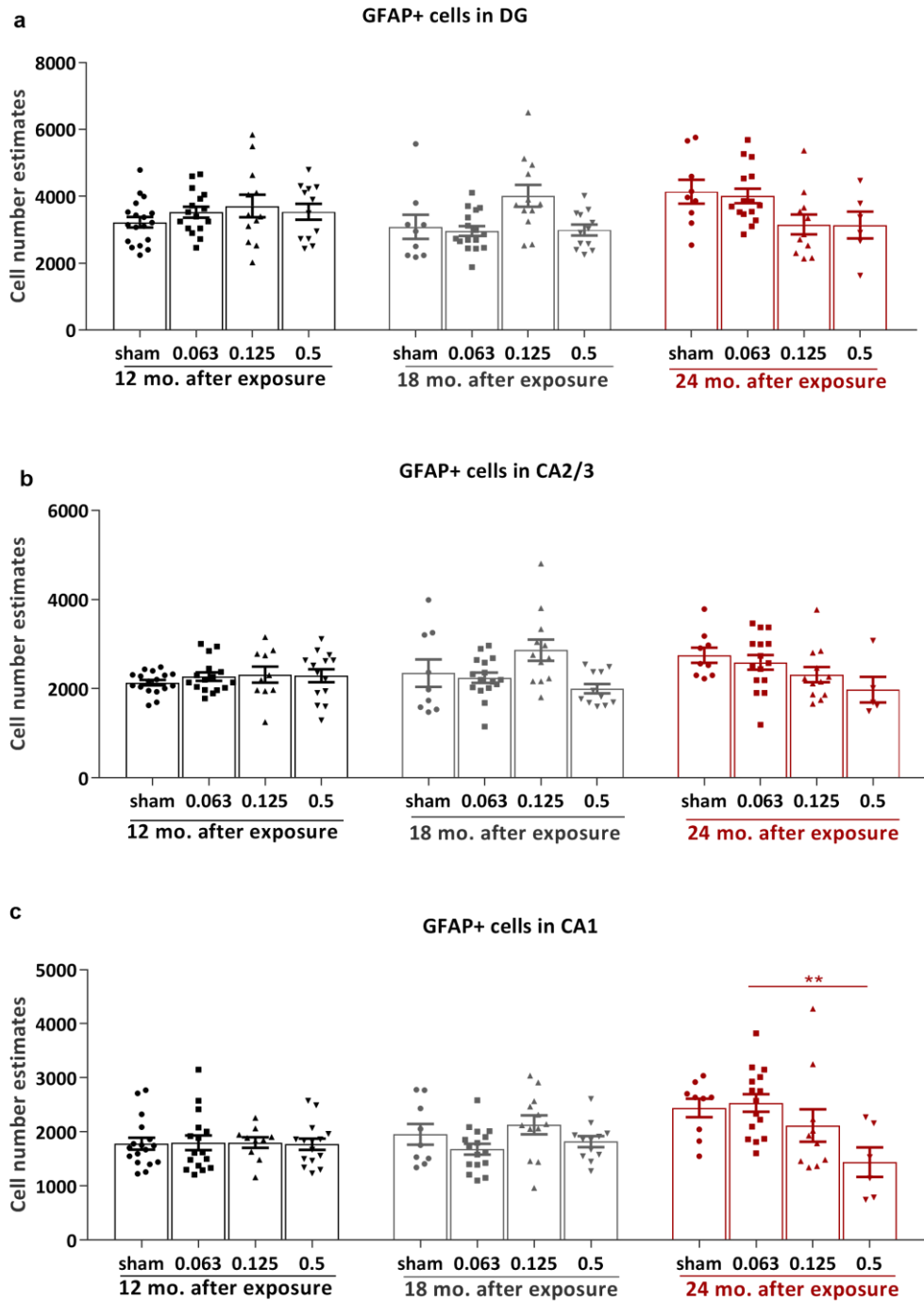


Fig.D.3.7. Linear Model Analysis: GFAP. Sexes and genotypes were pooled. Results of post-hoc tests are indicated by ** $p < 0.01$. Data are presented as scatter plots +/- SEM. No dose-dependent effects of radiation were observed in DG or in CA23 (a, b). A decrease in GFAP+ astrocytes in CA1 was observed at 24 months after exposure to 0.5 Gy, compared to 0.063 Gy-irradiated group.

3.8. Morphological analysis of astrocytic cells.

To see if radiation induced long-term effects morphological changes in the support cells of hippocampus, astrocytic morphology was reconstituted in the dentate gyrus of 24-months old wt and *Ercc2*^{S737P} het mice, exposed to doses from 0 to 0.5 Gy using Neurolucida software. Using this program, the number of nodes, endings, intersections and dendrite length of each observed astrocytic cell was estimated in order to provide information on their possible activation state. Results were analyzed with 2-way RM ANOVA and post-hoc tests performed with the Sidak's multiple comparisons test. Number of endings decreased after exposure to 0.125 Gy compared to sham-irradiated animals and after exposure to 0.5 Gy compared to 0.063 Gy-irradiated animals (Fig.D.3.8, a, $F(3, 44) = 5.819$; $p=0.0019$, post-hoc $p=0.0205$ and $p=0.0058$). Number of nodes decreased after exposure to 0.125 Gy compared to sham- and 0.063 Gy-irradiated animals and after exposure to 0.5 Gy compared to 0.063 Gy-irradiated animals (b, $F(3, 44) = 7.218$; $p=0.0005$; post-hoc $p=0.0148$; $p=0.0023$ and $p=0.0130$). Dendritic length decreased after exposure to 0.125 Gy compared to sham- and 0.063 Gy irradiated animals (c, $F(3, 44) = 5.950$; $p=0.0017$; post-hoc $p=0.0124$ and $p=0.0034$).

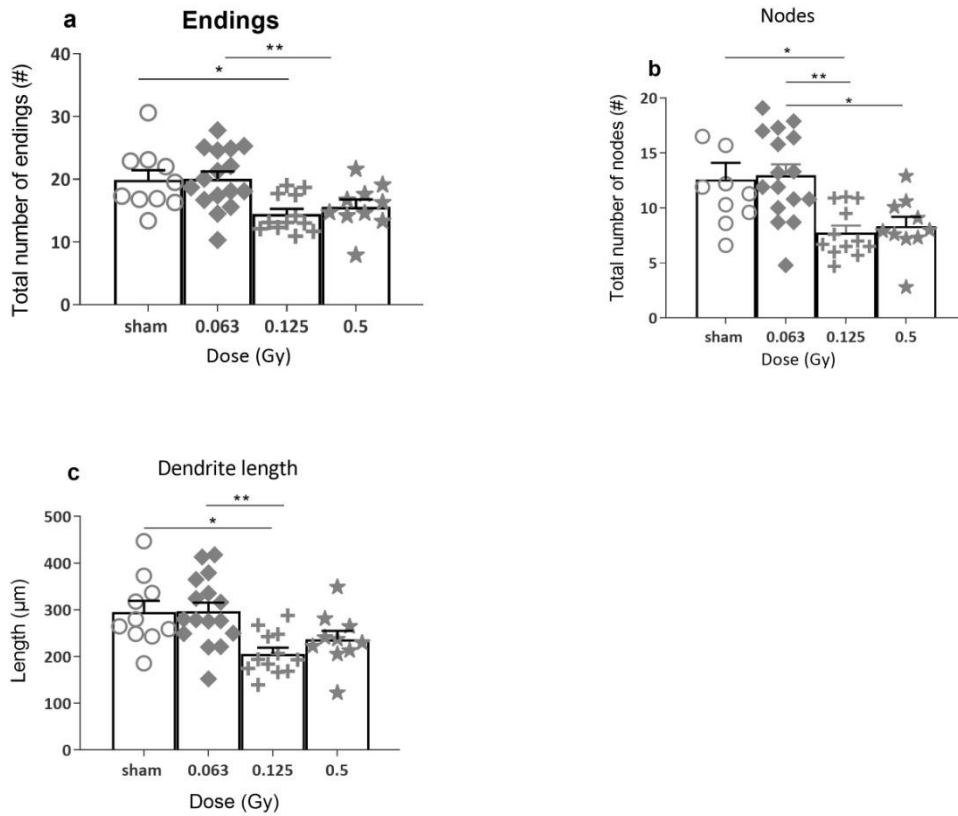


Fig.D.3.8.a. Dose-dependent radiation effects on astrocyte branching complexity. Total numbers of endings **a**, nodes, **b** and **c**, the total dendrite length show significant differences between 0.125 Gy irradiated cells in comparison with sham- and 0.063 Gy irradiated groups. Data are presented as means +/- SEM. 10 cells/animal were traced. n=10-16 animals/group * $p \leq 0.05$; ** $p \leq 0.01$; *** $p \leq 0.001$; **** $p \leq 0.0001$.

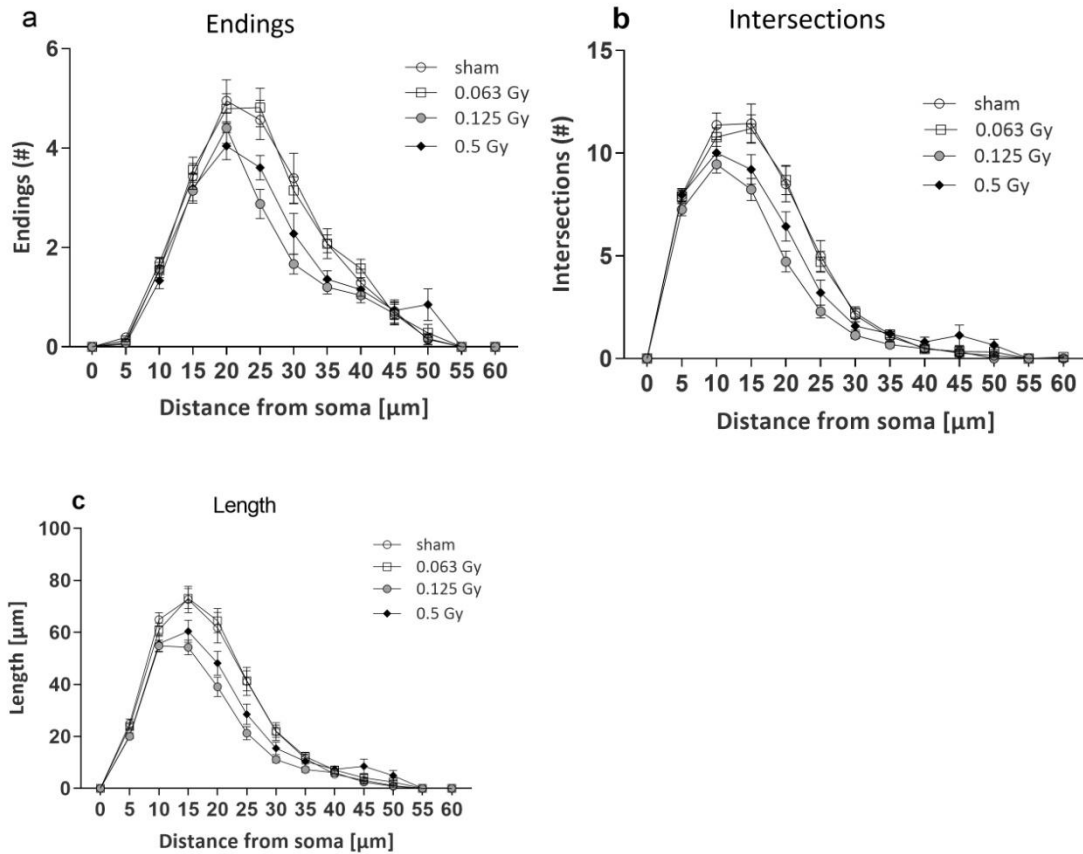


Fig.D.3.8.b. Sholl-analysis of astrocyte endings (a), intersections (b) and branch length (c). (n = 10-16, repeated measures ANOVA, $F(36, 572) = 2.531$ (for endings), 3.255 (for intersections) and 3.551 (for length), $p < 0.0001$). See Table D.3.8.d for Holm-Sidak's *post hoc* test results

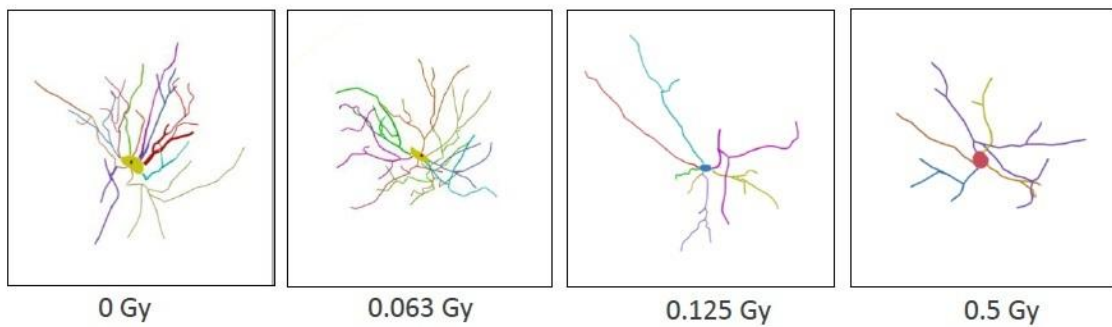


Fig.D.3.8.c. 3D-traced structures of exemplary hippocampal astrocytes of sham-, 0.063 Gy-, 0.125 Gy- and 0.5 Gy- irradiated animals, 24 months after exposure.

Table D.3.8. Dose-dependent radiation effects on astrocytic branching complexity. Data was analysed with 2-way Repeated Measures (RM) ANOVA and post-hoc tests were performed with Sidak's multiple comparisons. 10 cells/animal were traced. n=10-16 animals/group. * $p \leq 0.05$; ** $p \leq 0.01$; *** $p \leq 0.001$; **** $p \leq 0.0001$

Number of endings									
Radiation dose (Gy)	Distance from Soma [μm]								
	5	10	15	20	25	30	35	40	45
sham vs 0.063 Gy	-	-	-	-	-	-	-	-	-
sham vs 0.125 Gy	-	-	-	-	****	****	*	-	-
sham vs 0.5 Gy	-	-	-	*	**	**	-	-	-
0.063 Gy vs. 0.125 Gy	-	-	-	-	****	****	*	-	-
0.063 Gy vs. 0.5 Gy	-	-	-	-	*	*	*	-	-
0.125 Gy vs. 0.5 Gy	-	-	-	-	-	-	-	-	-

Number of nodes									
Radiation dose (Gy)	Distance from Soma [μm]								
	5	10	15	20	25	30	35	40	45
sham vs 0.063 Gy	-	-	-	-	-	-	-	-	-
sham vs 0.125 Gy	-	****	****	****	*	-	-	-	-
sham vs 0.5 Gy	-	****	**	**	-	-	-	-	-
0.063 Gy vs. 0.125 Gy	-	***	****	****	**	-	-	-	-
0.063 Gy vs. 0.5 Gy	-	****	****	****	*	-	-	-	-
0.125 Gy vs. 0.5 Gy	-	-	-	-	-	-	-	-	-

Number of intersections									
Radiation dose (Gy)	Distance from Soma [μm]								
	5	10	15	20	25	30	35	40	45
sham vs 0.063 Gy	-	-	-	-	-	-	-	-	-
sham vs 0.125 Gy	-	**	****	****	****	-	-	-	-
sham vs 0.5 Gy	-	-	**	**	*	-	-	-	-
0.063 Gy vs. 0.125 Gy	-	-	****	****	****	-	-	-	-
0.063 Gy vs. 0.5 Gy	-	-	**	***	*	-	-	-	-
0.125 Gy vs. 0.5 Gy	-	-	-	*	-	-	-	-	-

Branch length									
Radiation dose (Gy)	Distance from Soma [μm]								
	5	10	15	20	25	30	35	40	45
sham vs 0.063 Gy	-	-	-	-	-	-	-	-	-
sham vs 0.125 Gy	-	-	****	****	****	*	-	-	-
sham vs 0.5 Gy	-	*	**	**	**	-	-	-	-
0.063 Gy vs. 0.125 Gy	-	-	****	****	****	**	-	-	-
0.063 Gy vs. 0.5 Gy	-	-	**	****	***	-	-	-	-
0.125 Gy vs. 0.5 Gy	-	-	-	-	-	-	-	-	-

V. Discussion

This thesis focuses on the long-term effects of a single whole-brain low-dose radiation exposure on the brain and on the behavior of adult wildtype and *Ercc2*^{S737P} heterozygous mice. Long-term effects of low-dose radiation exposure are still unclear.

Up to now there is no clear definition of what is a low radiation dose. Legislation suggests that doses between 10 and 100 mGy would be considered as low doses. However, a clear understanding of the transition between very low and low doses with a potential biological risk is still not achieved.

The long-term consequences of low-dose radiation are also not well defined. Data provided by long-term epidemiologic studies on exposed cohorts are an important source of information but the presence of confounding factors such as environment or lifestyle can potentially strongly influence the results.

With the evolution of technology and the ever-growing use of X-ray technology for diagnostic and radiotherapy, low-dose radiation exposure is part of our lives and it is important to measure its risks. The importance of studying the effects of low-dose radiation exposure is vital for evaluating the potential risk for inhabitants of naturally high radioactive sites or decontaminated radioactive areas. Professionals exposed daily to radiation have the rights to know the later risks consecutive to their profession. In addition, several studies study actually the long-term effects of low-dose radiation exposure in preparation for spatial travel.

Numerous evidences show that biochemical pathways stimulated by low-dose radiation exposure are different that the ones activated by high-dose exposure. Simply adapting the risk model used at high-dose exposure to fit low-dose exposure is not functioning because the biological processes do not occur in a linear way.

Due to its low mitotic activity, the brain was previously considered not so sensitive to radiation. However, the presence of adult neurogenesis and the cognitive problems experienced by patients after brain radiotherapy are modifying this paradigm.

The aim of this thesis was to correlate potential behavioral changes occurring after low-dose radiation exposure with cellular changes observed on the neurons and on the brain microenvironment, over a long-time period (>1 year) to reproduce long-term effects occurring during adulthood and aging. For this purpose, the mouse model was considered the most suitable. A mutant mouse line, heterozygous *Ercc2*^{S737P} was included in the study, considering its potential increased radiation sensitivity compared to control mice. The reason behind was to compare long-term behavioral and cellular effects of low-dose radiation on healthy and on pathological conditions. These mutant mice did not show strongly significant behavioral or cellular long-term changes that could be correlated with low-dose radiation exposure. In fact, non-irradiated *Ercc2*^{S737P} het mice demonstrated higher

levels of total distance, speed and rearing in comparison to non-irradiated wt mice at 18 months after sham exposure.

1. Main findings

In the open field, no general sex or genotype effect could be statistically addressed meaningfully with the 2 way-ANOVA analysis.

In the acoustic startle test, no consistent effects were observed. So far, more effects were observed at higher doses and later time points. No effects after exposure to 0.125 Gy were present at 4 or 12 months. Could this dose be considered as a limit, at which positive and negative radiation effects hold the balance?

In the social discrimination test, the reduction in recognition index in male wt mice 4 months after exposure with 0.5 Gy might be related to an adult neurogenesis reducing effect of radiation. However, it is not clear why this effect is not seen in female wt mice irradiated with the same dose. It is also not seen in het mice irradiated with this dose but this could be due to differences in radiation sensitivity or in time course of cellular responses to radiation between het and wt. This reduction of recognition index is a transient effect since it is not seen again at later time points. The increase in recognition index in het mice irradiated with 0.125 Gy at 18 months after exposure might also happen because of differences between wt and het in radiation sensitivity or time course of cellular responses.

It is not clear if the observed reductions in investigation time in different male groups might be related to differences in housing conditions, which are sometimes necessary in long-term studies with male mice. Single housed mice explore conspecifics more than grouped-housed mice during this test. To sum up, no consistent dose-related effects were detectable with these individual analyses. Therefore, overall analyses that took all time points and groups into account were necessary to address the question if radiation affected the sexes and the genotypes differently (i.e. assessing treatment x sex or treatment x genotype interactions). This overall analysis also allowed the assessment of changes in the measured parameters over time.

The linear model analysis with random intercept provided a clear outlook on the long-term effects of low dose ionizing radiation. First of all, it confirmed that radiation affected general behavior, with a significant general dose effect on acoustic startle, spontaneous locomotion (total distance travelled and whole average speed) and explorative behavior (rearing). Second, it revealed the presence of delayed effects of radiation on behavior. While ASR/BW at 110 dB decreased already at 4 months after exposure to 0.5 Gy, the effects of radiation on spontaneous locomotion and explorative behavior started only at 12 months after exposure. Third, it revealed a possible genotype-dose interaction at 18 months on these parameters, possibly due to significant differences between sham-irradiated wt and sham-irradiated het animals that appeared only at this later age. Finally, significant differences between sham-

irradiated and 0.063 Gy-irradiated animals were also observed at 18 months after exposure in explorative behavior and acoustic startle, with increased levels in the irradiated group, demonstrating a possible beneficial effect of the lowest radiation dose at older age.

The data clearly showed that a single whole-body low dose ionizing radiation could actually affect adult mouse behavior and induces quantitative and morphological changes in cellular brain populations, with a dose as low as 0.063 Gy. Behavioral changes were observed as early as 4 months after exposure and persisted until 24 months after exposure, in parallel with cellular changes. In contrast to the starting hypothesis, *Ercc2*^{S737P} het mice did not show a higher sensitivity to ionizing radiation, but rather a resistance to age-related decline.

2. Early and delayed radiation effects

In this study, a decrease in sensorimotor response and spontaneous locomotion occurred after a single exposure to 0.5 Gy. Concretely, being exposed to such a dose can occur in daily life, for example after medical interventions (Sanchez et al., 2014). These behavioral responses did not happen at the same time points. The decrease in sensorimotor recruitment was observed already at 4 months and persisted to 12 months after exposure. Similar results were observed in the literature, with researchers hypothesizing the existence of a possible radiation-induced sensorineural hearing loss (Mujica-Mota et al., 2014). It was observed that doses of 2 and 5 Gy were triggering enhanced inflammation and cell death, inducing radiation damages on the cochlear structures through production of reactive oxygen species (ROS). Furthermore, exposure to 0.5 Gy decreased spontaneous locomotion and exploratory activity at 12 and 18 months after exposure. Acute locomotor reductions (within the first 24 hours after exposure) were observed in adult mice in similar exposure conditions (York et al., 2012), later attributed to neuro-immune activation-induced fatigue. It is less clear if this also explains the changes observed in the present results. Delayed effects of radiation exposure have been observed in human patients. 50 to 90% of radiotherapy-treated brain tumor survivors exhibit disabling cognitive brain function at 6 months to 1 year after radiotherapy (Makale et al., 2016).

3. Dose-dependent effects

Another finding of this study was the dose-dependent effect of radiation. A dose of 0.063 Gy induced no negative effect on early behavior and a beneficial effect at a later time point, no effect on cellular brain populations but increased ramification in microglial cells. These results are in line with other findings of the INSTRA study reported in 2018, i.e. increased survival probability in mice irradiated with such a dose (Dalke et al., 2018), compared to sham-irradiated mice and mice irradiated with higher doses. Tumorigenesis (excluding thyroid adenomas) was also shown to be reduced in the 0.063 Gy-irradiated group.

On the other hand, a dose of 0.5 Gy induced an early decrease in sensorimotor gating, a delayed decrease in spontaneous locomotion and explorative behavior, increased glial expression in the dentate gyrus and decreased dendritic arborization in microglial cells in the long term. This other part of the INSTRA study mentioned earlier (Dalke et al., 2018) showed that this dose increased significantly mortality probability and tumor formation.

From these results, it seems that a dose exists, between 0.063 Gy and 0.5 Gy, below which effects are beneficial and above which health risks increase significantly. However, there is still no precise number for this dose since few studies used doses as low as 0.063 Gy. 0.5 Gy is a dose more frequently encountered in studies. However, despite the more abundant literature, no clear consensus exists on the effects of this dose.

For example, a study in 2018 (Barazzuol et al., 2019) showed that after 6 hours post exposure to 0.5 Gy of X-ray radiation, the number of apoptotic cells increased in the subventricular zone and a proliferation arrest occurred in 3-months old wt mice. However, the loss of doublecortin (DCX) marker expression occurred only at doses higher than 0.5 Gy, showing that biological effects on neurogenesis were dose-dependent. The proliferation arrest (measured by Ki67 expression) was temporary after exposure to 0.5 Gy (recovering occurred after 48 hours) but persisted after exposure to 2 Gy (lasted after 48 hours), showing the biological effects of exposure could be repaired with time up to a certain dose, above which damages are permanent. In this example, 0.5 Gy (with a dose rate of 0.5 Gy/min) is causing temporary and reversible effects.

In our study, exposure to 0.5 Gy was inducing a general decrease of behavioral parameters, such as spontaneous locomotion, explorative behavior and acoustic startle, and these effects were persisting until a late age. Changes in microglial morphology after 0.5 Gy exposure were present in the dentate gyrus of 24 months-old mice.

These 2 examples illustrate the fact that with a same dose, depending on the experimental conditions and the type of observations performed, different outcomes can occur. Is this characteristic sufficient to name such a dose a “transition” dose?

4. Neuroinflammation

Exposure to ionizing radiation can induce increased neuroinflammation in the brain (Hladik and Tapio, 2016). Activated microglia and reactive astrocytes are the major components of the neuroinflammatory response (Betlazar et al., 2016), therefore these cell populations were investigated specifically in 3 regions of the hippocampus (dentate gyrus, CA1 and CA23) at 12, 18 and 24 months after exposure, to look at the development of both populations over time. Immunohistochemical staining with Iba1 (for microglia) and GFAP (for astrocytes) allowed quantification of the number of cells present after exposure.

No consistent dose effect was observed over time on microglial population but a general decrease of microglial number with age was noticed. A linear analysis, using 12 months

results as a baseline, showed that time effect was significant for cell counts in DG, CA23 and CA1.

No consistent radiation dose effect was observed on astrocytes population over time but the linear analysis showed a significant time effect for the cell counts in CA23 and CA1.

The decrease in microglia was surprising because one would expect increased microglial number related to age-related inflammatory processes (Nissen, 2017). However, the number of microglia may not reflect their activation state; a study in 2012 showed that in 8 to 28 months old-rats, after 10 Gy-whole brain radiation, the total microglial number decreased, at all ages, but microglial activation increased markedly, particularly in older animals (Schindler et al., 2008). The same could be hypothesized for astrocytes.

Due to the low case numbers and the lack of consistent radiation effects over time, the effects on the cell population at individual time points have to be considered with caution.

At 12 months after exposure, no significant differences were observed in the number of astrocytes but a decrease in microglia was observed after exposure with 0.063 Gy in CA23. According to (Hua et al., 2012) the CA3 region of the hippocampus appears to be differentially sensitive to effects of aging and radiation and radiation with 0.063 Gy might stimulate molecular and cellular protective mechanisms (Betlazar et al., 2016).

At 18 months after exposure, in the dentate gyrus, a decrease in microglial number was observed in the dentate gyrus after radiation with 0.125 and 0.5 Gy whereas an increase in astrocytes was observed after radiation with 0.125 Gy. If the increase in astrocytes can be related to radiation-induced inflammatory processes (Betlazar et al., 2016), the decrease in microglia is unexpected. It is important to note that 0.125 Gy-irradiated animals showed a high inter-individual variation, which could influence the results. For the 0.5 Gy-irradiated animals, number of cells and state of activation might be two independent parameters, especially in case of old animals. Fewer cells could be present after exposure at older age in total, because of potential radiation-induced or aging-related cell death, but the remaining cells could show an increased activated state (Schindler et al., 2008).

At 24 months after exposure, the higher radiation dose (0.5 Gy) compared to the lower doses increased the number of Iba1+ microglia and did not significantly alter GFAP+ astrocyte number in the dentate gyrus. This increase could be linked to radiation-induced neuroinflammatory changes, indicative of microglial proliferation in response to brain injury (Acharya et al., 2015). In the CA1 region a microglia decrease was found in response to the middle dose (0.125 Gy) and astrocytes decrease was found in response to the highest (0.5 Gy). 0.1 Gy radiation exposure prior to higher radiation doses could trigger expression of neuroprotective pathways that mitigate high dose effects (Alwood et al., 2012; Acharya et al., 2015). The latter, however, runs contrary to the generally accepted view that radiation always induces reactive astrogliosis (Hwang et al., 2006).

Nevertheless, the results here indicate that there are brain region and sub-region specific vulnerabilities to low dose radiation not necessarily applicable to the whole brain. Such regional heterogeneity would fit with, for example, known region-specific microglial functions and transcriptional heterogeneity (Dubbelaar et al., 2018). Furthermore, an undulating pattern (decreases returning to normal over time) of hippocampal GFAP activation was observed previously after high dose radiation in rats (Lumniczky et al., 2017). Thus, the dose and time point after exposure are critical for induction of effects.

These microglial alterations were further characterized at 24 months after exposure by assessing microglial morphology within the dentate gyrus. Microglia have a characteristic stellar shape, with processes which can extend and retract to survey the microenvironment of the brain for possible threats. This process is named ramification (Salter and Stevens, 2017). In the case of inflammation, microglia becomes activated, which is translated morphologically by a rounded, “amoeboid” shape, after retraction of the processes. This transformation is coupled with increased ROS production and cytokine release.

After exposure to 0.5 Gy, long-term de-ramification of the microglia occurred in the dentate gyrus. Exposure to 0.063 Gy increased microglial ramification, explained by some studies as experience-dependent remodeling (Beynon and Walker, 2012). This morphological evidence signifies that the higher and lower tested doses have opposite effects on dynamic microglial processes. Further research is required to understand the functional consequences of these alterations on the brain but it could be postulated that after exposure to 0.063 Gy, ramified microglia possessed a long-term enhanced ability to efficiently re-orientate their processes in response to immune challenge and changes in neural activity (Beynon and Walker, 2012).

In the adult brain, microglia can drive neuronal apoptosis, regulate synaptic plasticity, adult neurogenesis and hippocampal function (Sierra et al., 2010; Gemma and Bachstetter, 2013; Parkhurst et al., 2013; Schafer et al., 2013). Thus, it might be that, within the dentate gyrus, low dose radiation produces long-term persistent effects on these different processes through microglia.

24 months after exposure to 0.125 Gy, decreased branching complexity was observed in astrocytic morphology in the dentate gyrus. Change or loss of astrocytic morphology is known as one of the hallmarks of astrogliosis. This inflammatory phenomenon occurs after insult or injury to the brain tissue and is featured in many neurological diseases (Dossi et al., 2018). As a potential treat, it was shown that Ionizing radiation can induces astrocyte gliosis through microglia activation (Hwang et al., 2006). PGE2 released from irradiated microglia is a key mediator of irradiation-induced gliosis or astrocyte phenotype change. If a change in morphology in response to radiation exposure is seen in both cell types, since microglia and astrocytes do not fulfill the same role, their receptivity to radiation might be different. Astrocytes are support cells of the brain tissue and control the micro-environment where the neurons actually evolve (Palmer and Ousman, 2018). Potential changes consecutive to

radiation exposure might affect their work and therefore have influence on behavioral outputs.

5. Effect of the *Ercc2*^{S737P} mutation at young and older age

At the beginning of the study, it was hypothesized that biological effects of radiation exposure would be more visible in *Ercc2*^{S737P} het mice because their lymphocytes demonstrated an increased sensitivity to radiation-induced DNA damage *in vitro* (Kunze et al., 2015). The results did not confirm this hypothesis. No general effects of genotype over the whole time course of the study were found, neither on the linear analyzes of the behavior or of the cellular populations estimates in the hippocampus after radiation. *Ercc2*^{S737P} het mice carry a c.2209T>C mutation in the *Xpd/Ercc2* gene leading to a Ser737Pro exchange. In 2006 a review on XPD/ERCC2 single nucleotide polymorphisms and the risk of cancer indicated that this gene may not be involved in the repair of X-ray-induced damage that appeared to predominantly require the base excision repair mechanism (Manuguerra et al., 2006), excluding any role of XPD mutation in radiation sensitivity. In addition, at 18 months after exposure, sham-irradiated het mice showed increased total distance traveled, whole average speed and rearing compared to sham-irradiated wt mice. One hypothesis could be that the heterozygous state of the mutation has a protective effect that may be beneficial for ageing (Ven et al., 2012).

6. Health consequences following low-dose radiation exposure

In 2018, a review by (Shimura and Kojima, 2018) was gathering evidence for the lowest radiation dose having molecular changes in the living body, in animals and in humans. According to the authors, the smallest radiation dose causing the changes in the levels of biomarkers appears to be between approximately 0.1 and 0.5 Gy. This dose may overlap with the induction of some adaptive responses. Children and fetuses are shown to be especially vulnerable; DNA damage was observed in children after CT scans with an estimated blood radiation dose as low as 0.15 mGy shortly after examination (Vandevoorde et al., 2015). About the effects of a chronic low-dose exposure, the frequencies of chromosomal translocations were lower in residents of high radioactive background areas (Kerala region in India, South China) than in those of control areas (Hayata et al., 2004; Jain and Das, 2017). This means that systemic adaptive responses may have been prominently expressed in subjects exposed to radiation doses between 0.1 and 0.5 Gy. About 0.5 Gy, this dose was shown to increase genomic instability in human cells (Antonelli et al., 2015) and upregulate the expression of stress responsive genes or proteins. A single exposure was sufficient to elicit a persistent state of genomic instability (Sudo et al., 2008). On the other hand, stimulatory effects were also observed with this dose (Macklis and Beresford, 1991).

(Roch-Lefèvre et al., 2016) recently compared the induction of chromosomal damage in mouse lymphocytes after acute γ -irradiation with that in humans. They revealed that the ratio of the yield of chromosomal breakpoints in mice versus humans was approximately 2 at

all γ -doses delivered (0.1, 0.2, or 0.5 Gy) using fluorescence in situ hybridization. They suggested that this was partly due to the smaller size of the mouse genome from that of the human genome.

Long-term cognitive disability has been observed in subjects exposed to brain irradiation. About half of patients survive >6 months, many attain long term control or cure, but 50-90% of survivors overall exhibit disabling cognitive dysfunction (Makale et al., 2016). Relatively subtle early forms of radiation induced CNS damage may drive chronic pathophysiology leading to permanent cognitive decline. White matter deterioration has been presumed to be a major factor underlying progressive cognitive decline generally apparent a year or so after brain irradiation. It is important to note that the doses used in the radiotherapy are far beyond the scope of low doses.

One review published in 2015 investigated the relation between ERCC2 polymorphisms and radiation-induced adverse effects on normal tissue; no clear connexion was found and one polymorphism was shown to confer a possible radioresistance (Song et al., 2015).

However, extrapolating results obtained in a study using a mouse model to humans is not advised. Several studies reported discordant gene responses to radiation between both species (Ghandhi et al., 2019). (Nakamura, 2017) provided other arguments for why genetic effects of radiation are observed in mice but not in humans: selective mice breeding, lack of highly responsive genes in humans or limited experimental conditions of human studies.

7. Limitations in the techniques used to determine radiation damages

In this study, we assessed the effect of low-dose ionizing radiation using a whole-body irradiated mouse model, with three escalating doses to compare their impact on the behavior of the mouse, using standard behavioral tests, on the cellular composition and the morphology of the hippocampal brain tissue, using immunohistochemistry, stereological and morphological techniques. These tools provided us a phenotypical and pathological picture of consequences of low-dose radiation exposure. However, some parameters can bring variability in results.

Behavioral studies are particularly vulnerable to environmental factors, human-induced factors, females-oestrous cycles, pheromones and circadian rhythm (Holter et al., 2015b) as they can affect the reproducibility of the results. The influence of these factors was kept as minimal as possible, by housing the animals in the controlled environment of the German Mouse Clinic, with constancy in the identity and in the behavior of the experimenter (always the same experimenter following a strictly defined testing protocol) and always including in equal parts males and females in each testing group. The tests were also all carried at the exact same clock time for each session.

Immunohistochemistry procedures were performed with a defined protocol for each stain. Each batch included all brain tissues of the animals sacrificed at one specific time point,

using the same anatomical brain section, with code numbers for each animal and including in equal number males and females, wt and het animals.

The analyses were performed with the Stereoinvestigator software and the NeuroLucida software, always using the same parameters and the same version of the software.

8. Limitations of the study

The INSTRA project was designed in work packages, in which each group had its own research interests. Since the animals were shared between the groups, a limited number of samples was available per group and strict restrictions in term of collection and processing of the samples were put in place. In addition, it was a long-term study, where the animals were irradiated and sacrificed at precise time points, without any possibilities to repeat the experiments and a long waiting time until all the samples were available. One brain hemisphere per animal was available for all the experiments. Because other organs and blood were also sampled, PFA fixation was not possible. All these conditions restricted the type and number of experiments that could be performed. Stereological analysis requires anatomical integrity of the region of interest. Several sections per animal were discarded because they were broken. Four sections per animal was the maximal number of sections that could be included to have the highest animal number. This low number of sections could have partially caused a high inter-individual variation between animals. Sample management was very strict, especially with the 24 months-old animal tissues, which were behaviorally tested and in this sense, more valuable.

9. Conclusions and outlook

In this study, it was shown that a single whole-body exposure to a low-dose of ionizing radiation was able to induce persistent and delayed changes in adult mouse behavior as well as quantitative and morphological dose-dependent changes in hippocampal microglial and astrocytic cell populations. Contrasting effects were observed after exposure to 0.063 Gy or to 0.5 Gy. In addition, no enhanced radiosensitivity was observed in het *Ercc2*^{S737P} mice compared to wildtype mice but the mutation rather showed a protective effect at older age.

In terms of radiation risk for humans, this would mean that doses under 10 mGy, actually considered “harmless” or inducing only background effects, could induce long-term biological changes that could potentially affect our health. All humans will be exposed to low dose radiation in their lives. It is important to find out how this chronic exposure is going to affect them.

It was shown that a dose as low as 1.2 mGy was able to induce DSBs in human cells that remained unrepaired for many days (Rothkamm and Löbrich, 2003). A brain-specific microRNA was found to be consistently deregulated in health professionals exposed in average to 19 mGy during 16 years (Borghini et al., 2017), meaning that neurological

impairments could happen even at low doses. In context of a journey to Mars, where the astronauts would be exposed to space radiation during several months, this could be problematic (Lu et al., 2017). It would be also interesting to find out if genetic radiation risks of very low doses are hereditary (Schmitz-Feuerhake et al., 2016).

Doses between 10 and 100 mGy are actually defined as low doses, with potential cancer risks starting at 100 mGy. It was shown in this study that exposure to a very low dose, 63 mGy was able to induce long-term enhancing effects on mouse behavior and microglial cell morphology. No significant behavioral changes were observed after exposure to 125 mGy but astrocytic cell morphology was significantly affected by this dosage at 24 months. 500 mGy was affecting both behavior and glial cell morphology. These results show assimilating low doses to inoffensive doses is incorrect and that implying that the dose-response curve for biological risks at low doses is linear is also not conform to reality. Current legislation need to be revised to integrate these evidences.

To sum up, the results of this thesis are a valid contribution to radiation biology and neuroscience by providing biological evidences of the impact of low dose radiation exposure on behavior and cellular brain populations in adult mice. It was shown that a single non targeted radiation exposure in young adult mice was able to induce long term changes in behavior and that these changes had different onsets depending on the affected behavior. Depending of the dose and the time after exposure, these changes could be deleterious or beneficial for the irradiated subject. The observed changes in glial cell populations hint towards the influence of inflammatory response in behavioral changes. Further studies need to be done to understand clearly the molecular and cellular mechanisms activated by low dose irradiation and its evolution over time.

BIBLIOGRAPHY

- Abbott A (2015) Researchers pin down risks of low-dose radiation. *Nature* 523:17–18.
- Acharya MM, Baddour AA, Kawashita T, Allen BD, Syage AR, Nguyen TH, Yoon N, Giedzinski E, Yu L, Parihar VK, Baulch JE (2017) Epigenetic determinants of space radiation-induced cognitive dysfunction. *Sci Rep* 7:42885.
- Acharya MM, Patel NH, Craver BM, Tran KK, Giedzinski E, Tseng BP, Parihar VK, Limoli CL (2015) Consequences of low dose ionizing radiation exposure on the hippocampal microenvironment. *PLoS One* 10:e0128316.
- Alvarez LE, Eastham SD, Barrett SR (2016) Radiation dose to the global flying population. *J Radiol Prot* 36:93–103.
- Alwood JS, Kumar A, Tran LH, Wang A, Limoli CL, Globus RK (2012) Low-dose, ionizing radiation and age-related changes in skeletal microarchitecture. *J Aging Res* 2012:481983.
- Antonelli F, Campa A, Esposito G, Giardullo P, Belli M, Dini V, Meschini S, Simone G, Sorrentino E, Gerardi S, Cirrone GAP, Tabocchini MA (2015) Induction and Repair of DNA DSB as Revealed by H2AX Phosphorylation Foci in Human Fibroblasts Exposed to Low- and High-LET Radiation: Relationship with Early and Delayed Reproductive Cell Death. *Radiat Res* 183:417–431.
- Arena C, De Micco V, Macaeva E, Quintens R (2014) Space radiation effects on plant and mammalian cells. *Acta Astronaut* 104:419–431 Available at: <http://www.sciencedirect.com/science/article/pii/S0094576514001659>.
- Azizova T, Briks K, Bannikova M, Grigoryeva E (2019) Hypertension Incidence Risk in a Cohort of Russian Workers Exposed to Radiation at the Mayak Production Association Over Prolonged Periods. *Hypertens (Dallas, Tex 1979)* 73:1174–1184.
- Azzam EI, Jay-Gerin J-P, Pain D (2012) Ionizing radiation-induced metabolic oxidative stress and prolonged cell injury. *Cancer Lett* 327:48–60.
- Bakmutsky M V, Joiner MC, Jones TB, Tucker JD (2014) Differences in cytogenetic sensitivity to ionizing radiation in newborns and adults. *Radiat Res* 181:605–616.
- Barazzuol L, Hopkins SR, Ju L, Jeggo PA (2019) Distinct response of adult neural stem cells to low versus high dose ionising radiation. *DNA Repair* 76:70–75.
- Barnett GC, West CML, Dunning AM, Elliott RM, Coles CE, Pharoah PDP, Burnet NG (2009) Normal tissue reactions to radiotherapy: towards tailoring treatment dose by genotype. *Nat Rev Cancer* 9:134–142 Available at: <https://doi.org/10.1038/nrc2587>.
- Betlazar C, Middleton RJ, Banati RB, Liu G (2016) Redox Biology The impact of high and low dose ionising radiation on the central nervous system. *Redox Biol* 9:144–156 Available at: <http://dx.doi.org/10.1016/j.redox.2016.08.002>.
- Beynon SB, Walker FR (2012) Microglial activation in the injured and healthy brain: what are we really talking about? Practical and theoretical issues associated with the measurement of changes in microglial morphology. *Neuroscience* 225:162–171.
- Binley KE, Ng WS, Tribble JR, Song B, Morgan JE (2014) Sholl analysis : A quantitative comparison of semi-automated methods. *J Neurosci Methods* 225:65–70 Available at: <http://dx.doi.org/10.1016/j.jneumeth.2014.01.017>.
- Bolus NE (2017) Basic review of radiation biology and terminology. *J Nucl Med Technol* 45:259–264.

- Borghini A, Vecoli C, Mercuri A, Carpeggiani C, Piccaluga E, Guagliumi G, Picano E, Andreassi MG (2017) Low-Dose Exposure to Ionizing Radiation Deregulates the Brain-Specific MicroRNA-134 in Interventional Cardiologists. *Circulation* 136:2516–2518.
- Braff D, Stone C, Callaway E, Geyer M, Glick I, Bali L (1978) Prestimulus effects on human startle reflex in normals and schizophrenics. *Psychophysiology* 15:339–343.
- Brandsma I, Gent DC (2012) Pathway choice in DNA double strand break repair: observations of a balancing act. *Genome Integr* 3:9 Available at: <https://pubmed.ncbi.nlm.nih.gov/23181949>.
- Bundesamt fur Strahlenschutz (n.d.) Ionizing radiation - Bfs. Available at: https://www.bfs.de/EN/topics/ion/environment/environment_node.html.
- Burdak-Rothkamm S, Rothkamm K (2018) Radiation-induced bystander and systemic effects serve as a unifying model system for genotoxic stress responses. *Mutat Res* 778:13–22.
- Cannan WJ, Pederson DS (2016) Mechanisms and Consequences of Double-Strand DNA Break Formation in Chromatin. *J Cell Physiol* 231:3–14 Available at: <https://pubmed.ncbi.nlm.nih.gov/26040249>.
- Casciati A, Dobos K, Antonelli F, Benedek A, Kempf SJ, Belles M, Balogh A, Tanori M, Heredia L, Atkinson MJ, von Toerne C, Azimzadeh O, Saran A, Safrany G, Benotmane MA, Linares-Vidal M V, Tapio S, Lumniczky K, Pazzaglia S (2016) Age-related effects of X-ray irradiation on mouse hippocampus. *Oncotarget* 7:28040–28058.
- Chien L, Chen WK, Liu ST, Chang CR, Kao MC, Chen KW, Chiu SC, Hsu ML, Hsiang IC, Chen YJ, Chen L (2015) Low-dose ionizing radiation induces mitochondrial fusion and increases expression of mitochondrial complexes I and III in hippocampal neurons. *Oncotarget* 6:30628–30639.
- Cui J, Yang G, Pan Z, Zhao Y, Liang X, Li W, Cai L (2017) Hormetic Response to Low-Dose Radiation: Focus on the Immune System and Its Clinical Implications. *Int J Mol Sci* 18.
- d'Avella D, Cicciarelo R, Albiero F, Mesiti M, Gagliardi ME, Russi E, d'Aquino A, Tomasello F, d'Aquino S (1992) Quantitative study of blood-brain barrier permeability changes after experimental whole-brain radiation. *Neurosurgery* 30:30–34.
- Dalke C et al. (2018) Lifetime study in mice after acute low-dose ionizing radiation: a multifactorial study with special focus on cataract risk. *Radiat Env Biophys* 57:99–113.
- Davis CM, Roma PG, Armour E, Gooden VL, Brady J V, Weed MR, Hienz RD (2014) Effects of X-ray radiation on complex visual discrimination learning and social recognition memory in rats. *PLoS One* 9:e104393.
- Deng Z, Sui G, Rosa PM, Zhao W (2012) Radiation-induced c-Jun activation depends on MEK1-ERK1/2 signaling pathway in microglial cells. *PLoS One* 7:e36739.
- Deriano L, Roth DB (2013) Modernizing the nonhomologous end-joining repertoire: alternative and classical NHEJ share the stage. *Annu Rev Genet* 47:433–455.
- Desouky O, Ding N, Zhou G (2015) Targeted and non-targeted effects of ionizing radiation. *J Radiat Res Appl Sci* 8:247–254 Available at: <http://www.sciencedirect.com/science/article/pii/S1687850715000333>.
- Dossi E, Vasile F, Rouach N (2018) Human astrocytes in the diseased brain. *Brain Res Bull* 136:139–156.
- Dubbelaar ML, Kracht L, Eggen BJL, Boddeke EWGM (2018) The Kaleidoscope of Microglial Phenotypes. *Front Immunol* 9:1753.

- Eriksson PS, Perfilieva E, Bjork-Eriksson T, Alborn AM, Nordborg C, Peterson DA, Gage FH (1998) Neurogenesis in the adult human hippocampus. *Nat Med* 4:1313–1317.
- Fukuda A, Fukuda H, Swanpalmer J, Hertzman S, Lannering B, Marky I, Bjork-Eriksson T, Blomgren K (2005) Age-dependent sensitivity of the developing brain to irradiation is correlated with the number and vulnerability of progenitor cells. *J Neurochem* 92:569–584.
- Fuss JO, Tainer JA (2011) XPB and XPD helicases in TFIIH orchestrate DNA duplex opening and damage verification to coordinate repair with transcription and cell cycle via CAK kinase. *DNA Repair (Amst)* 10:697–713 Available at: <http://www.sciencedirect.com/science/article/pii/S156878641100125X>.
- Gage FH (2000) Mammalian neural stem cells. *Science (80-)* 287:1433–1438.
- Gemma C, Bachstetter AD (2013) The role of microglia in adult hippocampal neurogenesis. *Front Cell Neurosci* 7:229.
- Ghandhi SA, Smilenov L, Shuryak I, Pujol-Canadell M, Amundson SA (2019) Discordant gene responses to radiation in humans and mice and the role of hematopoietically humanized mice in the search for radiation biomarkers. *Sci Rep* 9:19434 Available at: <https://doi.org/10.1038/s41598-019-55982-2>.
- Haerich P, Eggers C, Pecaut MJ (2012) Investigation of the effects of head irradiation with gamma rays and protons on startle and pre-pulse inhibition behavior in mice. *Radiat Res* 177:685–692.
- Hamada N, Fujimichi Y (2014) Classification of radiation effects for dose limitation purposes: history, current situation and future prospects. *J Radiat Res* 55:629–640 Available at: <https://www.ncbi.nlm.nih.gov/pubmed/24794798>.
- Hammond GR (1973) Lesions of pontine and medullary reticular formation and prestimulus inhibition of the acoustic startle reaction in rats. *Physiol Behav* 10:239–243.
- Hayata I, Wang C, Zhang W, Chen D, Minamihisamatsu M, Morishima H, Wei L, Sugahara T (2004) Effect of high-level natural radiation on chromosomes of residents in southern China. *Cytogenet Genome Res* 104:237–239.
- Hendry JH, Simon SL, Wojcik A, Sohrabi M, Burkart W, Cardis E, Laurier D, Tirmarche M, Hayata I (2009) Human exposure to high natural background radiation: what can it teach us about radiation risks? *J Radiol Prot* 29:A29–A42 Available at: <https://pubmed.ncbi.nlm.nih.gov/19454802>.
- Hladik D, Tapio S (2016) Effects of ionizing radiation on the mammalian brain. *Mutat Res* 770:219–230.
- Holter SM, Einicke J, Sperling B, Zimprich A, Garrett L, Fuchs H, Gailus-Durner V, Hrabe de Angelis M, Wurst W (2015a) Tests for Anxiety-Related Behavior in Mice. *Curr Protoc Mouse Biol* 5:291–309.
- Holter SM, Garrett L, Einicke J, Sperling B, Dirscherl P, Zimprich A, Fuchs H, Gailus-Durner V, Hrabe de Angelis M, Wurst W (2015b) Assessing Cognition in Mice. *Curr Protoc Mouse Biol* 5:331–358.
- Hua K, Schindler MK, Mcquail JA, Forbes ME, Riddle DR (2012) Regionally Distinct Responses of Microglia and Glial Progenitor Cells to Whole Brain Irradiation in Adult and Aging Rats. 7.
- Hwang S-Y, Jung J-S, Kim T-H, Lim S-J, Oh E-S, Kim J-Y, Ji K-A, Joe E-H, Cho K-H, Han I-O (2006) Ionizing radiation induces astrocyte gliosis through microglia activation. *Neurobiol Dis* 21:457–467.
- IRCP (2003) Relative Biological Effectiveness (RBE), Quality Factor (Q), and Radiation Weighting

- Factor (wR)., ICRP Publi. Available at: [http://www.icrp.org/publication.asp?id=ICRP Publication 92](http://www.icrp.org/publication.asp?id=ICRP%20Publication%2092).
- ICRP (2010) Conversion Coefficients for Radiological Protection Quantities for External Radiation Exposures. In: ICRP Publication 116, Ann. ICRP 40, pp 2–5.
- ICRP (2019) Absorbed, Equivalent, and Effective Dose. Available at: http://icrpaedia.org/Absorbed,_Equivalent,_and_Effective_Dose.
- Jain V, Das B (2017) Global transcriptome profile reveals abundance of DNA damage response and repair genes in individuals from high level natural radiation areas of Kerala coast. *PLoS One* 12:e0187274.
- Kate-Louis D. Gottfried and Gary Penn (1996) Radiation in Medicine: A Need for Regulatory Reform. *Medicals Phys* 23:1472–1473.
- Katsura M, Cyou-Nakamine H, Zen Q, Zen Y, Nansai H, Amagasa S, Kanki Y, Inoue T, Kaneki K, Taguchi A, Kobayashi M, Kaji T, Kodama T, Miyagawa K, Wada Y, Akimitsu N, Sone H (2016) Effects of Chronic Low-Dose Radiation on Human Neural Progenitor Cells. *Sci Rep* 6:1–12.
- Keith Franklin George Paxinos (2019) Paxinos and Franklin's the Mouse Brain in Stereotaxic Coordinates, Compact. Elsevier.
- Kempf SJ, Casciati A, Buratovic S, Janik D, von Toerne C, Ueffing M, Neff F, Moertl S, Stenerlow B, Saran A, Atkinson MJ, Eriksson P, Pazzaglia S, Tapio S (2014) The cognitive defects of neonatally irradiated mice are accompanied by changed synaptic plasticity, adult neurogenesis and neuroinflammation. *Mol Neurodegener* 9:57.
- Klaften M, Hrabé de Angelis M (2005) ARTS: a web-based tool for the set-up of high-throughput genome-wide mapping panels for the SNP genotyping of mouse mutants. *Nucleic Acids Res* 33:W496-500.
- Koch M, Schnitzler HU (1997) The acoustic startle response in rats--circuits mediating evocation, inhibition and potentiation. *Behav Brain Res* 89:35–49.
- Koturbash I, Zemp F, Kolb B, Kovalchuk O (2011) Sex-specific radiation-induced microRNAome responses in the hippocampus, cerebellum and frontal cortex in a mouse model. *Mutat Res* 722:114–118.
- Kovalchuk A, Kolb B (2017) Low dose radiation effects on the brain – from mechanisms and behavioral outcomes to mitigation strategies. *Cell Cycle* 16:0.
- Krukowski K, Feng X, Paladini MS, Chou A, Sacramento K, Grue K, Riparip LK, Jones T, Campbell-Beachler M, Nelson G, Rosi S (2018) Temporary microglia-depletion after cosmic radiation modifies phagocytic activity and prevents cognitive deficits. *Sci Rep* 8:7857.
- Kunze S, Dalke C, Fuchs H, Klaften M, Rossler U, Hornhardt S, Gomolka M, Puk O, Sabrautzki S, Kulka U, Hrabé de Angelis M, Graw J (2015) New mutation in the mouse Xpd/Ercc2 gene leads to recessive cataracts. *PLoS One* 10:e0125304.
- Leach JK, Van Tuyle G, Lin P-S, Schmidt-Ullrich R, Mikkelsen RB (2001) Ionizing Radiation-induced, Mitochondria-dependent Generation of Reactive Oxygen/Nitrogen. *Cancer Res* 61:3894 LP – 3901 Available at: <http://cancerres.aacrjournals.org/content/61/10/3894.abstract>.
- Leitner DS, Powers AS, Hoffman HS (1980) The neural substrate of the startle response. *Physiol Behav* 25:291–297.
- Lowe XR, Bhattacharya S, Marchetti F, Wyrobek AJ (2009) Early brain response to low-dose radiation

- exposure involves molecular networks and pathways associated with cognitive functions, advanced aging and Alzheimer's disease. *Radiat Res* 171:53–65.
- Lu T, Zhang Y, Wong M, Feiveson A, Gaza R, Stoffle N, Wang H, Wilson B, Rohde L, Stodieck L, Karouia F, Wu H (2017) Detection of DNA damage by space radiation in human fibroblasts flown on the International Space Station. *Life Sci Sp Res* 12:24–31.
- Lumniczky K, Szatmári T, Sáfrány G (2017) Ionizing Radiation-Induced Immune and Inflammatory Reactions in the Brain. 8:1–13.
- Macklis RM, Beresford B (1991) Radiation hormesis. *J Nucl Med* 32:350–359.
- Makale MT, McDonald CR, Hattangadi-gluth JA, Kesari S (2016) Mechanisms of radiotherapy-associated cognitive disability in patients with brain tumours. *Nat Publ Gr* 13:52–64 Available at: <http://dx.doi.org/10.1038/nrneurol.2016.185>.
- Manuguerra M, Saletta F, Karagas MR, Berwick M, Vineis P, Matullo G (2006) Human Genome Epidemiology (HuGE) Review XRCC3 and XPD / ERCC2 Single Nucleotide Polymorphisms and the Risk of Cancer : A HuGE Review. 164:297–302.
- Marazziti D, Baroni S, Catena-Dell'Osso M, Schiavi E, Ceresoli D, Conversano C, Dell'Osso L, Picano E (2012) Cognitive, psychological and psychiatric effects of ionizing radiation exposure. *Curr Med Chem* 19:1864–1869.
- Matsuo M, Taira Y, Orita M, Yamada Y, Ide J, Yamashita S, Takamura N (2019) Evaluation of Environmental Contamination and Estimated Radiation Exposure Dose Rates among Residents Immediately after Returning Home to Tomioka Town, Fukushima Prefecture. *Int J Env Res Public Heal* 16.
- Mickley GA, Ferguson JL (1989) Enhanced acoustic startle responding in rats with radiation-induced hippocampal granule cell hypoplasia. *Exp Brain Res* 75:28–34.
- Mizumatsu S, Monje ML, Morhardt DR, Rola R, Palmer TD, Fike JR (2003) Extreme sensitivity of adult neurogenesis to low doses of X-irradiation. *Cancer Res* 63:4021–4027.
- Mohammadi M, Danaee L, Alizadeh E (2017) Reduction of Radiation Risk to Interventional Cardiologists and Patients during Angiography and Coronary Angioplasty. *J Tehran Hear Cent* 12:101–106.
- Mosley RL, Benner EJ, Kadiu I, Thomas M, Boska MD, Hasan K, Laurie C, Gendelman HE (2006) Neuroinflammation, Oxidative Stress and the Pathogenesis of Parkinson's Disease. *Clin Neurosci Res* 6:261–281.
- Můčka V, Červenák J, Reimitz D, Čuba V, Bláha P, Neužilová B (2018) Effects of irradiation conditions on the radiation sensitivity of microorganisms in the presence of OH-radical scavengers. *Int J Radiat Biol* 94:1142–1150.
- Mujica-Mota MA, Lehnert S, Devic S, Gasbarrino K, Daniel SJ (2014) Mechanisms of radiation-induced sensorineural hearing loss and radioprotection. *Hear Res* 312:60–68.
- Mullenders L, Atkinson M, Paretzke H, Sabatier L, Bouffler S (2009) Assessing cancer risks of low-dose radiation. *Nat Rev Cancer* 9:596–604.
- Najafi M, Fardid R, Hadadi G, Fardid M (2014) The mechanisms of radiation-induced bystander effect. *J Biomed Phys Eng* 4:163–172 Available at: <https://pubmed.ncbi.nlm.nih.gov/25599062>.
- Nakamura N (2017) Why Genetic Effects of Radiation are Observed in Mice but not in Humans. *Radiat Res* 189:117–127 Available at: <https://doi.org/10.1667/RR14947.1>.

- Nickoloff JA, Boss M-K, Allen CP, LaRue SM (2017) Translational research in radiation-induced DNA damage signaling and repair. *Transl Cancer Res* 6:S875–S891.
- Nissen JC (2017) Microglial Function across the Spectrum of Age and Gender. *Int J Mol Sci* 18.
- Olesen M V, Needham EK, Pakkenberg B (2017) The Optical Fractionator Technique to Estimate Cell Numbers in a Rat Model of Electroconvulsive Therapy. *J Vis Exp*.
- Otsuka K, Koana T, Tauchi H, Sakai K (2006) Activation of antioxidative enzymes induced by low-dose-rate whole-body gamma irradiation: adaptive response in terms of initial DNA damage. *Radiat Res* 166:474–478.
- Palmer AL, Ousman SS (2018) Astrocytes and Aging. 10:1–14.
- Parkhurst CN, Yang G, Ninan I, Savas JN, Yates JR 3rd, Lafaille JJ, Hempstead BL, Littman DR, Gan W-B (2013) Microglia promote learning-dependent synapse formation through brain-derived neurotrophic factor. *Cell* 155:1596–1609.
- Pecaut MJ, Haerich P, Zuccarelli CN, Smith AL, Zendejas ED, Nelson GA (2002) Behavioral consequences of radiation exposure to simulated space radiation in the C57BL/6 mouse: open field, rotorod, and acoustic startle. *Cogn Affect Behav Neurosci* 2:329–340.
- Perez EC, Rodgers SP, Inoue T, Pedersen SE, Leasure JL, Gaber MW (2018) Olfactory Memory Impairment Differs by Sex in a Rodent Model of Pediatric Radiotherapy. *Front Behav Neurosci* 12:158.
- Pittler SJ, Baehr W (1991) Identification of a nonsense mutation in the rod photoreceptor cGMP phosphodiesterase beta-subunit gene of the rd mouse. *Proc Natl Acad Sci U S A* 88:8322–8326.
- Powell SN, Kachnic LA (2003) Roles of BRCA1 and BRCA2 in homologous recombination, DNA replication fidelity and the cellular response to ionizing radiation. *Oncogene* 22:5784–5791.
- Roch-Lefèvre S, Martin-Bodiot C, Grégoire E, Desbrée A, Roy L, Barquinero JF (2016) A mouse model of cytogenetic analysis to evaluate caesium-137 radiation dose exposure and contamination level in lymphocytes. *Radiat Environ Biophys* 55:61–70.
- Rothkamm K, Löbrich M (2003) Evidence for a lack of DNA double-strand break repair in human cells exposed to very low x-ray doses. *Proc Natl Acad Sci* 100:5057 LP – 5062 Available at: <http://www.pnas.org/content/100/9/5057.abstract>.
- Ruhm W, Azizova T, Bouffler S, Cullings HM, Grosche B, Little MP, Shore RS, Walsh L, Woloschak GE (2018) Typical doses and dose rates in studies pertinent to radiation risk inference at low doses and low dose rates. *J Radiat Res* 59:ii1–ii10.
- Saeed Y, Xie B, Xu J, Wang H, Hassan M, Wang R, Hong M, Hong Q, Deng Y (2014) Indirect effects of radiation induce apoptosis and neuroinflammation in neuronal SH-SY5Y cells. *Neurochem Res* 39:2334–2342.
- Salter MW, Stevens B (2017) Microglia emerge as central players in brain disease. *Nat Med* 23:1018–1027.
- Sanchez RM, Vano E, Fernandez JM, Moreu M, Lopez-Ibor L (2014) Brain radiation doses to patients in an interventional neuroradiology laboratory. *AJNR Am J Neuroradiol* 35:1276–1280.
- Schafer DP, Lehrman EK, Stevens B (2013) The “quad-partite” synapse: microglia-synapse interactions in the developing and mature CNS. *Glia* 61:24–36.
- Schindler MK, Forbes ME, Robbins ME, Riddle DR (2008) Aging-dependent changes in the radiation response of the adult rat brain. *Int J Radiat Oncol Biol Phys* 70:826–834.

- Schmitz-Feuerhake I, Busby C, Pflugbeil S (2016) Genetic radiation risks: a neglected topic in the low dose debate. *Environ Health Toxicol* 31:e2016001.
- Shimura N, Kojima S (2018) The Lowest Radiation Dose Having Molecular Changes in the Living Body. *Dose Response* 16:1559325818777326.
- Sierra A, Encinas JM, Deudero JJP, Chancey JH, Enikolopov G, Overstreet-Wadiche LS, Tsirka SE, Maletic-Savatic M (2010) Microglia shape adult hippocampal neurogenesis through apoptosis-coupled phagocytosis. *Cell Stem Cell* 7:483–495.
- Song Y-Z, Duan M-N, Zhang Y-Y, Shi W-Y, Xia C-C, Dong L-H (2015) ERCC2 polymorphisms and radiation-induced adverse effects on normal tissue: systematic review with meta-analysis and trial sequential analysis. *Radiat Oncol* 10:247.
- Spitz DR, Azzam EI, Li JJ, Gius D (2004) Metabolic oxidation/reduction reactions and cellular responses to ionizing radiation: a unifying concept in stress response biology. *Cancer Metastasis Rev* 23:311–322.
- SSK (2007) Krebsrisiko durch mehrjährige Expositionen mit Dosen im Bereich des Grenzwertes für die Berufslebensdosis nach § 56 Strahlenschutzverordnung (StrlSchV). Available at: https://www.ssk.de/SharedDocs/Beratungsergebnisse_PDF/2007/Krebsrisiko_Berufslebensdosis.pdf?__blob=publicationFile.
- Stanley FKT, Irvine JL, Jacques WR, Salgia SR, Innes DG, Winkquist BD, Torr D, Brenner DR, Goodarzi AA (2019) Radon exposure is rising steadily within the modern North American residential environment, and is increasingly uniform across seasons. *Sci Rep* 9:18472 Available at: <https://doi.org/10.1038/s41598-019-54891-8>.
- Sudo H, Garbe J, Stampfer MR, Barcellos-Hoff MH, Kronenberg A (2008) Karyotypic instability and centrosome aberrations in the progeny of finite life-span human mammary epithelial cells exposed to sparsely or densely ionizing radiation. *Radiat Res* 170:23–32.
- Sun J, Chen Y, Li M, Ge Z (1998) Role of Antioxidant Enzymes on Ionizing Radiation Resistance. *Free Radic Biol Med* 24:586–593 Available at: <http://www.sciencedirect.com/science/article/pii/S0891584997002918>.
- Swerdlow NR, Braff DL, Taaid N, Geyer MA (1994) Assessing the validity of an animal model of deficient sensorimotor gating in schizophrenic patients. *Arch Gen Psychiatry* 51:139–154.
- Tharmalingam S, Sreetharan S, Brooks AL, Boreham DR (2019) Re-evaluation of the linear no-threshold (LNT) model using new paradigms and modern molecular studies. *Chem Biol Interact* 301:54–67 Available at: <http://www.sciencedirect.com/science/article/pii/S0009279718310858>.
- Thompson LH, Schild D (2001) Homologous recombinational repair of DNA ensures mammalian chromosome stability. *Mutat Res* 477:131–153.
- UNSCEAR (2017) What levels of radiation exposure do people receive? Available at: <https://www.unscear.org/unscear/fr/faq.html#Levels of radiation>.
- Vaiserman A, Koliada A, Zabuga O, Socol Y (2018) Health Impacts of Low-Dose Ionizing Radiation: Current Scientific Debates and Regulatory Issues. *Dose Response* 16:1559325818796331.
- Vandevoorde C, Franck C, Bacher K, Breyssem L, Smet MH, Ernst C, De Backer A, Van De Moortele K, Smeets P, Thierens H (2015) γ -H2AX foci as in vivo effect biomarker in children emphasize the importance to minimize x-ray doses in paediatric CT imaging. *Eur Radiol* 25:800–811.
- Ven M Van De, Andressoo J, Horst GTJ Van Der, Hoeijmakers JHJ, Mitchell JR (2012) Effects of

- compound heterozygosity at the Xpd locus on cancer and ageing in mouse models. *DNA Repair (Amst)* 11:874–883 Available at: <http://dx.doi.org/10.1016/j.dnarep.2012.08.003>.
- Verri M, Pastoris O, Dossena M, Aquilani R, Guerriero F, Cuzzoni G, Venturini L, Ricevuti G, Bongiorno AI (2012) Mitochondrial alterations, oxidative stress and neuroinflammation in Alzheimer's disease. *Int J Immunopathol Pharmacol* 25:345–353.
- Willers H, Dahm-Daphi J, Powell SN (2004) Repair of radiation damage to DNA. *Br J Cancer* 90:1297–1301.
- World Health Organization (2018) Cancer. Available at: <https://www.who.int/news-room/fact-sheets/detail/cancer>.
- Yamaoka K, Edamatsu R, Itoh T, Akitane M (1994) Effects of low-dose X-ray irradiation on biomembrane in brain cortex of aged rats. *Free Radic Biol Med* 16:529–534 Available at: <http://www.sciencedirect.com/science/article/pii/0891584994901325>.
- York JM, Blevins NA, Meling DD, Peterlin MB, Gridley DS, Cengel KA, Freund GG (2012) The biobehavioral and neuroimmune impact of low-dose ionizing radiation. *Brain Behav Immun* 26:218–227.
- Zou J, Wang W, Pan Y-W, Lu S, Xia Z (2015) Methods to measure olfactory behavior in mice. *Curr Protoc Toxicol* 63:11.18.1-11.18.21 Available at: <https://pubmed.ncbi.nlm.nih.gov/25645244>.

ACKNOWLEDGEMENTS

My first acknowledgment goes to PD Dr. Sabine Hölter-Koch for her constant support, thoughtful guidance and encouragement during my PhD. Thank you for your availability, your advices and your cheerful attitude.

I would like also to thank Prof. Dr. Wolfgang Wurst for supervising my thesis, and his support and advices on my research. I would like to acknowledge and thank the examination board, Prof. Dr. Angelika E. Schnieke, Prof. Dr. Michael J. Atkinson and Prof. Dr. Wolfgang Wurst for their time and effort to evaluate my thesis.

I would like to thank Dr. Daniela Vogt-Weisenhorn and Dr. Florian Giesert for their valuable inputs on my research work, especially on the experimental part.

I would like to thank Dr. Michael Rosemann for his encouragements.

I would like to thank Prof. Dr. Joachim Graw and Dr. Claudia Dalke for their time and effort in the creation and management of the INSTRA project.

I would like to acknowledge the members of the INSTRA consortium for being part of this project and sharing their expertise.

This thesis would not have been possible without my co-workers Dr. Lillian Garrett, Jan Einicke, Bettina Sperling, Dr. Annemarie Zimprich and the other members of the Behavioral Neuroscience group. I am grateful for the time you invested in my training, your respective contribution to my research work, your valuable inputs and the general good mood within our team. Working with you was very nice.

Thanks to my colleagues of the second floor's corridor in building 35.37, especially the PhD students: Sarah, Sharmilee, Daniel, Silviu, Maria, Susanne, Felix, Chris, Pannus, Ahne, Antonella, Michele, Sheryl... Thank you for sharing lunches, advices, happy and sad moments. Thanks to Monika and Erika for their delicious cakes!

José, thank you for your love and support and for being such a great partner.

Finally I would like to thank my parents and my brother for their ongoing support, and for giving me the possibility to pursue freely my studies until this stage.

